UNIVERSITY OF BIRMINGHAM

Potential involvement of epithelial-mesenchymal transition in the pathogenesis of periodontitis

By

Ali Abbas Abdulkareem

A thesis submitted to the University of Birmingham for the degree of DOCTOR OF PHILOSOPHY

School of Dentistry

College of Medical and Dental Sciences

The University of Birmingham

February 2017

Abstract

Epithelial-mesenchymal transition is reportedly important in loss of epithelial integrity and cell migration in inflammatory/infectious diseases and cancer. Since Gram negative anaerobic periodontal pathogens are well-recognized to induce intense inflammatory responses; the present study investigated their ability to induce EMT *in vitro*. A 2D chronic inflammatory model was developed using either the H400 oral keratinocyte cell-line or primary rat oral keratinocytes which were exposed to heat-killed *Fusobacterium nucleatum*, *Porphyromonas gingivalis* and *Escherichia coli* LPS for up to 8-days. EMT-associated changes were determined using semi-quantitative-RT-PCR, PCR-arrays, ELISA, scratch/transwell migration assays, immunocytochemistry/immunofluorescence, and transepithelial electrical resistance. Chronically stimulated cultures increased extracellular levels of the EMT regulatory cytokines, TGF-β1, TNF-α and EGF, whilst subsequent EMT-induction was indicated by up-regulation of mesenchymal markers, including vimentin and N-cadherin, and concomitant down-regulation of epithelial markers including E-cadherin and β-catenin. In addition, intracellular signaling activity of key EMT regulatory transcription factors, Snail-1 and NF-κB, increased following chronic bacterial exposure and was associated with enhanced cellular migratory activity and reduced epithelial barrier integrity. These results indicated for the first time that EMT may be involved in the compromised epithelial barrier function observed during periodontitis pathogenesis which may occur in response to prolonged local bacterial exposure.

To my Mother

Acknowledgements

I would like to express my sincere gratitude to my advisors Dr. Mike Milward, Prof. Paul Cooper, Dr. Richard Shelton, Prof. Gabriel Landini for the continuous support of my PhD study and related research, for their patience, motivation, and immense knowledge. Their guidance helped me in all the time of research and writing of this thesis. I could not have imagined having better advisors for my PhD study.

I gratefully acknowledge the funding received towards my PhD from Iraqi Ministry of Higher Education and scientific Research.

I would especially like to thank all laboratory technicians at School of Dentistry/ University of Birmingham. All of you have been there to support and teach me, without you I would not be able to collect data for my PhD thesis.

A special thanks to my family. Words cannot express how grateful I am to my mother, my brothers Akram and Basel, and my sister Maha for all sacrifices and help that they have made.

I would also like to thank all of my friends and colleagues in postgraduate room who supported me in writing, and incented me to strive towards my goal. I would also like to say a heartfelt thank you Nibras Khalid Al-Naimi for everything you have done for me since the first day till I finish.

Table of contents

List of Illustrations

List of tables

List of Abbreviations

AJ	Adherens junctions
Antibody	AB
BC	Breast cancer
bDNA	Bacterial DNA
BM	Basement membrane
BMP	Bone morphogenic protein
BSA	Bovine serum albumin
C. rodentium	*Citrobacter rodentium*
CagA	Cytotoxin-associated gene A
CC	Cholangiocarcinoma
CD	Crohn's disease
cfu	Colony forming unit
CRB	Crumbs complexes
CRC	Colorectal carcinoma
CT	Connective tissue
CTGF	Connective tissue growth factor
CVD	Cardiovascular disease
DAB	3,3'-diaminobenzidine
Des	Desmosomes
DLG	Discs large
DM	Diabetes mellitus
DMEM	Dulbecco’s modified Eagle’s medium
DMSO	Dimethyl sulfoxide
Dnase I	Deoxyribonuclease I
E. coli	*Escherichia coli*
ECM	Extracellular matrix
EDTA	Ethylenediaminetetraacetic acid
EGF	Epidermal growth factor
EGFR	Epidermal growth factor receptor

ELISA	Enzyme-linked immunosorbent assay
EMT	Epithelial-mesenchymal transition
EndMT	Endothelial-mesenchymal transition
F. nucleatum	*Fusobacterium nucleatum*
FCS	Foetal calf serum
FGF	Fibroblast growth factor
FSP-1	Fibroblast specific protein-1
GAPDH	Glyceraldehyde-3-phosphate dehydrogenase
GC	Gastric cancer
GFP	Fluorescent protein
H. influenza	*Haemophilus influenza*
H. pylori	*Helicobacter pylori*
HCV	Hepatitis C virus
HDMS	Hexamethyldisilazane
HGF	Hepatocyte growth factor
HSCSs	Hepatic stellate cells
ICC	Immunocytochemistry
IF	Immunofluorescence
IHC	Immunohistochemistry
IKK	IκB kinase
IL	Interleukins
ILK	Integrin-linked kinase
IκB	inhibitors of κB
JE	Junctional epithelium
KCM	Keratinocyte culture medium
LEF-1	Lymphoid enhancer-binding factor-1
LPS	Lipopolysaccharide
MAPK	Mitogen-associated protein kinase
MDCK	Madin-Darby canine kidney
MET	Mesenchymal-epithelial transition
MMC	Mitomycin C

MMP	Matrix metalloproteinases
NF-κB	Nuclear factor kappa-light-chain-enhancer of activated B cells
OC	Ovarian cancer
OD	Optical density
OSCC	Oral squamous cell carcinoma
P. aeruginosa	*Pseudomonas aeruginosa*
P. gingivalis	*Porphyromonas gingivalis*
PAMPs	Pathogen- associated molecular patterns
PAR	Partitioning-defective
PBS	Phosphate-buffered saline
PCR	Polymerase chain reaction
PI3K	Phosphatidylinositol-3-kinase
PRRs	Pathogen recognition receptors
RANKL	Receptor activator of nuclear factor kappa-B ligand
RCC	Renal cell carcinoma
SCRIB	Scribble complexes
SEM	Scanning electron microscope
sq-RT-PCR	Semi-quantitative reverse transcriptase-polymerase chain reaction
TEER	Transepithelial electrical resistance
TGF-β	Transforming growth factor-β
TJ	Tight junctions
TLR	Toll-like receptor
TNF-α	Tumour necrosis factor-α
UC	Ulcerative colitis
VE-cadherin	Vascular endothelial cadherin
ZEB-1	Zinc finger E-box-binding homeobox
ZO-1	Zonula occludens-1
α-SMA	α-smooth muscle actin

INTRODUCTION

The concept of epithelial-mesenchymal transition (EMT) was first reported by Elizabeth Hay working on the primitive streak of chick embryos (Hay, 1968). Briefly, EMT is a process by which epithelial cells acquire a mesenchymal-like phenotype in response to different pathological and physiological stimuli. There is now growing evidence for EMT as a mechanism which plays important roles in embryogenesis, inflammation and cancer metastasis. A series of distinct molecular events appear to be involved in triggering EMT such as activation of certain transcriptional pathways, alteration in expression of surface molecules and changes in cytoskeletal proteins (Kalluri and Neilson, 2003, Radisky, 2005, Kalluri and Weinberg, 2009). Several studies have highlighted the involvement of cytokines and bacterial products as EMT-predisposing factors (Ackland et al., 2003, Binder Gallimidi et al., 2015, Li et al., 2012a).

Periodontitis encompasses a group of inflammatory conditions affecting the supporting tissues of the dentition (Offenbacher, 1996). The disease is characterised by an aberrant host response in susceptible patients to a pathogenic plaque biofilm consisting of a predominance of Gram-negative anaerobic bacteria (Socransky et al., 1998). Some of these key periodontal pathogens are well-recognized for their ability to stimulate host cells, including junctional epithelium, which is intimately related to the plaque biofilm, to secrete a range of pro-inflammatory cytokines which have been implicated in initiating the EMT process (Kornman et al., 1997). It is proposed that the EMT process and the resulting shift from an epithelial to mesenchymal phenotype (Radisky, 2005) could result in the loss of the integrity of the epithelial barrier allowing bacterial invasion of the underlying tissues predisposing the patient to periodontal disease. To date the role of periodontal pathogens, particularly Gram-negative anaerobes, in initiating the EMT process has not been completely elucidated.

1: Epithelium

Epithelium is a major tissue covering almost all bodily external surfaces and lines body cavities, blood vessels and lymphatics. Epithelium is derived from all three embryonic germ layers; ectoderm (e.g. lining of the mouth), endoderm (e.g. lining of respiratory tract), and mesoderm (e.g. endothelium of blood vessels) (Eurell and Frappier, 2013).

Epithelium is composed of tightly packed continuous epithelial sheets in one or more layers. The epithelial cells adhere to each other with a classical cobble-stone appearance by specialised multiprotein structures called cell junctions which provide physical strength and maintain epithelial integrity, as well as mediating communication and metabolite transport between adjacent cells (Locke and Harris, 2009). Epithelium is an avascular tissue and receives nutrients and oxygen via diffusion through selective permeability of the thin, fibrous basement membrane, whose primary function is to anchor epithelial cells to the underlying connective tissue (CT). The attachment between basement membrane and epithelial cells is mediated by the interaction between BM-associated laminin and its integrin receptors in the basal epithelial layer. On the stromal side, extracellular matrix (ECM) components are attached to BM-associated collagen IV (Kubota et al., 1988, Paulsson, 2008). In addition, BM acts also as a barrier against invasion of bacteria and metastatic cells at the early stages of malignant change thereby confining cells to the epithelial compartment (Liotta et al., 1980).

In general, epithelia can be classified utilizing three morphological features. The first feature is based on the number of epithelial layers: simple epithelium (which consists of a single layer) or multilayered, also termed stratified epithelia. The second feature is based on the shape of the constituent cells, such as cuboidal, columnar and transitional. These, in turn could be simple or stratified. The presence of different surface specialised structures, such as cilia and keratinisation are the criteria used for the third categorization (Eurell and Frappier,

2013, Tortora and Derrickson, 2010). The primary function of epithelium is protective by acting as mechanical barrier against different threats such as microbial invasion and physical trauma; also, it secretes a range of inflammatory cytokines and antimicrobials that enable the induction of innate immunity. In addition, epithelia are specialised in certain organs such as glands, nervous, digestive, and respiratory systems to perform different functions including secretory, sensory, absorption, and diffusion respectively (Fritz et al., 2008, Marchiando et al., 2010). Epithelial cells exhibit a range of unique cellular molecules that can be used as markers to identify the epithelial phenotype (Table 1).

Protein	**Function**	**Reference**
E-cadherin	Major component of calcium-dependent adherens junction	(Hulpiau and Van Roy, 2009)
β-Catenin	Regulates cell-cell adhesion and signaling pathways; e.g. Wnt	(MacDonald et al., 2009)
Occludin	Integral protein of tight junctions	(Furuse et al., 1993)
Claudins	Structural units of tight junctions, regulates passage of molecules through epithelial layer	(Furuse et al., 1998)
Desmoplakin	Component of desmosomal structures	(Arnemann et al., 1991)
Plakoglobin	Major protein of cytoplasmic domain of Des and adherens junctions	(Cowin et al., 1986)
Desmocollin and desmoglein	Adhesion proteins of Des-mediated cell-cell adhesion	(Garrod et al., 2002)
Cytokeratins	Diverse group of intermediate filaments forming cytoskeleton that maintains stability and integrity of the cell	(Moll et al., 2008)
Laminin-1	Scaffolding unit of basal lamina that participate in cell-ECM attachment	(Aumailley et al., 2005)
Type-1 collagen	Major protein of ECM secreted by epithelial cells	(Hayashi et al., 1988)
MMP-9	Degradation of ECM components	(Hannas et al., 2007)
Integrin (e.g. α6β4)	Transmembrane protein participates in cell-ECM adhesion	(Kikkawa et al., 2000)

Table 1. Summary of molecules commonly used to define epithelial-phenotype.

1.1: Cell junctions

Epithelial cells have specialised structural proteins in the cellular membrane which enable robust adhesion between neighboring cells and this is a key factor in maintaining epithelial integrity (Figure 1).

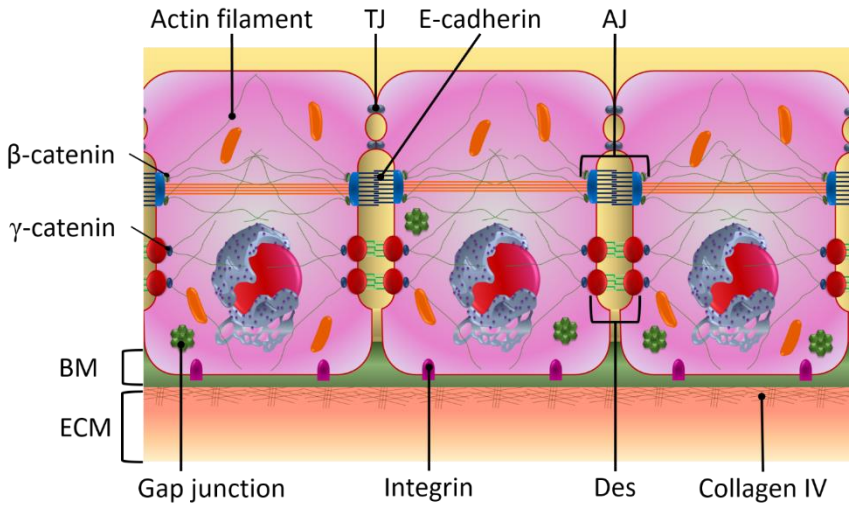

Figure 1. Diagram of epithelial cells and junctions demonstrating tight junctions (TJ), adherens junctions (AJ), desmosomes (Des), and gap junctions. Different types of catenin molecules strengthen the attachment by linking cadherins-associated cellular junctions with cytoskeletal actin. Epithelial cells attached to underlying fibrous BM, predominantly by Collagen IV, via integrins.

1.1.1: Tight junctions

Tight junctions (TJ) are located just beneath the apical surface of the cells and act mainly to maintain apical polarity and provide a seal between adjacent cells thereby regulating the passage of molecules into the intercellular space (Yamanaka et al., 2001, Goldstein and Macara, 2007). TJ consist of number of scaffolding proteins which include occludins and claudins which form the extracellular domain. These molecules complex together and form part of the Zonula occludens-1 (ZO-1) which binds intracellularly to the actin cytoskeleton of the cell thus joining the cytoskeleton of adjacent cells and is involved in transducing signaling to the nucleus (Kirschner and Brandner, 2012).

1.1.2: Desmosomes

These inter-cellular structures are composed of three distinct protein families: the cadherins, the armadillo proteins and the plakins. They are responsible for maintaining epithelial sheet integrity, together with AJ, through binding with the actin cytoskeleton internally via plakoglobin and desmoplakin (Garrod et al., 2002, Getsios et al., 2004). Disintegration of desmosomes by various stimuli such as bacterial enzymes result in compromised epithelial barrier function in adult and embryonic tissues. Furthermore, the knocking out of desmoplakin in a mouse model caused intercellular separation when the skin is exposed to mechanical stress. In addition, desmoplakin-null epithelial cells showed less Des and AJ in comparison with the wild type control along with a failure to organise actin causing a subsequent breach in epithelial adhesion and loss of cytoskeletal architecture (Vasioukhin et al., 2001).

1.1.3: Adherens junctions

AJ in combination with Des form the junctional-complex, an essential architecture-maintaining component of epithelial cells which anchors the cytoskeleton of each cell and bridges it to other cells. These protein complexes are usually located in more basal sites than TJ and appear as a band or belt encircling the cell (zonula adherens) thereby yielding structural reinforcement for TJ (Guo et al., 2007). Each AJ is composed essentially of three domains: an extracellular domain that binds to the extracellular component of an adjacent cell, a transmembrane domain and an intracellular part that links to the actin cytoskeleton, forming a network with cytoskeletal proteins of adjacent cells, through α- and β-catenin. The predominant structural protein in this domain is E-cadherin (Figure 2) which is a member of the cadherin family found in many tissues (Gumbiner, 2005, Halbleib and Nelson, 2006, Lien et al., 2006).

Levels of E-cadherin and hence AJ-mediated adhesion are affected mainly by the transcriptional activity of Snail/Slug, zinc finger transcriptional factors which act as major E-cadherin-suppressors by deacetylating histones at E-cadherin motif sites (Peinado et al., 2004). Indeed, ablation of Snail in a mouse embryo model resulted in retention of E-cadherin in mesoderm with subsequent early embryonic development failure. This finding was consistent with findings observed in Snail-negative *Drosophila* embryos (Carver et al., 2001).

Cadherins constitute a large family of cell-surface glycoproteins which represent the main structural component of calcium-dependent cellular junctions which are responsible for cell-cell adhesion and maintaining tissue integrity. In addition, cadherins play an important role in signal transduction and mediate the morphogenesis of different organs (Gumbiner, 2005, Halbleib and Nelson, 2006, Lien et al., 2006). Members of the cadherin family are widely distributed in the tissues of vertebrates such as N- (neural), VE- (vascular endothelial), K- (kidney), R- (retinal), and P- (placental) cadherin (Hulpiau and Van Roy, 2009). It has been shown that physiological and pathological events are associated with altered cadherin expression (Price et al., 2002, Honjo et al., 2000, Takeichi, 1995).

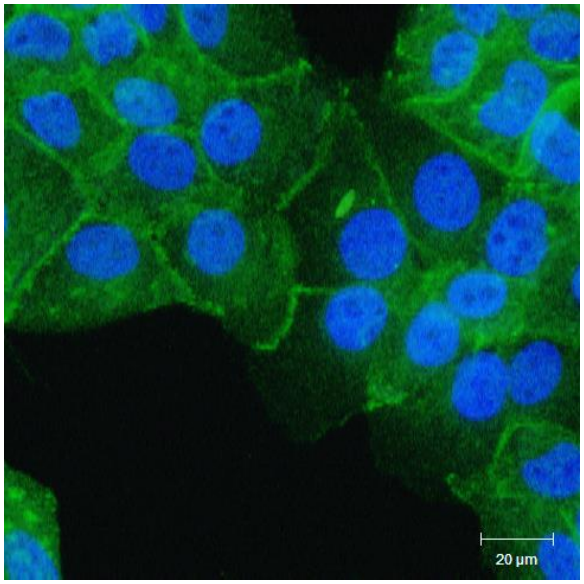

Figure 2. Immunofluorescence staining of H400 cells demonstrating E-cadherin (green) distributed throughout the cytoplasm of the cells. However, this protein is more concentrated around the periphery of the cells in the area contacting adjacent cells, indicating its role in maintaining attachment of epithelial cells. Nuclei are counterstained with DAPI (blue). Scale bars are shown.

1.1.3.1: E-cadherin-catenin complex

Each mature E-cadherin molecule is composed of intracellular, transmembrane, and extracellular domains (Overduin et al., 1995, Shapiro et al., 1995). The extracellular region is connected to the cytoplasmic or intracellular domain via a transmembrane component which in turn is connected to another structural protein, catenin that mediates the attachment between E-cadherin and the cytoskeletal proteins of the cell. The intracellular domain is either attached to β-catenin, in the case of AJ, or to plakoglobin (γ-catenin) when associated with Des (Shapiro and Weis, 2009). The strength of linkage between these two proteins in the Madin-Darby canine kidney cells (MDCK) cell line was measured by Chen et al. (2013b) showed that the adhesion shifts from a relatively weak to strong state in ~1 hour following temperature shifting from 40°C to 35°C. The terminal end of β- or γ-catenin binds to α-catenin which mediates the attachment to the cytoskeleton thereby adding more stability to the adhesion complex between the cells (Aberle et al., 1994).

2: Connective tissue

CT is a biological supporting tissue of mesodermal origin which provides structural strength and metabolites to other tissues. In addition, it provides the shape and maintains separation between organs. This tissue contains blood and lymphatic vessels which mediate nutrients and waste product exchange between the tissues and circulatory system (Ross and Pawlina, 2006).

In general, all CT have two primary components, ECM and cells. The physical properties of CT are determined by the ECM, the most abundant component, which is composed of loosely-attached cells lacking polarity, embedded in a ground substance containing a variety of fibres, and glycoproteins (Strum et al., 2007). The fibrous component is formed mainly from two fibre types, elastin and collagen. Collagen is the most commonly found fibre in the human body and is subdivided into up to 28 different types, collagen I, II, and III are well-distinguished due to their ability to withstand mechanical stresses while collagen IV and VII, which are non-fibrillar, are associated with BM attachment to the overlying epithelial layer (Sherman et al., 2015). Although increased collagen fibre production is a normal body response to different tissue injuries and considered to be part of the normal healing mechanism, excessive collagen fibre deposition following certain pathological conditions such as idiopathic pulmonary fibrosis and systemic sclerosis or large wounds may result in fibrosis and subsequent loss of tissue architecture and organ dysfunction (Rockey et al., 2015). Fibroblasts (Figure 3) are the main source of collagen fibre deposition in the ECM which can be activated by a range of cytokines released by inflammatory and epithelial cells. Many studies have demonstrated a central role of transforming growth factor- β1 (TGF-β1), the most well-known pro-fibrotic mediator, which is upregulated in fibrotic tissue and modulates fibroblast function and phenotype (Pohlers et al., 2009, Biernacka et al., 2011).

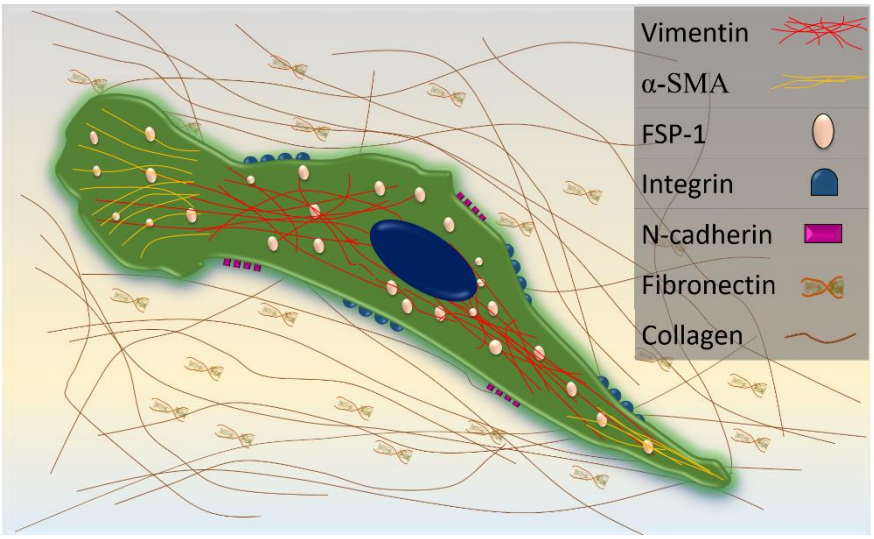

Figure 3. Diagram of a fibroblast (in green) located within the ECM and illustrating the location of essential mesenchymal molecules such as vimentin, α-SMA, and fibroblast specific protein-1 (FSP-1), and N-cadherin. A key is provided for the different molecules shown.

The major cellular constituents of CT are classified based on their function, i.e. fibroblasts, adipocytes, chondrocytes, osteoblasts, blood cells and immune cells. Fibroblasts are derived from mesenchymal precursors and are responsible for synthesis and maintenance of ECM components. Unlike epithelial cells, fibroblasts are less robustly attached to each other, they are not polarised nor attached to BMs and do not form layers but are randomly distributed in the ECM, they also exhibit higher mobility rates (Baum and Duffy, 2011). In addition, fibroblasts can express a range of mesenchymal markers (Table 2) including vimentin and transmembrane molecules (such as N-cadherin) (Shapiro et al., 1995, Dave and Bayless, 2014) which are not present in epithelial cells. The morphology of fibroblasts (Figure 4) is heterogeneous, they may appear as spindle-shaped, elongated or exhibit a flattened stellate shape (Baum and Duffy, 2011).

Protein	Function	References
N-cadherin	Cadherin-family member involved in mesenchymal cell-cell adhesion	(Takeichi, 1990, Shapiro et al., 1995)
α -Smooth muscle actin (α-SMA)	Implicated in fibrogenesis and motility of cell	(Cherng et al., 2008)
Vimentin	Major intermediate filament forming cytoskeleton	(Katsumoto et al., 1990, Dave and Bayless, 2014)
Fibroblast specific protein-1 (FSP-1)	Cytoplasmic protein participates in regulating cellular functions such as differentiation and motility	(Garrett et al., 2006)
Fibronectin	Binds the cell to ECM components.	(Pankov and Yamada, 2002)
Laminin 5	ECM constituent which is mediated adhesion and migration of cell	(Miyazaki, 2006)
Integrins (e.g. α5β1)	Bind cell to ECM components such as fibronectin and collagen, also participate in regulating cytokines production	(Boudreau and Varner, 2004)
MMP-2, and -3	Modulate components of ECM	(Hannas et al., 2007)

Table 2. Summary of molecules commonly used to define mesenchymal-phenotype.

The ECM provides the base from which epithelial sheets gain support, this adhesion is mainly mediated by interaction of epithelium-associated integrins and laminins which can be defined as high molecular weight proteins, associated with the basal lamina of BM and is involved in epithelial cell adhesion, migration and differentiation (Aumailley et al., 2005).

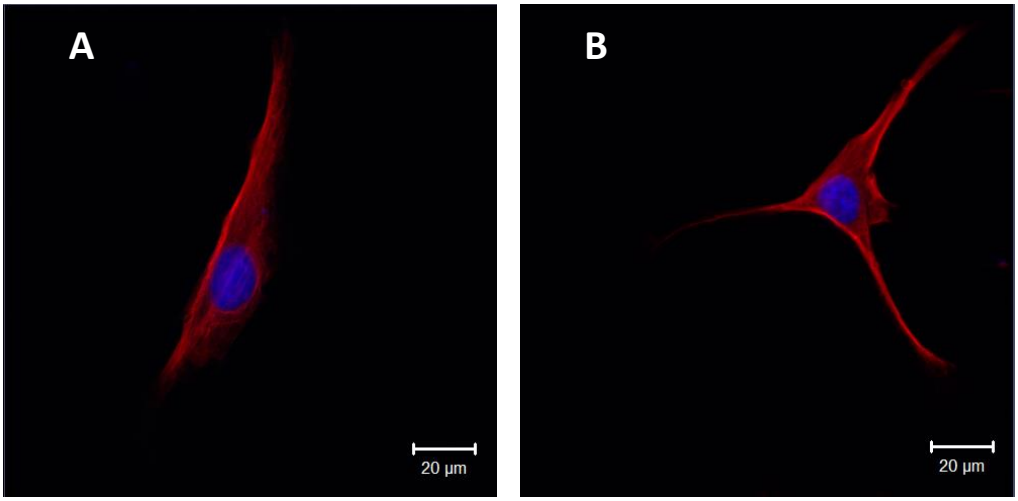

Figure 4. Vimentin (red) stained human gingival fibroblasts exhibiting different morphologies (A) Spindle-shape, (B) stellate shape. Nucleus counterstained with DAPI (blue) stain.

3: Epithelial-mesenchymal transition (EMT)

3.1: EMT history and definition

The first description of epithelial-mesenchymal transition (EMT) and its inverse process, mesenchymal-epithelial transition, was attributed to the work of Hay (1968) on the primitive streak of chick embryos. EMT is the process by which an epithelial cell switches to a more mesenchymal-like phenotype (Fig.5). This shifting in phenotype consists of a diverse range of cellular events including an increased resistance to apoptosis, loss of apico-basal polarity, dissociation of cellular adhesion junctions (cell-cell and cell-BM attachments), and major architectural reorganization of the cytoskeleton. These events are associated with simultaneous up-regulation of mesenchymal markers and downregulation of epithelial markers (Lamouille et al., 2014). The acquisition of mesenchymal properties increases motility of the cells together with increased enzymatic activity which causes remodeling of the BM. This facilitates migration of transitioned cells to gather in the interstitium of the tissue (Kalluri and Neilson, 2003, Radisky, 2005).

Treatment of MDCK epithelial cells with antibody against E-cadherin resulted in expression of EMT-like features in these cells *in vitro* (Hay and Zuk, 1995). In addition, certain factors including TGF-β and integrin 5β1, applied in a 3D model of lens epithelium, showed potential to alter phenotype of epithelial cells into mesenchymal-like cells (Hay and Zuk, 1995). Conversely, transfection of embryonic corneal mesenchyme with E-cadherin gene resulted in the conversion to an epithelial phenotype, i.e. mesenchymal-epithelial transition (MET) (Hay and Zuk, 1995). These processes are modulated by many epigenetic and molecular events which have been used as the main indicators for cells undergoing EMT (Kalluri and Weinberg, 2009). Notably EMT can be reversed upon removal of stimuli or by using certain anti-EMT agents or drugs (Tan et al., 2007, Nagai et al., 2011, Zhang et al., 2013a).

3.2: Controversy around EMT

Since it was first described (Hay, 1968), EMT has provided an attractive potential mechanism to explain largely undefined pathological and physiological conditions such as embryogenesis, inflammation, and cancer metastasis (Radisky, 2005, Kalluri and Weinberg, 2009). As described above the EMT process encompasses loss of an epithelial-phenotype and acquisition of mesenchymal-like features which facilitate migration of transitioned cells through breached BM (Radisky, 2005, Lamouille et al., 2014). However, there is significant debate regarding a core aspect of this process which is the origin of the active myofibroblasts responsible for increased collagen production. Indeed, many studies have indicated that these cells are derived from resident fibroblast rather than being derived from the epithelium during fibrotic conditions which affect many organs including liver and kidney (Taura et al., 2016).

Notably EMT-associated fibrosis has been extensively investigated in liver and kidney tissues over recent decades. In this section, studies on EMT in these organs will be described. Liver fibrosis is the consequence of different chronic conditions such as viral hepatitis, congenital biliary atresia, and alcoholic liver disease (Bataller and Brenner, 2005). Kaimori et al. (2007) indicated that cultured hepatocytes underwent EMT following treatment with TGF-β1, and this finding was supported by data from another study which showed increased expression of FSP-1 in TGF-β1-stimulated hepatocytes (Zeisberg et al., 2007). Further, experimentally-induce liver fibrosis in a murine model demonstrated increased expression of FSP-1 (Zeisberg et al., 2007) and vimentin (Nitta et al., 2008) in hepatocytes from a cirrhotic liver. Recently these findings were challenged by results from a study which utilised lineage tracing in a transgenic mouse model whereby green fluorescent protein (GFP) expression is detected in collagen synthesising cells. Data from this study showed that the myofibroblasts were not derived from hepatocytes (Taura et al., 2010) and these findings were supported by another

study which used the same technique to track fate of cells in transgenic mice model. Furthermore, data also excluded another liver cell type, cholangiocytes, from being the source of the myofibroblasts which arise during fibrosis of the liver (Scholten et al., 2010). Further evidence which opposes the EMT premise in liver cells was provided by an *in vitro* study using primary mice hepatocytes. Although results indicated morphological changes in the cultured epithelial cells, they did not upregulate their expression of the mesenchymal markers, FSP-1 and α-SMA (Chu et al., 2011).

Several *in vitro* and *in vivo* studies have also rejected EMT as a process involved in chronic inflammatory diseases of the kidney. Indeed, results from murine models of four kidney diseases have showed inconsistent results. While EMT was induced in association with unilateral ureteral obstruction and ischemic nephropathy, a ureteral obstruction and adriamycin nephrosis model failed to show induction of EMT (Inoue et al., 2015). Cultures of MDBK cells transfected with Snail resulted in an increased nuclear localization of Snail, however, the epithelial cells maintained their phenotype and did not express any features characteristic of EMT. Notably, expression of E-cadherin, N-cadherin, and fibronectin were not changed in comparison with control despite up-regulation of other EMT-related markers such as ZEB-1 and Slug (Izawa et al., 2015). Involvement of EMT in inflammatory disease *in vivo* was started with a landmark study on kidney disease (Iwano et al., 2002) which was further supported by other clinical studies (Rastaldi et al., 2002, Simonson, 2007, Rossini et al., 2005, Hertig et al., 2006). Data implicated EMT as a potential source of fibroblast during chronic kidney conditions. Notably this concept was under intense debate due to findings from other researchers which support alternative sources of fibroblasts during kidney tissue scaring induced fibrosis in mouse model by ureteral obstruction and their findings indicated that pericytes, following vascular injury, migrated and differentiated into collagen-producing

myofibroblasts (Lin et al., 2008). Following ligation of a rat ureter, resident fibroblasts showed increased expression of αSMA which charaterise active myofibroblasts. These events were associated with increased mitotic activity at the stressed sites (Picard et al., 2008).

While the reviewed body of evidence somewhat opposes EMT there are some inconsistences in the methodologies applied such as the use of lineage tracking failing to label all cells, i.e. only 40% efficiency in some studies (Scholten et al., 2010). Potentially this may result in a considerable percentage of the cells undergoing EMT without being detected. Also, previous studies have relied on the immunostaining of a limited number of EMT-indicators which may not robustly detect EMT. Furthermore, the experimental liver-fibrosis model used in mice may not completely reflect the process which occurs humans in term of type and strength of stimuli applied. Subsequently more research is required to better understand the EMT process and its involvement in human chronic inflammatory disease pathogenesis.

3.3: Biomarkers of EMT

The induction of motile, mesenchymal-like cells from non-motile, tightly packed epithelial cells is associated with alteration in key molecular markers, such as those that mediate cell-cell and cell-BM attachment, cytoskeletal proteins, ECM molecules and transcriptional factors. Changes in expression of many of these markers have been associated with EMT induction (*Table 3*) (Zeisberg and Neilson, 2009, Scanlon et al., 2013).

3.4: Molecular events in EMT

EMT (Figure 5) is a process which is responsible for a degree of epithelial-phenotype destabilization and acquisition of mesenchymal-like cellular features that alters the migratory abilities of cells (Kalluri and Weinberg, 2009). These events can be divided into changes

affecting cell-cell junctions, the cytoskeleton and cell-ECM adhesion as well as the migration of invasive cells.

3.4.1: EMT-associated cellular junction and cytoskeleton changes

EMT is characterised by a loss of cellular adhesive junctions accompanied by major cytoskeletal reorganization associated with loss of apico-basal polarity and which can result in acquisition of invasive properties. Furthermore, this can increase resistance to apoptosis (programmed cell death), and anoikis, which is programmed cell death initiated following loss of cell attachment to the surrounding ECM (Lamouille et al., 2014). EMT is modulated by a range of regulatory pathways; mainly, downstream of TGF-β signaling activity which is evident in many developmental and pathological situations in which EMT is reported, including embryogenesis, inflammation and tumor metastasis (Vittal et al., 2013, Zhang et al., 2013b). The active form TGF-β1 is a polypeptide chain dimer, derived from a precursor following enzymatic activation. Activated TGF-β1 then binds to two pairs of serine/threonine kinases receptors which are known as the type I and type II receptors, respectively. Following TGF-β1 binding to its receptor; the signal is transduced, by intracellular transcriptional factors called Smad, to the nucleus via phosphorylation of Smad-2 and -3 which then form the Smad-4 complex. This process requires additional DNA-binding molecules that are derived from the Snail, Twist, and the basic helix-loop-helix (bHLH) transcription factor, which are the main regulators of EMT (Shi and Massagué, 2003, Massagué, 2008).

Other signaling molecules also participate in EMT activation such as phosphatidylinositol-3-kinase (PI3K), mitogen-associated protein kinase (MAPK) and Rho-like GTPases. The sum effect of all these molecules is the suppression of certain epithelial markers involved in cell attachment and apico-basal polarity, via up-regulation of transcriptional repressors including Snail, Slug, ZEB-1, and Twist (Thiery and Huang, 2005, Peinado et al., 2007a). These

molecules compromise epithelial tissue cohesiveness by binding to E-box components of the promoter of the gene encoding the AJ protein E-cadherin, subsequently histone deacetylases and other suppressing factors are recruited which enhance chromatin condensation and downregulate E-cadherin transcription (Singh and Settleman, 2010). Simultaneously, N-cadherin (also known as Cadherin-2 or CDH2, associated with mesenchymal cell adhesion), is upregulated. This overall process is called ‘cadherin switching’ and the epithelial cadherin is replaced by mesenchymal cadherin and is considered as one of the hallmark EMT features (Hazan et al., 2004). Notably, N-cadherin and E-cadherin are similar in their molecular function i.e. mediating cell-cell adhesion; however, they are expressed by different tissues. N-cadherin is expressed mainly in mesenchymal cells which lack additional epithelial junctional and polarity molecules which, together with E-cadherin, maintain epithelial integrity and phenotype (Hulpiau and Van Roy, 2009).

Category/Function	Biomarker	EMT associated changes	Reference
Cell-cell attachment molecules	E-cadherin	Downregulated	(Peinado et al., 2004, Kalluri and Weinberg, 2009)
	ZO-1, Occludins, Claudins	Downregulated	(Ikenouchi et al., 2003, Polette et al., 2007)
	Desmoplakin, plakoglobin	Downregulated	(Savagner et al., 1997)
	N-cadherin	Upregulated	(Jiang et al., 2016)
Cytoskeletal molecules	β-catenin	Downregulated	(Medici et al., 2008, Yan et al., 2012)
	Cytokeratins	Downregulated	(Savagner, 2010, Serrano et al., 2014)
	α-Smooth muscle actin	Upregulated	(Ding et al., 2014)
	Vimentin	Upregulated	(Mendez et al., 2010)
	FSP-1	Upregulated	(Okada et al., 1997)
Transcriptional factors	Snail	Upregulated	(Medici et al., 2008, Lamouille et al., 2014)
	Slug (Snail-2)		
	Twist	Upregulated	(Eckert et al., 2011)
	LEF-1	Upregulated	(Kim et al., 2002)
	ZEB-1	Upregulated	(Takkunen et al., 2006)
	NF-κB	Upregulated	(Huber et al., 2004, Maier et al., 2010)
ECM proteins	Collagen I	Upregulated	(Shintani et al., 2008)
	Collagen III		
	Collagen IV	Downregulated	(Song et al., 2000)
	Fibronectin	Upregulated	(Sume et al., 2010)
	Laminin	Downregulated	(Kantarci et al., 2011)
Cell-BM attachment proteins	Integrin α6β4	Downregulated	(Lamouille et al., 2014)
	Integrin α5β1	Upregulated	(Li et al., 2003, Maschler et al., 2005)
	Integrin αVβ6		
Proteolytic enzymes	MMP-9	Upregulated	(Cheng and Lovett, 2003, Sume et al., 2010)
	MMP-2		
	MMP-3		

Table 3. Molecular Indicators/Markers expressed during EMT demonstrating changes in attachment, cytoskeletal, and ECM proteins in addition to increased activity of certain transcriptional factors and proteolytic enzymes.

Furthermore; EMT is associated with loss and/or reorganization of other epithelial markers, indeed cytoskeletal cytokeratins, which also interfere with E-cadherin expression and form together the cell-anchorage apparatus. This loss of keratin expression is considered an important EMT indicator (Lorenz et al., 2015). Beside E-cadherin, the expression of other junctional attachment proteins, such as occludin, claudin, and ZO-1, are repressed during EMT. Claudins and occludin, tight-junction associated protein, are reportedly downregulated in cultured epithelial cells (Ikenouchi et al., 2003) and this is regulated by Snail which binds to the E-box of the gene promoter and represses transcription in a similar manner to E-cadherin down-regulation (Ikenouchi et al., 2003). Following loss of cellular cohesiveness, subsequent EMT events are triggered in a chain reaction leading to epithelial-phenotype destabilization. Cell polarity is modulated by the number of molecules including Scribble complexes (SCRIB), Discs large (DLG), and partitioning-defective (PAR) complexes, in addition to Crumbs complexes (CRB) which are associated with TJs and determine the cell's apical compartment. Therefore, repression of attachment proteins subsequently disturbs polarity complex molecules expression and results in further loss of epithelial features (Lamouille et al., 2014). Increased resistance to apoptosis is also evident at this stage of EMT and this is mainly attributed to the activation of MAPK signaling downstream induced by TGF-β (Mulholland et al., 2012, Pickup et al., 2013). Consequently, disintegration of the cell-cell junctions allows the newly developed mesenchymal-like cells to migrate to the underlying CT.

3.4.2: Loss of Cell-ECM adhesion and acquisition of migratory-phenotype

This step requires degradation of BM due to proteolytic activity of matrix metalloproteinases (MMPs), in addition to structural modification due to actin cytoskeletal reorganization which is modulated via up-regulation of vimentin expression (Bourboulia and Stetler-Stevenson, 2010). Cell movement generally is achieved by forward extension of the plasma membrane by forming specialised cellular structures including blebs, filopodia, lamellipodia, and invadopodia. These

protrusions from the cell body uniquely participate in cell migration under specific conditions. Filopodia are consider as probing or exploratory tools for the cell to enable sensing of the surrounding environment while lamellipodia contribute to propelling the cell through the tissue as they can extend further than filopodia into the ECM. These functional specialisations are characterised by differences in actin arrangement; while actin filaments are arranged in a parallel pattern in filopodia, lamellipodia contain an actin mesh which forms highly active regions that facilitate forward protrusion of the plasma membrane.

Presence of both filopodia and lamellipodia, have been proposed as an EMT-phenotype characteristic of metastatic cancer cells (Ridley, 2011, Chen et al., 2013b). Invadopodia are a specialised form of lamellipodia in which actin polymerization is associated with secretion of MMPs e.g. MMP-2, and -9, thereby facilitating cell invasion through the tissue via local degradation of the ECM (Buccione et al., 2009). In addition, it has been shown that the activity of invadopodia are centrally regulated by Twist following exposure of epithelial cell lines to different EMT stimuli (Eckert et al., 2011). A recent study on human colorectal carcinoma samples showed that proteins associated with increased invadopodia activity, including Abelson interactor 1 and Cortactin, were upregulated together with down-regulation of E-cadherin expression (Steinestel et al., 2014). EMT-induced actin cytoskeletal rearrangement, a prerequisite for cellular projections formation, is understood to be mainly modulated by TGF-β signaling. Downstream signaling is regulated by small GTPases (including Rho, Rac and Cdc42) which mediate remodeling of the actin cytoskeleton in epithelial cells in different pathological and physiological conditions involving tubular, endothelial, and epithelial retinal cells (Kardassis et al., 2009). Furthermore, the migratory-phenotype is associated with up-regulation of vimentin which is essential for the process of cellular protrusion formation. This process starts with the assembly of actin networks that mature by inclusion of vimentin and microtubules filaments (Schoumacher et al., 2010).

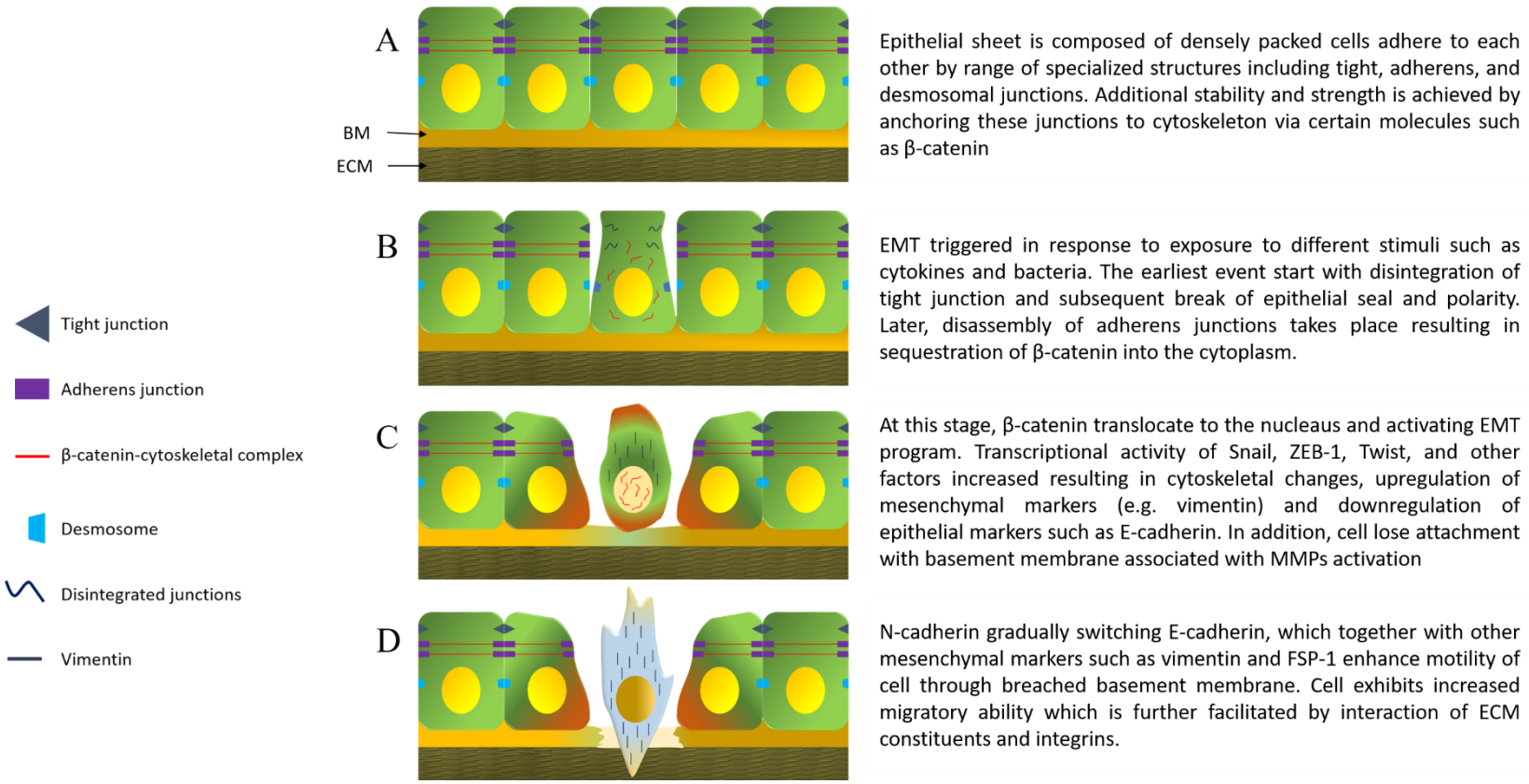

Figure 5. Molecular and cellular events of EMT. This process starts when intact epithelial layer (A) exposed to certain stimuli such as cytokines or bacteria (B) potentially responsible for EMT-induction. At earlier stages (C) adhesion of epithelial cells is lost due to down-regulation of essential attachment proteins such as E-cadherin followed by loss of BM integrity. Finally, cells acquire mesenchymal-like properties, including increased expression of vimentin and FSP-1 that facilitates their migration and invasion (D).

The EMT process is further propagated and sustained by release of MMPs, such as MMP-9, which facilitate the invasion and migration of cells through the breached BM. In addition, TGF-β released from ECM further drives the progression of EMT (Lin et al., 2011, Shah et al., 2012). Cooperation between EMT and MMPs has been demonstrated in mouse xenograft models of human gastric cancer, which showed that up-regulation of MMP-9 activity together with the EMT-phenotype increased the incidence of lung metastasis (Yoo et al., 2011). Other findings indicated that up-regulation of vimentin and the transcriptional factor, ZEB-1, were associated with poorly-differentiated and highly invasive breast cancer (Karihtala et al., 2013). Changes in the level of MMP-mediated EMT are also associated with alterations in integrin expression by the replacement of epithelial integrin with mesenchymal ones. For example, during EMT epithelial integrin α6β4 is downregulated whiles concomitantly there is up-regulation of mesenchymal integrin α5β1 which increases the tendency of cells to adhere to fibronectin in the ECM. Furthermore, alteration of integrin expression itself triggers EMT via activating signaling pathways including TGF-β, Smad, and integrin-linked kinase (ILK) (Kim et al., 2009).

The exact time-course for complete EMT-phenotype expression remain controversial (Picard et al., 2008, Inoue et al., 2015, Izawa et al., 2015) as different *in vivo* and *in vitro* studies suggested variable timelines ranging from one day to eight days (Chinnery et al., 2012, Choi and Diehl, 2009, Tanaka et al., 2010, Chu et al., 2011).

3.5: Types of EMT

The concept of increased tissue size resulting from cell proliferation was first described approximately a century and a half ago (Virchow, 1871). In this concept, all cells in the body were derived from continuous division of a single fertilised egg. From the middle of the 20th century, cell plasticity was recognized as occurring during embryogenesis when the cell phenotype alternates between epithelial-like and mesenchymal-like as potential consequences of EMT and MET (Hay,

1968). Differentiation is necessary for each cell type to perform its specific functions. This led to the understanding that phenotype maintenance after development is absolute and essential for cells to undertake their specific roles and functions (Kalluri and Weinberg, 2009). However, this concept was challenged due to observations from several studies, indeed in the early 1980s, it was claimed that even fully differentiated epithelium may dedifferentiate into a mesenchymal-like phenotype via triggering of *in vitro* EMT (Greenburg and Hay, 1982, Stoker and Perryman, 1985). It was proposed that this occurred as a function of the tissue repair mechanism (e.g. wound healing) and in pathological conditions including persistent inflammation and cancer. In general, EMT has been classified as 'complete EMT' in which all classical features of transition take place and 'partial EMT' is characterised by simultaneous expression of both mesenchymal and epithelial markers. Notably the latter type has mostly been associated with tissue healing (Savagner, 2010). EMT is now potentially implicated in three distinct situations including embryogenesis, post-injury tissue fibrosis and cancer metastasis. This classification of EMT into three distinct subtypes (Figure 6) was proposed following an expert panel meeting on EMT in Poland in 2007, and followed by a further meeting in Cold Spring Harbor Laboratories in 2008 (Zeisberg and Neilson, 2009).

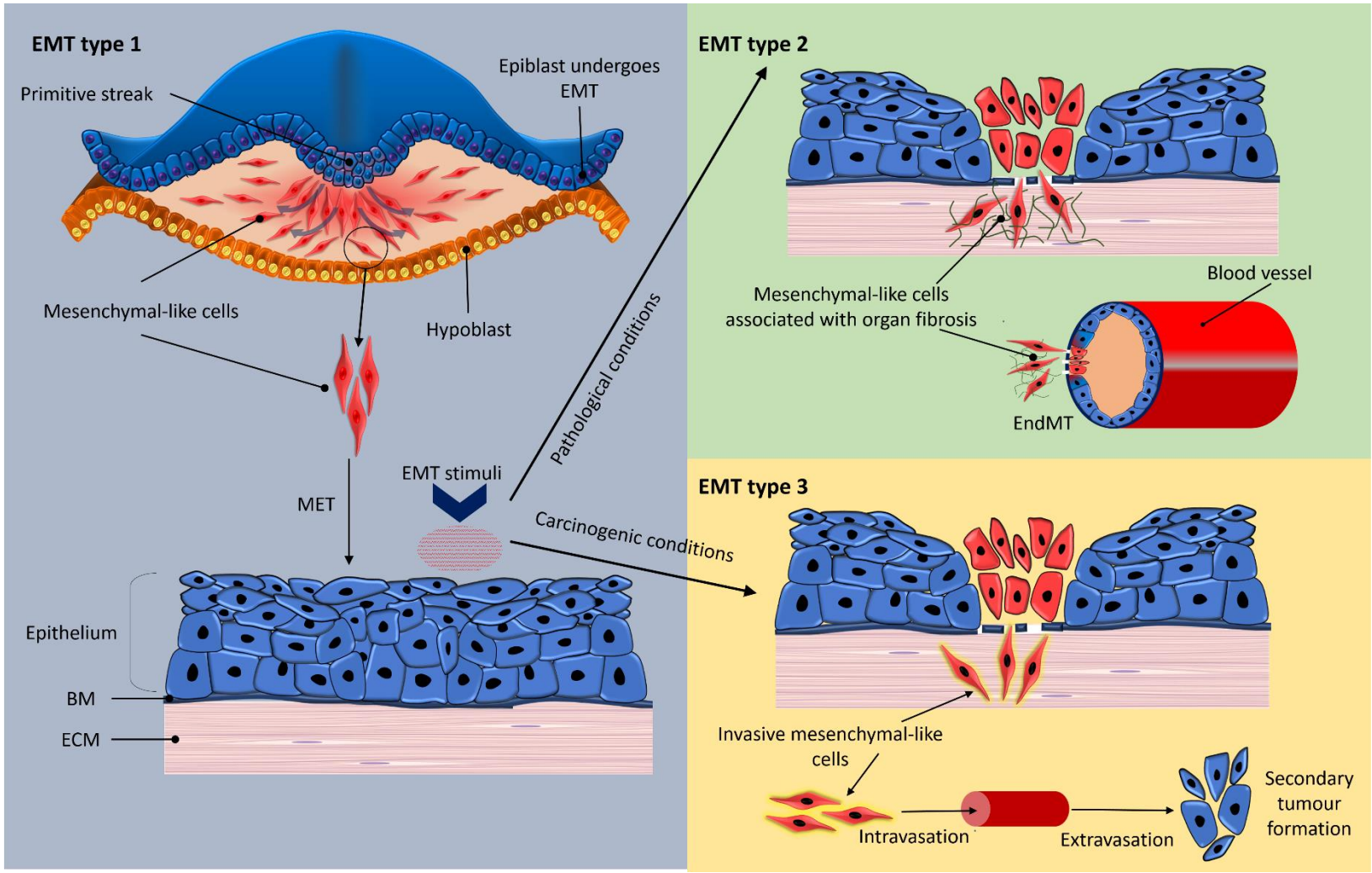

Figure 6. Types of EMT and the cellular processes involved. Type 1 is associated with gastrulation and embryogenesis, and types 2 and 3 are associated with fibrosis and cancer metastasis respectively.

3.5.1: Type 1 EMT

This type of EMT occurs during embryogenesis and is therefore not related to the potential role for EMT in chronic inflammatory diseases, such as periodontitis, however it will be briefly discussed here for completeness.

Type 1 EMT is considered as a potential physiological process necessary for implantation of the embryo and the subsequent transition into a three-layered structure via gastrulation. Gastrulation begins with the formation of the primitive streak which is formed by development of an invagination in the middle of epiblast that is located in the lower region of the developing embryo, and extends antero-posteriorly between the epiblast and hypoblast layer (Thiery and Sleeman, 2006). Cells of the primitive streak at this stage have an epithelial-like phenotype, expressing markers such as E-cadherin and displaying apico-basal polarity, from which cells implicated in gastrulation and development of germ layers originate (Mikawa et al., 2004). Following the formation of the primitive streak, activation of the EMT process takes place leading to the generation of the mesendoderm from which the mesoderm and ectoderm are subsequently derived (Hay, 1995). It has been proposed that the organogenesis of vital structures and organs (including muscles, heart, nervous system, and palate) requires the initiation of type 1 EMT (Hay and Zuk, 1995). The newly formed mesoderm layer acts as a source for the primary mesenchyme, potentially derived by EMT, and this shows increased migratory ability compared with the parental epithelial cells, i.e. epiblast and hypoblast (Hay, 2005). The increased migratory ability facilitates translocation of the embryonic mesenchymal cells to more distant sites where they undergo MET; forming secondary epithelia that further transition by subsequent EMT into different CT cells (Kalluri and Weinberg, 2009). A sub-division or modification of type 1 EMT which is called endothelial-mesenchymal transition (EndMT) has also been proposed. This unique EMT type is thought to induce transition of endothelial cells into mesenchymal-like cells, potentially responsible

for the formation of heart valves at later stages of development (Kalluri and Weinberg, 2009). Data from a study on mouse embryos suggested that EMT occurring during embryogenesis is regulated by several factors including Wnt signaling. Indeed, defective Wnt expression during gastrulation results in abnormal morphology of the embryo due to failure of EMT induction (Popperl et al., 1997, Thomas et al., 1997). The role of Wnt signaling in EMT was further confirmed by a study on chick embryos which demonstrated that blocking Wnt8 signaling was associated with failure of primitive streak formation (Skromne and Stern, 2001). Similar results were reported in association with Wnt3 signaling in mice (Liu et al., 1999). Several studies also demonstrated that Wnt signaling is mediated by members of the transforming growth factor-β (TGF-β) superfamily, including Nodal and Vg1 and their deficiency can result in EMT failure and in morphological consequences such as asymmetry of the embryo (Skromne and Stern, 2002, Chea et al., 2005). Furthermore, the role of Snail in EMT triggering was demonstrated as a major suppressor of E-cadherin expression. Snail exerts its activity via interaction with the E-cadherin promoter region thereby affecting E-cadherin-mediated cell attachment (Peinado et al., 2004, Peinado et al., 2007). In addition, Snail may induce EMT by blocking the transcription of occludins and claudins, the structural proteins of TJs, by direct binding to their promoter motifs (Ikenouchi et al., 2003). Other studies have demonstrated that Snail not only promotes EMT via repressing molecules mediating cell attachment but also through suppressing genes regulating epithelial cell polarity and maintaining architecture of the tissue such as human Disc large (DLG1) (Cavatorta et al., 2008), and the Crumbs complex (Whiteman et al., 2008).

3.5.2: Type 2 EMT

Chronic inflammation is reportedly a potent type 2 EMT inducer which is understood to be responsible for the loss of epithelial barrier integrity and organ dysfunction (Kalluri and Weinberg, 2009). Persistent and chronic inflammation results in increased production of inflammatory

cytokines and chemokines such as TGF-β1 and interleukins (ILs) which are considered as the main drivers for type 2 EMT (Wynn, 2008). Early evidence of type 2 EMT was generated from studies utilizing tubular epithelial cells from human tissue samples and murine models. Results indicated that the up-regulation of certain mesenchymal markers including α-SMA, FSP-1 and vimentin associated with increased expression of TGF-β1 and EGF (Okada et al., 1997, Strutz et al., 1995, Rastaldi et al., 2002). Similar changes were observed *in vivo* and *in vitro* in diseases, involving organs such as the liver (Corpechot et al., 2002, Yamaoka et al., 1993, Scharl et al., 2015) and in the biliary tract (Zhou et al., 2010, Omenetti et al., 2008). Additionally, EMT could result in an imbalance in collagen turnover by dysregulating production of MMPs and tissue inhibitors of metalloproteinases (TIMPs). Associated events lead to up-regulation of collagen synthesis and deposition causing scarring of the damaged area instead of normal wound healing (Wynn, 2008). While inflammation is a normal tissue defense mechanism associated with secretion of range of inflammatory cytokines and chemokines the aberrant regulation of these inflammatory mediators, in certain situations, are reported to be implicated in EMT induction (Corpechot et al., 2002, López-Novoa and Nieto, 2009, Zeisberg et al., 2007, Zhou et al., 2010, Sume et al., 2010).

A role for EMT in pathogenesis of many diseases has been proposed with studies investigating EMT in a range of organs including liver (Choi and Diehl, 2009, Wells, 2010), intestine (Flier et al., 2010), kidney (Iwano et al., 2002), and lung (Willis and Borok, 2007). The proposed involvement of type 2 EMT in disease processes in various organs are summarised in Table 4.

Cell type or tissue examined	Study type	Changes in EMT-related indicators and features			References
		Upregulated	Downregulated	Other features	
Tubular epithelial cells stimulated with FGF-2 with TGF-β1 and EGF	*In vitro*	FSP-1, collagen I, MMPs, and α-SMA	E-cadherin, collagen IV, and cytokeratin	increased migratory ability	(Strutz et al., 2002)
CC cell line co-cultured with activated macrophages	*In vitro*	FSP-1 and MMP-9	E-cadherin and cytokeratin 19		(Techasen et al., 2012)
Mouse hepatocytes induced by TGF-β1	*In vitro*	Snail and collagen I			(Kaimori et al., 2007)
human primary cholangiocytes treated with TGF-β1	*In vitro*	Vimentin, FSP-1, and MMP-2	E-cadherin, cytokeratins		(Rygiel et al., 2008)
Biopsies from HCV-infected liver and hepatocytes infected with HCV	*In vivo* and *in vitro*	FSP-1, Snail, Slug, Twist and vimentin	E-cadherin and β-catenin	morphology alteration *in vitro*	(Bose et al., 2012)
Mouse model of CD and small intestinal cell line (IEC-6) stimulated with TGF- β1	*In vitro* and experimental model	FSP-1	E-cadherin		(Flier et al., 2010)
CD-associated fibrosis samples	*In vivo*	TGF-β1 and Snail-2	E-cadherin and β-catenin		(Scharl et al., 2015)
Mouse cardiac fibrosis model and human coronary endothelial cells	*In vitro* and experimental model	FSP-1 and TGF-β1		Cells showed increased resistant to apoptosis	(Zeisberg et al., 2007)
Human umbilical vein endothelial cells and aortic endothelial cells treated with glucose	*In vitro*	FSP-1	VE-cadherin		(Widyantoro et al., 2010)
Human intrahepatic biliary epithelial cells stimulated with LPS	*In vitro*	S100A4, α-SMA, TGF-β1,	E-cadherin		(Zhao et al., 2011)

Cholangiocarcinoma (CC), hepatic stellate cells (HSCs), hepatitis C virus (HCV), ulcerative colitis (UC), Crohn's disease (CD), vascular endothelial cadherin (VE-cadherin)

Table 4. Summary of selected studies on type 2 EMT in different models showing changes in expression of key-EMT indicators.

3.5.3: Type 3 EMT

Malignancy is characterised by uncontrolled cell proliferation, evasion of apoptosis and sustained angiogenesis of the supporting stroma; which contribute to tumour growth and progression (Hanahan and Weinberg, 2000, Kaufhold and Bonavida, 2014). Cancerous cells can acquire invasive capabilities, enabling them to migrate into the underlying CT through the BM. Indeed, epithelial cells account for ~80% of human cancers (Van Roy and Berx, 2008). Additionally, an increased number of invasive malignant cells are associated with failure of E- cadherin expression or deficiency to form the E-cadherin-catenin complex (Huber et al., 1996, Bullions and Levine, 1998). Investigators have proposed that EMT induction in epithelial cancer cells could provide a potential mechanism allowing cells to invade locally and to spread to distant locations (metastasis) (Thiery, 2002). Reports from studies utilizing mouse models and a cancer cell line have shown that epithelial cancer cells acquired a mesenchymal-like phenotype characterised by increased expression of mesenchymal molecules such as vimentin, FSP-1, and α-SMA as well as a down-regulation of epithelial markers such as E-cadherin and β-catenin (Yang and Weinberg, 2008). The potential role of EMT in cancer metastasis is supported by findings from several different *in vivo* and *in vitro* studies as highlighted below (Table 5).

4: EMT-associated cytokines

Cytokines are a broad group of cell signaling small molecular weight proteins which are secreted by a wide range of cells including immune cells, endothelial cells, epithelial cells and fibroblasts (Chen et al., 2013a). They affect cell behavior either of the cell producing them (autocrine signaling) or in other cells (paracrine signaling) (Cheng and Lovett, 2003, Cherng et al., 2008). The cytokines most relevant to this study will be discussed in the following sections.

Cell type or tissue studied	**Study type**	**Changes in EMT-related indicators and features**			**References**
		Upregulated	**Downregulated**	**Other features**	
Human RCC cell line and human RCC biopsies	*In vitro* and *in vivo*	Vimentin *in vivo*. In addition to MMP-9 *in vitro*	E-cadherin *in vivo* and *in vitro*	Migration rate increased *in vitro*	(Ho et al., 2012)
Localised RCC	*in vivo*	Twist and clustrin			(Harada et al., 2012)
Epithelial OC cell line (A4)	*In vitro*	Snail and Slug		Increased resistant to apoptosis	(Kurrey et al., 2009)
CRC cell line (HT-29)	*In vitro*	N-cadherin	E-cadherin and ZO-1	increased mobility of the cells	(Wang et al., 2013)
GC biopsies infested with *H. pylori* and GC cell line stimulated with Cytotoxin-associated gene A (CagA)	*In vitro* and *in vivo*	Twist and vimentin	E-cadherin and programmed cell death factor 4 (PDCD4)	increased migratory ability *in vitro*	(Yu et al., 2014)
Human BC cell lines (MCF7, MDA-MB-231, MDA-MB-468, and MCF-10A)	*In vitro*	Vimentin and fibronectin	β-catenin, E-cadherin and occludin	migratory ability increased	(Yan et al., 2012)
Human BC cell lines	*In vitro*	Twist, and FOX	β-catenin		(Siletz et al., 2013)

RCC= Renal cell carcinoma, OC= Ovarian cancer, CRC = colorectal carcinoma, Gastric cancer= GC, Breast cancer= (BC)

Table 5. Summary of selected studies on type 3 EMT in different models showing changes in expression of key-EMT indicators.

4.1: Transforming growth factor-β1

It is a ubiquitous polypeptide member of TGFβ superfamily which comprises activins, inhibins, bone morphogenic protein and mullarian inhibiting substance (Lawrence, 1996). They are multifunctional cytokines involved in a wide range of cellular processes including differentiation, apoptosis, and proliferation (Kubiczkova et al., 2012). Structurally, TGFβ is a polypeptide which is a disulphide-linked homodimer with two chains, each one consisting of 112 amino acids (Lawrence, 1996). There are 5 different isoforms of TGFβ; however, only 3 are recognized as effecting cellular activity (Kubiczkova et al., 2012).

TGFβ-signaling is well-known as a potent EMT-stimulus (Zavadil and Böttinger, 2005, Xu et al., 2009). In response to TGFβ, transmembrane serine-threonine kinase receptors activated and subsequently trigger the downstream of Smad-signaling pathway which is potentially associated with an EMT-phenotype (Feng and Derynck, 2005). In addition, TGFβ could activate EMT through a non-Smad dependent pathway (Zhang et al., 2009). The hallmark of TGFβ signaling is up-regulation of Snail, an E-cadherin repressor, (Jamora et al., 2004) in addition to other cytokines potentially involved in EMT triggering such as fibroblast growth factor (FGF) (Barrallo-Gimeno and Nieto, 2005) and hepatocyte growth factor (Grotegut et al., 2006). The role of TGFβ-mediated EMT in different pathological and developmental conditions have been widely investigated including the *in vitro* effects on different cell lines (Kaimori et al., 2007, Rygiel et al., 2008, Taura et al., 2010, Chu et al., 2011, Zhao et al., 2011), during embryogenesis (Romano and Runyan, 2000, Martínez-Álvarez et al., 2004), pathological fibrosis (Yáñez-Mó et al., 2003) and drug-induced gingival overgrowth (Sume et al., 2010, Pisoschi et al., 2012).

4.2: Tumour necrosis factor-α

TNF-α was originally described in the mid-1970s as a circulating protein that caused death of cancerous cells (Carswell et al., 1975). Later, it was recognized as a key regulator of the acute

phase reaction during inflammation (Barrallo-Gimeno and Nieto, 2005). It is predominantly produced by activated macrophages but it is also produced by other cell types including endothelial cells and keratinocytes (Bradley, 2008). Soluble TNF-α is produced by proteolytic cleavage of its transmembrane precursor (Tang et al., 1996). Although TNF-α has anti-tumorigenic properties at relatively high concentrations it has been proposed that it may promote cancer cell proliferation and metastasis when chronically released at relatively low concentrations (Szlosarek et al., 2006). The presence of TNF-α in breast, ovary and pancreas tumours has been suggested as a marker of poor prognosis (Balkwill, 2006, Balkwill, 2009).

There are two types of receptors for this molecule, TNFR1 and TNFR2, and three main signaling pathways which can be activated by TNF-α, namely nuclear factor kappa-light-chain-enhancer of activated B cells (NF-κB), MAPK and apoptosis. The latter process is mostly masked by the anti-apoptotic effect of NF-κB (Chen and Goeddel, 2002, Wajant et al., 2003). NF-κB is a key pro-inflammatory transcription factor that has been shown to be activated in periodontal lesions (Coons et al., 1941) and in response to exposure to periodontal pathogens *in vitro* (Milward et al., 2007). In addition, some studies have proposed a central role of NF-κB in EMT-induction (Huber et al., 2004, Maier et al., 2010). These pathways are well-recognized during an inflammatory response, cell differentiation and EMT activation (Huber et al., 2004, Maier et al., 2010, Huang et al., 2015). Similar to TGFβ, exposure of different types of cell lines to TNF-α *in vitro* may stimulate the EMT process (Okada et al., 1997, Ekhlassi et al., 2008, Yan et al., 2010, Chu et al., 2011, Li et al., 2012a). Furthermore, TNF-α can synergistically act with TGFβ-1, mediated by p38 MAPK activity, to promote an invasive cell phenotype as has been demonstrated in samples of human colon carcinoma (Bates and Mercurio, 2003).

4.3: Epidermal growth factor

Epidermal growth factor is a low-molecular weight polypeptide involved in cell differentiation, proliferation, and survival. It was first discovered in saliva from the submandibular gland (Carpenter and Cohen, 1990). This growth factor exerts its biological activity through interaction with a specific cell surface receptor, the epidermal growth factor receptor, which initiates a cascade of signals mediated by tyrosine kinases (Fallon et al., 1984, Dawson et al., 2005).

EGF functions primarily in maintaining tissue integrity of the gastro-intestinal tract against various chemical and physical injuries (Yanaka et al., 2002). However, evidence from several studies suggests that it may contribute to disruption of the epithelial barrier integrity (Okada et al., 1997, Strutz et al., 2002, Gilles et al., 1999). Analysis of data following exposure of a breast cancer cell line to EGF showed down-regulation of E-cadherin, β-catenin, and collagen IV and an associated increased expression of vimentin and collagen I (Ackland et al., 2003). In addition, increased expression of EGFR in renal cell carcinomas resulted in increased resistance to chemotherapy via triggering of EMT as determined by EMT-related protein expression and signaling pathways in three renal cell carcinoma cell lines (Mizumoto et al., 2015). EGF-mediated EMT features can be facilitated by synergistic effect of TGFβ that increase cell surface expression of EGFR resulting in more aggressive and invasive breast cancer (Wendt et al., 2010).

In general, limited research has investigated the possible implication of EGF in EMT-induction; however, data from previously described studies support its role in cell-phenotype alteration.

5: Potential role of bacteria in EMT

Organ fibrosis and dysfunction is the outcome of persistent non-resolving chronic inflammation which can be induced by a range of physical, chemical, and bacterial stimuli. Persistent inflammation is a well-known predisposing factor for EMT (Kalluri and Weinberg, 2009) and bacterial associated infections have been implicated in EMT induction (Hofman and Vouret-Craviari, 2012). Prior to triggering signaling pathways, microbes must be recognized by the cell to be appropriately managed by the immune system. The first proposed cell microbe-recognition mechanism was described by Jenaway (1989) who demonstrated the recognition of certain conserved molecules associated with each microbial class, such as lipopolysaccharide (LPS), bacterial DNA and flagellin, referred as pathogen- associated molecular patterns (PAMPs). Each cell expresses surface proteins known as pathogen recognition receptors (PRRs) which are responsible for inducing an innate immune response following PAMP recognition (Janeway, 1989). This discovery was supported by the identification of the Toll transmembrane receptor following injection of bacteria into *Drosophila* which stimulated antimicrobial gene expression such as cecropins, insect defensin, antifungal peptide and drosomycin (Lemaitre et al., 1996). Later studies undertaken in mice, identified Toll-like receptor (TLR) 4 as the protein involved in LPS identification and transduction, suggesting the existence of a relationship between a microbial motif, LPS, and TLR4 (Poltorak et al., 1998). Currently 11 human TLRs have been identified with each one recognising specific PAMPs (e.g. lipopeptides, LPS, and lipoteichoic acid) which are associated with the pathogenesis of a variety of inflammatory conditions (Mahla et al., 2013). TLRs can be activated by different types of ligands including peptides from bacterial fimbriae, Lipoteichoic acid, and LPS (Schröder et al., 2003, Gillrie et al., 2010), LPS and bacterial DNA (bDNA) (Tabeta et al., 2000, Hemmi et al., 2000, Ren et al., 2005, Chinnery et al., 2012).

The role of bacteria, particularly Gram-negative anaerobic bacteria, in triggering EMT has been investigated in many studies. *Helicobacter pylori* (*H. pylori*), previously known as *Campylobacter pylori*, is a Gram-negative, microaerophilic bacterium mostly found in the stomach is associated with the loss of epithelial integrity of the gastric mucosa (Blaser, 2006). Furthermore, injection of *H. pylori*-associated protein, CagA, into gastric epithelial cells resulted in the disruption of epithelial barrier function. This bacterium acts mainly by downregulating ZO1-mediated TJ causing dissociation of cell-cell attachment and loss of the apical seal thereby facilitating invasion to underlying tissues. Persistent exposure of gastric epithelium to *H. pylori* resulted in morphological indicative of mesenchymal-like cells associated with loss of apico-basal polarity (Amieva et al., 2003). In addition, transfection of MDCK cells *in vitro* with CagA resulted in acquisition of an invasive-phenotype characterised by an increased migratory rate and spindle shaped cells together with up-regulation of MMP activity and loss of cell polarity (Bagnoli et al., 2005). Challenging human gastric epithelial cells with CagPAI+ H. pylori also upregulated transcriptional factor ZEB-1 through activation of the NF-κB signaling pathway which triggered EMT-like features (Baud et al., 2013).

Consequently, the potential role of different bacteria or their virulence factors in EMT has been investigated in several studies. Examples include the contribution of *P. aeruginosa*, a Gram-negative bacterium, infection in obliterative bronchiolitis following lung transplant (Borthwick et al., 2011). The collected primary bronchial epithelial cells from lung transplant recipients were exposed to *P. aeruginosa* or *P. aeruginosa*-activated monocytes (THP-1). They found that *P. aeruginosa* caused increased levels of inflammatory cytokines, IL-8, IL-1β, and TNF-α due to activation of TLR signaling. There was also significant E-cadherin down-regulation, associated with increased vimentin and fibronectin expression. Moreover, cells co-cultured with activated THP-1 exhibited a mesenchymal-like phenotype and this was

suggested to be due to activation of a TGF-β1-induced EMT. Further evidence was provided by two distinct bacteria, *Streptococcus pneumoniae* and *Haemophillus influenza*, which are present as part of the normal nasal flora but can cause opportunistic infections, and were studied in a murine model. Colonization of the nasal epithelium with these bacteria caused dramatic down-regulation of claudins which was mediated by a TLR-dependent mechanism. The associated compromised epithelial integrity enabled invasion of these bacteria through the epithelium. In addition, findings obtained from an *in vitro* model of primary human bronchial epithelial cells demonstrated a similar pattern with claudin down-regulation following increased expression of Snail, which required activation of p38 MAPK/ TGF-β signaling (Clarke et al., 2011). Similar results were obtained in infections of the upper respiratory tract by the same bacteria in a mouse model, which indicated a TLR-dependent response of the immune system in respiratory epithelium (Beisswenger et al., 2009).

A further example of bacteria inducing EMT-like features is provided by *Citrobacter rodentium* (*C. rodentium*), a Gram-negative enteric bacterium, which is opportunistic bacteria which rarely cause disease in humans; however, in mice it is responsible for transmissible murine colonic hyperplasia which is associated with a high mortality rate (Schauer et al., 1995). Subsequently, mice were experimentally infected with *C. rodentium* for 12 days following and the colonic cryptic cells were collected and cultured. Immunohistochemical analysis showed the presence of cells exhibiting a mesenchymal-phenotype as characterised by a positive expression of fibronectin and vimentin associated with negative staining for key epithelial markers such as E-cadherin and cytokeratins. Furthermore, cells stimulated with *C. rodentium* demonstrated increased activation of the NF-κB, TGF-β, Wnt/β-catenin, and Notch signaling pathways *in vivo* (Chandrakesan et al., 2012). LPS (also known as endotoxin) is the main virulence factor of Gram-negative bacteria and can elicit a strong immune response which is potentially involved in inducing EMT. Indeed, data have

demonstrated that exposure of human intrahepatic biliary epithelial cells to LPS triggered TGF-β1-induced-EMT as shown by decreased E-cadherin expression and increased transcription of S100A4 and α-SMA. In addition, the classical cobblestone epithelial cell morphology changed into a fibroblast-like appearance. Notably the knock-out of Smad 2/3 resulted in abolishing TGF-β1 signaling and reversal of LPS- induced EMT (Zhao et al., 2011). Further *in vitro* and *in vivo* studies utilised 4 hepatocellular carcinoma cell (HCC) lines and a mouse model. Results indicated that EMT induction occurred in response to LPS-TLR4 mediated NF-κB signaling activation. EMT features were confirmed by increased transcription of mesenchymal molecules (including N-cadherin, vimentin and α-SMA) and down-regulation of epithelial markers (including E-cadherin and β-catenin), in addition, cells demonstrated an increased migratory phenotype. The blocking of NF-κB resulted in the down-regulation of Snail activity associated with EMT suppression (Jing et al., 2012b). Consistent with these findings, intranasal inoculation of mice with LPS resulted in increased Snail activity and subsequent down-regulation of claudins, components of tight junctions, breaking the apical epithelial seal via activation of TLR-4 *in vivo* (Clarke et al., 2011).

Recently the effect of two distinct periodontal pathogens, *F. nucleatum* and *P. gingivalis*, on oral epithelial cells responses has been studied by Milward et al. (2007) using the H400 keratinocyte cell line which expressed TLR-2, -4, and -9, to investigate the molecular changes following bacterial exposure. Data demonstrated that there was subsequently increased NF-κB nuclear translocation associated with increased transcription of the cytokines TNF-α, IL-1β, IL-8, MCP-1/CCL2 and GM-CSF. Those results also indicated a greater magnitude of molecular changes occurred at 24hr exposure to *F. nucleatum* than *P. gingivalis in vitro* as compared to unstimulated controls. Notably however the EMT phenotype of these cells was not characterised in these or longer term cultures.

Kondo et al. (2012) investigated the role of another bacterial component, flagellin, the structural unit of bacterial flagella, in inducing EMT in lung epithelial cells. Flagellin-exposed cells showed increased activation of NF-κB and p38/ MAPK pathways which correlated with TGF-β1 signaling and subsequently resulted in the up-regulation of fibronectin and down-regulation of E-cadherin within 30hr of exposure. These data indicate that flagellin induced EMT via reacting with TLR-5 on alveolar cells and this may contribute to the pathogenesis of pulmonary fibrosis (Kondo et al., 2012).

Combined, data from these studies provide evidence that microbial challenge, particularly by Gram-negative anaerobic bacteria, triggers EMT either directly or indirectly (autocrine signaling) by binding to TLRs. Gram-negative anaerobic pathogens are strongly associated with periodontitis and this could have implications for EMT-activation in the periodontium and may indicate a novel mechanism which contributes to the pathogenesis of chronic periodontitis.

6: Periodontitis

6.1: Definition, prevalence and systemic disease-association

Periodontitis is a multifactorial, chronic inflammatory condition affecting the tooth's supporting tissues and is characterised by a progressive loss of attachment and resorption of alveolar bone (Matthews et al., 2001, Armitage, 1999). If not correctly managed in its early stages, disease progression may lead to tooth mobility and subsequent to tooth loss (Martin et al., 2010). Data collected by the UK Adult Dental Health Survey undertaken in 2009-2010 (including England, Wales, and Northern Ireland), indicated that the overall prevalence of periodontitis was ~45% of the adult population, with severe disease affecting approximately 9% of the population. Data from recent surveys suggest that there has been an increase in the severe form of periodontitis from 6% to 9% over the last decade. Although oral hygiene has

generally improved, a proportion of people included in the study suffered from poor oral hygiene and this was related to factors such as age and low socioeconomic groups (White et al., 2012).

Over recent years there has been considerable interest in the links between periodontitis and a range of systemic diseases and conditions including diabetes, cardiovascular disease (CVD), pregnancy, and rheumatoid arthritis. Notably Type 2 diabetic patients are at 3-fold higher risk of developing periodontitis when compared with healthy individuals (Mealey and Oates, 2006). The exact mechanism underpinning this association remains unclear, however both diseases are associated with a hyper-inflammatory phenotype, underpinned by the effects of hyperglycaemia which induces signaling pathways associated with increased inflammation and oxidative stress (Brownlee, 2005). Recent epidemiological studies indicated that diabetes mellitus (DM) is a risk factor for periodontitis and inflammation associated with periodontal disease and has a negative impact on the glycaemic state (Preshaw et al., 2012). Data from several studies indicated a higher prevalence and increased number of complications of DM in patients with periodontitis than periodontitis-free controls (Amar and Han, 2003). In addition, several meta-analysis studies have indicated that efficient periodontal treatment resulted in improvement in glycaemic control in diabetic patients (Paraskevas et al., 2008, D'Aiuto et al., 2004, O'Connell et al., 2008). Recently, the pathogenesis of type 2 diabetes has been attributed to an innate immunity disorder caused by a persistent low-level inflammatory response (Amar and Han, 2003). Interestingly periodontitis is associated with ulceration and high vascularity of pocket epithelium; this may facilitate systemic bacteremia by periodontal pathogens. Among these bacteria, *P. gingivalis* received attention due to its ability to invade tissues and alter systemic cytokine levels such as several interleukins and TNF-α, which potentially contribute to the pathogenesis of type 2 diabetes (Haraszthy et al., 2000, Chun et al., 2005).

CVD is another systemic condition that has been proposed to be associated with periodontitis. The presence of Gram-negative anaerobic bacteria in established periodontal lesions will likely provide a source of LPS and inflammatory cytokines, such as TNF-α, which potentially could enter the systemic circulation and exacerbate CVD. Data from a cohort study on patients with coronary heart disease indicated an association between severity of periodontitis and the incidence of this disease (Beck et al., 1996). A study by Geerts et al. (2004) also suggested a significant correlation between periodontitis and coronary artery disease. The findings showed that 91% of patients with CVD suffered from moderate to advanced periodontitis while this percentage reduced to 66% in healthy subjects. The correlation between periodontitis and pregnancy factors remains controversial. Interestingly, periodontitis has been suggested as a risk factor for preterm delivery and low birth weight, and results from 5-year prospective study supported this notion in which maternal periodontitis appear to be involved in premature births. Notably however, other studies reported a negative correlation between periodontitis and pregnancy. A recent clinical study undertaken on women in labour wards has however indicated a negative correlation between improved periodontal disease status and pregnancy outcome (Davenport et al., 2002). Isolation of the periodontitis-associated bacteria, *F. nucleatum*, from the placenta, amniotic fluid and chorioamnionic membranes from women that delivered prematurely indicated a potential mechanistic relationship between the two conditions

Osteoporosis is another systemic condition which has been proposed to be associated to periodontitis. Notably RANKL expression is proportionally increased with severity of periodontitis which is thought to be responsible for increased osteoclastic activity during alveolar bone destruction. Activated T-lymphocytes in periodontal lesions and local epithelium showed upregulated expression of RANKL which could be involved systemically in osteoclast differentiation, and down-regulation of osteoprotegerin, osteoclast inhibitor,

which may indicate a possible mechanism for association with osteoporosis induction (Liu et al., 2003).

6.2: Pathogenesis of periodontitis

The interaction between periodontal pathogens in dental plaque and the host immune response are considered central to the pathogenesis of periodontitis. During initiation of periodontitis, the first line of defense between bacteria in the plaque biofilm and the underlying connective tissues in the periodontium is the junctional epithelium (JE) which acts both as a mechanical and immunological barrier. The associated apical migration of the JE results in periodontal pocket formation which is a key clinical marker in patients with periodontal disease. The periodontal pocket is colonised by a wide diversity of bacteria and as disease progresses Gram-negative pathogens increase in number and proportion. The virulence factors produced, including LPS, can stimulate an intense immune response and subsequent inflammatory mediator release from the pocket epithelium (Tribble and Lamont, 2010). Furthermore, increased release of MMPs and prostaglandin E2 can be detected in addition to RANKL activation which participates in the increase in pocket depth and subsequent alveolar bone resorption (Kornman et al., 1997, Page and Kornman, 1997). Epithelial cells, when pro-inflammatory stimulated, secret MMPs, e.g. MMP-9, which is evident by the high levels found in periodontitis (Hannas et al., 2007, Offenbacher, 1996). Neutrophils are also a key first line defense cell and are part of the innate immune system. In healthy periodontal tissues, they are resident in relatively small numbers, however once bacterial infection induces a host pro-inflammatory response; neutrophils are recruited in relatively large numbers. Their passage through pocket epithelium together with their antimicrobial activity results in a release of enzymes and oxygen radicals which aim to reduce bacterial number. In periodontal disease patients, there is reportedly an exaggerated neutrophilic response which results in local tissue damage (Chapple, 2002). Knowledge of

immune mechanisms and inflammatory responses and how they are regulated is essential for understanding the pathogenesis of periodontitis. The primary aetiological agent for periodontal diseases is the bacteria in the dental biofilm (Carranza et al., 2014) however, determination of the pathogens which are entirely responsible for periodontal disease pathogenesis still unclear. There is evidence that certain bacteria are highly associated with the destructive forms of periodontitis; however, the presence of these microbes in healthy individuals and patients with no signs of active disease progression suggests that the disease is not merely dependent on bacterial presence but it is combined with the host immune and inflammatory response (Cekici et al., 2014). Regulation of this underpins patient susceptibility and this is also modulated by environmental factors (Van Dyke and Dave, 2005).

Other important cellular components in periodontal lesion are fibroblasts, which also contribute to the defensive mechanism by up-regulation of secretion of fibrous ECM molecules that encapsulate and confine the inflammatory cell infiltrates (Page and Kornman, 1997). However, similarly to epithelial cells, fibroblasts can also play a dual protective and destructive role. Notably resident periodontal fibroblasts that produce the ECM in health can participate in tissue destruction during periodontal disease. Indeed, during disease activated fibroblasts can produce proteolytic enzymes such as MMP-2 (Hannas et al., 2007) and prostaglandin E2 causing soft tissue destruction and promote bone resorption (Page and Kornman, 1997). Classically, the increasing fibroblast number during inflammation is attributed to their mitotic up-regulation. Notably studies performed analysing early gingival lesion in humans (Schroeder and Page, 1972) and in a baboon model (Simpson and Avery, 1974, Avery and Simpson, 1973) showed that the fibroblast population and CT mass are significantly decreased because of the cytotoxic effect of sensitised lymphocytes at sites of

inflammation. Later, in more advanced periodontal lesions fibroblast numbers begin to increase.

The influence of the plaque biofilm, which is defined by Costerton et al. (1994) as a "matrix enclosed bacterial population adherent to each other and/or to surfaces or interfaces", on the host response has been investigated. While the pathogenetic mechanisms at a cellular level has not been fully clarified evidence from advanced stages of periodontitis indicate that periodontal pathogens tend to invade deep tissues through dissociated pocket epithelium. In addition, bleeding on probing is evident in active periodontal pockets which indicate microulceration of pocket epithelium (Tribble and Lamont, 2010). These data suggest that EMT is a potential mechanism involved in compromising periodontal pocket epithelium.

Although periodontitis is characterised by a wide diversity of subgingival flora which may harbor more than 500 bacterial species (Moore and Moore, 1994), small groups of bacteria are strongly associated with destructive aspects of the disease, in particular these are *F.* nucleatum, *P. gingivalis, Bacteroides forsythus* and *Aggregatibacter actinomycetemcomitans* (Paster et al., 2001, Lovegrove, 2003). Socransky et al. (1998) classified the periodontal pathogens into five complexes of microorganisms depending on their pathogenicity and sequence of appearance in periodontal pockets and termed them "red", "orange", "green"," yellow", and "purple" complexes. Members of the "red" complex are strongly associated with increasing pocket depth and bleeding on probing however their existence requires prior colonization by bacteria of the "orange" complex. The bacteria belonging to "orange" complex, particularly *F. nucleatum*, have a central role in providing physical bridging and enhancing anaerobic conditions that protect congregating strictly anaerobic bacteria of "red" complex (Bullions and Levine, 1998). The "Orange" group is also highly associated with periodontal pocket deepening. The final three bacterial clusters, "yellow", "green", and "purple" complex, represent the early pocket colonisers which prepare the microenvironment

for more aggressive periodontal pathogens belonging to “orange” and “red” complexes (Socransky et al., 1998).

The organization and structure of the microbial communities within this biofilm allow them to exchange nutrients and eliminate by-products via a primitive circulatory system. In addition, this structure provides protection against host defensive mechanisms such as antibodies in the gingival crevicular fluid. Accordingly, the biofilms are resistant to locally and systemically administrated antibiotics and antimicrobials that can only be used as an adjunctive treatment following mechanical debridement which is still the first choice for treating periodontal disease (Costerton et al., 1994, Dennison and Dyke, 1997).

It is well known now that EMT could be triggered in response to inflammation in an attempt to promote healing and ‘wall off’ bacterial invasion; however, if inflammation chronically persists it may eventually result in tissue and organ fibrosis and dysfunction. Conversely, the EMT process would reverse once inflammation subsides (Kalluri and Weinberg, 2009). The role of EMT in periodontal disease pathogenesis has received no attention and is yet to be fully investigated. EMT may play a potential role in compromising junctional epithelial integrity allowing bacterial invasion to the underlying connective tissues and thereby initiating a destructive host response resulting in connective tissue breakdown which is characteristic of periodontal disease.

6.3: Possible implication of EMT in periodontal disease

Evidence from several studies has demonstrated EMT-related changes in periodontally diseased-tissues. Gingival samples collected from periodontitis patients have indicated that CT showed increased expression of fibronectin and αvβ6 integrin. Data from epithelial cultures, derived from the same patients, revealed increases in fibronectin, Slug, MMP-9, MMP-13, and MMP-2 while E-cadherin levels have been noted as being significantly

reduced in patients exhibiting drug- induced gingival overgrowth. Notably the authors suggested that TGF-β1 was a potent stimulator for these observed changes (Sume et al., 2010). The significance of TGF-β1 in triggering EMT in phenytoin-induced gingival enlargement was supported by another recent study (Pisoschi et al., 2012) whereby up-regulation of this cytokine was associated with increased expression of FSP-1, Snail and Smad in the basal epithelial layer together with diminished E-cadherin expression and evidence of BM disintegration. Consistently, treating human gingival epithelium with Cyclosporine-A resulted in decreased E-cadherin and increased α-SMA expression which was reversed upon addition of a TGF-β1 signaling inhibitor to the culture (Fu et al., 2015). Furthermore, examination of tissue samples collected from patients with overgrown gingiva demonstrated multiple discontinuities along the BM which contained epithelial-like cells aligned towards the CT. Areas of the disintegrated BM were associated with down-regulation of collagen type IV and laminin 5 (Kantarci et al., 2011). The effect of TGF-β1 is not only confined to epithelial cells, human gingival fibroblasts also stimulated with TGF-β1 release MMPs via stimulation of p38 MAPK signaling which causes further damage to the BM and locally stimulates the EMT process (Ravanti et al., 1999). Interestingly, treatment of normal human gingival fibroblasts with different concentrations of Cyclosporine-A resulted in increased TGF-β1 but failed to express α-SMA and CT growth factor (CTGF), markers of differentiation into myofibroblasts, *in vitro* (Sobral et al., 2010). Significantly periodontitis is a chronic inflammatory condition characterised by up-regulation of TGF-β in response to bacterial stimuli and periodontal tissue samples collected from patients with advanced chronic periodontitis have shown significantly increased expression of TGF-β compared with healthy controls (Mize et al., 2015).

Findings from previous studies of periodontal disease have indirectly suggested involvement of periodontal pathogens in stimulating EMT-like features. Exposure of an oral keratinocyte

cell line to heat-inactivated periodontal pathogens, *F. nucleatum* and *P. gingivalis*, resulted in increased transcription of EMT-related cytokines such as TNF-α, in addition to altered expression of cytokeratins (Milward et al., 2007). Additionally, exposure of primary mouse gingival cells to *P. gingivalis* LPS upregulated TNF-α and IL-6 *in vitro* (Ekhlassi et al., 2008). A further study showed that the effect of bacteria was not only limited to a molecular level only; as co-culturing bacteria with oral keratinocytes in organotypic model promoted migration of epithelial cells (Pöllänen et al., 2012). Analysis of tissue samples collected from chronic periodontitis patients has also demonstrated that the exposure of encounter of pocket epithelial cells to periodontal pathogens resulted in EMT-like features, including down-regulation of E-cadherin and altered cytokeratin expression (Nagarakanti et al., 2007). Furthermore, periodontal pocket tissue samples together with subgingival plaque samples showed up-regulation of RANKL transcription, also proposed as an inducing factor for EMT, which was associated with a significant increase in *P. gingivalis* bacterial numbers (Wara-aswapati et al., 2007).

These previous studies demonstrate the immune response to bacteria, mainly Gram-negative anaerobes, is characterised by production of potent inflammatory cytokines such as TNF-α, TGF-β1, and interleukins potentially involved in EMT-induction. Furthermore, pocket epithelial cells are chronically exposed to these cytokines which could trigger EMT via autocrine and paracrine signaling. In addition, infection with these bacteria in different organs is mostly associated with loss of epithelial barrier function, a hallmark of EMT process. Periodontal pockets are characterised by the prolonged presence and diversity of anaerobic pathogens associated with loss of epithelial integrity especially during active phases of periodontal disease. These underpinning findings require further investigation to determine the potential involvement of EMT in the initiation and progression of periodontitis.

7. Aims and objectives

7.1. Overall aims of the study

The overall aim of this thesis can be summarized as follow:

- Adjusting growth of oral keratinocytes to be confluent in monolayer in 8-days then investigating the effect of heat-killed periodontal pathogens (*F. nucleatum* and *P. gingivalis*) and *E. coli* LPS on the proliferation rate and viability of epithelial cells during culturing period.
- Investigate immunological response of oral epithelial cells to the presence of heat-killed periodontal bacteria by detecting activation of NF-κB signaling and changes in the expression of different TLR.
- To investigate possible EMT-induction and involvement in periodontitis using previously developed *in vitro* model systems which utilised both transformed and primary oral epithelial cells in response to relatively long term exposure to periodontal bacterial components.

7.2. Specific aims and objectives for chapter 3:

Aims:

- Adjusting growth of oral keratinocytes to be confluent in monolayer in 8-days then investigating the effect of heat-killed periodontal pathogens (*F. nucleatum* and *P. gingivalis*) and *E. coli* LPS on the proliferation rate, viability, and pro-inflammatory response of epithelial cells during culturing period.

Objectives:

1- To investigate different growth conditions (altering the FCS concentration and/or seeding number) to regulate the confluency of H400 cells to enable studies at 8-days post seeding.

Previous studies indicated that the average time required for EMT-induction ranged between 1-8 days (Chapter 1, section 3.4.2).

2- To compare manual and automated cell counting techniques and determine the reproducibility of an image-analysis based automated approach.

3- To investigate the effect of heat-killed periodontal pathogens, *F. nucleatum* and *P. gingivalis*, on the growth and viability of H400 cells in addition to examining whether such treatments induced a pro-inflammatory response via NF-kB activation.

4- To investigate changes in gene expression of TLR-2, -4, and -9 following exposure to bacterial components.

7.3. Specific aims and objectives for chapter 4:

Aims:

To investigate the potential of two key periodontal pathogens, *F. nucleatum* and *P. gingivalis*, to induce EMT *in vitro* in the H400 OSCC cell line.

Objectives:

EMT induction was investigated by using a range of assays including PCR, an EMT gene expression array, ELISA, IF, ICC, wound healing, transwell migration, and TEER.

7.4. Specific aims and objectives for chapter 5:

Aims:

1- To investigate the possible involvement of EMT in compromising epithelial barrier function following exposure of primary oral keratinocytes to periodontal pathogens in an *in vitro* periodontitis-model system.

2- Compare results obtained using primary keratinocytes with those obtained using the H400 cells following exposure to heat-killed periodontal pathogens.

Objectives:

1- EMT induction in primary cells cultures was investigated by range of different assays including PCR, IF, and ICC for selected EMT-indicators.

2- The integrity of the epithelial monolayers was investigated by using TEER.

3- Increased migratory ability of the cells was investigated by utilising transwell-migration and scratch-wound assay.

MATERIALS and METHODS

Methods used in this thesis included preparation of bacterial suspension, by heat-killing of bacterial cultures, to be used in stimulating epithelial cells cultures. This was followed by culturing epithelial cells under different conditions to optimise their growth to develop model to investigate EMT-induction. Morphological, molecular and behavioural changes associated with EMT then were detected by utilising range of assays. All methodologies used in this study are summarised in Figure 7.

1: Bacterial cultivation and heat-inactivation

Lyophilised stocks of *F. nucleatum* (ATCC 10953) and *P. gingivalis* (ATCC 33277) were commercially purchased from the American Type Culture Collection (ATCC, Rockville, MD). All materials used for bacterial culture were purchased from Difco laboratories, USA, unless otherwise stated. Bacteria were reconstituted using mycoplasma broth which was generated by mixing 21g of mycoplasma broth powder to 700ml of sterilised distilled water. Bacteria were cultured on trypticase soy agar supplemented with 5% sheep blood in an anaerobic chamber (Don Whitley, UK) at 37ºC in atmosphere of 80% Nitrogen, 10% Carbon dioxide, 10% hydrogen. The purity of bacterial colonies was confirmed by Gram staining (section 1.2) and morphology of colonies in cultures. Morphologically-identical colonies (Figure 8), produced by subculture, were inoculated into 10ml trypticase soy broth and incubated at 37ºC in anaerobic conditions for 24hr. Post-incubation, the growth of the bacteria was indicated by turbidity in suspension. A bacterial pellet was produced by centrifugation (Jouan, UK) at 3000rpm for 10min. The resultant pellet was washed three times in sterile PBS (see below), then resuspended in sterile PBS followed by heat-inactivation at 121°C and 15psi for 10min in the autoclave (Prestige medical, UK).

Phosphate-buffered saline (PBS) (x1) was synthesised by dissolving 8g of sodium chloride (NaCl), 0.2g potassium chloride (KCl), 1g of sodium phosphate dibasic (Na_2HPO_4), and 0.2g

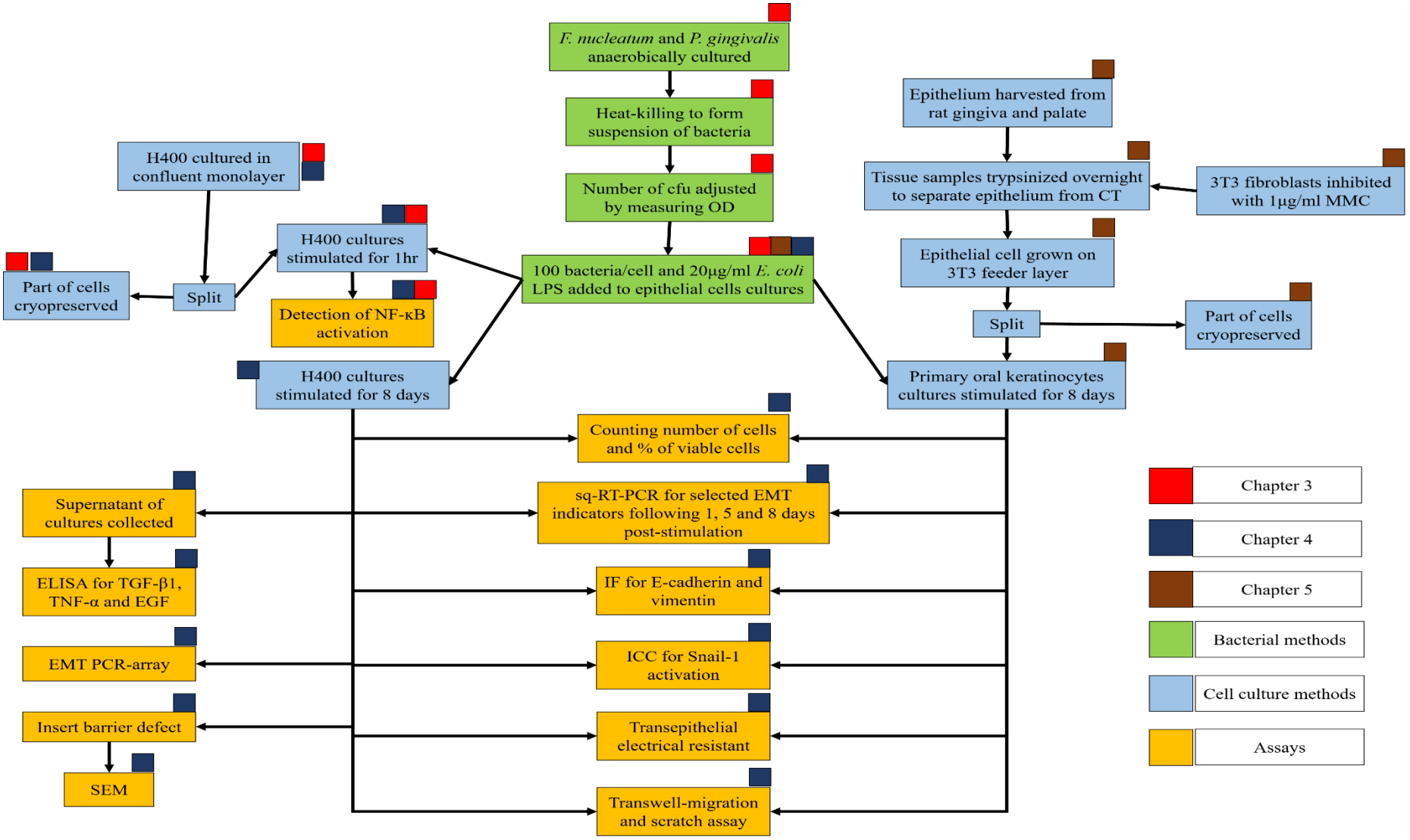

Figure 7: Summary of methodologies used to prepare heat-killed bacterial suspension, cell culture and EMT investigation

of potassium phosphate monobasic (KH_2PO_4) in 1L of distilled water. PBS was sterilised by autoclaving prior to use. The bacterial concentration in the suspension was determined by measuring optical density (OD) (Zhang et al., 2014, Liu et al., 2009) using a spectrophotometer (Jenway, Dunmow, UK) at 600nm using 1ml semi-micro cuvettes (Sarstedt, UK) and by comparison with a standard curve (OD vs. bacterial count) (Coons and Kaplan, 1950). This curve was produced by inoculating bacteria onto TSB broth and incubated anaerobically for 24hr until turbidity is evident which is then serially diluted. Spectrophotometer was blanked by placing cuvette containing broth only followed by inserting serially diluted samples and recording absorbance for each. Using Microsoft Excel, scatter graph was generated by plotting absorbance data on y-axis and dilution factor on x-axis. The resulted linear regression equation can be used later to determine colony forming unit (CFU) for new cultures same bacteria by measuring OD. A final suspension containing $4x10^8$ bacteria/ml was generated by diluting the suspension with sterile PBS. 50µl of the suspension was re-plated on a blood agar and incubated anaerobically for 48hr to confirm bacterial killing. Heat-inactivated bacterial suspensions were stored in 1ml aliquots at -30ºC prior to use.

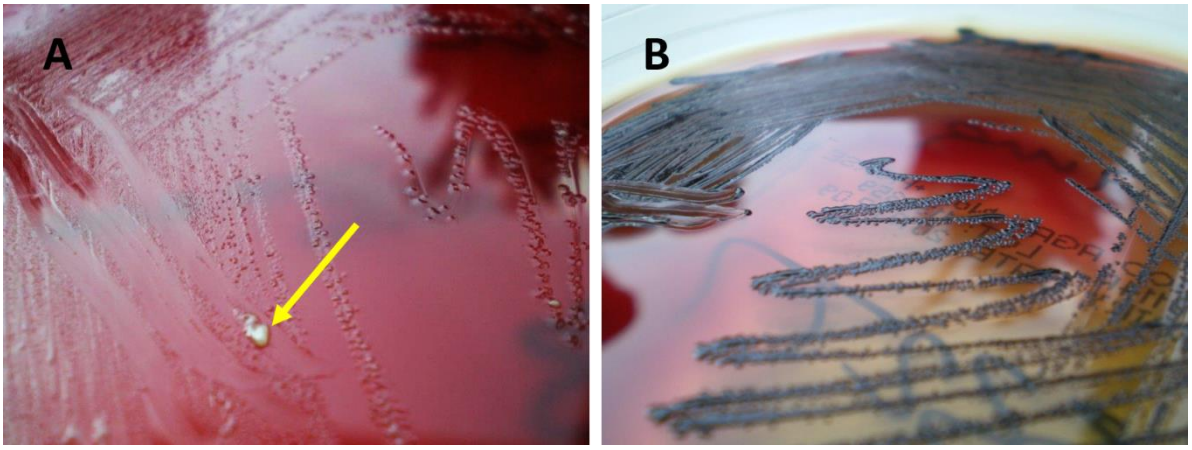

Figure 8. Streaks of *F. nucleatum*, and *P. gingivalis* grown on 5% sheep blood agar anaerobically cultured at 37°C for 48hr in a 15cm petri-dish. *F. nucleatum* form translucent grey colonies with no sign of hemolysis (A). While *P. gingivalis* (B) produced black-pigmented colonies on agar supplemented with blood.

1.2: Gram staining

Representative colonies were harvested using a sterile metal loop and resulting bacteria collected and emulsified into a single drop (~0.5ml) of NaCl solution, on a glass microscope slide (Fisherbrand, UK). The emulsion then was fixed by quickly heating several times over a Bunsen burner flame. This was then cooled before flooding with crystal violet (Prolab diagnostics, UK) for 30sec before gently washing under running tap water. This was followed by flooding Lugol's iodine (Prolab diagnostics, UK) onto the surface of the slide for 30sec before being washed off with distilled water. Bacteria were quickly (2-3sec) decolorised by acetone rinsed with distilled water and then counterstained with carbol fuchsin for 30sec before final washing. Slides were dried using absorbent tissue paper and viewed under light microscope (x10 objective) (Leitz Wetzlar, Leica Microsystems GmbH, Germany) using oil immersion. The morphology (cocci, rods) and the Gram staining (deep violet for Gram positive and pink for Gram negative) were determined microscopically.

2: Cell cultures

2.1: Culture of H400 cells

H400 cells (ECACC 06092006) are from human oral squamous cell carcinoma (OSCC) cell line which was first isolated from squamous cell carcinoma of alveolar process of a 55-years old female patient. This cell line was reported to be highly responsive to TGF-β (Prime et al., 1990). Passages number ranged between 19 and 30, were revived from liquid nitrogen storage by placing them in a pre-warmed water bath at 37°C for rapid thawing (approx. 30-60sec). All plasticwares used in this thesis were supplied from Thermo Scientific, UK. Cells were transferred to a Falcon tube containing 1ml of medium consisting of Dulbecco's modified Eagle's medium (DMEM) (Sigma, UK) containing 2.5mM L-Glutamine and supplemented with 25µl of 10mg/ml hydrocortisone and 10% foetal calf serum (FCS) (Biosera, UK). The mixture was then centrifuged (Jouan, UK) at 800rpm for 5min until a

pellet was formed, the supernatant was removed and the cells were re-suspended in 1ml of complete medium, then transferred into a T75 flask containing 9ml of medium (DMEM and 10% FCS) and placed in a humidified incubator (Thermo Scientific, UK) at 37° C with 5% CO_2. Growth of cells and indications of contamination were checked for daily and replacement of growth media occurred every 2 days. When cultures reached ~80% confluency they were sub-cultured (passaged) for ongoing growth and for use in a range of experiments.

2.1.1: Sub-culturing

Used growth media was removed and the T75 culture flask washed with 4ml pre-warmed sterile PBS. After removing PBS, 4 ml of trypsin 0.25% trypsin- Ethylenediaminetetraacetic acid (EDTA) (Sigma, UK) was added and re-incubated at 37°C for approximately 10min or until cells had become detached from the culture surface as determined by microscopic examination. The trypsin-EDTA solution, together with the detached cells, were transferred to a falcon tube containing 4ml of DMEM supplemented with 10% FCS, pre-warmed to 37°C, to stop the reaction. Collected cells were then centrifuged at 1000rpm for 5min to form a pellet. The supernatant was removed and the pellet re-suspended in 5ml of warmed media (DMEM supplemented with 10% FCS). Cells were frozen as described in (section 2.1.3).

2.1.2: Growth of primary oral keratinocytes with 3T3 feeder layer

The technique applied was originally described by Rheinwald and Green (1975) and utilised primary keratinocytes seeded in flasks containing growth-inhibited 3T3 feeder layer (Corpechot et al., 2002). The 3T3 fibroblast layer secretes ECM proteins which facilitate attachment of epithelial cells as well as producing of growth factors that stimulate proliferation of keratinocytes.

2.1.2.1: Experimental design for inhibiting proliferation of 3T3s fibroblasts using different Mitomycin C concentrations

Primary keratinocytes require support from a feeder layer to maintain their growth. The purpose of this experiment was to determine the minimum inhibitory concentration of MMC required for inhibiting proliferation of 3T3 fibroblasts which are used as feeder layer for primary oral keratinocytes. Identification of optimal conditions would minimise the frequency of replenishing primary epithelial cultures with new batches of 3T3 feeder fibroblasts and avoid unwanted side-effects associated with relatively high MMC concentrations. 3T3 cells were cultured with a range of MMC concentrations (1, 4, 6, 8, and 10μg/ml) or with media only. Three T75 flasks for each condition were established and 6 cell counts were performed for each flask for days 4-12 then averaged and analysed. Experiments repeated in triplicate.

2.1.2.2: 3T3 cell feeder layer preparation

3T3 cells at passages 10-20 were used to prepare feeder layers by culturing $2x10^4$ 3T3 cells in T75 flask containing 10ml of DMEM supplemented with 10% FCS and incubated at 37°C in 5% CO_2 humidified chamber. The cultures were routinely subcultured twice a week to provide a continuous supply of 3T3 fibroblasts.

The feeder layer was prepared by incubating confluent 3T3 cultures with 1μg/ml Mitomycin C (MMC) (Sigma, UK), in T75 flasks containing 10ml of DMEM and 10% FCS, for 2hr at 37°C and 5% CO_2 to inhibit proliferation. Media was removed and the cultures thoroughly washed with sterile PBS to remove all remaining MMC that may inhibit the division of keratinocytes. Number of MMC-inhibited 3T3 fibroblasts tends to decrease with time in cultures as they die and not replaced due to inhibition of mitotic activity. This requires replenishing with freshly inhibited 3T3 cells to maintain growth of primary keratinocytes. Replenishment of 3T3 fibroblasts was performed by repeating the same MMC-inhibition

process described above, and the freshly inhibited 3T3 cells were trypsinised and supplemented to cultures containing primary epithelial cells

2.1.2.3: Isolating and culture of primary oral epithelial cells

Oral epithelial cells were harvested from labial gingivae and palate of 6-week old male Wistar Han rats (weight between 120-200g), (Aston University, Birmingham, UK). Following excision of these tissues, samples were incubated overnight in universal tube containing 0.25% trypsin-EDTA solution at 4°C. The following day, keratinocyte culture medium (KCM) was synthesised from DMEM, supplemented with 2.5mM L-glutamine, 10% FCS, 10µl/ml of penicillin–streptomycin, $2x10^{-2}$µl/ml cholera toxin, $5X10^{-2}$µl/ml of EGF (ThermoFisher, UK), $5x10^{-2}$µl/ml Amphotericin-B (Sigma, UK) and 5µg/ml insulin (Sigma, UK). Samples were removed from the trypsin-EDTA solution and transferred to 15cm petri-dish and the epithelial layer carefully separated with forceps from the underlying connective tissue. The resulting epithelial sheet was dissected into smaller pieces by using a sharp scalpel blade (No.15) (Swann Morton, UK) and added to 5ml of KCM to create a cell suspension which was then seeded in T75 flasks containing KCM and MMC-inhibited 3T3 cell feeder layer and incubated at 37°C in 5% CO_2.

Cultures were monitored daily to make sure that primary oral keratinocytes were not overwhelmed by overgrowth of primary fibroblasts. Usually, 3T3 cells inhibit the growth of human fibroblasts however; when the density of 3T3 cells decreases, primary fibroblasts proliferate. When primary fibroblast contamination was observed, cultures were incubated with trypsin/EDTA for 30sec and aspirated vigorously which resulted in detachment of 3T3 cells and the primary fibroblasts, keratinocytes subsequently remained attached. Fresh MMC-inhibited 3T3 cells were then added to the cultures.

2.1.2.4: Sub-culturing primary cells

Evidence of keratinocyte growth was routinely detected after 7 days in cultures in the form of round colonies. To ensure optimal growth, cells were sub-cultured every 8-10 days as described below.

The KCM was removed and cultures washed with sterile PBS then incubated with 4ml of trypsin/EDTA for 30sec to remove the 3T3 feeder layer. Remaining keratinocytes were incubated for 10-15min with 4ml trypsin-EDTA solution at 37°C. The cells were then transferred to a Falcon tube containing an equal volume of KCM to inhibit the trypsin reaction, and then pelleted by centrifuging at 800rpm for 5min. The pellet was then re-suspended and seeded into culture plasticware dependent on the downstream experiments being undertaken.

Following each cell sub-culture a stock of primary cells was maintained by freezing and archiving as described in section 2.1.3. The highest passage number used for all experiments was 5. Notably primary cells have a finite life-span and lose their division potential, i.e. undergo senescence, compared with an immortalised cell line (Chun et al., 2005).

2.1.3: Cryopreservation

Following passage, cells were cryopreserved to maintain stocks at a low passage number for use in future studies. Cells ($1x10^6$) were suspended in 1ml of cryomedia consisting of 700µl of DMEM, 200µl FCS, and 100µl dimethyl sulfoxide (DMSO) (Sigma, UK). Vials were labelled and placed in polystyrene box at -80°C freezer overnight before long term storage in the vapour phase of liquid nitrogen.

2.2: H400 oral keratinocytes cell line growth models

H400 cells were cultured under a variety of different conditions to achieve a target of reaching ~80% confluency after 8 incubation days. Cell cultures were generated by varying (a) cell seeding numbers, and (b) FCS concentrations.

For the first approach, three different densities ($3x10^3$, $2x10^3$, $1x10^3$ cells/ml) were cultured in medium with a relatively low FCS concentration (1%). Subsequently two cell seeding densities ($2x10^4$ and $1x10^3$ cells/ml) were cultured in 4ml of media supplemented with three FCS concentrations (2, 5 and 10%). Cell counts and viability assay began at day 3 and continued every day until the end timepoint. For each time point, six readings, including the cell count and viability analysis, were obtained in triplicate. A total of 18 readings were averaged and analysed using ANOVA test, significant level was considered when $P<0.05$.

2.3: Stimulation of oral keratinocytes by periodontal pathogens

The stimulation of oral keratinocyte cultures was performed by using the two periodontal pathogens, *F. nucleatum* and *P. gingivalis*, belonging to orange and red complexes respectively (Socransky et al., 1998). These bacteria were heat-killed (Section 1) and applied to cultures at a ratio of 100 bacteria per epithelial cell to simulate the cell-bacteria ratio found in periodontal pockets (Dierickx et al., 2002). LPS from Gram-negative bacteria had been confirmed as a potent EMT inducer in several studies (Dave and Bayless, 2014, Dawson et al., 2005) and was used as positive EMT-control in this thesis. *E. coli* LPS (serotype 026:B6) (Sigma, UK), was dissolved in DMEM to produce a stock solution at 1mg/ml, and stored in aliquots at -20°C prior to use. For each study a final concentration of 20µg/ml of *E. coli* LPS was used (Milward et al., 2007).

To maintain the cell-bacteria ratio (1:100) additional bacteria (every 2 days) were added, together with changing media, to compensate for increasing cell number. The numbers of

additional bacteria required was estimated from previous growth curves which indicated total number of cells at the time points studied.

3: Cell Counting and viability assay

Cell counts were performed by manual and automated counting methodologies as described below. Data from both techniques were analyzed to compare the consistency and validity of each method and to determine which approach was most suitable for assaying the number and viability of cells.

3.1: Manual cell counting

3T3 fibroblasts and oral keratinocytes cultures, H400 and primary cells, were trypsinised and trypsin was equilibrated with equal volume of DMEM supplemented with 10%FCS followed by centrifugation to form a pellet which was re-suspended with media. A cell suspension volume of 100µl was pipetted into an eppendorf containing an equal volume of trypan blue (Sigma, UK) and mixed well using a vortex mixer. The mixture was incubated at room temperature for 10min to allow cell uptake of the dye. Subsequently dead cells are stained blue due to a breached cell membrane while viable cells remain unstained (Costerton et al., 1994).

Cell counts were performed using haemocytometer (Improved Neubauer, Hawksley, UK) which was prepared for use by applying a moistened cover slip to the haemocytometer, correct positioning was confirmed by the presence of Newton's diffraction rings. The trypan-cell suspension was mixed and 10µl was gently pipetted onto the edge of the cover slip, allowing the mix to flow until it filled the whole counting chamber. The construct was then viewed using a microscope (Primovert, Zeiss, Germany) with a x10 objective and cells in the primary square counted. The boundaries of each primary square are defined by the middle of the triple line separating each. For consistency, when counting, cells touching the upper or

left boundary lines were included while those touching the lower or right lines were excluded. The suspension examined was mixed to enable uniformity with no cells clumps which would result in inaccurate counts.

Viable and non-viable cells were counted separately to estimate the percent of viable cells in each sample. Counts were performed on 3 separate cell culture dishes with each being counted 6 times. The mean cell count from the 18 readings was determined along with the percentage cell viability (Freshney, 2005).

3.2: Automated cell counts

Automated cell counting was undertaken using the Luna automated cell counter (Luna, Logos Biosystems Inc., USA (Figure 9). This device can calculate cell count, viability, and cell size and this is achieved in approximately 10sec. Images of cell suspensions can be captured (5MP image resolution) with manual focus mode. Images are then analysed, immediately or later, using a built-in image analysis algorithm. Accurate detection limits cell count analysis between $5x10^4$- $1x10^7$ cells and cell size between 3-60µm. Measurements were performed by taking 50µl of the cell suspension, mixed with equal volume of trypan blue (1:1), and then 10µl was pipetted into chamber of Luna cell counting slide (Figure 9). The plastic slide was inserted into the automated counter so that magnified section appeared on the display screen which is then manually focused to select a representative plane to be measured. Readings, counts and viability, were recorded and the slide was removed from the device and re-inserted again to take another set of readings.

1- Counting execution
2- Magnification option
3- Results display showing total cell number, percent of viable and dead cells, percent of viability, average size of cells measured, and dilution factors used
4- Dilution factor option to set dilution used in each sample
5- Graphic presentation of results
6- Save option, images can be saved as TIF file and re-analysed later

A

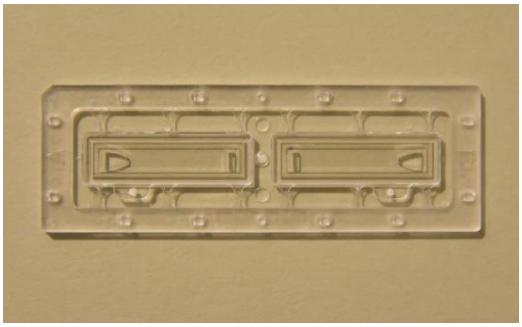

B

Figure 9. (A) Main features of Luna image analysis based automated cell counter, (B) Luna-cell counting slide.

3.3: Automated cell count validation

Two studies were performed in order to validate automated cell counts, the first was to assess the reproducibility of the automated cell counter and the second compared the automatic with the haemocytometer counts.

3.3.1: Reproducibility analysis of the automated cell counter

Measuring cell count was undertaken using a bright-field automated cell counter (Luna, Logos Biosystems Inc., USA). Initially a study was performed to estimate the consistency of the readings obtained by the device using a high- ($3x10^6$ cells/ml) and low- cell density

($2x10^5$ cells/ml). The sample size (i.e. the number of cultures analysed) necessary for this study was estimated to be n=12, using the N-query advisor ver.7 software (Statistical solutions, USA) using data from a pilot study. Subsequently high- and low-density groups were serially diluted (1:2, 1:4, and 1:8) with media supplemented with 10% FCS. For each dilution, the cell count was determined using the automated counter 12 times.

3.3.2: Manual vs automated cell count methods

The comparison between manual and automated cell count methods was performed to determine the consistency of readings obtained using the two techniques. Cells were seeded, $3x10^3$ cells/ml, in 35mm tissue culture dish containing 4ml of media and cultured for 8 days. Cell counts were performed on a daily basis from day 4-8 for both techniques.

4: Polymerase chain reaction assay

In this thesis, two types of polymerase chain reaction (PCR) were utilised and these included; semi-quantitative reverse transcriptase-polymerase chain reaction (sq-RT-PCR) and the Human EMT PCR-array (Qiagen, UK). The methods used for these studies are described below.

4.1: Semi-quantitative reverse transcriptase-polymerase chain reaction

This technique involves two steps starting initially with the reverse transcriptase reaction followed by the PCR. The amplification program of PCR consists of denaturation, annealing, and elongation. The products of this reaction were then separated using gel electrophoresis and analysed by GeneTools software (Syngene, USA) software.

4.1.1: Cell culture preparation for harvest of total RNA

Oral keratinocytes ($5x10^4$ cells) were cultured in T75 flasks, containing 10ml of DMEM and 10%FCS. Cultures were either treated with media only or stimulated with bacterial

components. RNA was harvested after 1, 5, and 8-days. Supernatants of all H400 cell cultures were aliquoted into 1.5ml tubes and stored at -80°C prior to ELISA (section 5.1).

4.1.2: Cell lysis

Media was aspirated from the flasks and cultures washed with PBS to remove remaining media which may interfere with the lysis process. Total RNA was extracted from cultures by using the RNeasy Mini Kit (Qiagen, UK) consisting of RTL lysis buffer and washing buffers (RW1 and RPE). Lysis was performed as follow:

- Addition of 350µl of RLT lysis buffer to the flask and lysate was collected and placed in eppendorf and homogenised by aspiration with an equal volume of 70% ethanol.

- 700µl of the mixture was transferred to Rneasy spin column assembly mounted in a 2ml collection tube, prior to centrifugation (5415D Centrifuge, Eppendorf, Germany) at 10000rpm for 30sec.

4.1.3: Total RNA extraction

Cell lysate produced in the previous step then was processed to obtain pure RNA, which will be used later for reverse transcription, according to following steps:

- 350µl of Buffer RW1 was added to column and centrifuged at 10000rpm for 30sec and flow through was discarded. Buffer RW1 contains guanidine salt and ethanol which is used mainly to eliminate unwanted biomolecules in the sample e.g. proteins, carbohydrates, and fatty acids.
- 80µl of Deoxyribonuclease I (Dnase I) (Sigma, UK) was added for each sample to eliminate DNA. Samples were incubated with Dnase I for 15min at room temperatue.
- 350µl of Buffer RW1 was added to column and centrifuged at 10000rpm for 30sec and flow through was discarded.

- Buffer RPE is a washing salt used to remove traces of salts that were used earlier from the samples. 500µl of Buffer RW1 was added to column and centrifuged at 10000rpm for 30sec and flow through was discarded. Then the same volume of Buffer RPE was added and centrifuged at 10000rpm for 2min and flow through was discarded.
- Column was placed in new collection tube and centrifuged at 10000rpm for 1min. Then column was transferred to 1.5ml collection tube and 30µl of RNase free water was added to the membrane and centrifuged at 10000rpm for 1min to elute RNA.

The whole RNA isolation process is summarised in Figure 10.

4.1.4: RNA quantification

The total amount and purity of RNA yielded from the samples was quantified using a spectrophotometer (BioPhotometer plus, Eppendorf, Germany) set at an analytical wavelength of 260nm. Initially, the device background was set by using 70µl of water in clean UVette (Eppendorf, Germany). Subsequently, 68µl of RNase free water was added to 2µl RNA sample in clean UVette, and then placed in the spectrophotometer which had been adjusted according to the dilution used. The digital read-out was recorded as concentration (µg/ml) and purity (260/280). This process was repeated in triplicate for each sample and the average of the readings used to determine the concentration of the total RNA.

4.1.5: RNA integrity visualisation

Agarose gel (1%) was generated by adding 0.7g of agarose (bioline, UK) to 70ml of 1x TAE (Severn Biotech, UK) buffer in conical flask. The mixture was heated in microwave for 2min to solubilise the mixture, and then cooled by placing the flask under running water. To enable the RNA bands to be visualised, 3µl of SYBR Gold (Invitrogen, USA) was added to the agarose solution. The solution was poured into a tape-dammed tray with insertion of comb to generate wells and allowed to set at room temperature for 30min.

A volume ranging between 0.5-2.5µl of RNA samples, depending on the concentration obtained, was added to x1 loading buffer (Invitrogen, UK) to generate a total volume of 6µl which was then pipetted into the wells of agarose gel placed in an electrophoresis tank (VWR, USA) filled with 1x TAE running buffer. Voltage was set to 120V and applied to electrophoresis tank containing gel-loaded RNA samples. Samples together with ladder control (PCR Ranger, NORGEN, Canada) were allowed to electrophorese for 20min. The gel was transferred to G:BOX (Syngene, USA) which is equipped with a UV transilluminator for ethidium bromide gels and 5.5MP camera. Images of RNA bands were captured by built-in digital camera and analysed using Genesnap software (Syngene, USA). The purpose of using this technique is to check integrity of RNA bands and absence of contamination of the samples with other products such as proteins or genomic DNA.

4.1.6: Reverse transcription of total RNA

Single stranded cDNA was synthesised from 1-2µg of DNase-digested total RNA, using the Tetro kit (Bioline, UK). A volume of 8µl mastermix was made for each sample (Table 6). 2µg of RNA was used to make up a final volume of 12µl. The 8µl mastermix was synthesised for each freshly prepared RNA sample then incubated in thermal cycler (Mastercycler, Eppendorf, Germany) at 45°C, annealing temperature, for 30min followed by 85°C for 5min to activate DNA polymerase which allows extending DNA template by adding complementary dNTPs at 5' to 3' direction. Cycles end with incubation at 4°C; this temperature allows short-term storage and maintains integrity of product prior to moving tubes from the machine. Samples were either used immediately were or stored at -80°C prior to use.

Reagent	Volumes (µl)
5x RT Buffer	4
(200u/µl) Reverse Transcriptase	1
(10u/µl) RNase Inhibitor	1
dNTP Mix 10mM	1
Oligo (dT)18 Primer Mix	1

Table 6. Constituents of reverse transcription mastermix.

4.1.7: Concentrating cDNA

Reversed transcripted DNA was pooled and concentrated using 0.5ml microcon filters (Amicon Ultra, Millipore, USA). Samples of cDNA previously produced were transferred to the microcon filter membranes then 480µl of DNase-free water was added to achieve a final volume of 500µl. Samples were centrifuged at 10000rpm for 2min, then twice at 8000rpm, flow through was discarded after each centrifuging step, for 1min. Level of DNA in the column was visually inspected after each spin until only 50-60µl was left which was determined by markings on the filter. At this point, columns were inverted in fresh tube and centrifuged at 800rpm for 1min to collect cDNA which were then stored at -20°C prior to use.

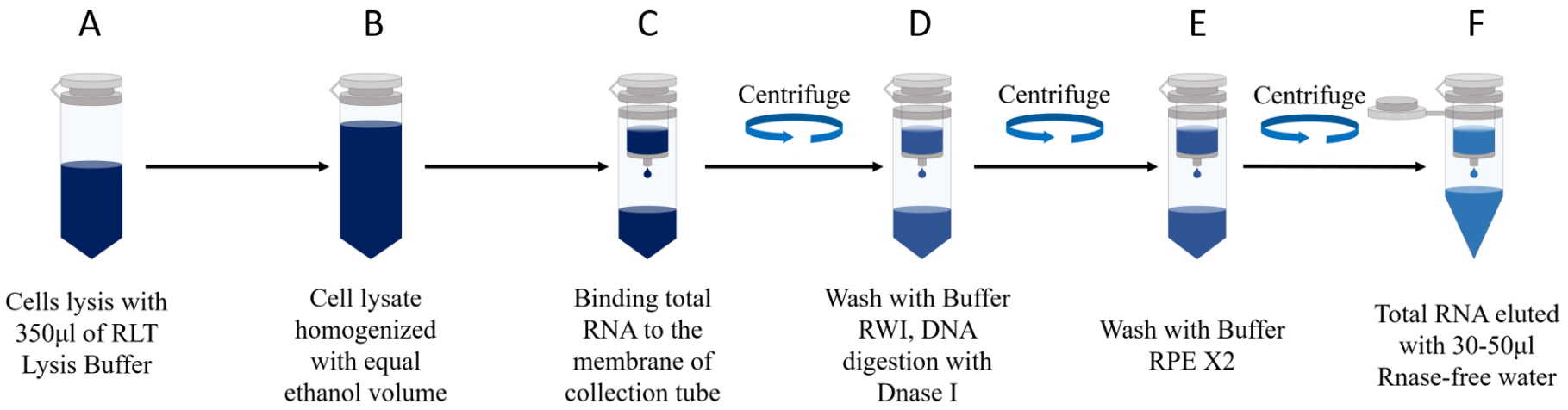

Figure 10. Illustration of total RNA extraction process from cell suspension for downstream sq-RT-PCR analysis. Following cell lysis with Buffer RLT (A), equal volume of 70% ethanol added to homogenise cell lysate. 700µl of homogenised mix was transferred to spin column mounted on 2ml collection tube and centrifuged at 10000rpm for 30sec (C). This followed by adding Buffer RW1 and centrifuging at 10000rpm for 30sec. Then DnaseI added for 15min at room temperature and washing again with Buffer RW1 (D). Total RNA finally washed twice with Buffer RPE and centrifuged at 10000rpm for 30sec and 2min (E), before eluting total RNA with Ranse-free water to 1.5ml collection tube (F). Flow through discarded after each centrifuging step.

4.1.8: Sq-RT-PCR amplification reaction

For analysis, 1µl of single-stranded cDNA template, containing ~50ng, was combined with 24µl RedTaq mastermix consisting of 12·5µl RedTaq ready reaction mix (Sigma, UK), 9·5µl dH2O, 2µl of 25µM forward and reverse primer. Details and primer sequences used for PCR assay are listed in Table 7 and Table 8. For primer design, accession number for each primer, after specifying species, were obtained from NCBI (http://www.ncbi.nlm.nih.gov/pubmed) or iHOP database (http://www.ihop-net.org/UniPub/iHOP/). These accession numbers were used to design the primers using online tool (https://www.ncbi.nlm.nih.gov/tools/primer-blast/index.cgi?LINK_LOC=BlastHome).

Templates of cDNA were amplified in a thermal cycler (Mastercycler, Eppendorf, Germany), in a range between 18-40 cycles. Each cycle consisted of an initial denaturation step which lasted for 5min at 94°C, which was followed by an amplification cycle consisting of 94°C for 20sec, 60–61°C for 20sec and 72°C for 20sec ending with a 10min extension at 72°C.

For initial experiments, 6µl of the reaction was collected, after the designated number of cycles, and stored in a 96-well plate on ice until all cycles have finished. Samples were transferred to a 1.5% agarose gel, 0.9g of agarose in 60mls 1x TAE buffer, containing 0·5µg/ml ethidium bromide (Sigma, UK). Gels, containing DNA ladder for sizing amplification products, were electrophoresed for 30min at 120V to separate reaction products then placed in UV box to be visualised. After image capture of the gels using GeneSnap software (Syngene, USA) they were analysed using GeneTools software (Syngene, USA), data were exported to Excel (Microsoft, US). Volume and density of PCR products were calculated and normalised against the housekeeping gene, Glyceraldehyde 3-phosphate dehydrogenase (GAPDH) control.

Gene name	Gene symbol	Supplier	Accession number	Sequence (5' → 3')	T_m (°C)	Product (bp)	Number of cycles
Glyceraldehyde-3-phosphate dehydrogenase	GAPDH	Invitrogen	AJ005371	F-TCT AGA CGG CAG GTC AGG TCC R-CCA CCC ATG GCA AAT TCC ATG	60	597	18,21,24,27
Interleukin-1beta	IL-1β	Thermohybaid	NM_000576.2	F-TCC AGG GAC AGG ATA TGG AG R-TTC TGC TTG AGA GGT GCT GA	61	292	25
Interleukin-8	IL-8	Thermohybaid	NM_000584.2	F-TAG CAA AAT TGA GGC CAA GG R-GGA CTT GTG GAT CCT GGC TA	61	204	30
Transforming growth factor beta-1	TGF-β1	Invitrogen	NM_014266	F- CGCCTTAGCGCCCACTGCTCCTGT R-GGGGCGGGACCTCAGCTGCAC	60	533	30
Tumor necrosis factor-α	TNF-α	Thermohybaid	NM_000594.2	F-AAG AAT TCA AAC TGG GGC CT R-GGC TAC ATG GGA ACA GCC TA	60	402	38
Epidermal growth factor	EGF	Invitrogen	NM_001963	F-CTTGGGAGCCTGAGCAGAAA R-TGGTTGTGGTCCTGAAGCTG	60	521	32
Matrix metallopeptidase 9	MMP-9	Invitrogen	NM_004994.2	F- TTCGACGGGAAGGACGGGCT R- ACCGTCGAGTCAGCTCGGGT	60	470	31
Matrix metallopeptidase 13 (collagenase 3)	MMP-13	Invitrogen	NM_002427	F-TAT GAC TAT GCG TGG CTG GA R- TCT GTG TGA AGA AGG GCA CA	60	395	29
Matrix metallopeptidase 2	MMP-2	Invitrogen	NM_013035	F- CCTCATCTTTGGGGCGTGTA R- GCAGCCAGACTCCTCATGTT	61	554	34
β-catenin	CTNNB1	Invitrogen	NM_001904	F- GCGCCATTTTAAGCCTCTCG R- ATTGCACGTGTGGCAAGTTC	60	682	28
Lymphoid enhancer-binding factor 1	LEF-1	Invitrogen	NM_001166119	F-CGGGCGATAGAGCTGGTAAC R- GATGTTCTCGGGATGGGTGG	60	577	28
N-cadherin	CDH2	Invitrogen	NM_001792.3	F-GCCCGGTTTCATTTGAGGGCACA R-TGACGGCCGTGGCTGTGTTT	60	418	35
E-cadherin	CDH1	Invitrogen	NM_004360	F-CAAGTGCCTGCTTTTGATGA R-GCTTGAACTGCCGAAAAATC	60	339	34
Vimentin	VIM	Thermohybaid	NM_003380.3	F-CGGGAGAAATTGCAGGAGGA R-ACGAAGGTGACGAGCCATTT	60	588	31

Fibroblast specific protein-1	FSP-1	Thermohybaid	NM_002966.1	F-AAA TTC GCT GGG GAT AAA GG R-TCT TAT CAG GGA GGA GCG AA	60	276	38
Snail-1	SNAl1	Invitrogen	NM_005985.3	F-CGGACCCACACTGGCGAGAAG R-CAGCTGCCCTCCCTCCACAGA	60	433	30
Snail-2 (*Slug*)	SNAl2	Invitrogen	NM_003068.4	F-CAACGCCTCCAAAAAGCCAA R- GGCCAGCCCAGAAAAAGTTG	60	400	32
Twist family bHLH transcription factor 1	TWIST1	Invitrogen	NM_000474	F- AGACCTAGATGTCATTGTTTCCAGA R-CAGGCCAGTTTGATCCCAGT	60	454	28
nuclear factor kappa-light-chain-enhancer of activated B cells	NF-κB	Invitrogen	NM_003998	F-CCT GGA TGA CTC TTG GGA AA R-CTT CGG TGT AGC CCA TTT GT	61	366	26
Toll-like receptor-2	TLR-2	Invitrogen	NM_003264.3	F-GAT GCC TAC TGG GTG GAG AA R-CGC AGC TCT CAG ATT TAC CC	61	392	31
Toll-like receptor-4	TLR-4	Invitrogen	NM_138444-2	F-AAC CAT CCT GGT CAT TCT CG R-CGG AAA TTT TCT TCC CGT TT	61	315	36
Toll-like receptor-9	TLR-9	Invitrogen	AB045180.1	F-CTG CGT CTC CGT GAC AAT TA R-GTC CTG TGC AAA GAT GCT GA	61	443	36

Table 7. Details of genes (Homo sapiens) studied, primer sequences and semi-quantitative RT-PCR conditions. Accession numbers were obtained from GenBank (Tm: Melting temperature).

Gene name	Gene symbol	Supplier	Accession number	Sequence (5' → 3')	T_m (°C)	Product (bp)	Number of cycles
Glyceraldehyde-3-phosphate dehydrogenase	GAPDH	Invitrogen	NM_017008	F- CGA TCC CGC TAA CAT CAA AT R-GGA TGC AGG GAT GAT GTT CT	60	597	18,21,24,27
Matrix metallopeptidase 2	MMP-2	Sigma	NM_031054	F- GACGGGCCGTACAATCTTCA R- AGGAGGGGAGCCATCCATAG	60	596	28
N-cadherin	CDH2	Invitrogen	NM_031333	F- CACCCGGCTTAAGGGTGATT R- CGTCTAGCCGTCTGATTCCC	60	470	36
E-cadherin	CDH1	Invitrogen	NM_002417.3	F-TTCTCCGCGCTCCTGCTCCT R-TTGTCAGCTCCTGGGCCGGT	60	385	32
Vimentin	VIM	Sigma	NM_031140	F- CCCTCGCTCTCTTCTTGCAG R- AATGACTGCAGGGTGCTCTC	60	681	32
β-catenin	CTNNB1	Invitrogen	NM_012618	F- TCTCTTGGTCTGGTCTCAACG R- AAGGCACTATGCTCACAGCC	60	400	34
Snail-1	SNAl1	Invitrogen	NM_053805	F-AGTTGTCTACCGACCTTGCG R- TGGCTTCGGATGTGCATCTT	60	587	31
Toll-like receptor-4	TLR-4	Sigma	NM_0191778.1	F-TTGAAGACAAGGCATGGCATGG R - TCTCCCAAG ATCAACCGATG	60	507	35

Table 8. Details of genes (Rattus norvegicus) studied, primer sequences and semi-quantitative RT-PCR conditions. Accession numbers were obtained from GenBank (Tm: Melting temperature).

4.2: Human EMT PCR-array

The real-time PCR based assay, profiles the changes in the gene expression of 84 EMT-related key markers. The RT2 profiler EMT PCR-array kit was purchased from QIAGEN, UK and includes the following components:

- RT^2 First Strand Kit, consists of Buffer GE, 5x Buffer BC3, RE3 Reverse Transcriptase Mix, Control P2, RNaes-free water
- RT^2 SYBER Green qPCR Mastermix
- PCR-array plate (96-well format)

4.2.1: cDNA synthesis

Total RNA previously harvested from H400 cells as described in section 4.1.3, was utilised as a template to synthesise cDNA using the First Strand Kit. Following manufacturer's instruction, 0.5µg total RNA (containing at least 100ng RNA) was used. All incubations were performed by using a thermal cycler (Mastercycler, Eppendorf, Germany).

Genomic DNA elimination mix, for each sample, was prepared by adding total RNA to 2µl of Buffer GE and a range of volumes of RNase-free water to make up to a 10µl total volume. The mix was incubated for 5min at 42°C followed by immediate placement on ice for at least 1min.

A total volume, 10µl, of reverse transcription mix (volume for 1 reaction) was prepared (Table 9) and added to the previously synthesised 10µl genomic DNA elimination solution. The mix was incubated at 42°C for exactly 15min, the reaction then was stopped by incubating at 95°C for 5min. RNase-free water, 91µl, was added to each reaction to make cDNA synthesis reaction. At this stage the reaction can be proceeded to real-time PCR or stored at -20°C to be used later.

4.2.2: Real-time PCR protocol for EMT-array

All reagents and PCR components were combined to prepare a total volume of 2700µl in a 5ml tube (Table 9).

The PCR component mixture was dispensed into a 96-well plate, at 25µl/well, using 8-channel pipettor (Gilson, USA). The multiwell plate was tightly sealed with adhesive film then loaded into a thermal cycler (LightCycler® 480, ROCHE, Switzerland). Cycling conditions were 1 cycle at 95°C for 10min, followed by 45 cycles at 95°C for 15sec, then terminated by incubation at 60°C for 1min. Results were collected using the LightCycler 480 software and analysed later by using online tool at Qiagen website (www.SABiosciences.com/pcrarraydataanalysis.php).

Reverse transcription mix	
Reagent	**Volume (µl)**
5x Buffer BC3	4
Control P2	1
RE3 Reverse Transcriptase Mix	2
RNase-free water	3
PCR components mix	
Reagent	**Volume (µl)**
2x RT^2 SYBER Green Mastermix	1350
cDNA synthesis reaction	102
RNase-free water	1248

Table 9. Table showing composition of (a) Reverse transcription mix and (b) PCR component mix used in the EMT-array.

5: Enzyme-linked immunosorbent assay

In this study, three cytokines (TGF-β1, TNF-α and EGF) which have been reported as being key EMT promoters (Maschler et al., 2005, Yan et al., 2010, Buonato et al., 2015) were selected for investigation. The presence of these markers was analyzed in archived supernatants from H400 cells exposed to bacteria (section 3.1.1). All cytokines levels were measured using ELISA kits purchased from R&D systems (Quantikine ELISA, USA). Components of ELISA kit, used in this study, are as described in Table 10.

Component	Description
Microplate (96-well format)	Coated with a monoclonal antibody against the human cytokine to be assayed
Standard solution	recombinant human EGF, TGF-β1, and TNF-α
Conjugate solution	Polyclonal antibody against chosen cytokines, conjugated with horseradish peroxidase
Assay diluent	Buffered protein base
Calibrator diluent concentrate	Buffered protein base with different concentrations
Calibrator diluent	Animal serum prepared by adding Calibrator Diluent Concentrate to deionised or distilled water
Wash buffer concentrate	Concentrated, 25-fold, buffered surfactant, deionised or distilled water used to prepare final volume of 500ml.
Colour reagent A	Stabilised hydrogen peroxide
Colour reagent B	Tetramethylbenzidine (stabilised chromogen)
Stop solution	Either 2N sulfuric acid or diluted hydrochloric acid

Table 10. Details of components of ELISA kits (R&D Systems, UK) used to assay for TGF-β1, TNF-α and EGF levels in the supernatants of H400 cell cultures.

5.1: ELISA protocol

5.1.1: Sample activation (for TGF-β1 only)

TGF-β1 is secreted in latent form, which is the most predominant, and active form that has a relatively short half-life of ~2min (Clarke et al., 2011). Commercially available ELISA kits cannot recognize the latent form and thus this molecule requires acid activation of TGF-β1 in the sample before performing the assay. Hence for each 100µl of cell culture supernatant, 20µl of 1N HCl, was generated by slowly adding 8.33ml of 12N HCl to 91.67ml of deionised water, and this was combined with samples and incubated for 10min at room temperature. The acidified mixture was then neutralised by adding 20µl of 1.2N NaOH/0.5M HEPES, 12ml of 10N NaOH added to 75ml of deionised water and 11.9g HEPES. The samples are then assayed immediately and as the samples were diluted the final concentration must be adjusted by multiplying by 1.4.

5.1.2: Assay procedure

After preparing all reagents, working standard, and samples, 50µl of Assay Diluent was added per well followed by adding standards and samples (50µl for TGF-β1, and 200µl for TNF-α and EGF) then incubated for 2hr at room temperature. The plate was then washed,

using an autowasher (Biotek EL_X50, USA), four times with wash buffer. Cytokine Conjugate then was added (100µl for TGF-β1, and 200µl for TNF-α and EGF) and incubated for 2hr at room temperature. Substrate solution, Colour reagents A and B were mixed 15min prior to use, and added to the microplates. The reaction was protected from light by wrapping microplates with tin foil and further incubated for 20min at room temperature. The reaction was stopped by adding 50-100µl of stop solution to each well.

5.1.3: Determining Cytokine levels

The optical density was determined within 30min of adding the stop solution using a microplate reader (Biotek EL_X800, USA) at a wavelength of 450nm. The absorbance value of a blank well was subtracted from the absorbance of all standards and samples assayed. The results obtained for the standards were used to produce a calibration curve by using Microsoft excel to plot the mean absorbance of each standard on the Y-axis against the log concentration of the standard on the X-axis (Figure 11). The regression equation generated from the calibration curve was utilised to determine cytokine concentrations for TGF-β1, TNF-α and EGF in the samples. Final concentrations (pg/ml) of TGF-β1 were determined by multiplying by 1.4 to compensate for dilution by the activation solution.

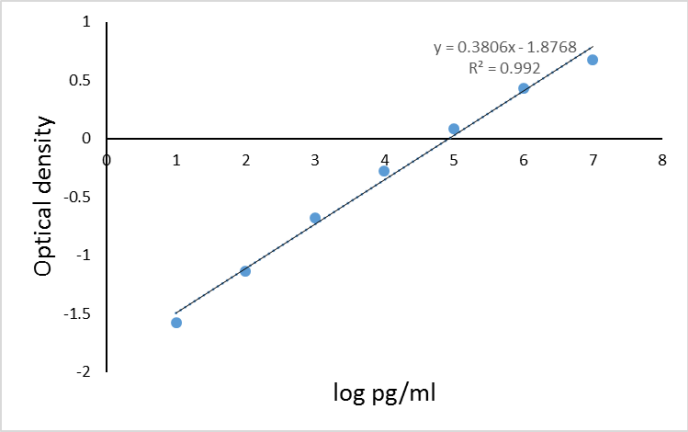

Figure 11. Example of ELISA-standard curve produced by plotting log of mean of absorbance of each standard on the Y-axis against the log of concentration on the X-axis. The resulted linear regression equation was calculated (shown on graph) and used to determine the cytokines concentrations in the culture supernatants. Experiments were run in triplicate.

6: Immunofluorescence staining

Immunofluorescence (IF) is a laboratory technique used to identify the presence of a particular antigen in cells in culture or in a tissue sample. It utilises an antigen-antibody interaction where the antibodies are labelled with a fluorescent dye thereby allowing specific antigen detection using fluorescence microscopy. In this thesis, an indirect IF technique was used which utilises a secondary antibody, labelled with a fluorophore, specific to the primary antibody investigated. The indirect technique involves more steps and is more time-consuming than the direct method, however, indirect IF has the advantage of signal amplification as the number of fluorophore molecules per antigen is higher than for direct IF (Cowin et al., 1986).

6.1: Culture and stimulation of keratinocytes for immunofluorescence

Primary oral keratinocytes and H400 cell cultures were established by seeding $1x10^3$ cells on pre-sterilised glass coverslips (22x22mm) placed in 6-well plates containing DMEM supplemented with 10% FCS for 8 days. Cells were allowed to adhere overnight and then stimulated separately with bacterial components, as described in section 2.3, for 8 days and E-cadherin and vimentin IF detection performed.

6.2: Negative control

A negative diluent control was generated by omitting the primary antibody. This control was used for calibrating the baseline setting of the microscope and to exclude the possibility of non-specific binding of the secondary antibody to the sample. Expected results were that no signal would be recorded during image acquisition for the negative control. These settings were utilised as the threshold for examination of all subsequent images to exclude false-positive signals by the secondary antibody.

6.3: Positive control

Cultures stimulated with 20µg/ml *E. coli* LPS were used as a positive control based on data from previous studies which indicated that LPS is a strong EMT-inducer and is associated with up-regulation of vimentin expression (Jing et al., 2012). Therefore, the expected results from cells treated with this stimulant are increased expression of vimentin and decreased expression levels of E-cadherin.

6.4: Staining procedure

Initial experiments were performed to determine the optimal antibody dilution. In addition, the optimal concentrations of blocking buffer and permeability solution were also confirmed in this experiment. Details of antibodies used in these studies are provided in

Table 11. All polyclonal antibodies used for immunostaining (IF and ICC) were from the same patch to avoid discrepancies in results. Cultures were prepared for immunofluorescence staining by first removing media and washing for 2min with PBS, this was then followed by fixing in 4% paraformaldehyde (Sigma, UK) for 15min at room temperature. The fixative solution was then removed by aspiration and cultures again washed twice with PBS. Cells were permeabilised with 0.25% Triton X-100 (Sigma, UK) in PBS 10-15min at room temperature. Washing twice with PBS was repeated prior to the blocking of non-specific binding of antibodies. Cultures were flooded with blocking buffer (5% BSA in PBS) for 1hr at room temperature. This was immediately followed by incubation with the primary antibody, i.e. Anti-E-cadherin or Anti-Pan-Cytokeratin, and Anti-vimentin, overnight at 4°C.

Subsequently samples were flooded with washing buffer and washed three times, 20min each, using PBS-Tween (0.1%) wash buffer to remove unbound primary antibodies. Secondary antibodies were applied in a darkened room for 1hr at room temperature, antibodies used were FITC-conjugated and TRITC-conjugated for immunofluorescence.

After incubation, samples were washed with PBS three times, 10min each. Samples were dried by gently decanting coverslips onto a piece of absorbent tissue. The cell nuclei were counter-stained with DAPI (Fluoroshield, Sigma, UK) and images captured using a confocal microscope (Zeiss, Germany). Analysis was performed on 5 random fields of view; clusters of cells expressing vimentin were selected, for each group to determine the number of vimentin positive cells in the total cell number.

The same staining procedure described above, using the same antibodies, was repeated on 3T3 cells, which were used as feeder layers for primary cells as previously described, to check the cross-reactivity of the primary antibodies which may result in false-positive results.

Antibody	Type	Supplier	Code	Species of origin	Reactivity	Dilution
Anti-pan-Cytokeratin	Primary	Santa Cruz Biotechnology	sc-15367	Rabbit polyclonal IgG	Human, rat	1:100
Anti-Vimentin	Primary	Santa Cruz Biotechnology	sc-373717	Mouse monoclonal IgG	Rat	1:100
Anti-Vimentin	Primary	Santa Cruz Biotechnology	sc-53464	Mouse monoclonal IgG	Human	1:100
Anti-E-cadherin	Primary	Santa Cruz Biotechnology	sc-7870	Rabbit polyclonal IgG	Human, rat	1:100
IgG-FITC	Secondary	Santa Cruz Biotechnology	sc-2365	Bovine	Anti-rabbit	1:200
IgG-TRITC	Secondary	Santa Cruz Biotechnology	sc-3796	Goat	Anti-mouse	1:200

Table 11. Details of primary antibodies and dilution factor utilised in immunofluorescent staining.

7: Immunocytochemistry

The principle of immunocytochemistry (ICC) is similar to that of the IF technique (section 6), except the fluorophore, in IF, is replaced with marker that enables the target antigen to be directly visible to the naked eye under light microscopy. In this thesis, activation of two proteins, NF-κB and Snail-1 were studied. Their role in EMT-induction was previously reviewed (section 4.2 for NF-κB) and (section 3.4 for Snail-1). Details of antibodies used are provided in Table 12. The principle of the ICC technique used in this thesis is illustrated in Figure 12.

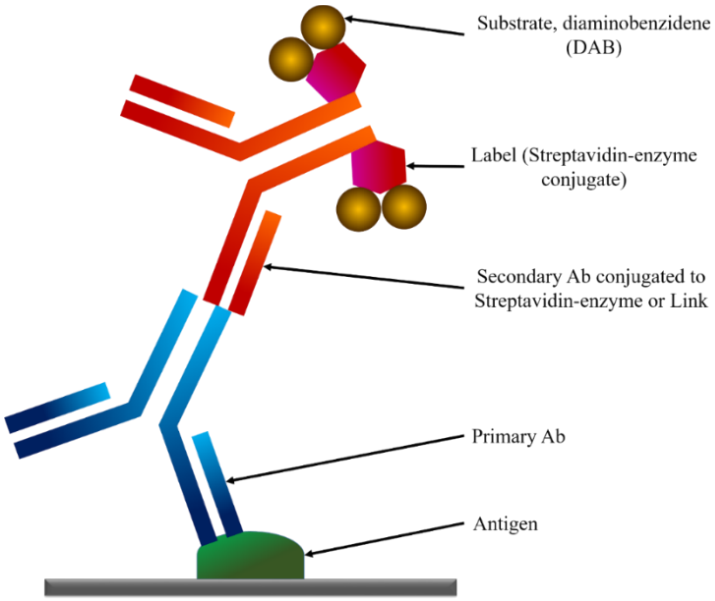

Figure 12. Diagrammatic illustration of ICC technique utilised for Snail and NF-κB staining.

Antibody	Type	Supplier	Code	Species of origin	Reactivity	Dilution
Anti-Snail	Primary	Abcam	ab180714	Rabbit polyclonal	Human, rat	1:100
Biotin-conjugated IgG	Secondary	Abcam	ab6720	Goat	Anti-rabbit	1:200
Anti-Ki67	Primary	Abcam	ab15580	Rabbit polyclonal	Rat	1:100
Anti-Ki67	Primary	NovacastraTM	NCL-L-Ki67-MM1	Mouse	Human	1:100
Anti-NF-κB p65 subunit	Primary	Santa Cruz Biotechnology	sc-8008	Mouse monoclonal IgG	Human, rat	1:100

Table 12. Details of antibodies and dilutions used for ICC.

7.1: Cell culture preparation for ICC staining

Cultures were established on 4-well slides (Hedley-Essex, UK) placed in pre-sterilised glass petri-dish containing 15ml of DMEM supplemented with 10% FCS. Each slide was divided into the experimental group, negative control, and positive control. The inclusion of positive and negative control in each slide was to determine the success of the staining procedure.

7.2: Positive control

This control was used to ensure that the staining procedure worked appropriately. Cells were treated with a monoclonal antibody to the Ki-67 nuclear protein. This protein is not expressed in the cytoplasm and therefore brown staining should be confined to the nucleus as is shown in Figure 13A; therefore, any staining in the cytoplasm indicates cross contamination between wells of primary antibody or unspecific binding.

7.3: Negative control

Cells were treated with 1% BSA in PBS instead of a primary antibody and secondary antibody, therefore the cells should not show brown staining otherwise this would indicate cross contamination of antibody or a lack of specificity in the staining system (Figure 13B).

7.4: Experimental groups

Each slide was treated either with media only, whole dead bacteria or *E. coli* LPS. Activation of NF-kB or Snail is characterised by translocation from the cytoplasm to the nucleus, therefore DAB staining in the nucleus indicates activation of NF-kB or Snail depending on the primary antibody used (Figure 13C). Cells where NF-kB or Snail is not activated will result in DAB staining being visible in the cytoplasm (Figure 13D).

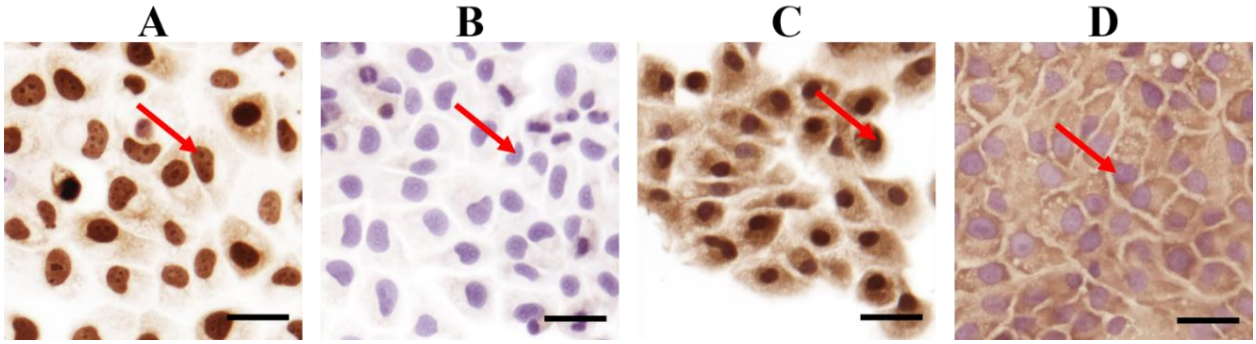

Figure 13. Results of ICC staining (red arrows) showing (A) positive control demonstrating DAB staining localised to the nucleus characteristic of Ki67 staining, (B) negative control demonstrating an absence of DAB staining, (C) stimulated cells with bacteria showing DAB stained nucleus indicating Snail or NF-κB activation, and (D) Cells treated with media only showing cytoplasmic DAB-stained NF-κB without translocation to the nucleus. Scale bars=30μm.

7.5: Culturing and stimulation of keratinocytes for Snail and NF-κB ICC

H400 and primary oral epithelial cells, were seeded, 4 x 10^5 cells, on pre-sterilised 4-well slides. These were then placed in glass petri dishes containing 15ml DMEM and cultured for a total of 5 days until they reached ~80 % confluency with the media changed after 4 days of initial seeding. On the day of analysis, for NF-κB, used growth media was removed and carefully replaced with 15ml of fresh medium. The media added was either DMEM supplemented with 10% FCS or the same media containing the relevant bacterial stimuli (section 2.3). Cultures were then re-incubated for 1hr to obtain maximum NF-κB activation (Coons et al., 1942, Nelson et al., 2004), followed by washing, fixing and drying. The resulting slides were than stained for NF-κB. For Snail, cells were cultured in the same way except that stimulation began from day 1 through until day 8. This difference in time of measurement for these two proteins was because Snail-1 translocates to the nucleus as long in the presence of stimulation. In contrast, activity of NF-κB peaks to its highest level in a relatively short time period, 1hr, and subsequently is then recycled to the cytoplasm regardless of the presence of the stimulation present (Coons et al., 1942, Nelson et al., 2004).

7.6: Protocol for NF-κB immunocytochemical staining

The staining process was performed by using the Super Sensitive™ Link-Detection Kit (BioGenex, USA). Reagents used are described in Table 13.

Reagent	Description
Link	pre-diluted biotinylated anti-immunoglobulins for primary antibodies
Label	horseradish peroxidase-conjugated streptavidin in PBS with carrier protein
Chromogen	3,3'-diaminobenzidine (DAB) chromogen solution
Substrate	hydrogen peroxide substrate solution

Table 13. Reagents used in the Super Sensitive™ Link-Label IHC Detection System.

Following stimulation cultures were stained simultaneously in all experimental groups to facilitate consistency of the results.

1. Cultures in glass petri-dishes were washed with PBS to remove residual media then fixed with acetone (Sigma, UK) for 15min at room temperature in a fume hood. Petri-dishes were covered with their lids to prevent evaporation of acetone. Slides were removed and allowed to air dry for 10min.

2. After fixing the cells, wells in each slide were circled using a water-repellent PAP pen (Sigma, UK) which helps to keep solutions within the wells and minimise the possibility of cross contamination of different antibodies between wells.

3. Cultures in wells designated as experimental and positive controls were treated with 100µl of Anti-NF-κB and Anti- Ki-67 primary antibodies, respectively. While cultures in the negative control well were treated with 100µl of 1% BSA in PBS only.

4. Cultures were then incubated in a humidity box for 1hr at room temperature. Slides were then washed in PBS for 2min (3 times).

5. Each well was then flooded with 2-3 drops of ‘Link’ reagent and incubated for 20min in a humidified box.

6. Slides were again washed as described in step 5 then horseradish peroxidase-conjugated streptavidin, 2-3 drops, were added to each well ensuring that the whole well was covered and incubated for 20min at room temperature.

7. DAB reagent was freshly prepared by adding 2 drops of 'Chromagen' to a 2.5ml vial of 'Substrate Buffer'. Washing process described in step 5 was repeated and 2-3 drops of DAB reagent was added to each well and incubated for 5min at room temperature.

8. Slides were washed under running water, to remove DAB reagent for 2min and then counterstained with Mayer's haematoxylin (BioGenex, USA) for 5min.

9. Slides were then washed in running deionised water for 2min, followed by dehydration through graded alcohol baths and finally cleared in xylene (Sigma, UK). Slides then were mounted in XAM mounting medium and kept horizontally in the dark overnight to allow the mounting medium to set.

7.7: Quantification of NF-κB translocation

The slides were viewed under phase contrast microscopy (Primo Vert, Zeiss, Germany), fitted with an eyepiece graticule divided into 10x10 squares, and using x10 objective lens. Cells with p65 NF-kB staining, defined as brown staining in the nuclei with clear cytoplasm, were determined as showing NF-kB activation and were counted as positive. In situations where staining was unclear these cells were recorded as negative to avoid over estimating NF-kB activation.

To determine a suitable number of fields for counting, Hunting curves were used (Davenport et al., 2002). This was achieved by plotting cumulative cell count per square against field number. i.e. adding the 1st square count to the 2nd and divided by 2 and subsequently repeating this process. The point at which the curve became stable indicated the field number which needs to be counted. Initial analysis of 4 slides indicated that the counts from a total of

19 microscopic fields, randomly selected, were required to provide an accurate estimate of the percentage of NF-κB-positive cells. Figure 14, shows an example Hunting curve. All cells counted within a 19 graticule area were recorded as positive or negative. For each sample, the percentage of cells expressing NF-κB activation was determined by using total and mean number of positive cells.

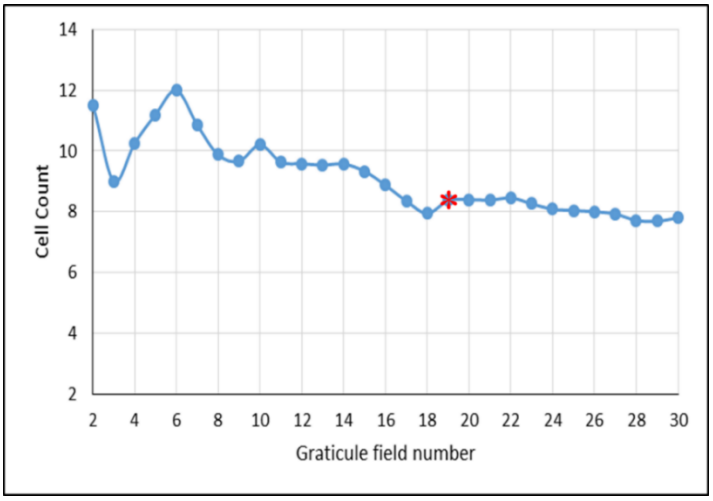

Figure 14. Example of Hunting curve showing cell counts plotted against cumulative mean of percentage of positively stained cells showing 19 counts (red asterisk) of 30 cells is sufficiently representative for quantification of NF-κB activation.

7.8: Protocol for Snail ICC staining and quantification

The stepwise protocol used for Snail activation analysis is described below.

1- Slides were washed rapidly with ice cold PBS. Then cultures were fixed with 4% paraformaldehyde for 10-15 min and washed again with PBS.

2- Cultures were incubated with anti-Snail antibody for 1hr at room temperature.

3- Slides were washed with 5µl Tween20 in 5ml PBS, for 10min (3 times) on a slow orbital mixing platform during washing to gently agitate the washing solution.

4- Cell-conjugated with primary antibody were then incubated with the biotin-conjugated secondary antibody for 1hr at room temperature.

5- The remainder of the staining procedure was performed as described in steps 7-9 in section 7.6.

Images were captured by using phase contrast microscopy (Olympus BX50, Japan) equipped with a digital camera and liquid crystal RGB filter (QImaging Retiga2000 R camera, Canada). The percentage of cells with positive Snail activation was determined by counting the cells expressing a dark brown nuclear stain relative to the total number of the cells in the field viewed. Quantification of the number of Snail-positive cells was performed as described above in section 7.7.

8: Transepithelial electrical resistance

This method was first introduced in mid-1980s by World Precision Instruments (WPI). It can be described as a non-destructive and reliable measurement technique used to monitor and assess growth and integrity of epithelial sheets *in vitro*. This technique is based on measuring the electrical resistance of epithelial monolayers to the passage of an electric current. This resistance is decreased upon losing cellular attachment. This results in increase in intercellular spaces which permits passage of electrical current more easily than coherent, intact epithelial sheet.

8.1: Epithelial Voltohmmeter (EVOM2), components and principle of action

The device used measured the epithelial sheet integrity and was called the EVOM2 (WPI, USA) and is an AC-based volt ohmmeter. This device has two main components, the meter itself (Figure 15) and the STX2 electrode set (Figure 16).

For measuring epithelial layer impedance, the inner pair of STX2 probe is placed in the tissue culture insert containing the epithelial sheet, the other pair (outer) is positioned in the well.

Resistance is measured between the two electrodes. Increased electrical resistance of epithelial layer develops as the epithelial monolayer develops and becomes confluent at which point it shows maximum resistance indicating an intact epithelial barrier. Figure 17, demonstrates the principle of Transepithelial electrical resistance (TEER) measurement of epithelial sheets grown on tissue culture inserts.

Figure 15. The EVOM2 meter used for assessment of epithelial integrity (A) instrument control panel, (B) EVOM2 assembled with STX2 probe.

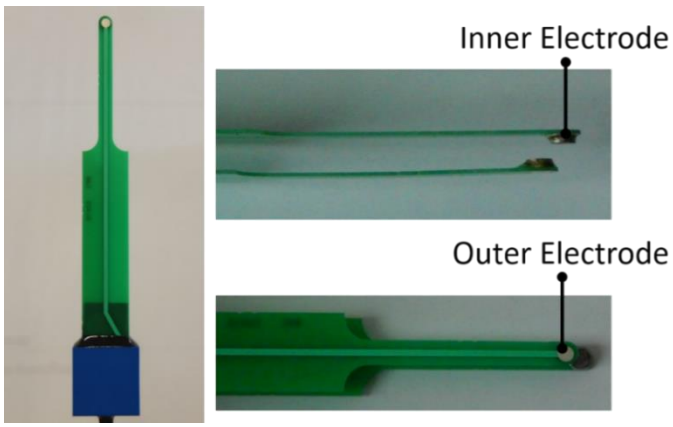

Figure 16. The electrodes of STX2 probe, the electrodes are of different lengths to accommodate the cell culture insert. When placed in the wells the electrodes are used to measure electrical resistance across the epithelial monolayer.

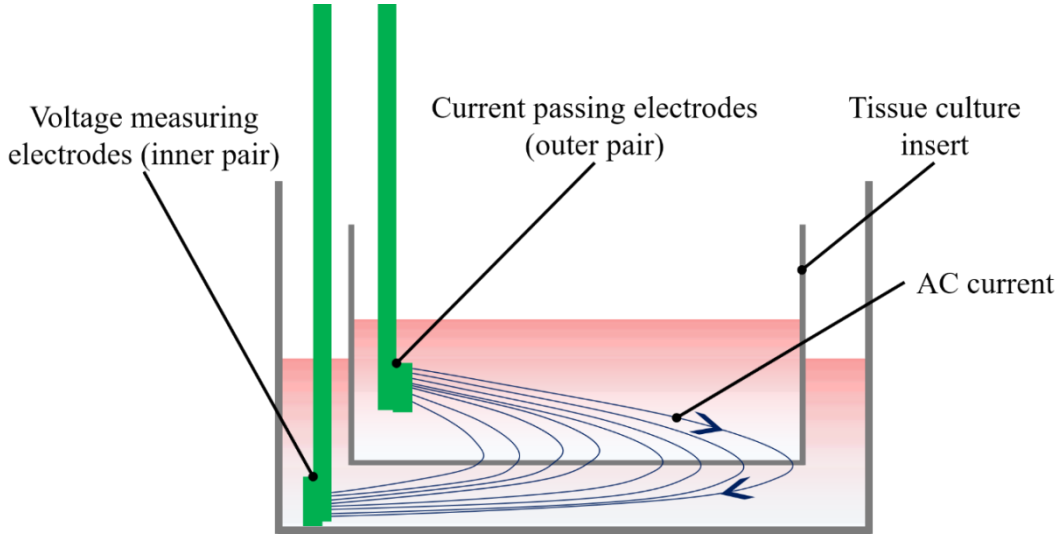

Figure 17. Diagram of TEER used to measure resistance across an epithelial monolayer.

8.2: Culture preparation for TEER

H400 and primary oral epithelial cells, under investigation were seeded ($7x10^4$ cells) in the upper chamber of tissue culture inserts supplied with 0.4µm pore membrane (Greiner bio-one, Germany) mounted in a 24-well plate (Sume et al., 2010). Media, 200µl, was added to the upper chamber and 500µl was added to the lower compartment of each well.

The resistance of the epithelial layer was checked daily until stable recordings were observed from all cultures which indicated that cells had formed confluent monolayers covering the whole insert membrane. This was considered the baseline reading. The presence of incomplete epithelial monolayer resulted in a decrease in resistance to a value very close or equal to the blank reading. Once a constant baseline reading was obtained (~2-3 days), cells were stimulated with bacterial components. TEER resistance values (Ω) were then recorded three times for each well over a 5-day period with 'true epithelial sheet resistance' for each reading calculated according to the formula

$R_{true\ tissue} = R_{Total} - R_{blank}$

The final readings were averaged and compared with unstimulated controls. Experiments were repeated in triplicate.

9: Transwell migration assay

This assay was originally developed by Dr. Stephen Boyden in 1961 to quantify cell migration. The set-up of this assay consists of tissue culture inserts equipped with a porous membrane placed in multiwell plates thereby dividing the well into upper and lower compartments. Then cells seeded on the membrane in the upper compartment and chemoattractant agent is placed in the lower chambers. Following incubation, cells that have migrated to the lower compartment are fixed and counted.

9.1: Cell cultures used for transwell migration assay

Epithelial cells were seeded ($5x10^4$) in T75 flasks and either stimulated (bacterial components) or unstimulated for 8 days, until they reached ~80-90% confluency. Tissue culture inserts (Greiner Bio-One, Germany) containing 8µm-pore membranes were mounted in a 24-well plate. Cells were trypsinised and $2.5x10^5$ cells were seeded in 300µl FCS-free media on the upper compartment of the tissue culture insert. In the lower chamber of each well, 700µl of media supplemented with 10% FCS was added. Cultures were incubated at 37°C and 5% CO_2 for 12hr.

9.2: Transwell migration assay procedure

The stepwise approach for the migration assay is provided below

1- Media were removed from the inserts and washed twice with PBS.
2- Cells present on the inserts were fixed with 100µl of 4% paraformaldehyde for 2min at room temperature.
3- Cells were permeabilised with 100% methanol for 20min at room temperature.

4- The Giemsa stain (Sigma, UK), a stain that specifically binds to phosphate group of DNA, was added to each well and the plate was wrapped with tin foil and incubated for 15min at room temperature.
5- Non-migrated cells in the upper chamber of the membrane were removed using a cotton swab (Schaeffer et al., 2014). Migrated cells, as indicated by a dark violet colour, present in the lower part of the membrane were counted under phase contrast microscopy (Primo Vert, Zeiss, Germany) using 4 random fields, one field from each quadrant of view.

10: Scratch assay

The ability of EMT to increase cells migratory ability was further investigated by using the scratch assay. This is a relatively simple and low-cost assay frequently used to assess cell migration *in vitro*. The principle of this method is based on inflicting an artificial gap in the confluent monolayer, the cells on either edge of this scratch will move towards each other in attempt to bridge this defect. Any factor increasing the migratory ability of the cells can be detected by an increased rate of gap-closure (Cory, 2011).

10.1: Preparation of cultures for scratch assay

H400 or primary oral keratinocytes, were seeded ($1x10^3$) in 6-well plates, each well containing 5ml of media (consisting of DMEM and 10% FCS), and either treated with culture media only or supplemented with bacterial components until reaching a confluent monolayer after 8 days.

10.2: Scratch assay procedure

A straight scratch-wound was produced on the confluent cell monolayer using a 10μm sterile pipette tip (Bao et al., 2012). The pipette tip was dragged across the monolayer using a ruler as a guide over the centre of the well to ensure production of a consistent straight line.

Cultures were rinsed with 1ml of PBS to remove cell debris and followed by the addition of 5ml of FCS-free medium per well. To ensure a consistent orientation of the scratch wound a reference point was created on the outer bottom of each well, either by etching the plastic using a sharp blade or with a fine permanent marker (Liang et al., 2007). The resulting cultures were viewed under x10 objective of phase contrast microscopy (Primo Vert, Zeiss, Germany) using the reference marks as a guide for orientation. Initial images (0hr) were captured, cultures were returned to the incubator and further images acquired after 12 and 24hr (for H400 cells), and 36hr (for primary oral keratinocytes). Notably the scratch wound in the H400 cells was closed more rapidly compared with the primary cells.

The images captured for each sample were analyzed quantitatively using Java-based ImageJ software (Rasband, 2016). Images were imported to ImageJ and scale bar was identified by using set scale function, then grid tool was used to place grid over the image and width of the gap was measured by drawing 10 lines across gap area following grid lines. The experiment was repeated in triplicate.

11: Experimental design using an insert-barrier approach

Wounds were generated in epithelial cultures either by scratching using a 10µl pipette tip or by utilising an insert-barrier. Conventional wound-healing assays have generally utilised the physical scraping of a confluent monolayer to investigate migration. This physical injury induces migration reportedly mainly due to release of cytokines, as part of haemostasis, and due to lack of contact inhibition (Guo and DiPietro, 2010). The purpose of using the insert-barrier in this experiment however was to exclude the effect of physical injury, which could have modulated the response of the cells to bacterial stimuli and to investigate the effect of each bacteria (*P. gingivalis* and *F. nucleatum*) alone on the migratory behaviour of the H400 oral epithelial cells.

11.1: Generating a 'gap-wound' in confluent H400 monolayer cultures by using an insert-barrier

H400 oral keratinocytes in culture were stimulated with the different bacterial components. Two-well tissue culture inserts (ibidi, Germany) were placed in sterile 35mm petri-dishes and gently pressed until the lower adhesive side was securely attached to the plastic surface. Cultures previously treated with media alone or heat-killed bacteria (*P. gingivalis* and *F. nucleatum*), or 20μg/ml *E. coli* LPS for 8-days were trypsinised to dissociate cells before reseeding $5x10^3$ cells in each well containing the insert and allowed to form confluent monolayers (2 days culture) prior to removal of the insert. Images were captured immediately after removal of the inserts (0hr), then at 12, 24, and 36hrs, then analysed by using ImageJ as previously described in scratch-assay. Experiments were performed in triplicate.

11.2: Preparing tissue culture samples for scanning electron microscopy analysis

The aim for using electron microscopy was to visually investigate physical damage inflicted on epithelial monolayers by using conventional scratch-assay or insert barrier. Media were removed and cells fixed using 2.5% glutaraldehyde (Sigma, UK) for 30min at room temperature. The fixative was removed and cultures were dehydrated with graded ethanol concentrations (30, 50, 70, 80, 90, 100 and 100%, 10min each) and cultures were dried by adding Hexamethyldisilazane (HDMS) (Sigma, UK) using a syringe and needle in a fume hood. The samples were left overnight to air dry and then mounted onto 25mm aluminum stubs using copper tape and gold sputter coated (K550X, EMITECH, UK) at 25mA for 2min. Then samples were transferred to the SEM (EVO/MA10, Zeiss, Germany) to be observed at a range of magnifications.

12: Statistical analysis

The reproducibility of the automated cell counter was estimated by using the coefficient of variation. Linear regression equation was calculated by using Microsoft Excel and was used

to determine bacterial concentration and level of cytokines in supernatants of cultures. Comparison of multiple groups was performed by ANOVA test followed by *post-hoc* test using statistic package (IBM SPSS Statistics, USA). A significant level was considered when $P \leq 0.05$.

DEVELOPING A TWO-DIMENSIONAL ORAL EPITHELIAL MODEL FOR EMT ANALYSIS

1: General introduction

This chapter discusses the development of a 2D-oral epithelium model utilizing an immortalised cell line to investigate the potential for EMT-induction in response to periodontal pathogens. Previous studies of EMT have used either primary cells (Acevedo et al., 2007, Bao et al., 2012) or cell lines (Maschler et al., 2005, Strutz et al., 2002). Although primary cell lines are understood to mimic more realistically the in *vivo* conditions, primary cells require specialised isolation and culture requirements that can increase the possibility of contamination with other cell types (Kaur and Dufour, 2012).

Using well characterised cell lines for developing *in vitro* models provides the advantage of population purity and consistency in growth and these cells do not require ethical permission for their use. However, their use has been subject to criticism because the *in vitro* model differs from the *in vivo* situation in several aspects including chromosomal aberrations and loss of tissue specific markers (Kaur and Dufour, 2012).

To study cell growth and viability in the presence or absence of bacteria, it is necessary to count cells at different time points. Traditionally, cell counting is performed by using a haemocytometer-based technique which is a relatively simple approach but time consuming and can be subject to inter- and intra-examiner variability. More recently, automated counting methods have been developed. Several manufacturers claim their devices generate data that is superior to results obtained with traditional manual counting approaches. Indeed, studies have been conducted to compare the degree of correlation, accuracy and the consistency between manual and automated cell counts. Platelet counts using both methods have indicated a positive correlation between the two approaches (Bakhubaira, 2013). In another study, four types of cells were utilised to compare these two techniques and data showed that both methods were correlated with higher consistency than the image-based automated cell

counting approach (Barber et al., 2001). White blood cell counts obtained using a Coulter automated cell counter indicated that this automated method provided advantages in time-saving, higher precision and was more accurate than manual approaches (Salinas et al., 1997).

Detection of bacteria or their products by epithelial cells is mediated by specialised cell surface proteins known as TLRs (described in Chapter 1, section 5). Oral keratinocytes are known to express TLR-2, -4, and -9 which recognize a range of bacterial components form periodontal pathogens (Milward et al., 2007). Furthermore, previous studies have reported that periodontal pocket microenvironment is characterised by the presence of several bacterial ligands including lipoteichoic acid, LPS, and bDNA, molecules which are specific for these receptors (Mori et al., 2003, Kusumoto et al., 2004, Ren et al., 2005). Activation of TLRs is associated with the triggering of a number of different signaling pathways related to the innate immune response (Guijarro-Muñoz et al., 2014) and potential EMT-induction (Jing et al., 2012). One of the main pro-inflammatory signaling pathways activated involves NF-κB which comprises a protein complex present in an inactive state in the cytoplasm of a non-stimulated cell (Freudenthal et al., 1998, Merlo et al., 2002). Unstimulated NF-κB protein is located in the cytoplasm of the cell bound to IκB kinase (Jacobs and Harrison, 1998). The presence of bacteria deactivates IκB kinase by phosphorylation and subsequent ubiquitination and degradation of IκB which results in NF-κB activation (Karin and Ben-Neriah, 2000, Ghosh and Karin, 2002, Zandi et al., 1997). Subsequently the NF-κB molecule translocates to the nucleus where it binds to specific DNA-motif sites thereby increasing gene transcription and release of pro-inflammatory mediators (Nelson et al., 2004). However, NF-κB cycles are characterised by their relatively short duration, ~1hr, due to a negative auto-feedback of IκB which re-inhibits the NF-κB activity (Nelson et al., 2004, Coons et al., 1942). Gram negative bacteria, associated with periodontal lesions, are well-known activators of the NF-κB

signaling pathway that leads to stimulation of the immune system and subsequent release of a range of inflammatory cytokines and enzymes (Ambili et al., 2005). Notably molecular changes occur in H400 oral keratinocytes in response to TLR-2, -4, and -9 by periodontal pathogens (Milward et al. 2007). Data showed a significant increase in NF-κB nuclear translocation which associated with increased transcription of several inflammatory mediators such as TNF-α, IL-1β, and IL-8, molecules which have previously been related to periodontal disease pathogenesis (Graves, 2008, Yucel-Lindberg and Båge, 2013). Interestingly several studies have shown that NF-κB activation is involved in triggering EMT (Li et al., 2012a).

In this thesis, oral keratinocytes (H400) (Prime et al., 1990) were used to develop a model to study the effect of bacterial stimuli on the number and viability of epithelial cells.

2: Specific aims and objectives of the studies described in this chapter:

Aims:

- Adjusting growth of oral keratinocytes to be confluent in monolayer in 8-days then investigating the effect of heat-killed periodontal pathogens (*F. nucleatum* and *P. gingivalis*) and *E. coli* LPS on the proliferation rate, viability, and pro-inflammatory response of epithelial cells during culturing period.

Objectives:

1- To investigate different growth conditions (altering the FCS concentration and/or seeding number) to regulate the confluency of H400 cells to enable studies at 8-days post seeding. Previous studies indicated that the average time required for EMT-induction ranged between 1-8 days (Chapter 1, section 3.4.2).

2- To compare manual and automated cell counting techniques and determine the reproducibility of an image-analysis based automated approach.

3- To investigate the effect of heat-killed periodontal pathogens, *F. nucleatum* and *P. gingivalis*, on the growth and viability of H400 cells in addition to examining whether such treatments induced a pro-inflammatory response via NF-kB activation.

4- To investigate changes in gene expression of TLR-2, -4, and -9 following exposure to bacterial components.

3: Results

3.1: Validation of the reproducibility of the automated cell counter

The results indicated discrepancies in cell count and viability obtained from low cell density samples ranged between $1x10^5$-$4x10^4$ cells/ml when using the automated cell counter. In contrast, the consistency of readings obtained at higher cell densities repeatedly measured, increased with increasing cell density in the sample (Table 14). This showed that the device yielded more consistent results in relatively high cell density samples compared with lower cell density samples, even though the low cell number measured were twice the minimum recommended cell density indicated by the manufacturer.

Groups		Low density			High density		
Dilution		1:2	1:4	1:8	1:2	1:4	1:8
Average cell count		2x10^5	1x10^5	4x10^4	3x10^6	1x10^6	5x10^5
Coefficient of variation	Cell count	0.06238	0.13058	0.11217	0.00621	0.02644	0.02258
	Viability	0.07988	0.14468	0.36239	0.00638	0.02119	0.04365

Table 14. Reproducibility of automated cell counter by utilizing two cell density samples (low and high) were serially diluted (1:2, 1:4, and 1:8) to obtain a series of cell densities. Data obtained from the low cell density groups showed higher coefficient of variation (shaded fields) when compared with higher cell density groups.

3.2: Comparison of manual vs automated cell counting approaches

Automated cell counts were compared with the conventional haemocytometer-based cell counting technique to determine the consistency of readings obtained using the two methods. Cell count and viability assay were undertaken using both techniques on the same samples. To ensure that wide ranges of cell numbers were compared, four time-points were selected (day 4, 6, 8, and 9). No statistically significant difference in cell counts (Figure 18) was

identified between the two methods. However, the automated method showed a higher variance ($F<0.05$) in readings associated with low cell density samples (day 4 and 6) which decreased with increasing cell density. This was consistent with the findings of the previous validation experiment (Section 3.1).

Cell viability was calculated after 4, 5, 6, 7, 8, and 9 days of H400 cell culture. Analysis of data from both methods showed significant differences ($P<0.001$) between days 4-6. The percent of viable cells estimated by the automated counter was almost half (~40%) that recorded using a haemocytometer (~80%).In contrast between days 7-9, there were no significant differences in cell viability detected between the manual and automated techniques (Figure 19). Viability results from day 4 to 6 again highlight issues with low cell density samples. The use of automated cell counting in later experiments was excluded due to the discrepancies detected and further analyses relied on manual counting only.

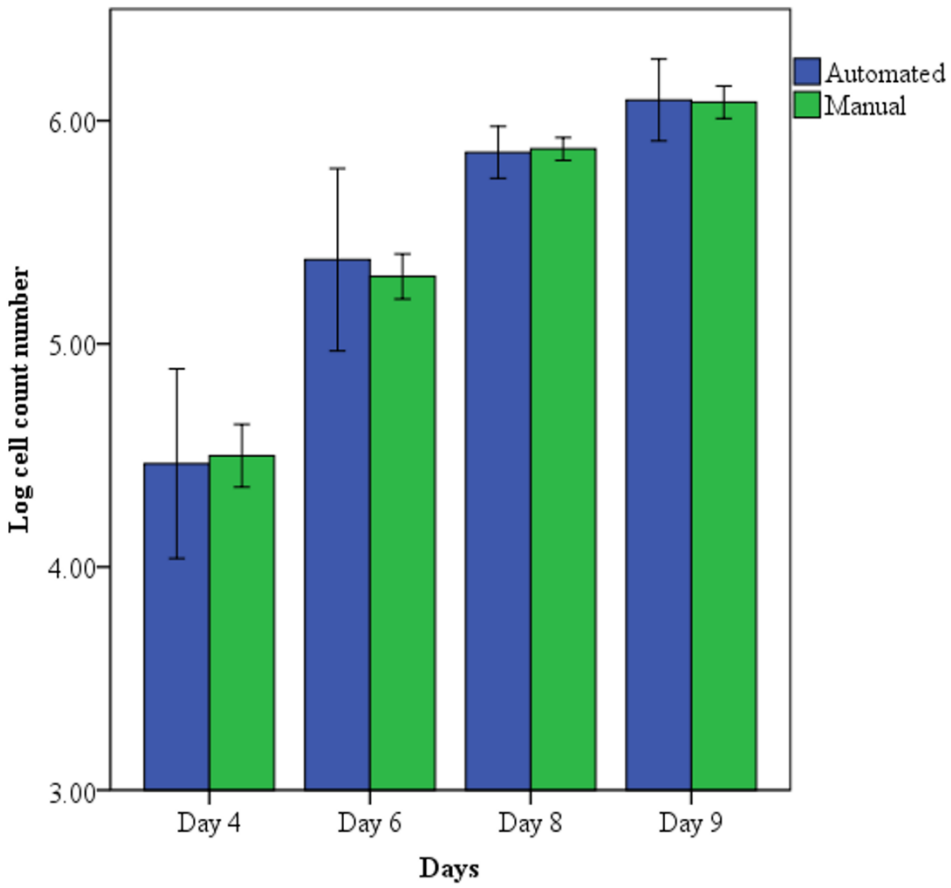

Figure 18. Comparison of the automated (Luna) and manual (haemocytometer) cell counts using the same samples showed no significant differences between the two counting methods over the four-time points investigated over a cell count range of ~$5x10^4$-$1x10^6$. Higher variance was associated with the automated technique. The experiment was performed in triplicate. n=12.

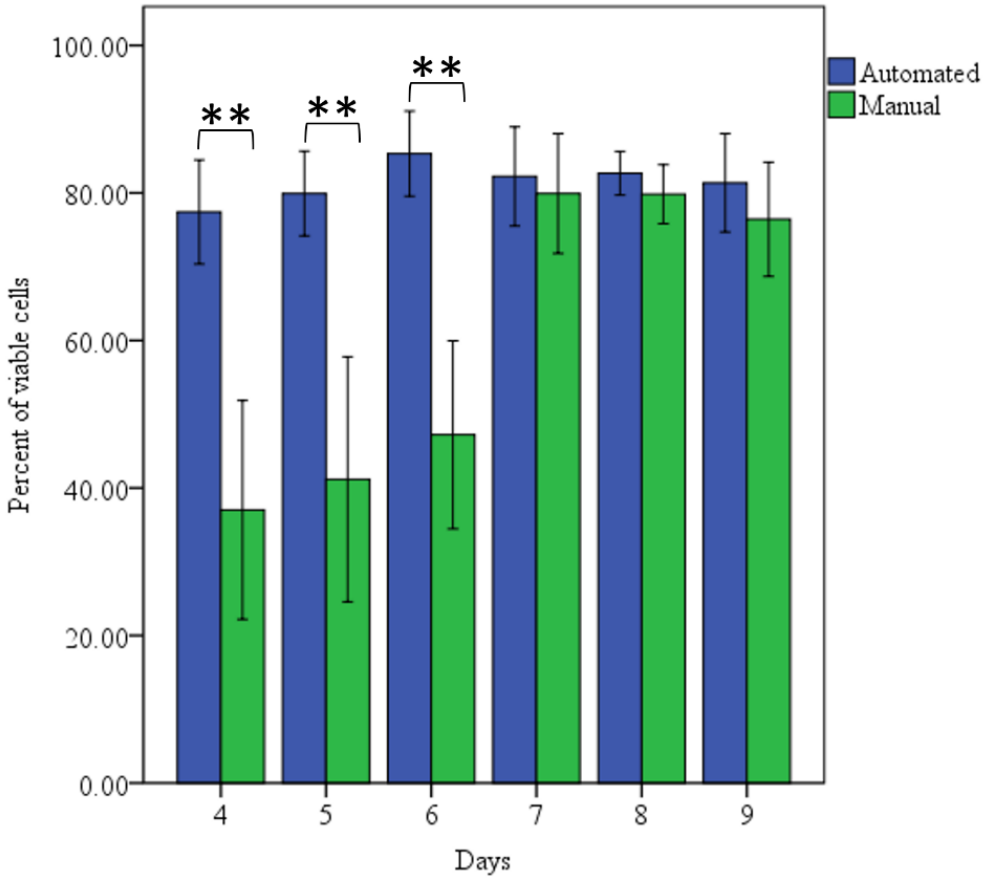

Figure 19. Comparison of cell viability as determined by automated and manual cell count methods. Data showed that the percent of viable cells detected was significantly lower using the automated technique compared with the manual viability counts obtained on days 4, 5, and 6 of culture. In contrast viability assessment on days 7, 8, and 9 showed no significant differences in percent of viable cells obtained between the two methods. The study was performed in triplicate. n=12, **=P<0.001.

3.3: Growth models

3.3.1: H400 cells cultured at different seeding densities and low FCS concentration

In the first model, H400 cells were cultured using different seeding numbers in medium containing 1% FCS to investigate the effect of medium supplementation and variable seeding densities on cell growth. Cells seeded at relatively low number ($1x10^3$ cells) in 1% FCS-medium resulted in cultures approaching confluency after 14 days. The cell seeding number cultured was increased to $2x10^3$ cells while maintaining the same FCS level resulted in

cultures reaching confluency at an earlier time point of day 12. The effect of increasing number of seeded cells in the same FCS concentration was further explored by raising the seeding number to $3x10^3$ cells. Growth curve analysis (Figure 20) showed that the degree of confluency was further increased and the cultures were confluent at 11 days.

Light microscope images (Figure 21) illustrate different degrees of culture confluency at the same time point. H400 cells were confluent, at day-11, when the initial seeding number was $3x10^3$ cells while other lower initial cell seeding densities investigated resulted in lower confluency when examined using phase contrast microscopy. Altering cell seeding number and reducing FCS concentration in the medium resulted in relatively long culturing times prior to confluency being achieved. However, lowering the FCS level may subject the cells to nutritional stress with potentially unfavourable consequences on viability or gene expression. Therefore, the subsequent model focused on adjusting both seeding number and FCS concentration to control degree of confluency.

Oral keratinocytes were seeded ($5x10^4$ cells) and grown in 35mm tissue culture dishes containing growth media supplemented with three different FCS concentrations (2, 5, and 10%). For the lowest FCS concentration (2%) the cultures reached 80-90% confluency after 6 days, while cells grown in 5 and 10% FCS medium cultures reached confluency in 5 days. Up to day 3, no significant differences in cell number were recorded between the three FCS concentrations used, however at days 4 and 5 cells grown in media containing 5 and 10% FCS showed significantly higher cell counts compared with cells cultured in 2% FCS (Figure 22). Levels of confluence were estimated by inspection under light microscope at the range of time points investigated (Figure 23).

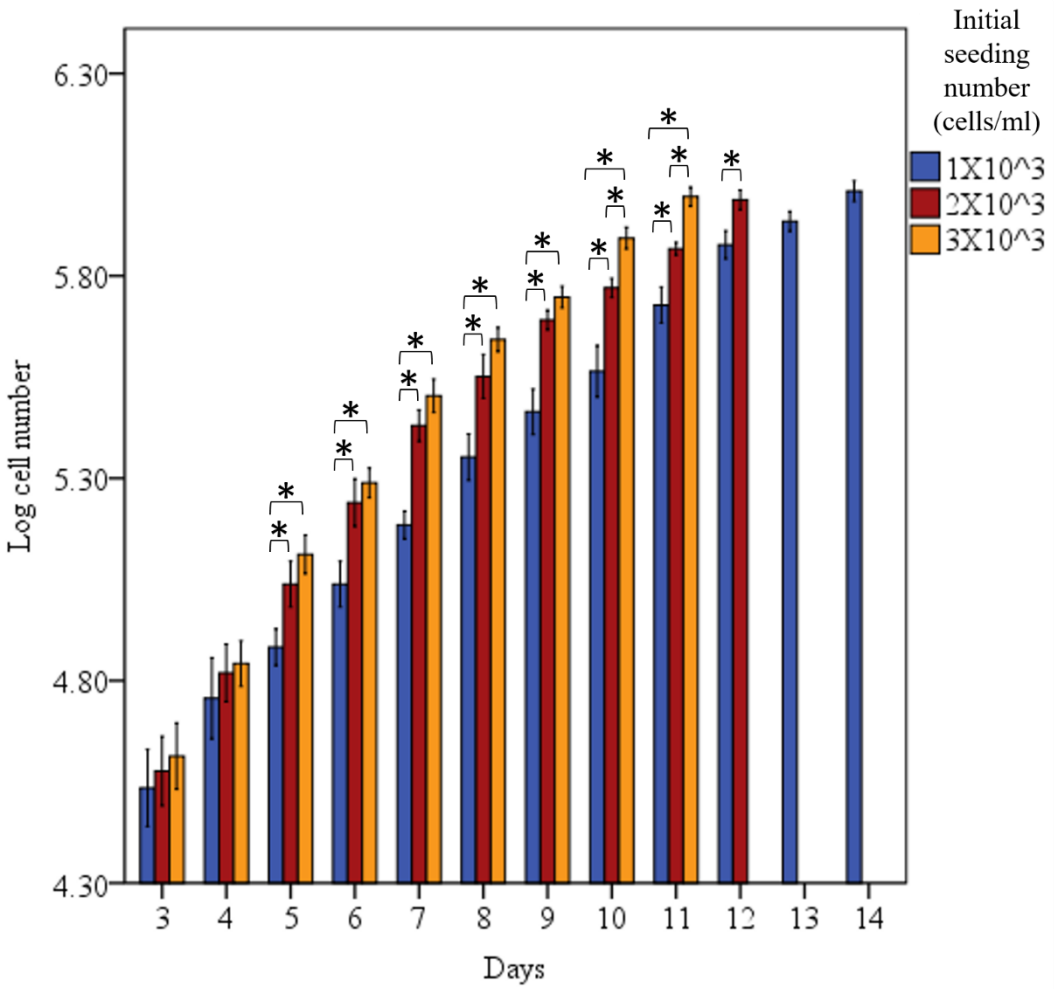

Figure 20. H400 cell growth analysis in medium supplemented with 1% FCS and with different cells seeding numbers (1, 2, and $3x10^3$ cells). Cell counts were significantly higher from day 5-12 among cell densities used. n=18, *=P<0.05.

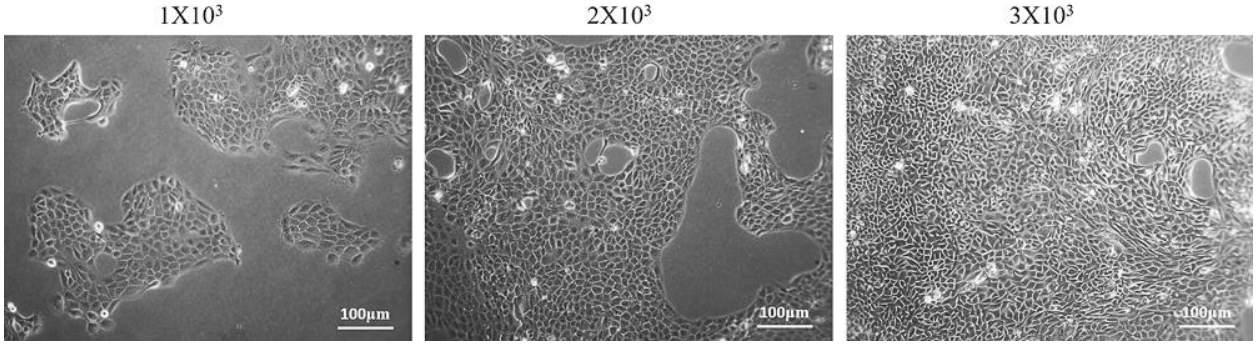

Figure 21. Representative phase contrast photomicrographs of H400 cells grown in media supplemented with 1% FCS and different initial seeding numbers (1, 2, and $3x10^3$ – shown above images). At day-11, cultures seeded with $3x10^3$ cells were almost confluent in contrast with the other seeding densities, 1 and $2x10^3$, which show a lesser degree of culture confluency. Scale bars are shown.

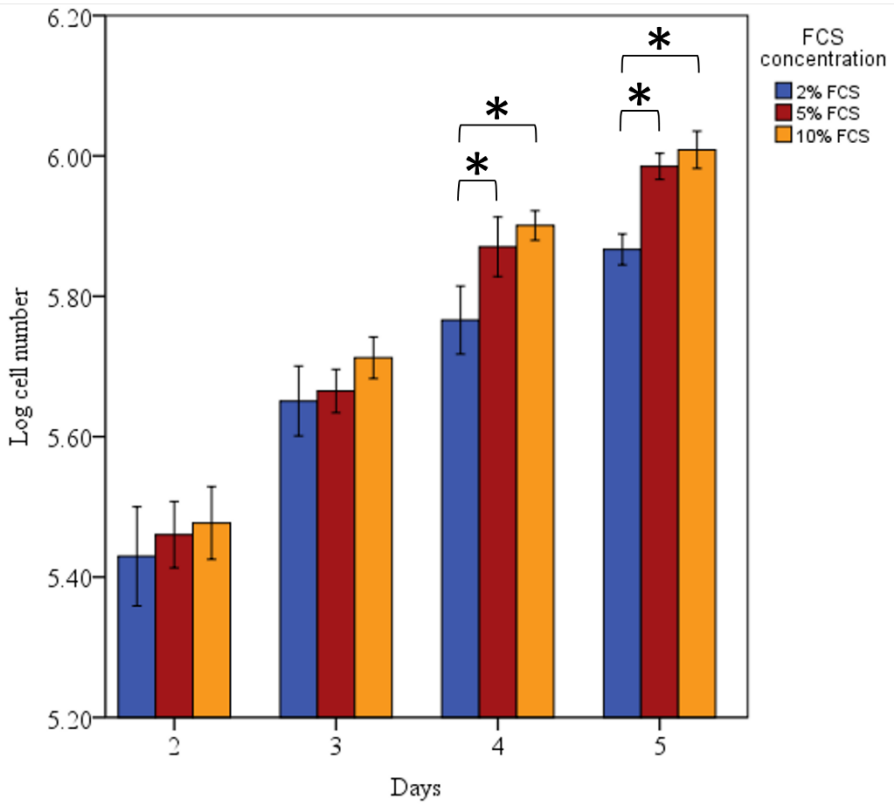

Figure 22. Growth curves for H400 cells cultured in media supplemented with 2, 5, and 10% FCS and with an initial seeding number $5x10^4$ cells. Data show significant differences in cell counts obtained between 5 and 10% FCS supplemented cultures compared with cells grown in 2% FCS at days 4 and 5. n=18, *=P<0.05.

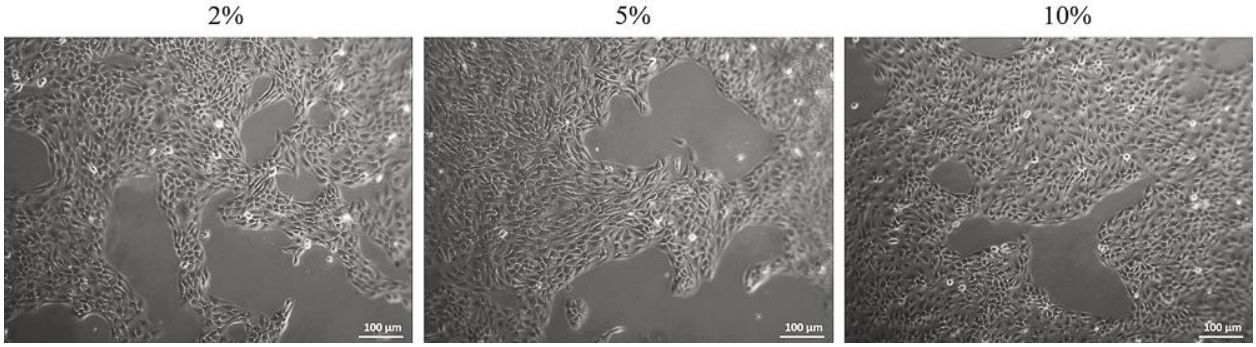

Figure 23. Representative light microscope images of H400 cells cultured in a range of FCS concentrations (2, 5 and 10%) and seeded with a fixed seeding number ($5x10^4$ cells). Images are for cultures containing 5 and 10% FCS and seeded at $5x10^4$ cells showing higher confluence than 2% FCS supplemented cultures at day 5. Scale bars are shown.

3.3.2: H400 cells cultured at low seeding number and different FCS concentrations

Results from the previous experiments did not identify conditions suitable for the intended EMT model as H400 cells reached confluence earlier than 8 days. In the subsequent experiment, H400 cells were cultured in supplemented FCS concentrations (2, 5, and 10%)

however the initial seeding number was reduced to $1X10^3$ cells. For each concentration, the experiment was terminated when cells reached confluence as determined visually using a phase contrast microscope.

Decreasing seeding number prolonged the time required for H400 cells to reach confluence in comparison with the previous experiments using the same FCS concentrations. For 2% FCS cultures, cells reached confluence after 11 days. Cultures supplemented with 5 and 10% FCS, cells required 10 and 8 days respectively to reach confluency. This was consistent with previous findings indicating that changing growth media FCS concentrations whilst using the same initial seeding number ($1X10^3$ cells) caused significant differences in cell counts from day 3 onwards until the end of the experiment. In this experiment the increased FCS concentration resulted in a significantly higher degree of confluency ($P<0.05$) for cells grown in 10% FCS compared with those cultured in 5 and 2% FCS. Following the same trend cultures grown in media containing 5% FCS showed higher cell counts than cultures incubated in media supplemented with 2% FCS (Figure 24). Representative light microscope images for cell cultures at day 8 utilizing different FCS concentrations are shown in Figure 25.

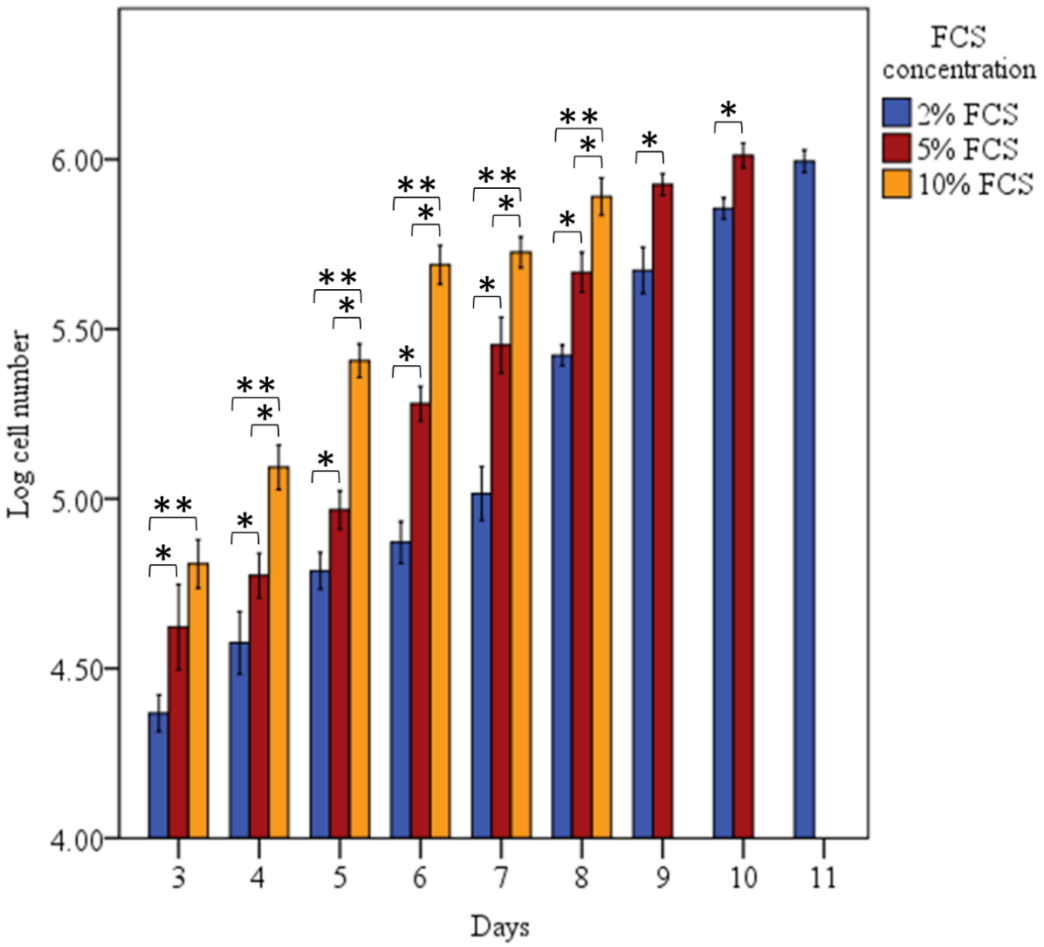

Figure 24. Growth curves of H400 cells cultured in media supplemented with 2, 5, and 10% FCS and an initial seeding number ($1x10^3$ cells). Data shows significant differences in cell counts between cultures supplemented with the range of FCS concentrations. Cell counts increased proportionally with increasing FCS levels in the media. n=18, *=P<0.05, **=P<0.001.

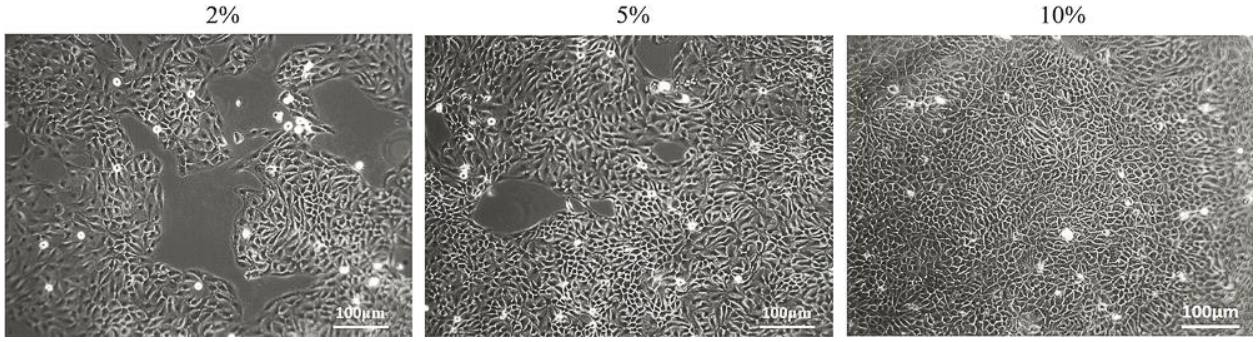

Figure 25. Representative light microscope images of H400 cells cultured in growth media containing different FCS concentrations (2, 5 and 10%) and with a fixed initial seeding number ($1x10^3$ cells). Images indicate that cultures containing 10% FCS reached a higher degree of confluence than those cultured in medium containing 2 and 5% FCS by day 8. Scale bars are shown.

Data from the previous three models suggested that the level of cell confluency was directly proportional to the growth media FCS concentration and initial cells seeding number. Growing cells in cultures containing the commonly used 10% FCS concentration and seeding number of $1X10^3$ cells resulted in the reaching of near confluency within desired targeted time point of 8 days. Subsequently these conditions were selected to investigate EMT *in vitro* in all downstream analyses.

3.3.3: Effect of bacterial components on H400 cell count

H400 cell cultures were exposed to heat-killed periodontal pathogens (*F. nucleatum* & *P. gingivalis*) and *E. coli* LPS to determine the effect of these bacteria and their components on cell numbers as assessed using the manual cell counting method.

The differences in number of cells for all groups (Figure 26) was not statistically significant for days 7 and 8 ($P > 0.05$), while results from day 4 - 6 showed that the cell count of cultures exposed to bacterial components were significantly lower than those in the unstimulated control group ($P<0.05$). This may be due to increase in the death of cells due to the toxicity of these components (Gonçalves et al., 2016, Sharifi et al., 2010). The compromised viability of H400 cells, as a possible reason for growth alteration in the presence of bacteria was investigated in the following section.

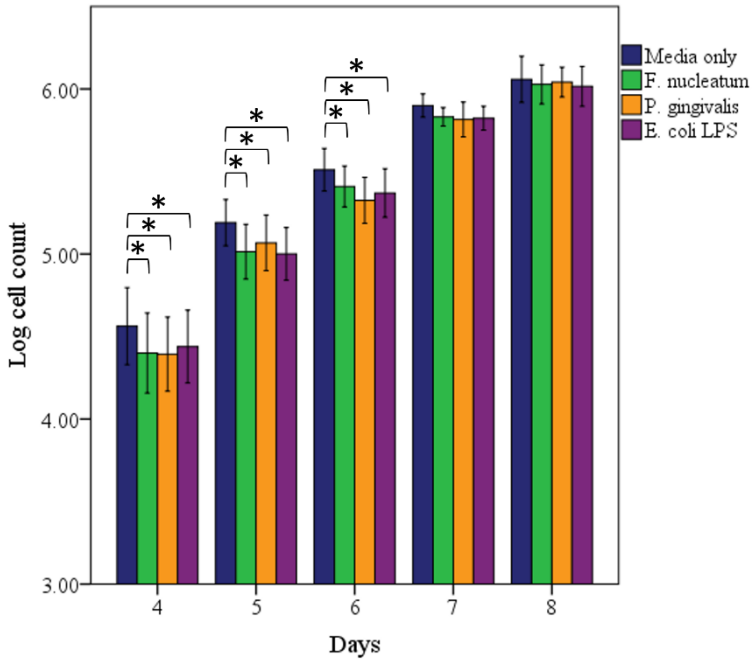

Figure 26. H400 growth over 8-days incubation with media only, or supplemented with *F. nucleatum*, *P. gingivalis* or *E. coli* LPS. Results showed significant difference in cell count, from day 4-6, between cultures exposed to bacterial components and cultures treated with media only. n=18, *=P<0.05.

3.3.4: Effect of bacterial components on H400 viability

A viability analysis was performed using the trypan-blue exclusion assay as the previous validation study showed a high discrepancy in estimated percent of viable cells in association with the automated cell counter. Analysis of viability assay data (Figure 27) showed no significant differences (P>0.05) between cultures treated with media only and those exposed to heat-killed bacteria or *E. coli* LPS during the experimental period (day 4-8).

The concentrations of heat-killed periodontal pathogens (100 bacteria/cell) or *E. coli* LPS (20μg/ml) appeared not to be toxic to H400 cells in the experimental conditions used and excluded the possibility that increased cell death after bacterial exposure was the reason for the decreased number of cells detected in the previous experimental study.

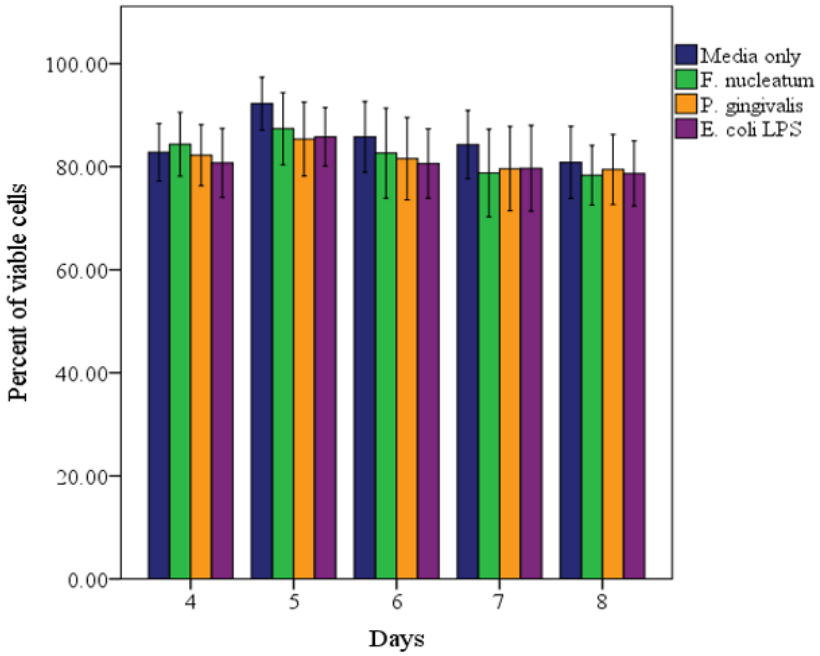

Figure 27. Trypan-blue exclusion viability assay for H400 cultures exposed to heat-killed bacteria or *E. coli* LPS for up to 8 days. Results showed no significant difference in percentage of viable cells detected between stimulated and unstimulated control. n=18.

3.4: Immunocytochemical analysis of NF-κB activation

Exposure of H400 keratinocytes to heat-killed *F. nucleatum*, *P. gingivalis* and *E. coli* LPS for 1hr caused an increased nuclear translocation of NF-κB indicating activation of this key pro-inflammatory regulatory transcription factor (Figure 28). Activated NF-kB was shown by immunostaining in the nuclei. Analysis of data showed a significantly higher ($P<0.001$) number of cells with NF-κB activation in association with *F. nucleatum* stimulation (79%), followed by cells exposed to *E. coli* LPS (73%). Both groups (*F. nucleatum* and *E. coli* LPS) were also significantly ($P<0.001$) higher than *P. gingivalis* stimulation which showed the lowest level of NF-kB activation (17%) (Figure 29). However, the latter group also showed significantly higher number of positive cells in comparison with the unstimulated group ($P<0.05$).

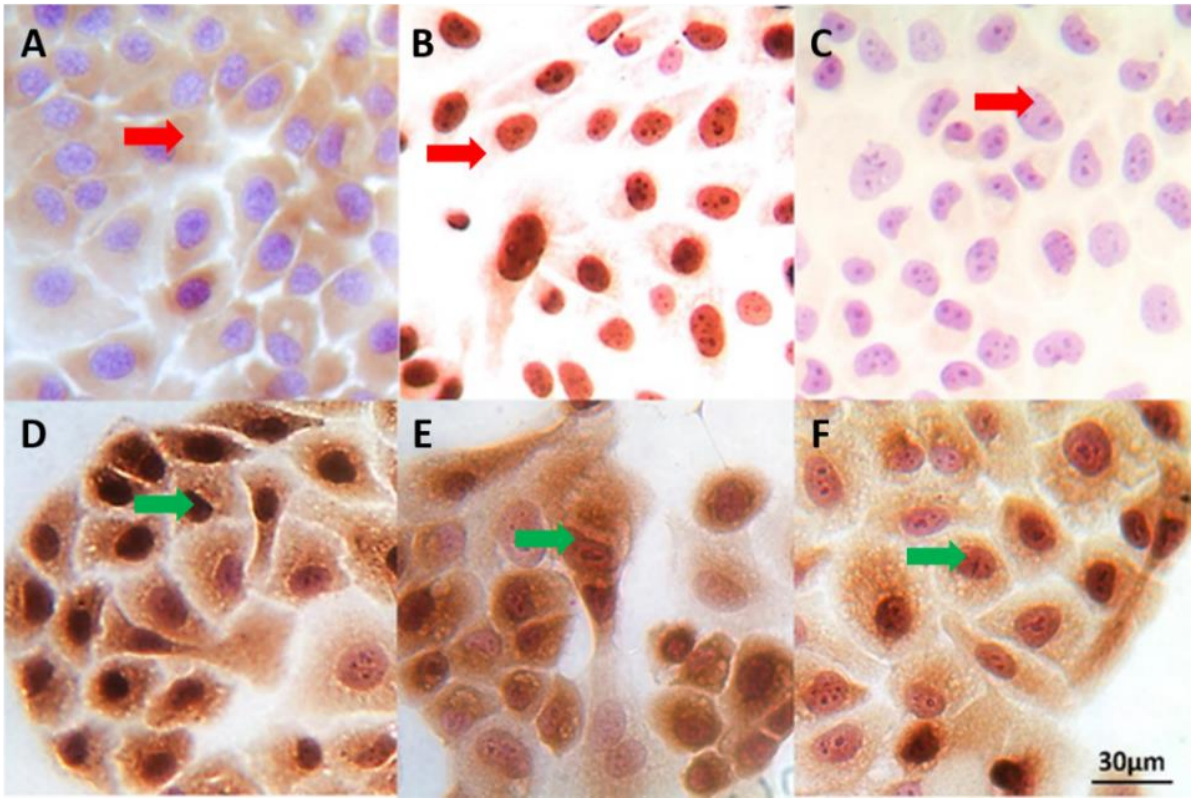

Figure 28. Representative light microscopy photomicrographs of immunocytochemical staining of H400 cells to demonstrate activation of NF-κB following exposure to bacterial stimuli. Arrows (red) indicate cytoplasmic activity with minimal nuclear involvement in unstimulated cells (A), positive control cells showing nuclear staining with Ki67 (B) clear cytoplasm of negative control group treated with 1% BSA only (C), nuclear translocation (green arrows) of NF-κB detected in cells stimulated with *F. nucleatum* (D), *P. gingivalis* (E), and 20µg/ml *E. coli* LPS (F). Experiment performed in triplicate. Scale bar = 30µm for all images.

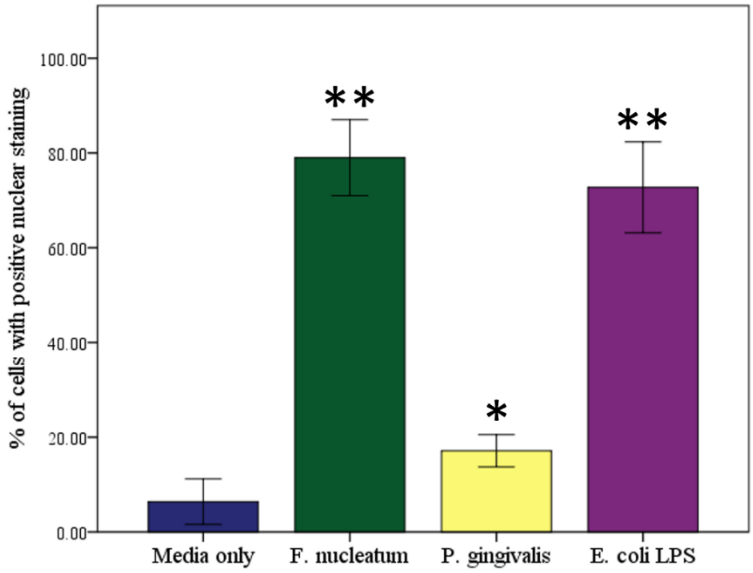

Figure 29. Semi-quantitative immunocytochemical analysis of NF-κB activation in H400 cells following 1hr stimulation with *F. nucleatum*, *P. gingivalis*, or 20µg/ml *E. coli* LPS. The highest activity was associated with exposure to *F. nucleatum* (79%), followed by *E. coli* LPS (73%) and *P. gingivalis* (17%). *=P<0.05, **=P<0.001 compared with unstimulated control.

3.5: TLR-2, -4, and -9 gene expression analysis

Signaling downstream of TLR, following bacterial stimulation, is known to lead to activation of the transcriptional factor NF-κB (Murray and Lopez, 1997) and this is potentially involved in EMT induction (Li et al., 2012a). Therefore, expression of TLR-2, -4, and -9 in cultured H400 in presence of bacteria was investigated.

3.5.1: TLR-2

Generally, results showed a significant decrease (P<0.05) in transcription of TLR-2 (~1.5-3 fold) in all stimulated groups compared with unstimulated controls (Figure 30A). Expression of TLR-2 associated with *P. gingivalis* stimulation gradually increased from day 1 until day 8 and it was significantly lower than in cultures stimulated with *F. nucleatum* on days 1 and 5, and *E. coli* LPS at day 5. TLR-2 expression in the *E. coli* LPS exposed group peaked at day 5 then decreased again at day 8 which suggested a general down-regulation of TLR-2 transcription following stimulation of H400 cells with bacteria or *E. coli* LPS.

3.5.2: TLR-4

Analysis of data showed significant up-regulation ($P<0.05$) of TLR-4 transcription in all stimulated cultures in comparison with the unstimulated controls from day 1 to 8 (Figure 30B). The highest up-regulation of TLR-4 was associated with *E. Coli* LPS stimulation and this was significantly higher compared with heat-killed periodontal pathogens at days 1 and 8. *F. nucleatum* and *P. gingivalis* stimulation demonstrated a similar degree of increased transcription of TLR-4, except at day 1 where *P. gingivalis* exposure resulted in a higher transcription level of this receptor. Cultures treated with LPS showed the highest up-regulation in TLR-4 expression when compared with other bacterial exposures.

3.5.3: TLR-9

Stimulation of H400 cells with different bacterial components resulted in significant up-regulation of TLR-9 expression compared with unstimulated controls, except for *E. coli* LPS at day 5 (Figure 30C). The highest up-regulation was associated with *F. nucleatum* stimulation on days 1 and 8 (up to 3-fold) and with *P. gingivalis* at day 5 (2 fold) relative to control. Analysis of data showed that the highest up-regulation of TLR-9 expression was associated with periodontal pathogen exposure following 24hr stimulation; this then relatively decreased at days 5 and 8. This may have suggested an oversaturation of this receptor or the cells becoming tolerant which is a regulatory mechanism that prevent excessive immune response following a prolonged exposure to the stimulus (Medvedev et al., 2006, Wang et al., 2002).

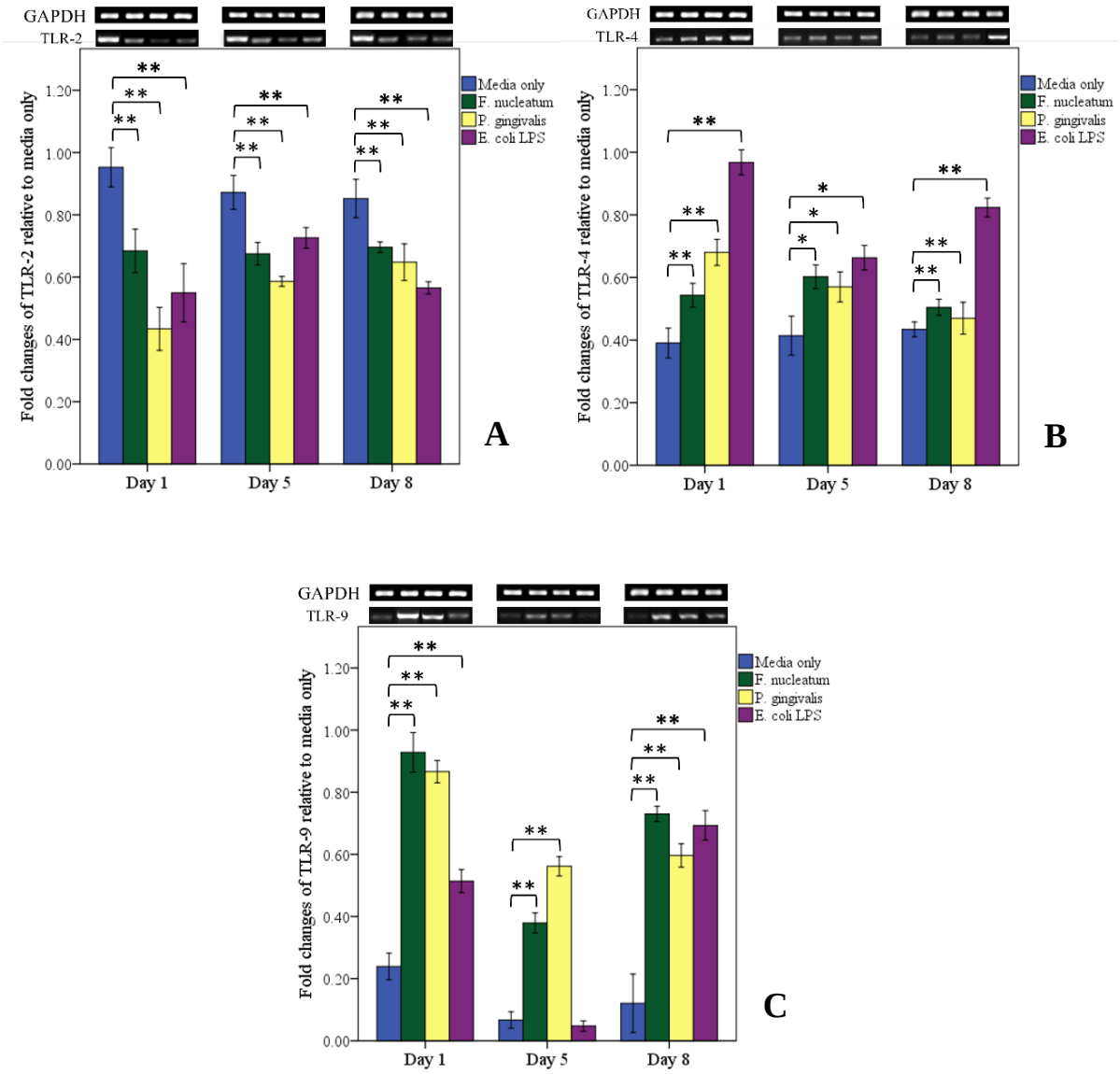

Figure 30. Gel images and densitometric analysis of TLR-2, -4, and -9 PCR products, showed that treatment of H400 cells with different bacterial components resulted in significant changes of these receptor transcriptional activity in comparison with unstimulated controls from day 1 - 8. Heat-killed bacteria (FN/PG) resulted in significant down-regulation of TLR-2 (A), while expression of TLR-4 (B) and -9 (C) were significantly upregulated. Experiments were performed in triplicate. *=P<0.05, **=P<0.001 indicate significant differences compared with controls.

4: Discussion

To study the potential of *F. nucleatum* and *P. gingivalis* to induce EMT in epithelial cells during periodontitis, a model system needed to be developed. For this purpose, a well characterised oral epithelial (H400) cell line was used. Although this cell line is of cancer origin and the cells have inherent mutations but still possess epithelial markers and are representative. The initial aim was to determine the growth characteristics required to produce a monolayer approaching confluence within a period of 8 days in order to investigate cellular response following extended exposure of epithelium to periodontal pathogens and *E. coli* LPS in an attempt to mimic the *in vivo* situation.

4.1: Validation of the automated cell counter

The bright-field automated cell counter yielded a higher discrepancy in cell count and estimation of viable cells in sample containing a relatively low density of cells. This discrepancy could be due to errors in the software algorithm that analyses the images captured by a built-in digital camera. In addition, manual focusing of automated counter to select the best representative plane to be measured is a further issue related to the use of this method. This is due to that when measuring low densities, cells are scattered in different planes which make it more difficult to choose the right detection plane compared with higher cell densities and this makes the method sensitive to the appropriate initial setup. In addition, clumping of cells may result in inadequate identification of cells and generate inaccuracies. In general, data showed that the automated cell counting device used in this study was less reproducible in counting the percentage of viable cells as compared to haeomocytometer.

4.2: Manual vs automated-cell count

Comparisons between manual and automated cell counter indicated no significant difference in cell count between the two techniques. This agrees with findings of a previous study which suggested that the methods correlated well (Barber et al., 2001). In contrast, when viability of

cells was assayed using both techniques, automated method showed significantly lower estimates than the manual method when low cell densities were measured.

The advantage of automated cell counting is however that a relatively rapid time enables acquisition of results (7-10 seconds) whilst manual cell counting requires additional steps for preparation of the haeomocytometer and counting the cells in the chamber. The subjectivity, which is one of the main disadvantages of manual cell counts, was also eliminated. These conclusions agree with another study which supports the use of the automated method over the manual technique (Salinas et al., 1997). Another factor that could interfere with the manual counting approach is that additional incubation at room temperature of the suspended cells, especially necessary for large number of samples, could cause cell clumping resulting in reading errors.

4.3: H400 growth models with different initial seeding numbers and FCS supplementation

Analysis of the model utilizing 1% FCS concentration and different cells seeding numbers showed that cultures with higher initial seeding numbers cultures reach confluency faster than lower ones. This is consistent with a previous study (Rodriguez et al., 2001). Although this model met the targeted incubation criteria for an EMT-model (i.e. 8-day), however concerns arise from cells cultured in low nutrient medium because this could rapidly result in starvation and failure of cultures to reach confluency.

Data from cultures, supplemented with three FCS concentrations (2, 5, and 10%) and an initial seeding number ($5x10^4$ cells), generally showed no difference in cell count amongst the different FCS levels used. These results suggested that cell seeding levels were too high and masked the effect of the different FCS concentrations. The seeding number was subsequently lowered to $1x10^3$ cells, and using the same FCS concentrations this resulted in cultures reaching confluency at 11, 10, and 8 days for 2, 5, and 10% FCS supplementations,

respectively. This suggests that confluency was proportional to FCS concentration used as the seeding number applied was the same in all groups.

Both cell seeding number and FCS concentration are key variables affecting confluency degree of cultures under these experimental conditions. This observation was further supported by initially seeding 500 cells; this resulted in failure of cells to obtain confluence, with cultures demonstrating minimal growth. This outcome could be due to a loss of contact between cells due to large distances separating them independent of the FCS concentration used. A similar result was obtained when growing cells in media without any FCS supplementation, causing cells to multiply in relatively small scattered islands in the cell culture before growth was halted. The initial cell multiplication may be due to that the cells could access available nutrients from the cell re-suspension step with media and 10% FCS to inhibit trypsin activity, after which cells stopped growing following the depletion of their nutrient store.

Confluency can be controlled by altering initial cells seeding number and FCS concentration together or independently. However, it was decided that the lower FCS concentrations (1, 2, and 5%) would be excluded from further studies to avoid any possibility of subjecting cultures to nutrient starvation which may adversely affect results.

4.4: Effect of heat-killed periodontal pathogens on cell count and viability of H400 cells

Epithelial cells were cultured with either media alone or *E. coli* LPS, heat-killed *F. nucleatum* and *P. gingivalis*. Although viable bacteria provide a more realistic disease model, use of heat-killed bacteria removes the risk of culture infection and bacterial overgrowth. In addition, heat-killed bacteria still retain many virulence factors that are present in their viable counterparts including LPS, bacterial DNA and lipoteichoic acid (Taverniti and Guglielmetti, 2011). Furthermore dead bacteria are present in the periodontal pocket and likely contribute to the pathogenesis of periodontitis as the subgingival biofilm contains both live and dead

bacteria (Marsh, 2009). Cell counts showed that while there was no significant difference in cells number between stimulated and unstimulated groups by the end of the experimental period, there was a significant difference in cell counts in stimulated compared with unstimulated cultures at days 4, 5, and 6. This difference could have been due to compromised vitality or decreased proliferation of epithelial cells by bacterial antigens (Bhattacharya et al., 2014). The reduction in the effect of bacterial components on number of cells at days 8 and 9 might be related to cell survival strategies stimulated through downstream transcription of factors such as NF-κB (Freudenthal et al., 1998, Merlo et al., 2002). This was further supported from data from viability analysis which showed no significant difference between cells treated with media alone or exposed to bacterial components. The other possible explanation was that the presence of bacteria caused diversion of cellular resources from replication to induction of protective mechanisms (Hausmann, 2010). Although the bacterial components used may provoke similar signaling pathways and autocrine feedback producing cytokines to *in vivo*. However, the levels produced may be too low to affect cell growth or morphology as has been proposed by Borthwick et al. (2011).

4.5: NF-κB activation in H400 cells following exposure to bacterial components

Exposure of keratinocytes to heat-killed periodontal pathogens and to 20µg/ml of *E. coli* LPS led to the induction of a pro-inflammatory response manifested by activation of the NF-κB pathway. The response of the oral keratinocytes to the bacterial stimuli used in this study somewhat varied. The most potent induction and highest percentage of cells with positive NF-κB nuclear translocation detected was associated with *F. nucleatum*, followed by *E. coli* LPS and the lowest was associated with *P. gingivalis* exposure which was consistent with previous findings (Milward et al., 2007, Jing et al., 2012b). This differential response seen between *F. nucleatum* and *P. gingivalis* may be explained due to *P. gingivalis* reportedly

mostly activating TLR-2 (Bainbridge et al., 2002, Nemoto et al., 2006). Interestingly the expression of TLR-2 was suppressed upon bacterial stimulation potentially due to tolerance of cells to bacterial stimulation which is a protective mechanism preventing excessive inflammatory response (Wang et al., 2002, Medvedev et al., 2006), while TLR-4 and -9 expression were up-regulated. This suggested a possible reduction in the ability of *P. gingivalis* to trigger the NF-κB pathway, although TLR-4 and -9 are potential receptors for components of *F. nucleatum* and *E. coli* LPS, which could have resulted in a subsequent increase of NF-κB nuclear translocation. Although the dead bacteria suspension used contained a number of different pathogenic components the most potent virulence factor of Gram negative anaerobic rods is cell-wall associated LPS which is released after the death of these bacteria (Rietschel et al., 1994). However, LPS extracted from different pathogens is known to induce different cytokines and distinct immune responses (Pulendran et al., 2001) and *P. gingivalis*-LPS has been reported by several studies as being a weak inducer of the immune system responses (Reife et al., 1995). This may suggest a reason for lower levels of NF-κB activation in *P. gingivalis* exposed cells compared with the other bacterial stimulants used in this study.

4.6: TLR gene transcription alteration in response to bacterial components

Stimulation of TLRs, by different PAMPs, induces innate immune responses which trigger various signaling pathways culminating in activation of NF-κB (Kawai and Akira, 2007). In this study, treatment of H400 cells with bacterial components resulted in altered TLR-2, -4, and -9 gene transcription in a similar pattern to that previously reported (Milward et al., 2007). Among the ligands present, LPS is a well-known inducer for NF-κB signaling downstream and activation of TLR-4 by LPS results in NF-κB nuclear translocation associated with increased transcription of many genes encoded cytokines and chemokines such as IL-1, 6, and 8 (Guijarro-Muñoz et al., 2014). Analysis of the PCR data generated here

indicated similar results in which treatment of H400 cultures with pure LPS resulted in up-regulation of TLR-4 expression associated with increased NF-κB nuclear translocation. The other two exposure groups (*F. nucleatum* and *P. gingivalis*) also produced a similar effect but to a lesser extent. This could have been due to the presence of other microbial components that may compete with LPS as a TLR-4 ligand. In addition, different bacteria produce different types of LPS which may vary in their potency (Pulendran et al., 2001).

Similarly, TLR-9 expression was up-regulated in response to bacterial stimulation and its activation is also known for inducing the secretion of a range of inflammatory cytokines. All stimulated groups showed evidence of increased transcription of TLR-9 which indicated that it was activated by *E. coli* LPS as well as other bacterial components. These data are consistent with findings from a previous study which utilised purified *H. pylori*-bDNA and LPS which up-regulated the expression of TLR-9-associated NF-κB activation (Tsujimura et al., 2004). Conversely, TLR-2 was down-regulated following exposure of H400 cells to bacterial components in all groups. This could have been due to a desensitizing response of epithelial cells to bacterial stimulation which caused a tolerance state of the cells. Additionally, these receptors could be competitively blocked by other less potent components available in the suspension.

Periodontal pathogens therefore appear to up-regulate expression of TLR-4, and -9 and activate downstream signaling pathways in oral keratinocytes, which are known to induce EMT. Furthermore, this process ultimately can result in release of a range of pro-inflammatory cytokines that contribute to the dual tissue protection-destruction role and potentially induce EMT via autocrine mechanisms.

5: Conclusions

- Confluency of epithelial cultures can be controlled by altering cell seeding numbers and/or varying FCS media concentration.
- Comparison of automated and manual cell counts showed that results achieved with both methods correlated. However, automated cell counts were associated with difficulty in obtaining reproducible measurements of samples with low cell number.
- The effect of culturing H400 cells, in terms of cell number and viability, with heat-killed *F. nucleatum* and *P. gingivalis* and *E. coli* LPS was not significantly different from the control group. This suggested potential abilities of epithelial cells to adapt to bacterial assault. Furthermore, vitality of epithelial cells was not affected by periodontal bacteria as reflected by data of viability assay.
- Bacterial components could stimulate a pro-inflammatory response on H400 cells as determined by the activation of the nuclear translocation of NF-κB. *F. nucleatum* showed greater stimulatory effects compared with *P. gingivalis*, possibly due to interaction with different TLR-types. This was supported by differential TLRs expression in response to bacterial component exposure.

The following chapters will explore the potential induction of EMT in oral keratinocytes in response to periodontal pathogens using the *in vitro* model developed here.

INDUCTION OF EMT IN AN H400 ORAL EPITHELIAL CELL LINE IN RESPONSE TO PERIODONTAL PATHOGENS

1: General Introduction

Oral cancer is a life-threatening condition if it is not diagnosed and treated in its early stages (Jemal et al., 2011). Epidemiological data indicate that oral cancer is the sixth most common cancer in the world. In the UK, it is ranked as the nineteenth most common malignancy causing mortality, with OSCC being the predominant form accounting for over 90% of cases (Choi and Myers, 2008, Feller and Lemmer, 2012). Generally, OSCC reportedly has 40-50% 5-year survival rates due to its tendency for recurrence and metastasis (Marsh et al., 2011). The most common risk factors for oral cancers include smoking, alcohol, genetic disorders, viruses, and malnutrition (Warnakulasuriya, 2009). Notably, recent data from case-control studies have indicated that periodontitis could represent a risk factor for OSCC independent of other risk factors (Tezal et al., 2007, Narayan et al., 2014). Indeed, poor oral hygiene and periodontal diseases have been proposed as potential factors involved in the initiation and progression of oral malignancy (Narayan et al., 2014, Rosenquist et al., 2005, Moergel et al., 2013).

In chronic periodontitis, Gram-negative anaerobic bacteria have the ability to induce a pro-inflammatory host response initiated by the crevicular epithelium (Paster et al., 2001). Notably the presence of chronic inflammation due to microbial challenge has been suggested to induce EMT-induction in a number of organs including the lungs, liver, and intestine (Hofman and Vouret-Craviari, 2012). Recent data suggest that infection by the periodontal pathogens *P. gingivalis* and *F. nucleatum* can drive the inflammatory host response and might also be implicated in OSCC invasiveness (Binder Gallimidi et al., 2015, Ha et al., 2015). Thus, cancer cell invasion has been partly attributed to the EMT process (Jechlinger et al., 2002, Radisky, 2005, Lee et al., 2006). Examination of samples from OSCC has revealed the presence of relatively large numbers of *P. gingivalis* bacteria in association with late stage metastatic cancer (Katz et al., 2011).

Notably the down-regulation of attachment molecules, such as E-cadherin, has been shown to increase cytoplasmic levels of free β-catenin (Kim et al., 2002, Nawshad et al., 2007b). This is followed by translocation of β-catenin to the nucleus where it activates LEF-1 transcription which facilitates acquisition of a migratory-phenotype (Nawshad et al., 2007, Kim et al., 2002). Furthermore, nuclear translocation of β-catenin was also associated with increased expression of the mesenchymal marker, vimentin (Gilles et al., 2003). The final stages of EMT involve increased production of proteolytic enzymes associated with increased migration and invasiveness (Kalluri and Weinberg, 2009). In addition Gram-negative periodontal pathogens and their virulence factors such as LPS stimulate up-regulation members of the MMP family in epithelial cells (Sapna et al., 2014), not only during periodontal disease but also in OSCC *in vivo* and *in vitro* in different cancer models (Inaba et al., 2014, Gursoy et al., 2008, Binder Gallimidi et al., 2015)

Periodontal pathogens such as *P. gingivalis* and *F. nucleatum* are well known to be able to elicit intense chronic inflammatory and immune responses which could trigger EMT. This chapter therefore explores the potential role of these bacteria in driving EMT in an OSCC cell line (H400) *in vitro* and this process may also identify a possible novel mechanism underpinning the pathogenesis of periodontitis.

2: Specific aims and objectives of the studies described in this chapter:

Aims:

To investigate the potential of two key periodontal pathogens, *F. nucleatum* and *P. gingivalis*, to induce EMT *in vitro* in the H400 OSCC cell line.

Objectives:

EMT induction was investigated by using a range of assays including PCR, an EMT gene expression array, ELISA, IF, ICC, wound healing, transwell migration, and TEER.

3: Results

3.1: sq-RT-PCR analysis of EMT-associated genes

One of the most frequently used methods for detecting EMT-induction is by monitoring changes in gene expression of several EMT-markers such as transcriptional factors, cytokines, cell-surface protein, cytoskeletal molecules, and proteolytic enzymes.

3.1.1: Changes of transcriptional factor expression

Activation of transcription factors is considered a key step in triggering the EMT process (Nawshad et al., 2007, Vincent et al., 2009). Based on data from previous studies, selected factors (twist, Snail-1, Snail-2, and NF-κB) have been closely associated with EMT-induction and were therefore selected for investigation.

Analysis using sq-RT-PCR demonstrated that exposure of H400 cells to heat-killed periodontal pathogens (*P. gingivalis* and *F. nucleatum*) and *E. coli* LPS resulted in gene expression profiles reportedly to be representative of EMT (Minafra et al., 2014, Lamouille et al., 2014). Eight days of cell culture in the presence of bacterial stimulation resulted in a significant up-regulation ($P<0.001$) of twist, Snail-1 and -2, LEF-1 and NF-κB compared with unstimulated controls (Figure 31). Twist mRNA showed an approximately 2-fold up-regulation in expression in oral epithelial cells in response to bacterial stimulation (Figure 31A). Furthermore, Snail-1 and -2, also showed significant up-regulation ($P<0.001$), of approximately 6- and 4-fold respectively, in comparison with unstimulated controls following 8-days of stimulation (Figure 31B and C). Cultures exposed to *P. gingivalis* and *F. nucleatum* showed similar increases in expression level of these markers. Transcript levels of NF-κB (Figure 31D) also increased ($P<0.001$), between 2- and 6-fold, relative to unstimulated controls. The pattern of NF-κB expression in response to bacterial stimuli was variable from day 1-5, however at the end of the experiment (day 8) all stimulated cultures showed similar expression levels. Expression of another EMT-regulator, LEF-1, was also significantly

increased (up to 6-fold) with the highest transcription associated with stimulation of H400 cells in the presence of *F. nucleatum* (Figure 31E).

3.1.2: Pro-inflammatory cytokines gene expression in oral keratinocytes

Stimulation of oral keratinocyte cultures with bacterial components resulted in up-regulation of EGF, TNF-α, TGF-β1, IL-1β, IL-6, and IL-8 (Figure 32). Transcription of EGF was up-regulated up to 6-fold ($P<0.001$), while TNF-α and TGF-β1 showed a 2-3-fold up-regulation at all time-points studied compared with unstimulated controls. At the end of the experiment, cells treated with *F. nucleatum* showed the highest up-regulation of EGF and TGF-β1 (Figure 32C), while cells exposed to *P. gingivalis* showed the highest transcription of TNF-α (Figure 32B). Expression levels of IL-1β, IL-8, and IL-6 also showed significant up-regulation ($P<0.001$), at approximately 3-, 4-, and 5-fold, respectively, in response to exposure to heat-killed bacteria (Figure 32D, E, and F). These data indicated that H400 epithelial cells responded to bacterial challenge by increasing the production of cytokines implicated in initiation of EMT.

3.1.3: Periodontal pathogens induced transcriptional changes in cell surface and cytoskeletal molecules

The earliest changes associated with EMT have been reported to be the down-regulation of attachment proteins with subsequent compromised epithelial cell adhesion (Zeisberg and Neilson, 2009). Exposure of H400 keratinocytes to bacterial components, over 8 days, resulted in significant down-regulation (~2-5 fold) ($P<0.001$) of E-cadherin transcription relative to the unstimulated control. The highest down-regulation (approximately 5-fold) was associated with *P. gingivalis* and *F. nucleatum* exposure (Figure 33A). Down-regulation of E-cadherin was associated with increased expression of the mesenchymal N-cadherin, ($P<0.001$) over the same time-period (Figure 33B). All bacterial groups showed a gradual increase in N-cadherin expression over the 8-day time-course (between 5-6-fold) with *P.*

gingivalis producing the highest up-regulation compared with the unstimulated control. Another mesenchymal marker, FSP-1, was also significantly up-regulated (up to 8-fold) in response to stimulation with the periodontal pathogens in cultures as compared with the unstimulated control (Figure 33C).

In general, all stimulated cultures demonstrated a 2- to 4-fold β-catenin down-regulation at the end point of the experiment and the highest changes detected were associated with *E. coli* LPS exposure (Figure 34A). The mesenchymal associated cytoskeletal protein, vimentin, showed increased expression in cells exposed to all bacterial components. Indeed, vimentin transcription was significantly ($P<0.001$) up-regulated in all stimulated cultures from days 1-8. The expression of this protein was increased from 2- to 6-fold during the experimental period relative to the unstimulated control (Figure 34B) with *F.* nucleatum stimulated cultures showing the greatest increase. Analysis of data indicated that stimulation of epithelial cells with whole dead *P. gingivalis* or *F. nucleatum* resulted in modulation of key-EMT cytoskeletal markers. β-catenin, an epithelial-phenotype protein, was down-regulated in a similar pattern to E-cadherin which suggested a compromised E-cadherin-catenin complex. Further, mesenchymal-associated proteins, vimentin and FSP-1, were up-regulated which may have indicated a shift towards a mesenchymal-phenotype in response to bacterial stimulation.

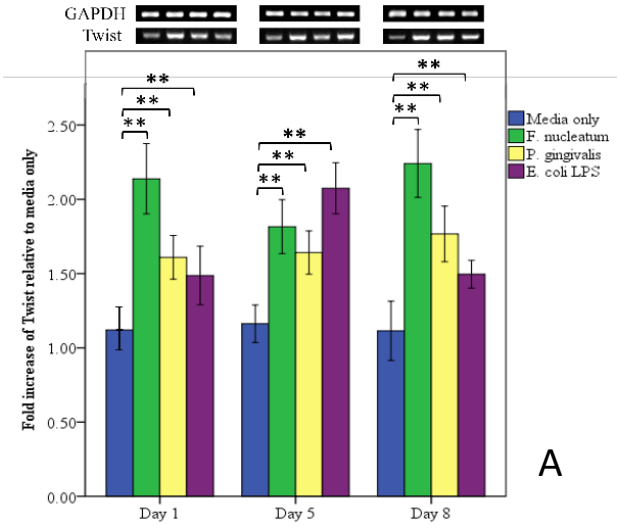
GAPDH
Twist
Fold increase of Twist relative to media only
0.00
0.50
1.00
1.50
2.00
2.50
Day 1
Day 5
Day 8
Media only
F. nucleatum
P. gingivalis
E. coli LPS
A

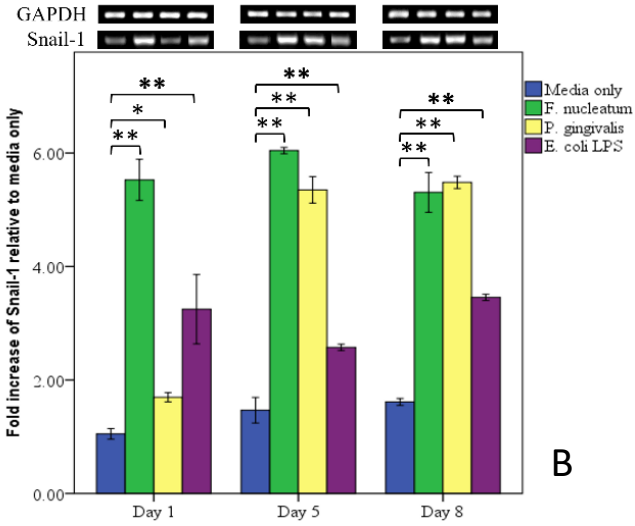
GAPDH
Snail-1
Fold increase of Snail-1 relative to media only
0.00
2.00
4.00
6.00
Day 1
Day 5
Day 8
Media only
F. nucleatum
P. gingivalis
E. coli LPS
B

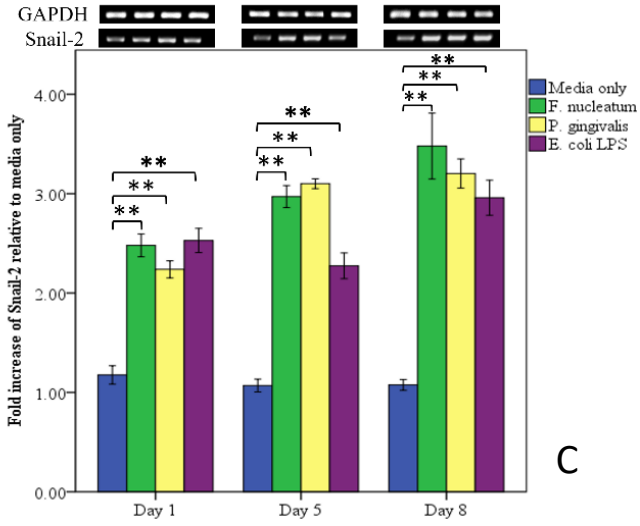
GAPDH
Snail-2
Fold increase of Snail-2 relative to media only
0.00
1.00
2.00
3.00
4.00
Day 1
Day 5
Day 8
Media only
F. nucleatum
P. gingivalis
E. coli LPS
C

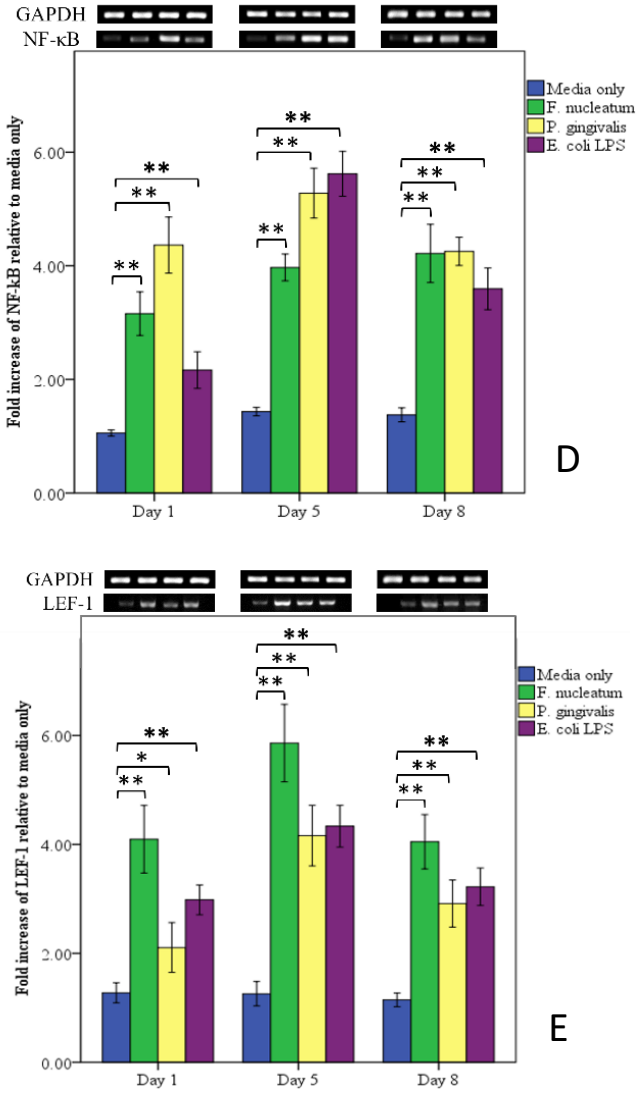

Figure 31. Heat-killed periodontal pathogens significantly upregulated expression of key-EMT transcriptional factors (A) twist (B) Snail-1, (C) Snail-2, (D) NF-κB, (E) LEF-1. Expression of Snail-1, NF-κB, and LEF-1 increased up to 6-fold during experimental period, while twist and Snail-2 showed ~2- and 3-fold, respectively. (*=P<0.05, **=P<0.001).

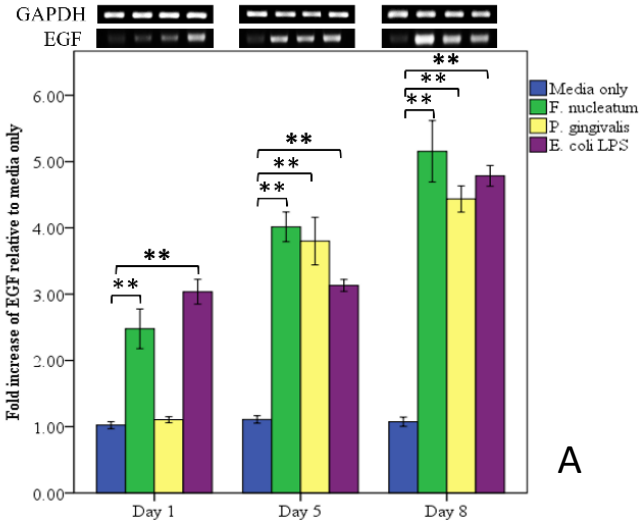
GAPDH
EGF
Fold increase of EGF relative to media only
6.00
5.00
4.00
3.00
2.00
1.00
0.00
Day 1
Day 5
Day 8
Media only
F. nucleatum
P. gingivalis
E. coli LPS
**

A

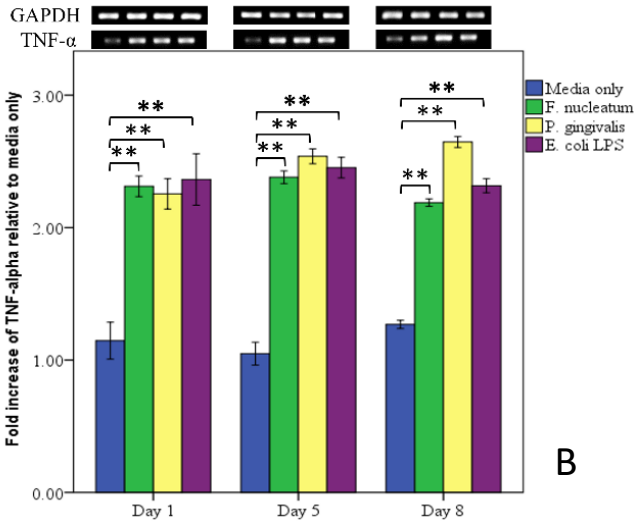
GAPDH
TNF-α
Fold increase of TNF-alpha relative to media only
3.00
2.00
1.00
0.00
Day 1
Day 5
Day 8
Media only
F. nucleatum
P. gingivalis
E. coli LPS
**

B

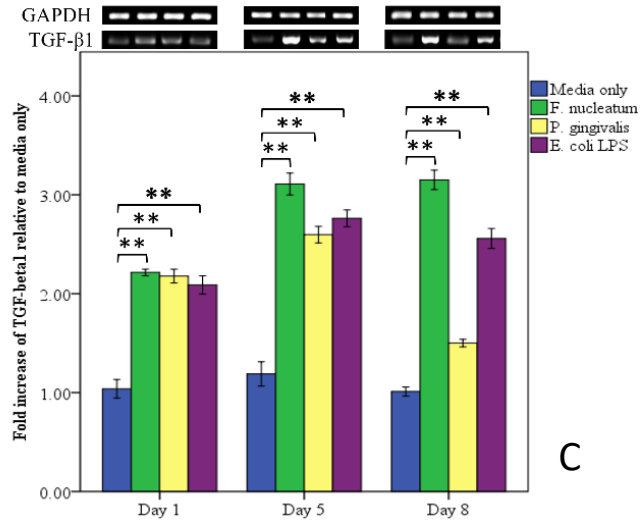
GAPDH
TGF-β1
Fold increase of TGF-beta1 relative to media only
4.00
3.00
2.00
1.00
0.00
Day 1
Day 5
Day 8
Media only
F. nucleatum
P. gingivalis
E. coli LPS
**

C

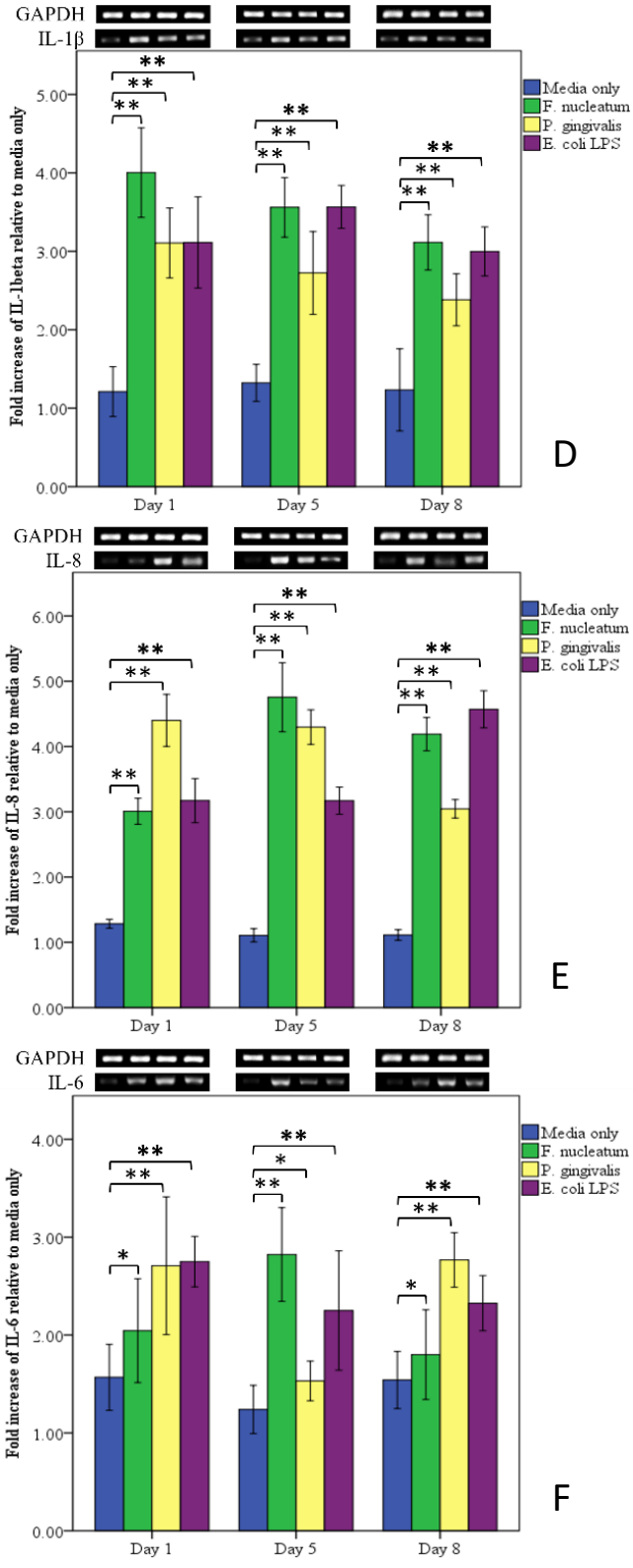

Figure 32. Exposure of H400 cells to bacterial components significantly increased the transcription of inflammatory cytokines (A) EGF, except for *P. gingivalis* at day 1, (B) TNF-α, (C) TGF-β1, (D) IL-1β, (E) IL-8, and (F) IL-6. The average increase in transcription for all cytokines, in stimulated cultures investigated, ranged between 2 to 6-fold relative to cells treated to media only over 8-days. Experiment run in triplicate, (*=P<0.05, **=P<0.001).

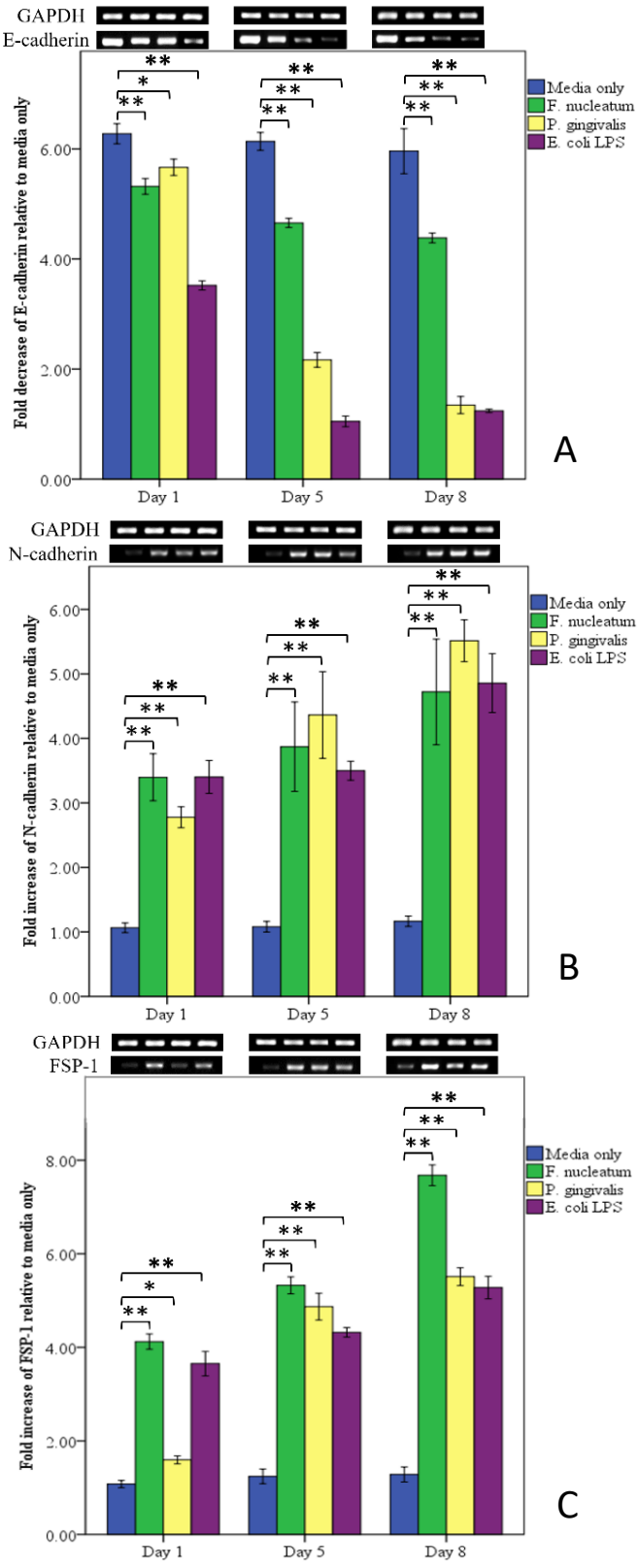

Figure 33. Stimulation of H400 keratinocytes with periodontal pathogens resulted in down-regulation of the epithelial molecular marker transcription (A) E-cadherin (almost 3-fold) whilst resulting in the up-regulation of mesenchymal proteins transcription (B) N-cadherin, ~6-fold, and (C) FSP-1, ~8-fold, in comparison with unstimulated controls. Experiments were performed in triplicate, (*=P<0.05, **=P<0.001).

3.1.4: Changes in matrix metalloproteinase gene expression in oral keratinocytes following bacterial exposure

The later stages of EMT are characterised by increased proteolytic activity which disrupts the basement membrane thereby facilitating the migration of transitioned cells (Lee et al., 2006, Lamouille et al., 2014). Analysis of selected genes showed significant up-regulation ($P<0.001$) of transcripts for the MMP enzymes -2, -9 and -13 following epithelial cell exposure to bacteria in comparison with cultures treated with media only (Figure 35). The gene expression of all transcripts for the MMPs investigated was significantly increased from days 1-8 in association with all bacterial component treatments as compared with the unstimulated controls. During the experimental period, expression of MMP-2 and -9 was increased up to 4-fold in response to bacterial exposure relative to the unstimulated control. The expression of MMP-13 was increased to almost 9-fold in response to these same stimuli.

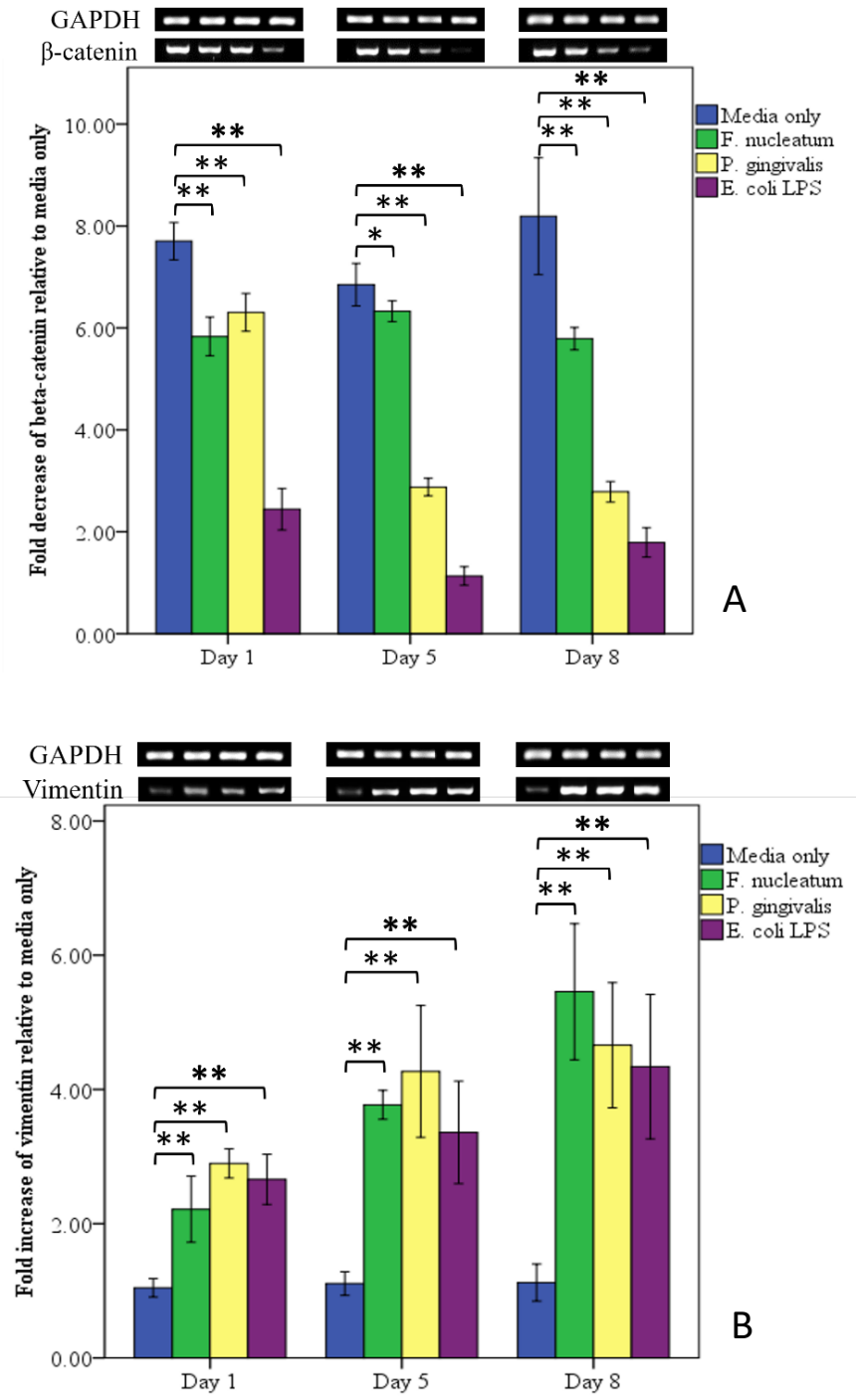

Figure 34. Expression of cytoskeletal genes in H400 cultures treated with media only, or heat-killed *P. gingivalis* and *F. nucleatum*, and *E. coli* LPS indicate down-regulation of (A) β-catenin in epithelial cells, accompanied by increased transcription of vimentin (B) following exposure to bacterial challenge. Expression of vimentin increased up to 6-fold which is almost equal to the level of β-catenin down-regulation when compared to media only group. The experiment was performed in triplicate, (*=P<0.05, **=P<0.001).

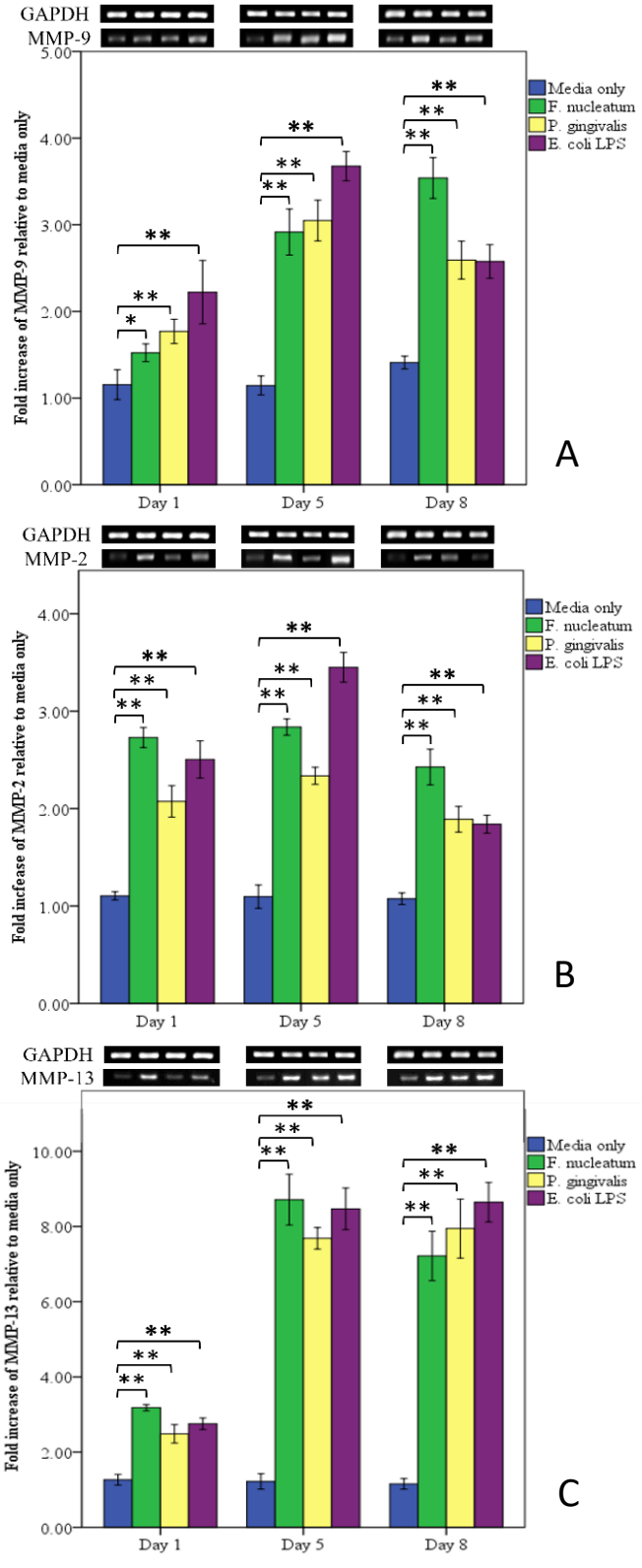

Figure 35. Transcription of the MMP enzymes, which are associated with the migratory-phenotype, significantly increased in response to bacterial stimulation. Expression of (A) MMP-9 and (B) MMP-2 peak to ~4-fold. (C) MMP-13 expression showed ~9-fold increase relative to controls. Experiments were undertaken in triplicate, (*=P<0.05, **=P<0.001).

3.2: Human EMT-PCR array analysis of H400 cells treated with bacterial components

Further analysis of changes in expression of EMT-related genes was performed by utilizing specific EMT PCR-arrays. This technique is real-time PCR-based and allowed profiling of multiple genes in a single analysis providing an accurate and highly sensitive assay (Quellhorst et al., 2006). Based on previous findings obtained from sq-RT-PCR and due to the relatively high cost of PCR-array kits, only one time point was selected for investigation (day 8), when changes in most of EMT-indicators expression were observed.

Analysis of data (Table 15) demonstrated a comparable pattern of EMT-related gene expression relative to the individual sq-RT-PCR data previously obtained. Indeed, both techniques yielded the same pattern for fold change in gene expression, at day 8, for twist, Snail-1, Snail-2, TGF-β1, E-cadherin, β-catenin, N-cadherin, vimentin, MMP-2 and -9. Transcripts for the epithelial molecules such as E-cadherin, β-catenin, and cytokeratin-14 were significantly down-regulated ($P<0.05$) from 2- to 5-fold in the stimulated cells in comparison with the unstimulated control. These changes were also associated with a 5-fold up-regulation of vimentin in comparison with the unstimulated control. In addition, up-regulation of Snail-1, Snail-2, twist, and bone morphogenic protein-7 (BMP-7) were observed relative to control cultures. Moreover; PCR-array analysis indicated changes in transcription levels had occurred to several other EMT-related indicators such as Jagged 1, Notch 1, ZEB 1, and Smad which further supported the induction of a mesenchymal-phenotype in this cell system.

The purpose of applying this technique was to support the previous findings obtained by sq-RT-PCR. In addition, the EMT-array provided additional evidence of EMT-related changes by demonstrating gene expression changes in oral keratinocytes in other important EMT-indicators such as NOTCH1, JAG1, ZEB1 and GSK3β.

Gene name	Gene Symbol	Fold changes relative to unstimulated control		
		F. nucleatum	***P. gingivalis***	***E. Coli* LPS**
Transforming growth factor β1	TGF-β1	2.8	2.2	1.6
Bone Morphogenic protein 7	BMP-7	2.5	4.7	6
Glycogen synthase kinase 3β	GSK3β	1.6	4.6	2.7
Jagged 1	JAG1	4.5	2	1.3
Notch 1	NOTCH1	6.9	2.1	1.9
Snail-1	SNAl1	4.3	6.3	1.9
Slug	SNAl2	1.5	3.1	1.6
Zinc finger E-box binding homeobox 1	ZEB1	3.2	7.8	2.9
E-cadherin	CDH1	-5.4	-4.3	-3.5
β-Catenin	CTNNB1	-2	-3.1	-1
Cytokeratin 14	KRT14	-2.1	-2.5	-1.1
N-cadherin	CDH2	6.3	2.4	5.7
Vimentin	VIM	5.5	4.8	2.6
Matrix metalloproteinases-2	MMP2	2.4	2	3.1
Matrix metalloproteinases-9	MMP9	6.5	2.1	2.4
Smad family member 1	SMAD1	2.4	1.8	2.4
Twist transcription factor 1	TWIST1	2	4	6.6

Upregulated Downregulated

Table 15. EMT PCR-array analysis showing fold changes in transcription of EMT-related genes following exposure to bacterial components. The table was generated by using the Qiagen online analysis tool (www.SABiosciences.com/pcrarraydataanalysis.php).

3.3: Protein and gene expression analysis in potential EMT-inducing cytokines

Levels of three selected cytokines (TGF-β1, EGF and TNF-α), previously reported in many studies (Chapter 1, Section 4) to be associated with EMT-induction, were measured in the supernatant of H400 cultures stimulated with bacteria (Figure 36). All cytokines were significantly increased ($P<0.05$) over the 8-day culture period in comparison with cells treated with media only. Interestingly, cells exposed to *P. gingivalis* on day 1 did not demonstrate a significant increase in cytokine levels measured. *F. nucleatum* produced the highest increase (~4 to 6-fold, $P<0.001$) in levels of all cytokines assayed throughout the study period. The increases in cytokine production detected identify a potential autocrine mechanism for these molecules in triggering EMT. Notably ELISA data for EGF was consistent with PCR results of cultures treated with *P. gingivalis* (Figure 32A) which also showed no difference with unstimulated control at day 1. In contrast, PCR results for TGF-β1 and TNF-α in cultures stimulated with *P. gingivalis* showed increased gene expression from day 1-8.

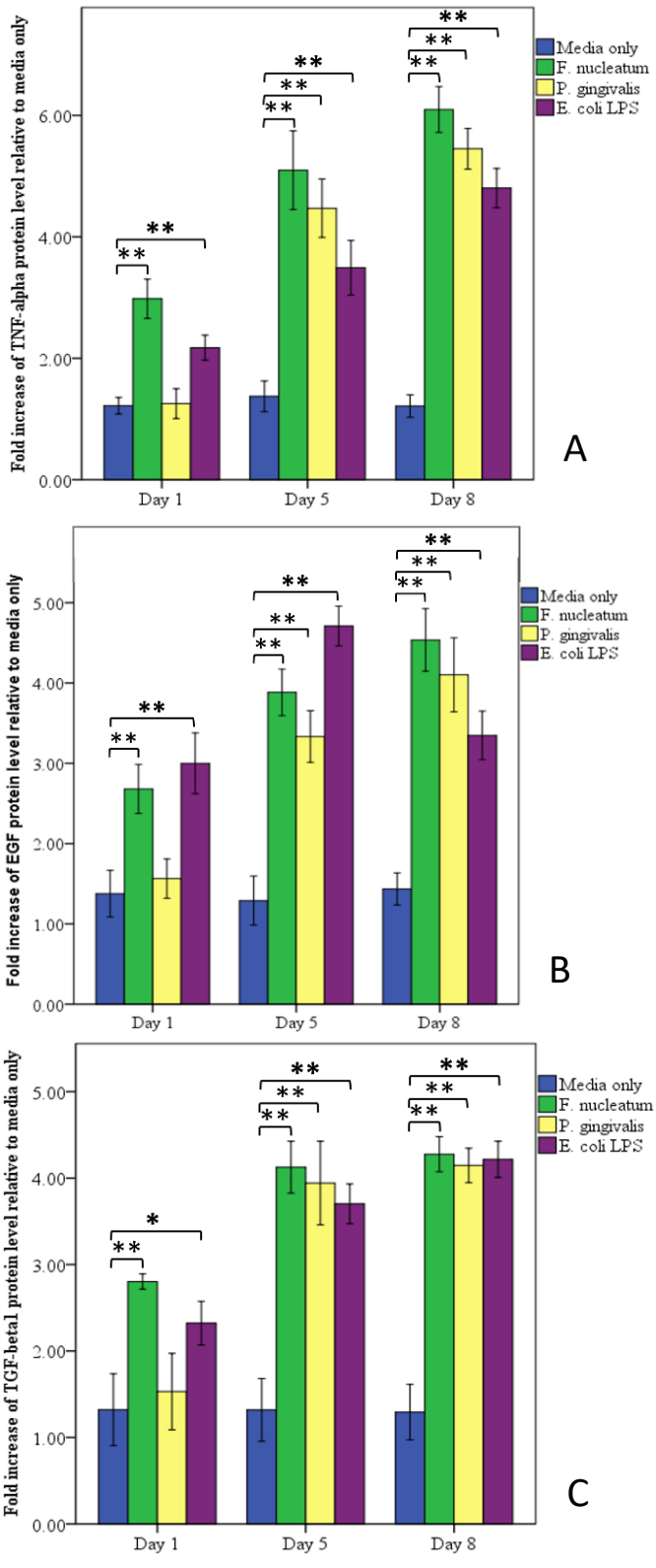

Figure 36. Supernatant collected from H400 cultures and assayed using ELISA for (A) TNF-α, (B) EGF, and (C) TGF-β1. Data indicates significant increases in the levels of all cytokines tested in the supernatants, except for the *P. gingivalis* group at day 1 which did not show significant increases in the level of any cytokine. Experiments were undertaken in triplicate, *=P<0.05, **=P<0.001.

3.4: Immunofluorescence analysis for E-cadherin and vimentin expression in H400 cells in response to bacterial stimulation

The purpose of analysis using immunofluorescence (IF) technique on H400 cultures, was to detect the presence of two important epithelial and mesenchymal EMT-markers (E-cadherin and vimentin). The increased number of vimentin positive cells associated with down-regulation of E-cadherin expression has been proposed by several studies as an important indicator of EMT (Medvedev et al., 2006, Strutz et al., 2002, Zeisberg and Neilson, 2009). Data from this thesis has now indicated that Gram-negative periodontal pathogens (*P. gingivalis* and *F. nucleatum*) modulate vimentin and E-cadherin gene expression in H400 cells over an 8-day culture period. Subsequently cells with vimentin positive staining were counted and expressed as a percentage of the total number of cells in the fields viewed. Analysis of immunofluorescence images (**Error! Reference source not found.**) showed an increase in the percentage of vimentin-positive H400 cells following bacterial stimulation in comparison with unstimulated controls (P<0.05).

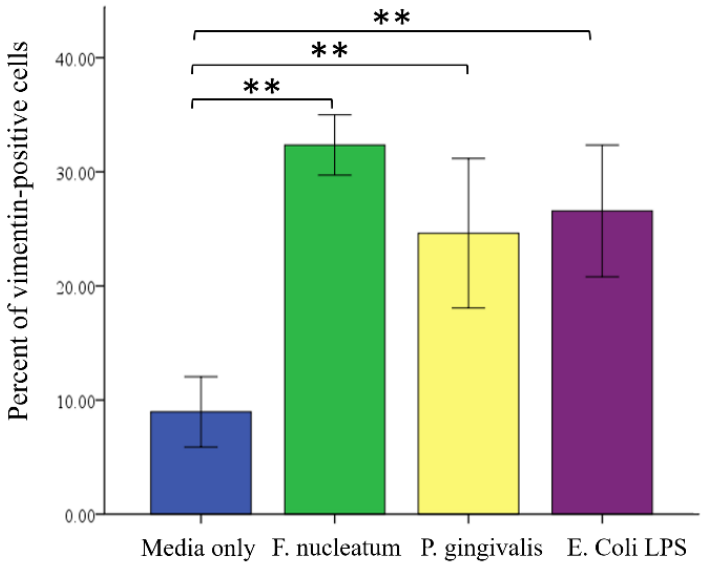

Figure 37. vimentin and E-cadherin expression in H400 cells after eight-day culture. (A) Analysis indicated a significant increase between cells stimulated with bacteria and unstimulated controls in terms of vimentin expression. (**=P<0.001).

Data indicated that the highest percentage of cells expressing vimentin were associated with cultures stimulated with *F. nucleatum*. The resulting transitioned cells, determined by positive-vimentin staining, either exhibited elongated, mesenchymal-like morphology whilst retaining some epithelial characteristics, i.e. by expressing internalised E-cadherin (Figure 38iv), or showing clusters of epithelial cells simultaneously expressing vimentin and E-cadherin. This was in contrast to other cell clusters which expressed E-cadherin only. These changes were also accompanied by a decrease of E-cadherin expression on the cell membrane of stimulated cells (Figure 38iv) when compared with cells treated with media only (Figure 38iii).

These findings indicated that exposure of epithelial cells to periodontal pathogens, resulted in down-regulation of an integral epithelial protein, E-cadherin, together with exhibiting increased expression of vimentin. This was also associated with morphological changes which resulted in cells changing from exhibiting classic epithelial cell morphology to a more fibroblast-like shape.

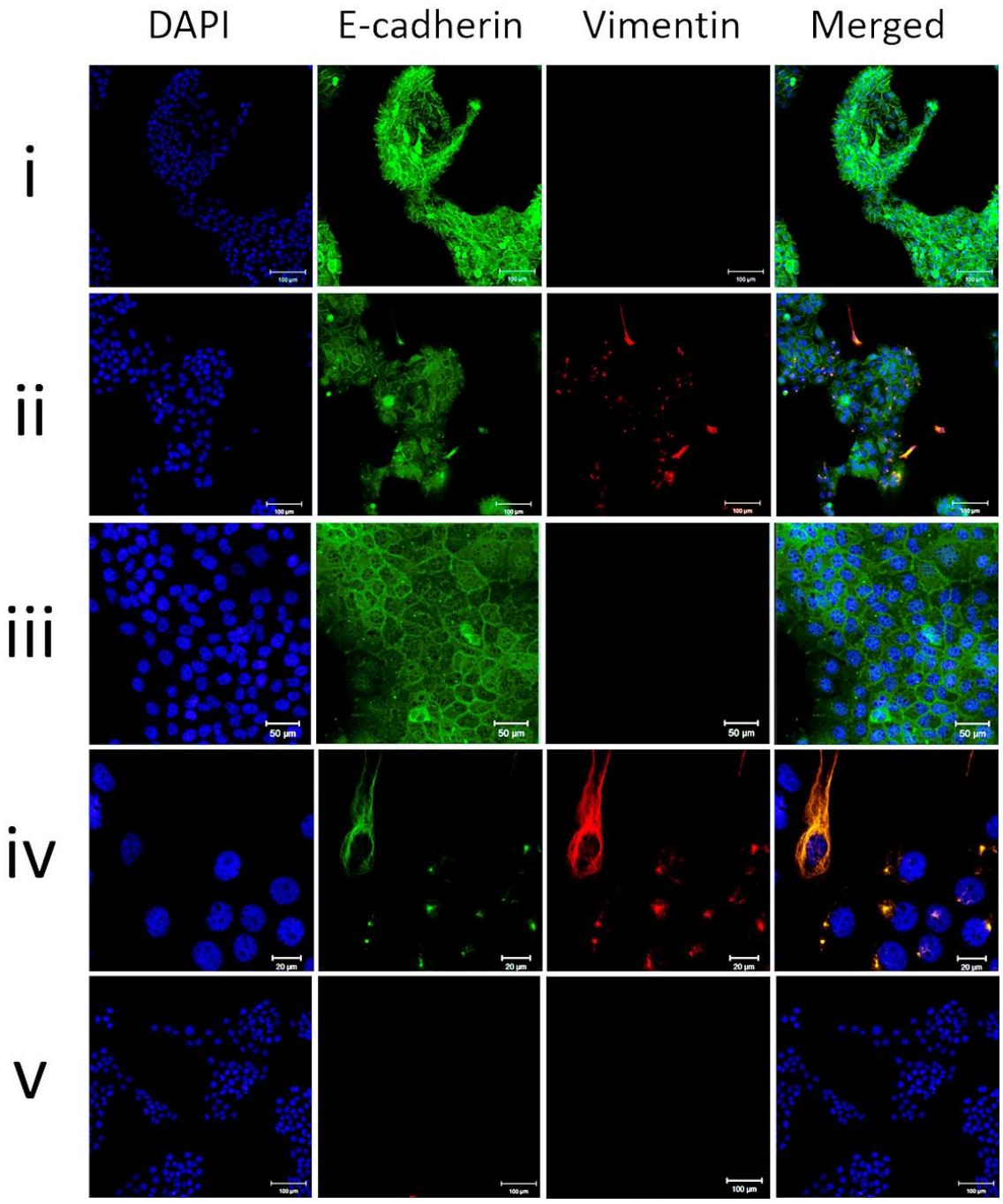

Figure 38. Representative IF staining indicates that *F. nucleatum* modulated expression of vimentin (red) (ii) when compared with the unstimulated control (i). Higher magnification showing that unstimulated control (iii) maintained normal E-cadherin distribution and negatively expressed vimentin. Scale bar=50μm. while stimulated cultures (iv) showed presence of vimentin-positive cells which either exhibit mesenchymal-like morphology and retained some characteristics of their parental origin by expressing E-cadherin or cluster of epithelial cells simultaneously expressing vimentin with downregulation of E-cadherin from periphery of cells. Scale bars= 20μm. Negative controls (cultures treated with secondary antibodies only) were included to exclude possibility of unspecific staining (v).

3.5: Immunocytochemical analysis of Snail activation in bacterial exposed H400 keratinocytes

Transcriptional factor, Snail-1, is well-known for its master regulatory role during EMT mainly by repressing E-cadherin expression (Wu and Zhou, 2010, Teng et al., 2007) Therefore, its activity was further explored using an immunocytochemistry assay for H400 cultures exposed to bacterial stimulation. Notably it is reported in the literature that Snail-1 activation is increased in response to inflammatory stimuli and may induce EMT-phenotype (Wu et al., 2009). Epithelial monolayers were treated with bacterial components over eight days then stained to investigate activation of Snail-1. Immunocytochemistry analysis (Figure 39A) indicated a significant increase ($P<0.05$) in the percent of Snail-positive cells, following the same period of stimulation as compared with the control. Both *P. gingivalis* and *F. nucleatum* activated Snail-1 in H400 keratinocytes to a similar extent. Immunocytochemical images (Figure 39B) showed Snail-1 positive cells which are characterised by dark brown discoloration of their nuclei in contrast to unstimulated cells which exhibit clear violet nuclei. These results were consistent with the previous PCR findings which showed down-regulation of E-cadherin following exposure of epithelial cells to periodontal pathogens. This could be due to increased Snail-1 transcriptional activity which is well-known for its E-cadherin-suppressive activity.

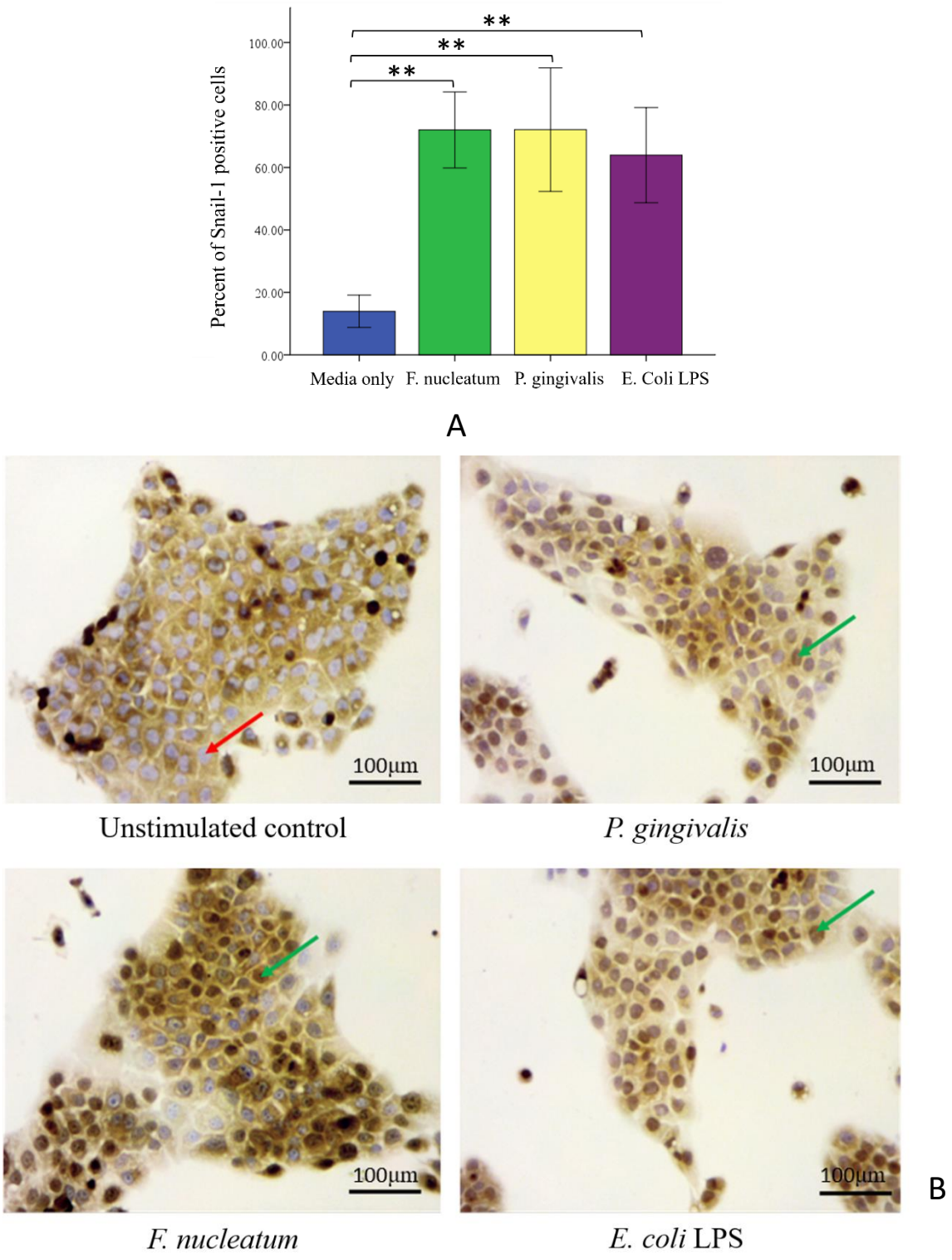

Figure 39. Stimulation of H400 cells with periodontal bacteria resulted in significant increase in Snail-positive cells. (A) Semi-quantitative analysis of Snail-positive cells showing that *P. gingivalis* and *F. nucleatum* elicited the highest response (up to 70%) when compared with unstimulated controls (B) ICC staining of H400 cells showing increased Snail expression as indicated by dark brown discoloration of the (green arrows), while unstimulated cells treated mainly exhibited dark blue nucleus (red arrow). Experiments undertaken in triplicate, Scale bars are shown. (**=P<0.001).

3.6: Epithelial integrity of H400 cultures exposed to bacteria

As EMT is associated with a decrease in expression of proteins involved in cellular attachment, it has been proposed that this contributes to cell dispersion with subsequent loss of epithelial barrier function (Sume et al., 2010). Furthermore, the loss of epithelial integrity has been associated with malignant tissue invasion and plays a potential role in the initiation and propagation of periodontal disease. H400 culture monolayer integrity was investigated by using *in vitro* trans-epithelial electrical resistance (TEER) following exposure of epithelial monolayers to bacterial components. This technique was previously described in Chapter 2, Section 8. The electrical resistance of H400 monolayers was significantly lower in stimulated H400 cells in comparison with unstimulated controls ($P<0.05$) from days 4-8 following exposure to *F. nucleatum* and *E. coli* LPS, indicating that integrity of epithelial sheets in the cultures were compromised following exposure to periodontal pathogens (Figure 40).

3.7: Transwell migration assay of H400 cells following exposure to bacteria

Following loss of cellular attachment and acquisition of mesenchymal proteins, transitioned cells in the late stages of EMT have been reported to migrate into the underlying connective tissue and increased migratory ability is regarded as an indicator of acquisition of a mesenchymal phenotype in malignant tumours (Zeisberg and Neilson, 2009). Subsequently H400 cells were exposed to periodontal bacterial components over 8 days, then harvested and used in the Transwell migration assay.

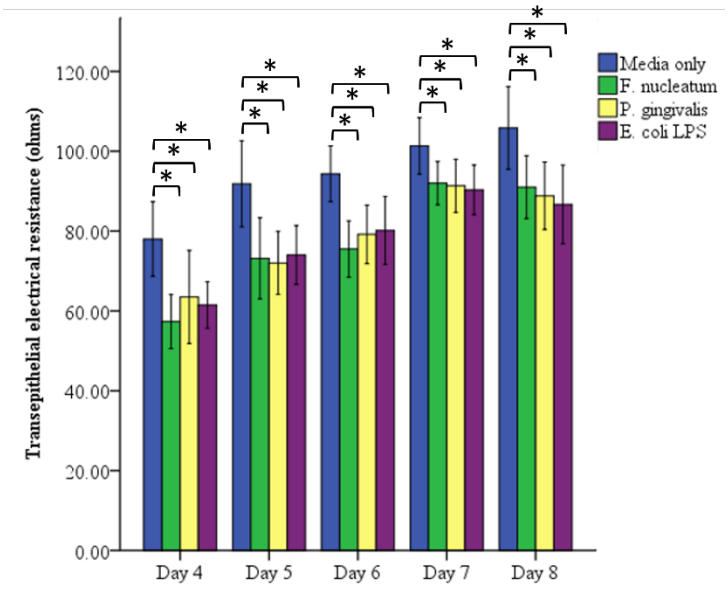

Figure 40. Electrical resistance of epithelial monolayers in response to bacterial stimulation showed a significant decrease in comparison with controls. On day 4, electrical resistance was significantly reduced in all stimulated groups in comparison with unstimulated controls. Data is shown as mean + SD. Experiments were performed in triplicate. (*=P<0.05).

The number of cells that migrated, after 12hr, through the membrane inserts was counted and averaged. The migration of H400 cells in the transwell migration assay was significantly increased (P<0.001) when cells were previously exposed to periodontal pathogens, indicating enhanced cell mobility following bacterial exposure when compared with control cultures (Figure 41). The highest number of migrated cells was associated with *F. nucleatum* stimulation, followed by *E. coli* LPS, and *P. gingivalis*. These findings suggest the acquisition of a migratory-phenotype by epithelial cells following bacterial stimulation which was further investigated using the scratch wound assay.

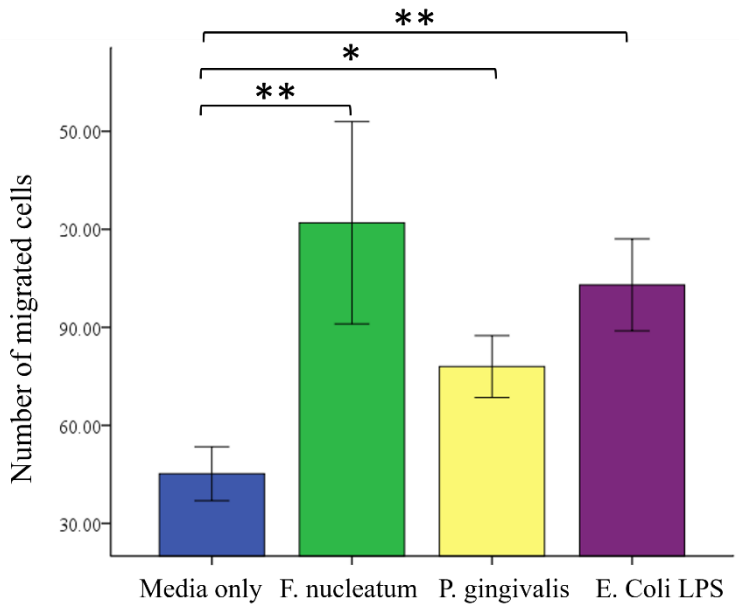

Figure 41. Transwell migration assay for H400 cells stimulated over 8 days with periodontal pathogens, *E. coli* LPS or media negative control. Data demonstrated that the higher number of cells had migrated through the membrane in comparison with control. The highest number of migrated cells was associated with cultures treated with *F. nucleatum* followed by *E. coli* LPS and *P. gingivalis*. Experiments were performed in triplicate, (*=P<0.05, **=P<0.001).

3.8: Migratory ability of stimulated H400 cells using scratch and barrier-insert models

To explore the migratory ability of H400 cells exposed to bacteria for 8 days, an artificial wound was created in a confluent cell monolayer and the rate of closure determined. The first approach used was by means of the well documented scratch-wound assay. The monolayers were wounded by using a 10µl sterile pipette tip, this was repeated until a technique was developed to allow consistent wound gap creation (~500µm). This distance was selected for consistency with the other technique studied which utilised the ibidi tissue-culture insert. This approach enabled better comparison of closure rates between the two techniques.

For the scratch-wound assay, images were captured as previously described (Chapter 2, Section 9.2) (Figure 42A). Up to 12hr after scratching, no significant differences were observed in gap closures between stimulated and unstimulated control groups. However, after 24hr, bacteria treated cultures exhibited a greater degree of gap closure (P<0.05) when

compared with controls (Figure 42B). A similar pattern of gap closure was observed when the second method using the insert-barrier was performed (Figure 43). Nonetheless, gaps created by using tissue culture inserts, where no mechanical stress was applied, showed slower closure rate when compared with the conventional scratch-wound method (Table 16). H400 cultures stimulated with *F. nucleatum* and *P. gingivalis* which were mechanically disrupted, showed a significantly higher rate in gap closure ($P<0.05$) after 12hr when compared with the barrier-insert created gap, however this was not the case for the *E. coli* LPS treated and unstimulated control groups. After 24hr, all epithelial scratched monolayers treated with bacteria and unstimulated controls, showed a higher degree of gap closure ($P<0.001$) as compared with the insert-barrier groups (Table 16). Additionally, the defects created by both methods were examined using SEM (Figure 44). Notably the scratch-wound approach showed apparent cellular damage and higher magnification imaging showed that cells bordering the scratch wound had been damaged and generated cellular remnants (Figure 44D, F, and H). In contrast, cells bordering the cell gap created using insert barriers showed intact cell membranes and the surrounding area was relatively free of cellular debris (Figure 44C, E, and G).

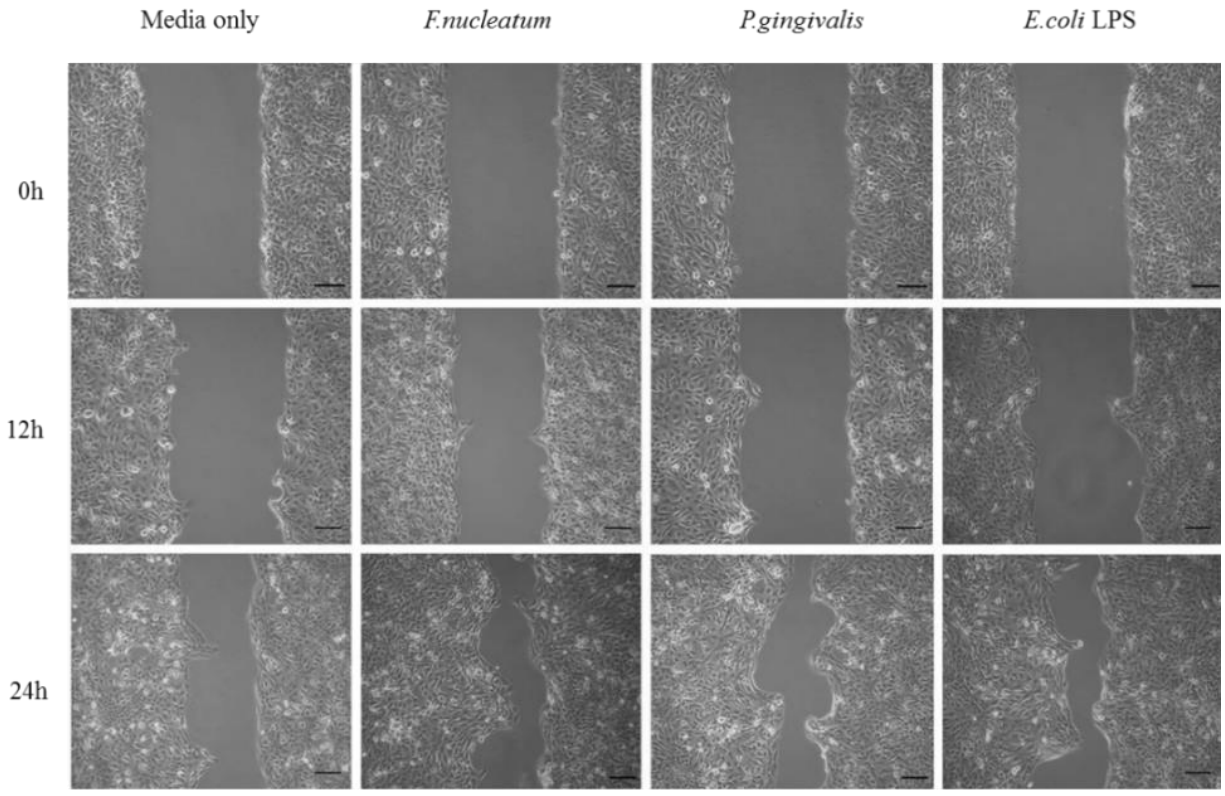

A

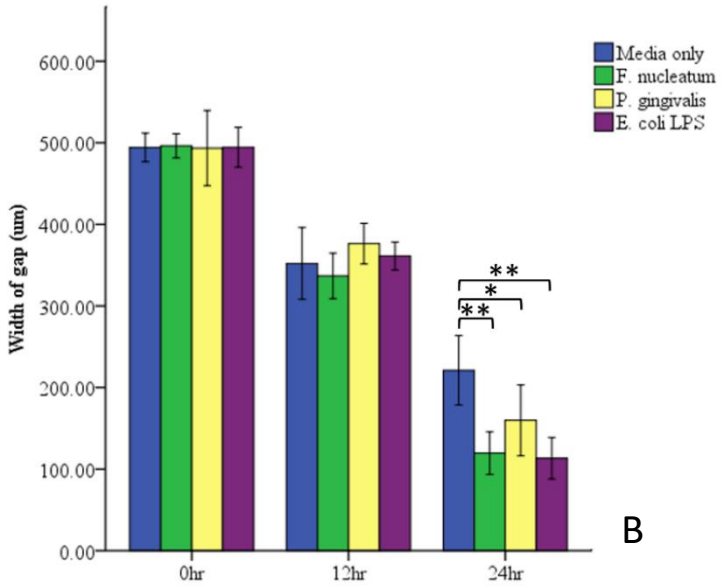

B

Figure 42. Confluent monolayers of H400 cells were disrupted by scratching with a 10μm pipette tip following 8 days of exposure to heat-inactivated *F. nucleatum* and *P. gingivalis* and 20μg/ml *E. coli* LPS. (A) Images were captured immediately following scratching and then after 12 and 24hr culture. Scale bars=100μm. (B) Measurements of the wound width at 12hr indicated no significant difference, however at 24hr scratch closure was significantly increased in all cultures exposed to bacterial components in comparison with unstimulated control. Experiments performed in triplicate, *=P<0.05, **=P<0.001.

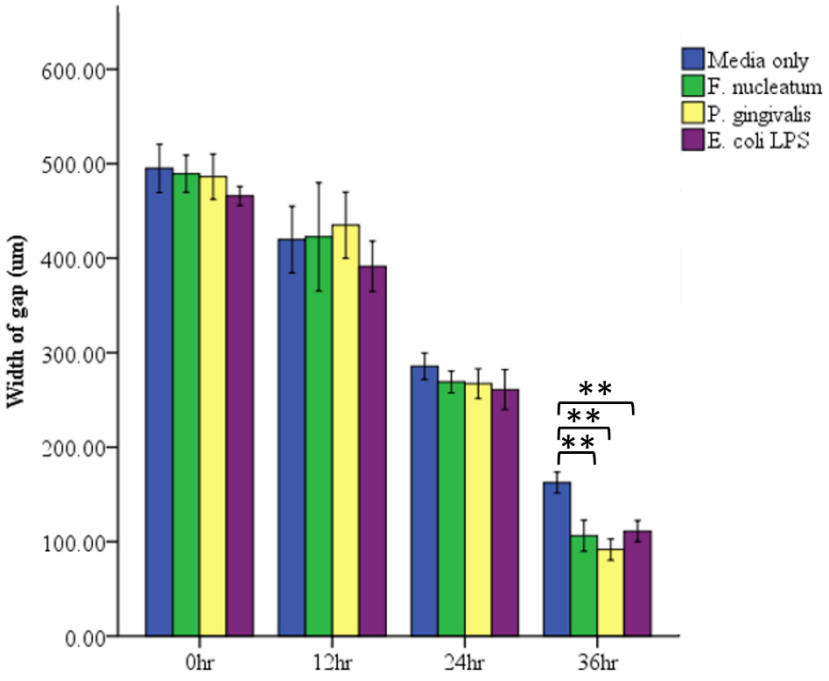

Figure 43. Analysis of barrier-defect measurements indicated no significant difference at 12hr and 24hr between cultures exposed to heat-inactivated periodontal pathogens and unstimulated controls. The rate of closure significantly increases after 36hr of treatment with bacterial components. Experiment performed in triplicate, *=P<0.05, **=P<0.001.

Both the scratch and barrier-insert assays further support data from the Transwell migration assay. In addition, the effect of bacteria on increased proliferation of cells was previously excluded as a mechanism which contributed to differences in gap closure (Chapter 3, Section 3.3.3). Subsequently data indicated that the increased migratory ability of epithelial cells, following 8-day exposure to bacterial components, was the main reason for the increased rate of gap closure in stimulated cultures as compared with unstimulated controls.

		Scratch	Insert	P-value	Scratch	Insert	P-value	Scratch	Insert	P-value
		0hr			12hr			24hr		
Mean gap width (μm)	Media only	500.2±3.2	495.4±25.6	N.S	384.5±59.8	419.6±35.1	N.S	239.5±17.6	285.6±14.2	<0.001
	F. nucleatum	486.3±23.9	502.3±12.3	N.S	317.3±15.9	422.5±57.3	<0.05	126.2±13.9	268.9±11.5	<0.001
	P. gingivalis	489.4±19.7	500.3±7.8	N.S	374.7±27.3	434.9±35.1	<0.05	160.1±22.9	267.3±15.6	<0.001
	E. coli LPS	506.5±13.1	485.9±35.6	N.S	367.2±27.9	391.3±26.5	N.S	103.3±9.7	261.0±21.1	<0.001

Table 16. Comparison of closure rate of defect created by scratch-wounding and insert-barrier approach showed significantly higher rate of gap closure in the scratch model compared with the insert-barrier method. After 12hr, both periodontal pathogen exposures in the scratch group significantly exhibited an increased rate of defect closure. However, media only and *E. coli* LPS in the same group failed to produce any significant change compared with barrier groups. At 24hr, all scratch groups exhibited a higher rate of gap closure in comparison with the barrier-insert groups.

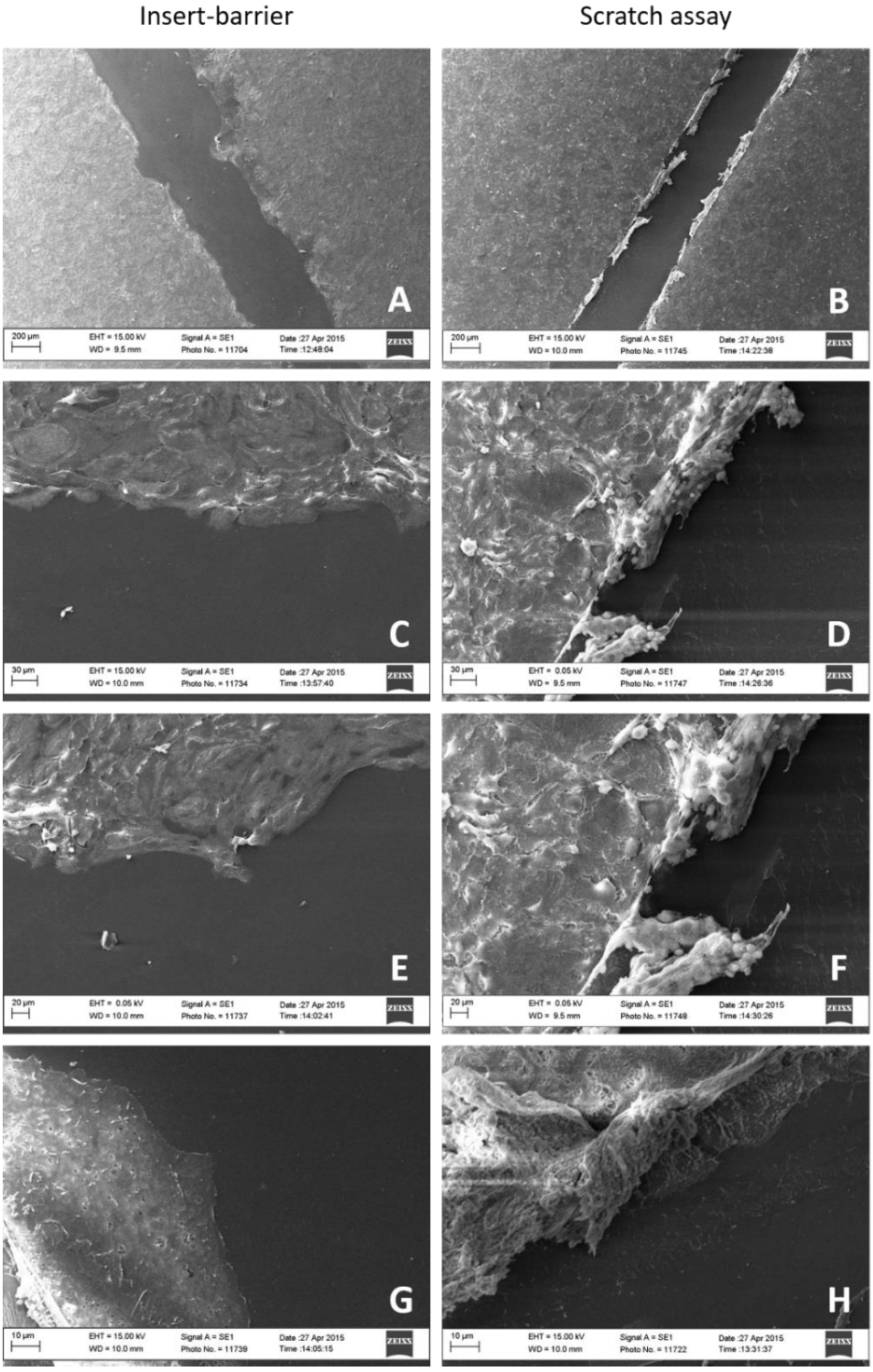

Figure 44. SEM images of gaps generated in confluent H400 monolayers by using the insert-barrier (A) and the scratch method (B). Higher magnification shows intact cells and a gap space free of debris in the insert-barrier cultures (C, E, and G) compared with damaged cells surrounded by cellular remnants generated by scratching (D, F, and H). Scale bars are shown. Images are representative of studies performed in triplicate.

4: Discussion

Oral malignancies are a major health problem that is characterised by high recurrence and metastasis rates that are closely associated with excessive tobacco and alcohol consumption (Feller and Lemmer, 2012). However, a proportion of patients develop OSCC in the absence of any known risk factor which suggests there may be other predisposing risk factors in the oral cavity such as infectious agents (Acay et al., 2008). Although viruses; e.g. human papilloma virus, were reported to be highly associated with oral malignancies, evidence from several studies suggested a potential role of bacteria in oral cancer (Lax and Thomas, 2002). Furthermore, data from different studies have suggested that oral cancer is associated with tooth loss and poor oral hygiene, irrespective of other risk factors (Narayan et al., 2014). A clinical study undertaken on 165 patients showed that poor oral hygiene is an independent risk factor in 80% of OSCC cases examined (Rosenquist et al., 2005). Similar findings were reported in a study of 60 patients where other potential risk factors for OSCC were excluded (Oji and Chukwuneke, 2012). Therefore, it is proposed that inflammatory conditions within the oral cavity such as chronic periodontitis could increase the risk of oral malignancies. Indeed, a retrospective study carried out on 178 OSCC patients, using radiographic and clinical examination, recommended considering treatment of periodontitis as a preventive measure which could potentially reduce the risk of neoplasm (Moergel et al., 2013). In addition, findings from a clinical study concluded that two out of four patients with chronic periodontitis are at risk of developing OSCC. This could be due to the negative impact of the inflammatory cascade, triggered in response to periodontitis, on the integrity of the oral mucosa (Krüger et al., 2013). Periodontal diseases are associated with a diverse population of potentially pathogenic bacteria, in particular, Gram negative anaerobes (Paster et al., 2001). Studies by Mager et al. (2005) have indicated the presence of a significantly higher number

of these bacteria in salivary samples of OSCC patients as compared with healthy controls. In OSCC, *P. gingivalis* potentially facilitates cancer metastasis via up-regulating MMP-9 expression and increasing resistance to apoptosis which is a characteristic feature of EMT (Inaba et al., 2014). Furthermore, recent studies have highlighted the potential involvement of periodontal pathogens, including *F. nucleatum* and *P. gingivalis*, in increased invasiveness of OSCC by potentially inducing the EMT process (Binder Gallimidi et al., 2015, Ha et al., 2015). Samples derived from highly invasive gingival squamous cell carcinoma cases showed an abundant presence of *P. gingivalis* compared with primary non-metastatic cancer (Katz et al., 2011), however the bacterial role and reason for the observed association remain unclear.

The accumulating evidence on EMT suggests that this process provides a potential mechanism to facilitate some of the required steps leading to metastasis (Jechlinger et al., 2002, Lee et al., 2006).

4.1: Exposure to periodontal pathogens promotes expression of EMT-related cytokines

EMT is characterised by several molecular changes involving cell surface proteins, cytoskeletal proteins, transcriptional factors, and proteolytic enzymes. These events require signaling from different cytokines (Kalluri and Weinberg, 2009, Lamouille et al., 2014). While the inflammatory response is essential to orchestrate the elimination of the sources of infection and cellular damage and restore homeostasis of tissues these, cytokines may subsequently modulate the behaviour and progression of malignant tumours. A range of inflammatory cytokines such as TGF-β1, TNF-α, EGF, and interleukins are potentially involved in this process and evoke several mechanisms including angiogenesis, reactive oxygen species generation, and the triggering of EMT (Landskron et al., 2014)

In the current study, gene expression of several cytokines in stimulated H400 cultures (TGF-β1, TNF-α, EGF, IL-1β, IL-6, and IL-8) showed significant increases following exposure to heat-killed periodontal pathogens and *E. coli* LPS. This agrees with previous findings reported by Milward et al. (2007) which indicated that oral keratinocyte (H400) exposure to non-viable periodontal pathogens increased expression of TNF-α, IL-1β, and IL-8. Similarly, exposure of gastric mucosa to another Gram-negative bacteria, *H. pylori*, resulted in up-regulation of IL-1β, -8, and TNF-α (Noach et al., 1994), molecules associated with driving EMT-related changes (Yu et al., 2014, Baud et al., 2013, Amieva et al., 2003). Under normal physiological conditions, TGF-β1 is a potent anti-inflammatory cytokine, with well-recognized roles in embryogenesis, cell proliferation, differentiation, apoptosis, invasion, and adhesion (Santibañez et al., 2011). In addition, TGF-β signalling has been reported to induce EMT and cancer metastasis in a range cell types (Xu et al., 2009). Indeed treatment of mammary epithelial cells with TGF-β1 induced expression of vimentin which was associated with increased cell invasiveness (Yoshida et al., 2013). In addition, N-cadherin up-regulation was reported in association with TGF-β1-induced EMT in pancreatic cancer cells (Nakajima et al., 2004). TGF-β1-may induce EMT through stabilizing Snail (Wu and Zhou, 2010, Wang et al., 2013) and facilitating nuclear translocation of β-catenin (Masszi et al., 2004). The current study has now demonstrated increased expression of TGF-β1 in oral keratinocytes following exposure to periodontal pathogens as well as concomitant N-cadherin and vimentin.

Although TNF-α is a major proinflammatory cytokine, its role in cancer progression remains controversial (Balkwill, 2006). Data from mouse models of experimentally-induced colon cancer, injected with LPS, showed an increase in TNF-α-dependent metastasis. This study suggested that TNF-α enhanced cancer progression was driven by activation of NF-κB which

increased the proliferation and survival of malignant cells (Gonçalves et al., 2016). In addition, deletion or inhibition of TNF-α production in mice increased their resistance to chemically-induced skin malignancy and liver cancer (Rezaei et al., 2013). Previously prolonged exposure of an OSCC cell line to TNF-α resulted in activation of EMT via Notch signalling and has been associated with increased malignancy invasion (Lee et al., 2012). Chronic treatment with TNF-α resulted in NF-κB activating twist-induced 'stemness' in both normal and malignant breast cells (Li et al., 2012a). Notably in the study presented here, stimulation of oral keratinocytes with heat-killed periodontal pathogens and *E. coli* LPS also increased transcription of EGF, IL-1β, IL-6, and IL-8. This may activate EMT independently or synergistically with other potent EMT-inducing cytokines such as TGF-β1 and TNF-α (Li et al., 2012b, Sullivan et al., 2009, Palena et al., 2012, Li et al., 2015, Wendt et al., 2010). Data from the PCR EMT array also indicated a significant increase in expression of TGF-β1 and BMP-7. Notably the role of BMP-7 in EMT induction is currently not clear in the literature. Data from work by Lim et al. (2011) showed that BMP-7 induced EMT in 2D and 3D models of prostate cancer cells, however others have suggested that this cytokine blocks TGF-β1-induced EMT in chronic kidney injury (Zeisberg et al., 2003) and in cholangiocarcinoma (Duangkumpha et al., 2014). It is unclear from current findings whether increased BMP-7 transcription contributed to EMT-signalling or functions to maintain epithelial cells.

In this study, TGF-β1, EGF and TNF-α were initially selected for investigation as they share a common EMT-signaling pathway which results in stabilization and increased nuclear activity of Snail. In addition, these cytokines have been reported as major EMT-inducing molecules in different pathological and physiological conditions (Wu and Zhou, 2010, Wang et al., 2013). It was originally hypothesised that these factors may drive the EMT phenotype

chronically due to local inflammatory events induced by bacteria which stimulate production of a range of cytokines with increasing levels due to autocrine signaling (Pandit, 2007, Schlange et al., 2007). Assaying levels of TGF-β1, EGF and TNF-α in the supernatant from H400 cell cultures showed that the presence of non-viable bacteria (*F. nucleatum* and *P. gingivalis) or E. coli* LPS significantly upregulated production of these cytokines although this was not as evident for *P. gingivalis* at 24hr post-stimulation. Notably these findings were consistent with previous reports indicating that *P. gingivalis* exerted a weaker effect (compared with *E. coli* LPS) in stimulating TNF-α over a 24hr period both *in vivo* and *in vitro* (Liu et al., 2008).

4.2: Presence of bacterial components provoke expression of transcriptional factors and signalling molecules

Reprogramming of epithelial cells into more motile, mesenchymal-like cells requires activation of key-transcriptional factors which regulate this process. Members of the Snail family, twist-1, LEF-1, and NF-κB are well-known for roles in modulating EMT during different physiological and pathological conditions (Lamouille et al., 2014, Lee et al., 2006).

Snail-1 and -2 are well characterised zinc-finger transcription factors, that increase in activity during inflammation and are well-known suppressors of E-cadherin transcription that subsequently causes dissociation of cells (Wu and Zhou, 2010). Treatment of three OSCC cell lines with TGF-β1 over 6 days has previously shown increased expression of Snail-1. Furthermore, immunocytochemical staining, following scratching monolayers of these cells, indicated increased activity of Snail-1 at the wounded margins that was associated with increased MMP-2 and -9 activity (Takkunen et al., 2006). Notably PCR data presented here showed that gene expression of transcriptional factors, Snail-1 and -2, were significantly increased (6- and 4-fold respectively) over eight days of culture following bacterial

stimulation and this response was associated with a decrease in transcription of E-cadherin. Notably the activation of these transcriptional factors requires activation of signaling pathways by a range of cytokines. Indeed TGF-β1 appears to provide a relevant candidate for activation of Snail-mediated repression of the gene encoding E-cadherin (Shirakihara et al., 2007, Vincent et al., 2009). Furthermore, Snail activation not only reportedly attenuates E-cadherin expression, it also activates MMP-9 transcription which enhances potential metastatic behavior (Lamouille et al., 2012).

Activation of NF-κB may contribute to EMT-induction by stabilizing Snail-1 (Wu et al., 2009). Indeed, the data presented in Chapter 3, Section 4.4 showed increased NF-κB nuclear translocation in oral keratinocytes following exposure to bacterial components which was further supported by PCR findings which indicated increased transcription of this factor. Increased nuclear activity of Snail, a major E-cadherin repressor, in response to induction by periodontal pathogens was further confirmed by immunocytochemical staining. Analysis of Snail activation images following 8 days of bacterial stimulation demonstrated that nuclear activity of Snail was evident in ~70% of cells exposed to *F. nucleatum* and *P. gingivalis* (Figure 39A).

Twist-1 is another transcriptional factor which was identified as being up-regulated in response to treatment of H400 cells with non-viable periodontal pathogens. This molecule is well established as being key to triggering EMT and promoting an invasive-phenotype in many types of malignancies such as breast and gastric carcinoma (Yang et al., 2008). Notably the increased expression of twist by breast cancer cells leads to activation of inflammatory cytokines (e.g. IL-6) and Snail transcription which in turn activates EMT (Yadav et al., 2011). The resulting activated Snail-twist combination could play a central role in activating EMT-signaling during development, fibrosis, and malignancy (Peinado et al., 2007b). Down-

regulation of the E-cadherin gene and EMT is also mediated by transcriptional activity of LEF-1 which is up-regulated following nuclear translocation of β-catenin following destabilization of adherens junctions (Nawshad et al., 2007, Kim et al., 2002). In agreement with this, LEF-1 expression was found to be up-regulated in H400 epithelial cells in response to bacterial stimulation. In addition, consistent with this was data from the EMT PCR-array which indicated increased transcription of these factors alongside essential molecules involved in EMT-signaling pathways ZEB-1, GSK3β, JAG1, and NOTCH. However, the changes in molecules in these signaling pathways differed in magnitude dependent on the bacterial stimuli investigated (Table 15). This may provide insight into the differential activation of certain pathways by different bacteria and the resultant ability to drive EMT.

4.3: Periodontal pathogens potentially compromise epithelial integrity via EMT

Transcription of E-cadherin was reportedly decreased significantly following increased transcription of Snail (Batlle et al., 2000) and twist (Smit et al., 2009). E-cadherin down-regulation was also accompanied by up-regulation of N-cadherin and supports the switching from epithelial into a mesenchymal cadherin profile which is considered one of the main features of EMT (Kalluri and Weinberg, 2009, Lamouille et al., 2014)

E-cadherin, a major molecule of epithelial adherens junctions, was significantly down-regulated (~3-fold) relative to the control after treating epithelial cells with bacteria. This finding was consistent with previous studies indicating that E-cadherin down-regulation was a major step in EMT induction (Kalluri and Weinberg, 2009, Lee et al., 2006). In addition, EMT-related decrease of E-cadherin expression is considered a prerequisite for cancer metastasis (Zeisberg and Neilson, 2009, Wendt et al., 2011, Onder et al., 2008). Investigation of metastatic carcinoma cells from different organs such as breast, stomach, ovary, and thyroid, showed a poorly differentiated epithelial-phenotype associated with either a decrease

in E-cadherin expression or the presence of a mutation, which is believed to facilitate cell detachment from the original primary tumour (Berx et al., 1998, Machado et al., 1999).

Virulence factors produced by periodontal pathogens such as *P. gingivalis* are reportedly capable of decreasing epithelial junctional attachment particularly through down-regulation of E-cadherin (Arun et al., 2010). Indeed co-culturing of epithelial monolayers with *P. gingivalis* resulted in the breakdown of E-cadherin of adherens junctions (Katz et al., 2002). Chronic infection with *F. nucleatum* may also lead to EMT in colorectal carcinoma cells via down-regulation of E-cadherin expression and increasing β-catenin-associated transcriptional factors such as LEF and NF-κB (Kumar et al., 2016). Data from this study regarding the up-regulation of LEF and NF-κB was consistent with that of these previous publications which demonstrated similar responses in oral keratinocytes exposed to periodontal pathogens. Previously, Jing et al. (2012) indicated E-cadherin down-regulation in hepatic malignant cells was mediated by LPS-TLR-4 signalling and the current study demonstrated that exposure of H400 cells to *E. coli* LPS resulted in a ~3-fold up-regulation in gene expression of TLR-4 (see Chapter 3, Section 3.5.2). Decreased expression of epithelial E-cadherin was also associated with up-regulation of mesenchymal N-cadherin transcription and the switching of cadherin types is a potential indicator of an EMT-phenotype (Kalluri and Weinberg, 2009). Indeed a recent immunohistochemical study carried out on primary and metastatic pancreatic cancer cells showed that TGF-β-induced N-cadherin overexpression which was associated with EMT-related morphological changes (Nakajima et al., 2004). Up-regulation of gene and protein expression of TGF-β1 and other growth factors such as EGF and TNF-α was demonstrated in this study and may provide a mechanistic explanation for increased N-cadherin expression in H400 cells following bacterial challenge. Notably increased levels of N-cadherin in OSCC undergoing EMT have been reported in several other studies

(Krisanaprakornkit and Iamaroon, 2012, Scanlon et al., 2013). Indeed, it has been proposed that assay of N-cadherin could provide a prognostic tool for metastatic malignancy. Examination of tissue samples from patient with gastric cancer showed that increased N-cadherin positive cells were associated with increased cancer aggressiveness (Kamikihara et al., 2012). Similarly, Gravdal et al. (2007) demonstrated the significance of switching from E-cadherin to N-cadherin expression and indicated that it may provide a valid indicator for progression of prostate carcinoma. Data also indicated that up-regulation of another mesenchymal molecule, FSP-1, which is a protein involved in motility and morphology of mesenchymal cells, is mainly mediated by TGF-β1 and EGF signalling and plays a key-role in EMT-induction *in vitro* (Okada et al., 1997, Teng et al., 2007, Li et al., 2015, Wendt et al., 2010)

Changes to the cytoskeletal architecture and loss of cell polarity are among the key features of the EMT process. The shifting of phenotype during cancer progression requires down-regulation of epithelial molecules coupled with up-regulation of mesenchymal cytoskeletal proteins (Sun et al., 2015). In this study, one mesenchymal (vimentin) and one epithelial (β-catenin) protein were shown to be highly implicated in EMT and were selected for further investigation. Cellular junctions are essential to maintain tissue polarity and integrity due to their association with the actin cytoskeleton via different types of catenin, such as β-catenin, which also mediates Wnt signalling. This relationship not only maintains the integrity of epithelium but also facilitates transduction of vital signalling and transcriptional pathways (Green et al., 2010). The β-catenin-E-cadherin complex is stabilized by Wnt signalling, which prevents β-catenin from entering the nucleus, thereby allowing accumulation of β-catenin in the cytoplasm (Amit et al., 2002, Lickert et al., 2000). Subsequently the degradation of adherens junctions leads to breakdown of E-cadherin and the subsequent release of β-catenin.

This results in translocation of β-catenin to the nucleus where it activates transcription of LEF which affects cell-cell adhesion and contributes to a migratory cell phenotype (Clevers, 2006, Kim et al., 2002). Absence of Wnt signalling finally leads to ubiquitination and breakdown of β-catenin (Luo and Lin, 2004). In the studies presented here exposure of H400 cells to heat-killed periodontal pathogens resulted in down-regulation of β-catenin expression by almost 6-fold. In addition, free β-catenin has been shown to play a synergistic role in TGF-β1-induced EMT, which was not triggered in an intact confluent monolayer, however loss of epithelial integrity and disassembly of cellular junctions followed by loss of E-cadherin and release of β-catenin triggers phenotype reprogramming associated with EMT (Masszi et al., 2004).

Gilles et al. (2003) identified *de novo* expression of vimentin in 8 cell lines following EMT-induction was mainly due to targeting vimentin-motif sites by β-catenin which was translocated to the nucleus. Up-regulation of vimentin expression is an indicator of EMT-phenotype and potentially contributes to increased cellular invasiveness. Indeed, data from several studies indicated that vimentin can be expressed in epithelial cells under certain pathological conditions that require cell migration such as wound healing and cancer metastasis (Ramaekers et al., 1983, Gilles et al., 1996). In this study, exposure of H400 keratinocytes to bacterial components up-regulated vimentin expression, which is consistent with a recently published study which demonstrated similar results when four epithelial cell lines (hepatocellular carcinoma cell lines) were exposed to LPS (Jing et al., 2012). Another study also showed that a plant extract which inhibited LPS induced NF-κB activation caused a decrease vimentin expression and restored an epithelial-phenotype (Cho, 2015). Increased transcriptional activity of vimentin has been proposed as an important regulator of EMT-associated cell migration during cancer progression in different organs, e.g lung (Kidd et al., 2014) and prostate (Wei et al., 2008). Further support for potential EMT-induction in H400

OSCC was provided from IF staining, together with PCR data, which showed a simultaneous up-regulation of vimentin expression after stimulation with heat-killed periodontal pathogens and *E. coli* LPS (Scanlon et al., 2013). Up-regulation of vimentin has been reported to be induced by EGF, which is a key regulator of proliferation and migration of cells (Paccione et al., 2008). Transitioned cells co-expressed vimentin and E-cadherin and showed two phenotypes, either the cells were elongated with internalization of E-cadherin, or cells formed epithelial clusters with E-cadherin distributed around the cell membrane; however, vimentin was detected in their cytoplasm which could indicate that these cells are at an early transition stage. Loss of cell-cell junctions was also supported by data from the TEER experiment, which demonstrated decreased resistance of epithelial monolayers to electrical current transmission following exposure to bacteria. This was in agreement with a previous study which demonstrated the decreased electrical resistance of oral keratinocytes chronically stimulated with periodontal pathogens (Sume et al., 2010).

5.4: Increased migratory ability of H400 cells exposed to bacterial components

The degradation of the basement membrane is a prerequisite for epithelial cells that acquired an invasive-phenotype to facilitate migration into underlying tissue or to distant sites (Kalluri and Weinberg, 2009). The present study showed that the MMPs-2, -9, and -13, which are proteolytic enzymes that degrade ECM, were up-regulated following eight days of exposure to bacteria. PCR-array data was consistent with the sq-RT-PCR findings and in addition identified other up-regulated genes (including MMP-3 and -9) involved in the breakdown the basement membrane, which could facilitate tumor metastasis (Kalluri and Weinberg, 2009, Lamouille et al., 2014). Periodontal pathogens, particularly *F. nucleatum* and *P. gingivalis*, are well-known for an ability to modulate host production of these enzymes which could contribute to increased cell motility and invasion (Gursoy et al., 2008, Fravalo et al., 1996,

Pattamapun et al., 2003). Indeed the culturing of eight different strains of *Fusobacterium* with HaCaT keratinocytes resulted in the up-regulation of MMP-2, -9, and -13 in addition to IL-8 (Gursoy et al., 2008). Furthermore challenging OSCC cells *in vitro* with *F. nucleatum* and *P. gingivalis* resulted in up-regulation of MMP-9 (Binder Gallimidi et al., 2015). In addition, exposure of oral keratinocytes to these bacteria triggered TLR-NF-κB signalling which induced up-regulation of genes such as MMPs (Philip et al., 2004). These data are further supported by findings from other studies which demonstrated that LPS-activated MMP was dependent on NF-κB signalling (Rhee et al., 2007). Increased cell migratory ability was investigated by scratch and transwell migration assays. Exposure of epithelial cells to periodontal pathogens resulted in a higher rate of closure of the scratch-wounds inflicted on H400 cell monolayers. These findings indicated that wound closure was consistent with an increase in numbers of migrated cells as supported by the transwell migration assay and growth models which showed no effect of bacteria used in this study on cell proliferation. The same pattern of migration rates was detected in both assays for the *F. nucleatum* and *P. gingivalis* treatments. These findings were also consistent with the PCR and immunofluorescence data demonstrating down-regulation of E-cadherin as well as the TEER results showing decreased epithelial integrity which could potentially have promoted cell motility. Increased vimentin expression is a potential indicator of the presence of cell populations with increased migratory capabilities (Yoon et al., 2007). These data are also in agreement with previous results (Misra et al., 2012) which demonstrated increased cell motility was correlated with increased vimentin expression and were associated with E-cadherin down-regulation.

A recent study indicated that wounding of an epithelial barrier resulted in initiation of a pro-inflammatory response by cells to manage the induced cellular stress (Leoni et al., 2015). The

epithelial-derived cytokines, secreted in response to wound trauma, such as TGF-β1 and EGF contribute to increasing motility of keratinocytes and facilitate repair of the epithelial barrier (Leydon et al., 2014). Electron microscopy images presented here showed damaged cells along the scratched area which may have caused increased release of growth factors in addition to those stimulated by bacterial stimulation of the epithelial cells. Subsequently there may be a combined molecular response in cytokine signaling when culture scratching occurs in the presence of bacteria. Based on these data, a study was undertaken comparing data from the scratch assay and the insert-barrier technique which excluded cell trauma in order to investigate the effect of bacterial component presence alone on the migratory rate of cells. Although the barrier group demonstrated an increased rate of gap closure in the presence of bacteria compared with controls this rate was significantly lower than the closure rate in the scratch wound assay. This potentially provided evidence for acquisition of a migratory-phenotype induced by periodontal pathogens. In addition, the closure rate, after 24hr, was higher in cultures treated with media only, which highlighted the important impact of physical cell damage on increased cell motility. It is well-known that healing of a small wound is mainly dependent on the sum of migration and increased proliferation which increases the number of cells populating the wound area (Crosnier et al., 2006, van der Flier and Clevers, 2009). It was previously shown (Chapter 3, Section 3.3.3) that the presence of bacterial components in cultures of H400 cells did not affect the proliferation rate or cell viability. Considering all the data it is proposed that increased cell migratory ability in response to bacterial challenge is the main factor in increasing wound closure in these *in vitro* model systems.

5: Conclusion

The periodontal pathogens *P. gingivalis* and *F. nucleatum* elicited changes in H400 epithelial cells, at a molecular, structural and behavioural level which were potentially indicative of EMT. However, transitioned cells observed in this study did not entirely lose their epithelial phenotype nor completely differentiate into mesenchymal cell as some of the parental phenotype was retained and mesenchymal markers were expressed concomitantly. In addition, the wound healing assay suggested that physical cell trauma induced a migratory-phenotype which was enhanced in the presence of *P. gingivalis* and *F. nucleatum*. These epithelial cells, in the presence of bacteria, acquired a migratory-phenotype which was indicated by the increase of motility related molecules such as vimentin and FSP-1. Furthermore, this study also suggested involvement of periodontal pathogens in compromising epithelial barrier function which is evident during periodontitis. Therefore, the potential involvement of EMT in the pathogenesis of periodontitis will be discussed in the following chapter.

EPITHELIAL-MESENCHYMAL TRANSITION AND ORAL EPITHELIAL BARRIER FUNCTION

1: General introduction

This chapter focuses on the potential of EMT (as induced by periodontal pathogens) in compromising the epithelial-barrier function in periodontitis by analysing responses in an *in vitro* primary oral keratinocyte model system. Indeed, persistent inflammation elicited by bacteria has previously been reported as a potential predisposing factor for EMT-induction in various organs such as lungs, liver, and intestine (Shen et al., 2014, Bose et al., 2012, Scharl et al., 2015). The inflammatory signaling induced by microbial challenge shares common pathways with EMT (Hofman and Vouret-Craviari, 2012). It has previously been shown that when pocket epithelial lining cells encounter *F. nucleatum* and *P. gingivalis* there is up-regulation of proteolytic enzymes such as MMP-2 (Gursoy et al., 2008, Grayson et al., 2003) which is, in turn, necessary for the EMT process (Radisky and Radisky, 2010, Duong and Erickson, 2004, Lin et al., 2011). Furthermore, Nagarakanti et al. (2007) have shown that gingival samples collected from patients with chronic periodontitis exhibit significant down-regulation of E-cadherin compared with healthy controls. Subsequently Yutori and co-workers have proposed that the attenuation of epithelial barrier function is due to E-cadherin down-regulation following co-culture of human gingival epithelial cells with *P. gingivalis*-LPS (Abe-Yutori et al., 2016). Consistent with these findings, prolonged stimulation of the gingival sulcular epithelium with *E. coli* LPS was shown to result in loss of tight junctions associated protein (claudin-1) (Fujita et al., 2012) and those changes support the potential induction of EMT in this cell type (Zeisberg and Neilson, 2009, Kalluri and Weinberg, 2009). Furthermore immunohistochemical analysis of samples derived from patients with gingival overgrowth has demonstrated the presence of areas exhibiting basement membrane disintegration that have been invaded by epithelial-like cells (Kantarci et al., 2011).

Whilst the host response to plaque biofilm has received considerable attention (Silva et al., 2015, Hasan and Palmer, 2014) the aetiology of periodontitis at a cellular level has not been fully elucidated. EMT appears as a potential mechanism which may affect the integrity of the periodontal pocket epithelium during periodontal disease pathogenesis, however thus far this process has received limited attention.

2: Specific aims and objectives of the studies described in this chapter:

Aims:

1- To investigate the possible involvement of EMT in compromising epithelial barrier function following exposure of primary oral keratinocytes to periodontal pathogens in an *in vitro* periodontitis-model system.
2- Compare results obtained using primary keratinocytes with those obtained using the H400 cells following exposure to heat-killed periodontal pathogens.

Objectives:

1- EMT induction in primary cells cultures was investigated by range of different assays including PCR, IF, and ICC for selected EMT-indicators.
2- The integrity of the epithelial monolayers was investigated by using TEER.
3- Increased migratory ability of the cells was investigated by utilising transwell-migration and scratch-wound assay.

3: Results

3.1: Inhibitory effect of different Mitomycin C concentrations on 3T3 fibroblasts

Analysis of 3T3 cultures showed that at all MMC concentrations used there was a significant decrease ($P<0.001$) in numbers of 3T3 cells compared with controls from days 5-12 (Figure 45). At the end of experiment, day 12, cell numbers in cultures treated with the higher MMC

concentrations (8 and 10μg/ml) were significantly lower ($P<0.05$) when compared with other MMC concentrations utilised (Figure 45). Comparison of cell number for each concentration with its initial seeding number (Table 17), showed that lower MMC concentrations (1 and 4μg/ml) did not significantly affect number of 3T3 till day 11 and 12. While higher MMC concentrations resulted in reduction in number of 3T3 at earlier time starting from day 7, for 6 and 8μg/ml, and from day 6 for 10μg/ml. This indicated that lower concentrations maintained higher number of 3T3 in cultures for longer time relative to higher concentrations.

3.2: Characterisation of epithelial-phenotype

Culture of primary oral keratinocytes was visualised using light microscopy. In contrast to randomly distributed fibroblasts, epithelial cell growth was characterised by the formation of round-tightly adherent epithelioid colonies, giving the classical 'cobble-stone' appearance of epithelial sheets (Figure 46). The epithelial-phenotype of primary rat oral keratinocytes was further confirmed by their reaction with antibodies to pan-cytokeratin which is the main intermediate filament present in epithelial cells (Figure 47).

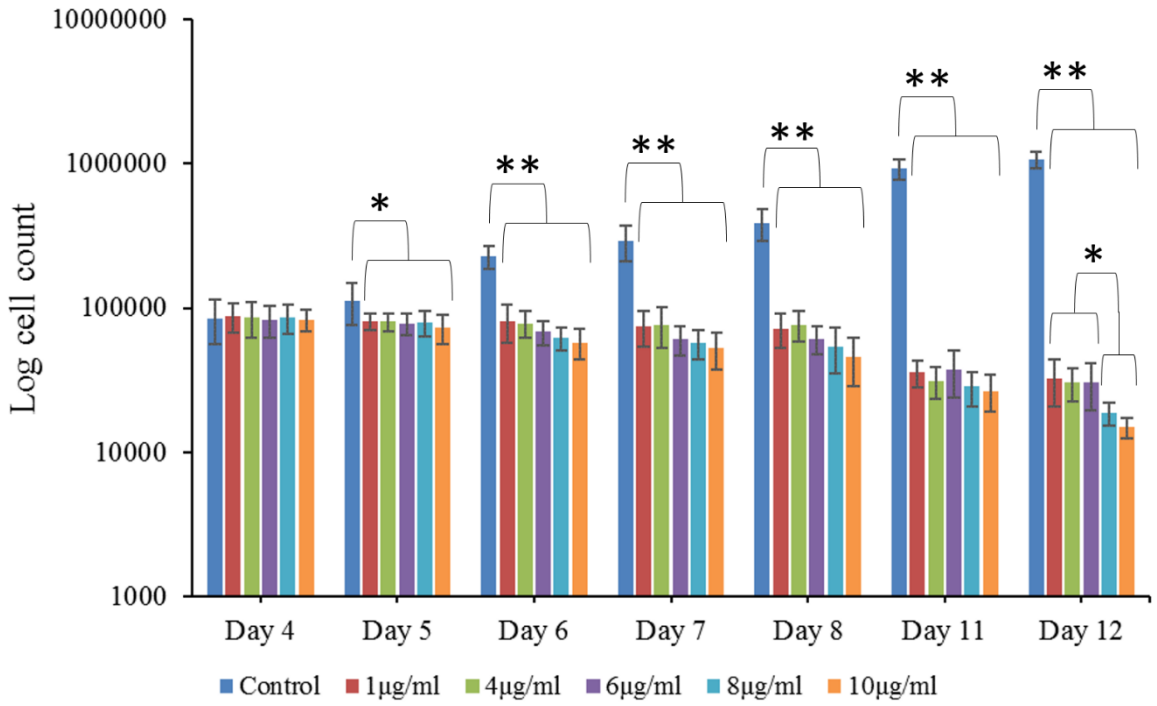

Figure 45. Treatment of 3T3 fibroblasts with a range of concentrations of MMC (1, 4, 6, 8, and 10µg/ml) for 2hr resulted in inhibition of growth as compared with the unexposed control. The number of 3T3 cells assayed in culture, at day 12, at the higher MMC concentrations, 8 and 10µg/ml, were significantly lower than in cultures treated with the lower MMC concentrations. Initial seeding number=$1x10^4$ cells. Experiments were performed in triplicate, *=P<0.05, **=P<0.001.

MMC concentration	Time (days)	3T3 cell count± SD	P-value	MMC concentration	Time (days)	3T3 cell count± SD	P-value
1μg/ml	4	84444±10356		8μg/ml	4	80000±19403	
	5	81111±10226	N.S.		5	78889±15676	N.S.
	6	78349±13736	N.S.		6	62222±11660	N.S.
	7	75000±9651	N.S.		7	57667±13394	P<0.05
	8	72222±10268	N.S.		8	54000±18838	P<0.05
	11	35778±5519	P<0.001		11	28500±7763	P<0.001
	12	32667±8802	P<0.001		12	18667±3308	P<0.001
MMC concentration	**Time (days)**	**3T3 cell count± SD**	**P-value**	**MMC concentration**	**Time (days)**	**3T3 cell count± SD**	**P-value**
4μg/ml	4	80222±13979		10μg/ml	4	78889±14507	
	5	79556±11618	N.S.		5	73333±16803	N.S.
	6	78333±16539	N.S.		6	57778±13956	P<0.05
	7	76667±23764	N.S.		7	52778±15265	P<0.05
	8	72901±17823	N.S.		8	49391±17083	P<0.001
	11	31222±7975	P<0.05		11	26667±7700	P<0.001
	12	30500±7883	P<0.05		12	14944±2485	P<0.001
MMC concentration	**Time (days)**	**3T3 cell count± SD**	**P-value**				
6μg/ml	4	79111±16237					
	5	78333±13394	N.S.				
	6	65556±12935	N.S.				
	7	67778±10371	P<0.05				
	8	66111±15346	N.S.				
	11	37333±13390	P<0.001				
	12	30333±10830	P<0.001				

Table 17. Data obtained from comparing the number of 3T3 fibroblasts in cultures to the initial seeding number, for each MMC concentration, showed that 1 and 4μg/ml did not reduce the number of cells until day 11. However, higher MMC concentrations significantly decreased number of 3T3 from day 7 in association with 6 and 8μg/ml. While the highest MMC concentration utilized (10μg/ml) resulted in reduction of 3T3 number at an earlier time (day-6).

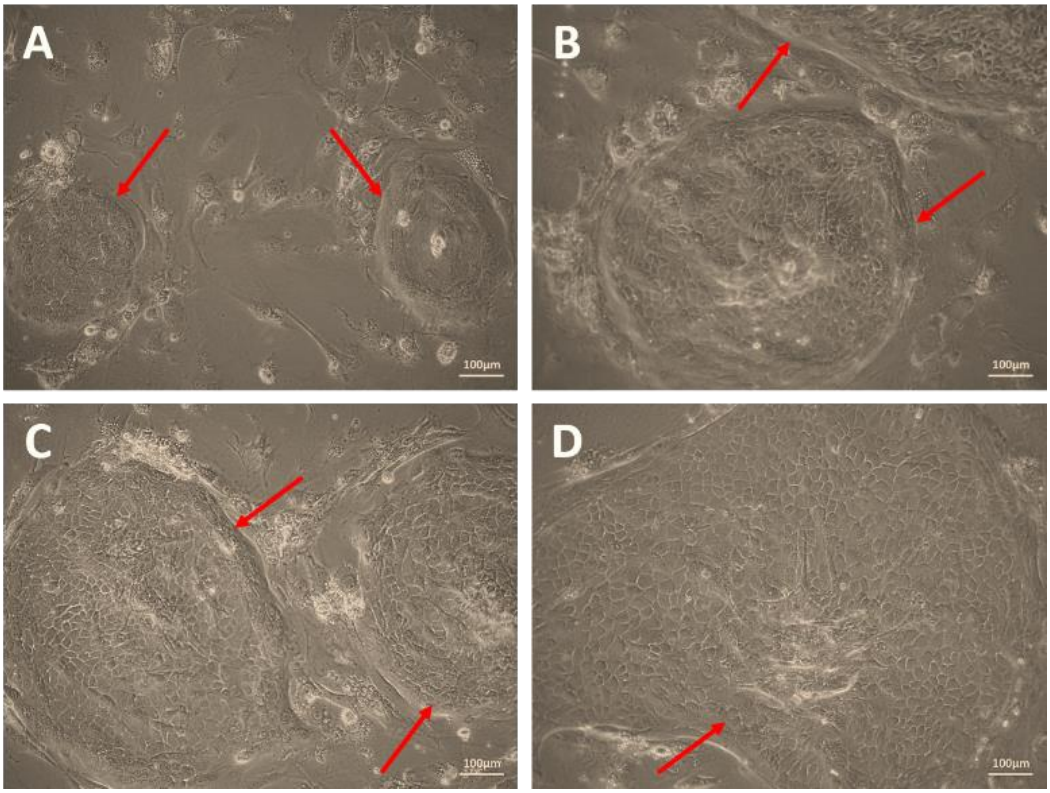

Figure 46. Phase contrast photomicrographs showing the growth of rat primary oral keratinocyte cultured on 3T3 cell feeder layers. Epithelial cells are densely packed forming round islands that gradually expand and form confluent layer (red arrows). Keratinocytes islands after 7 days (A), 10 days (B), 12 days (C), and 14 days (D). Cultures were incubated at 37^{o}C in 5% CO_2. (E). Images are representative of triplicate cultures. Scale bars are shown.

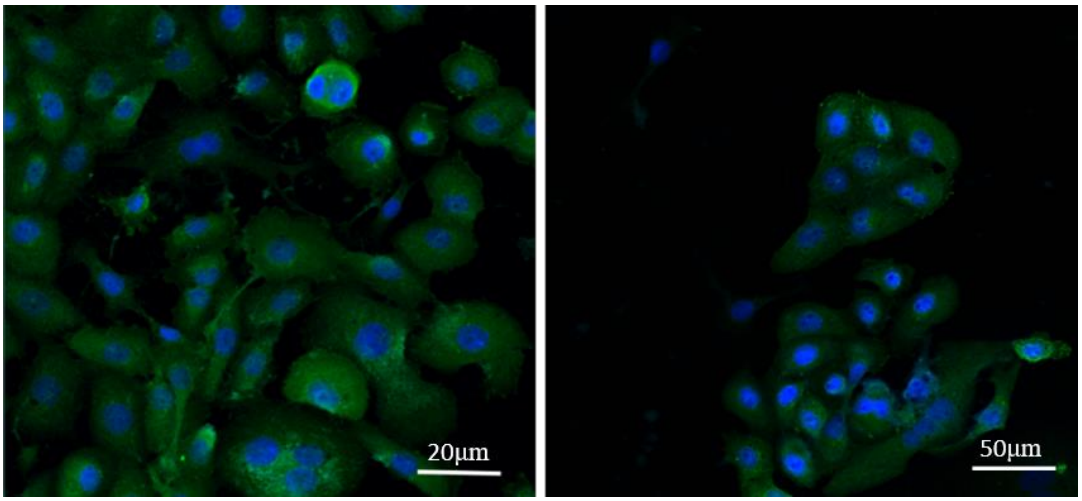

Figure 47. Confocal microscopy of primary oral keratinocytes showing pan-Cytokeratin (green) characteristic of Epithelial-phenotype. Nuclei were defined by counterstaining with DAPI (blue). Image are representative of studies run in triplicate. Scale bars are shown.

3.3: Effect of periodontal pathogens on growth and viability of primary oral keratinocytes

During the experimental period of 10 days, the growth rate of oral keratinocytes cultures exposed to heat-killed *F. nucleatum*, *P. gingivalis* and 20μg/ml *E. coli* LPS, did not show significant differences when compared with cultures in media only (Figure 48A). The same profile was also apparent for the percentage of viable cells determined in the same period. Exposure of primary oral keratinocytes to bacterial components did not cause any significant effect on growth when compared with controls, except at day 7 for the *F. nucleatum* exposure group ($P<0.05$) and at day 8 for all bacterial exposure groups, as the percentage of live cells under these conditions decreased significantly ($P<0.001$) (Figure 48B). The concentration of bacterial stimuli used in this experiment did not have an inhibitory or toxic effect on primary oral epithelial cells cultured *in vitro*.

3.2: EMT-related marker gene transcriptional changes following bacterial exposure

Exposure of oral epithelial cells to heat-killed periodontal pathogens and *E. coli* LPS for 8 days resulted in changes in expression of key genes related to EMT. Transcription of E-cadherin, and its associated cytoskeletal molecule, β-catenin, in stimulated cultures was significantly down-regulated (~3-4-fold respectively, $P<0.001$) in comparison with controls (Figure 49). At the same time, there was a significant up-regulation ($P<0.001$) of the two mesenchymal markers investigated, vimentin (~4-fold) and N-cadherin (~3-fold) (Figure 50). The expression of the transcriptional factor, Snail-1, was increased up to 5-fold in response to bacterial stimulation (Figure 51A), as well as a significant up-regulation of the transcript for the proteolytic enzyme (MMP-2) compared with unstimulated cultures at the same time point (Figure 51B). The greatest level of up-regulation of mesenchymal molecules, at the end point of the experiment, was associated with cells treated with *F. nucleatum*. Furthermore, levels of

TLR-4 expression (responsible for bacterial recognition, particularly LPS) were also significantly ($P<0.001$) increased in stimulated cultures when compared with cells treated with media only (Figure 51C).

Comparison of EMT-associated gene expression between primary oral keratinocytes and H400 cells, following bacterial exposure, showed similar patterns. However, H400 cells expressed greater changes in transcript levels for the genes investigated in this study. E-cadherin and β-catenin (Figure 52), were downregulated about 4-fold in association with H400 cultures in comparison to unstimulated control, while transcription of E-cadherin and β-catenin was decreased about 3-fold in stimulated primary cells cultures. In addition, vimentin, N-cadherin (Figure 53), Snail-1 and MMP-2 were increased in H400 cultures treated with bacteria compared with primary oral epithelial cells (Figure 54). However, primary oral keratinocytes exhibited higher expression of TLR-4 (~4-fold) compared with H400 cells.

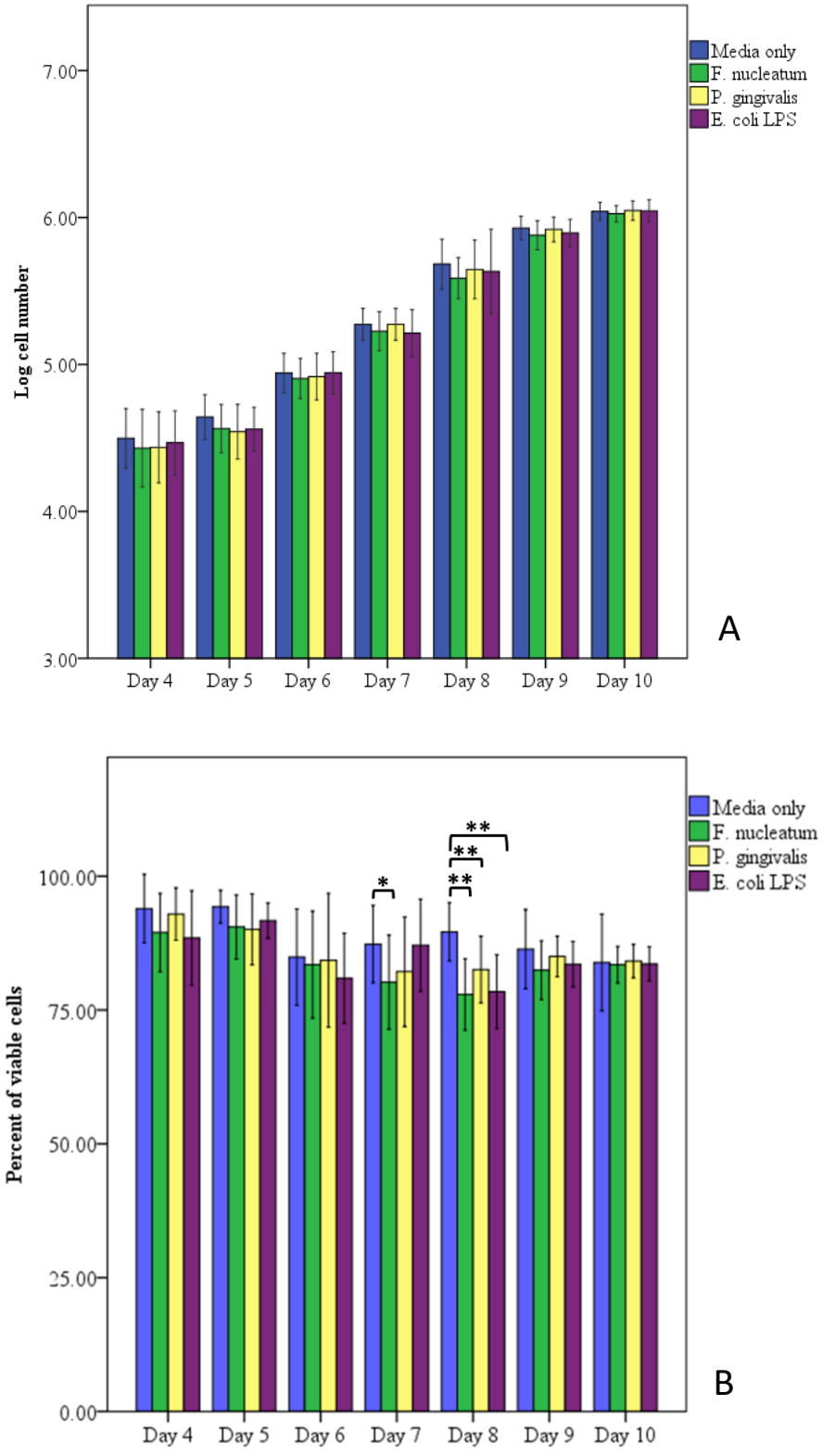

Figure 48. Exposure of primary oral epithelial cells to heat-inactivated *F. nucleatum*, *P. gingivalis*, and 20µg/ml *E. coli* LPS, over 10 days, did not produced any significant differences in (A) cell numbers of epithelial cells or (B) viability of cells, except for *F. nucleatum* exposure at day 7 and all stimulated groups at day 8 where the percentage of viable cells significantly decreased when compared with the unstimulated control at the same time points. n=18, (*=P<0.05, **=P<0.001).

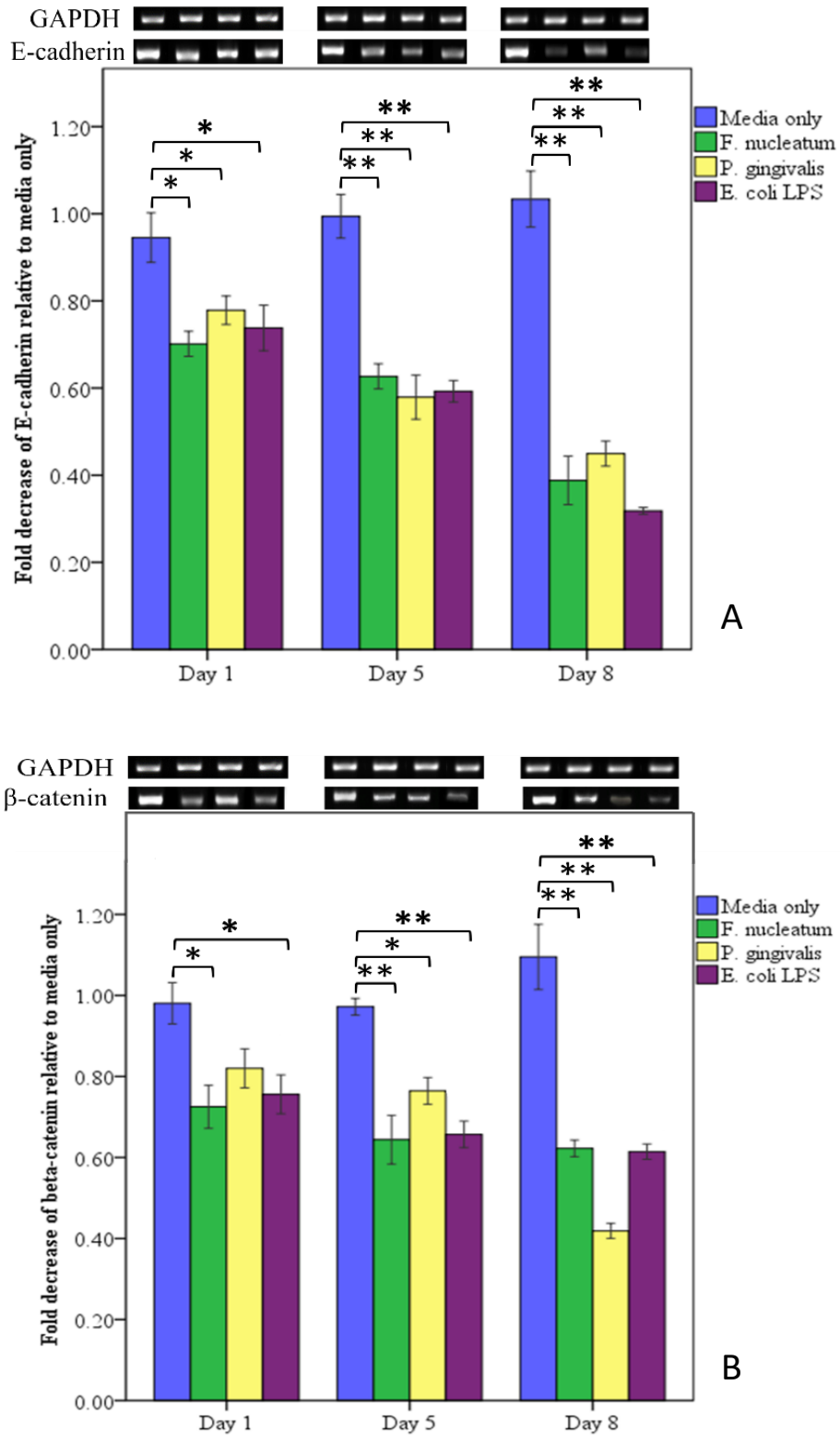

Figure 49. Gel images and densitometric analysis of sqRT-PCR data indicated that periodontal pathogens produced significant down-regulation of the epithelial related transcripts (A) E-cadherin, down-regulated up to 3-fold, and (B) β-catenin expression which was down-regulated up to 4-fold, except for *P. gingivalis* after one day of exposure. Experiments were performed in triplicate, (*=P<0.05, **=P<0.001).

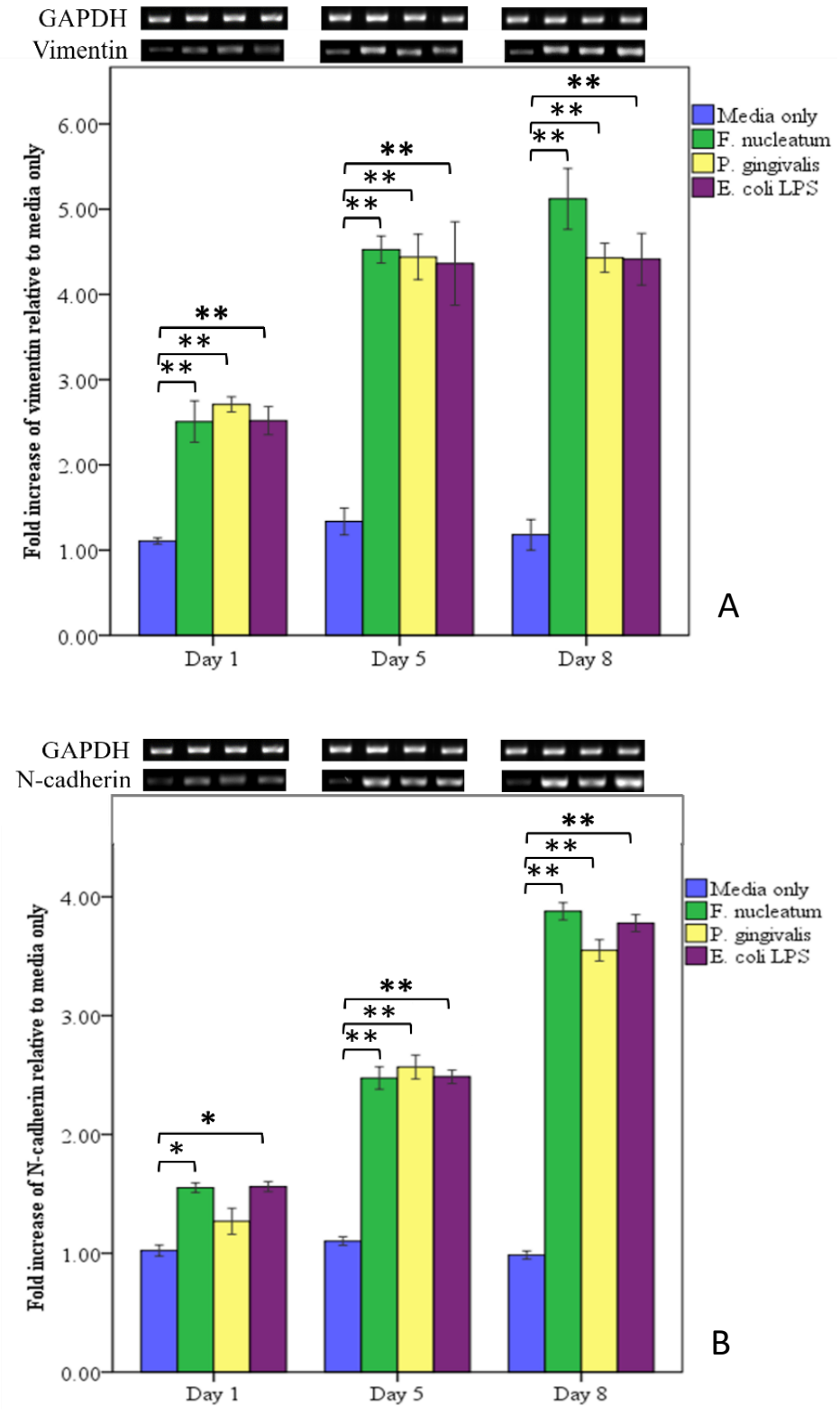

Figure 50. Transcriptional analysis of levels of selected key mesenchymal marker molecules. (A) Vimentin and (B) N-cadherin were upregulated in response to treatment with bacterial components by approximately 3-, and 4-fold respectively relative to unstimulated controls. *P. gingivalis* exposure did not stimulate any significant changes in gene expression of N-cadherin at day 1. Experiments were performed in triplicate, (*=P<0.05, **=P<0.001).

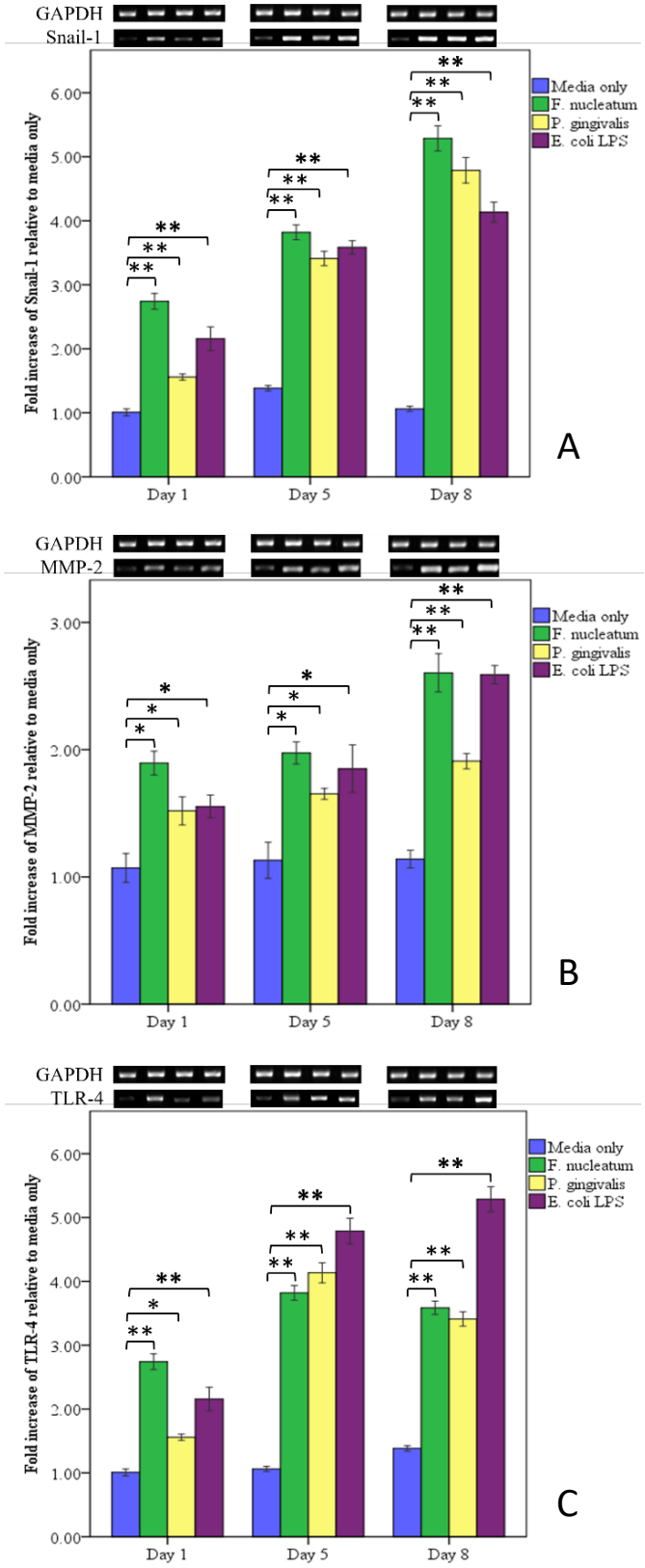

Figure 51. Treatment of primary rat oral keratinocytes with bacterial components resulted in significant increases in the expression of (A) Snail-1, ~5-fold, (B) MMP2, up to 2.5-fold, and (C) TLR-4 which showed 6-fold up-regulation in comparison with cultures in media only, over the 8-day culture period. Experiments were performed in triplicate, (*=P<0.05, **=P<0.001).

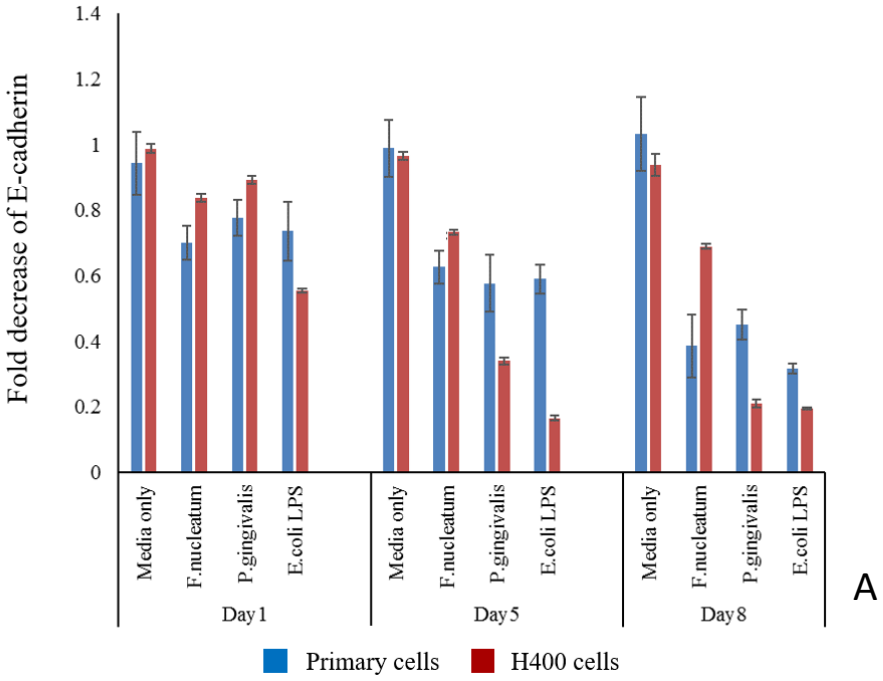

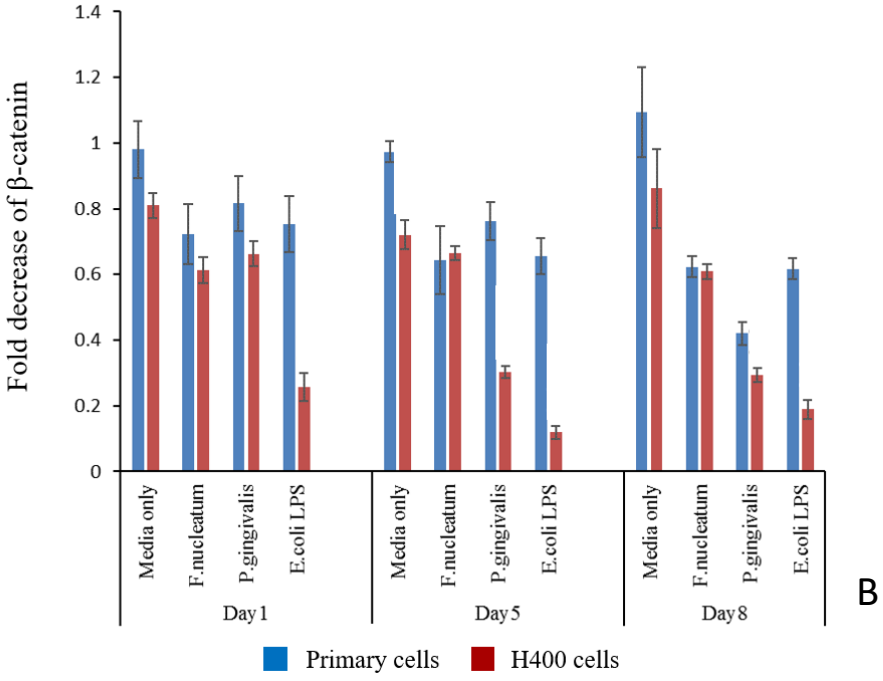

Figure 52. Comparison of (A) E-cadherin and (B) β-catenin expression in rat primary oral keratinocytes and H400 cultures stimulated with bacterial components showed that these transcripts were down-regulated with a similar profile in both cell types studied in comparison with unstimulated controls. However, H400 cells showed a more marked down-regulation of E-cadherin and β-catenin (about 4-fold) than primary cells.

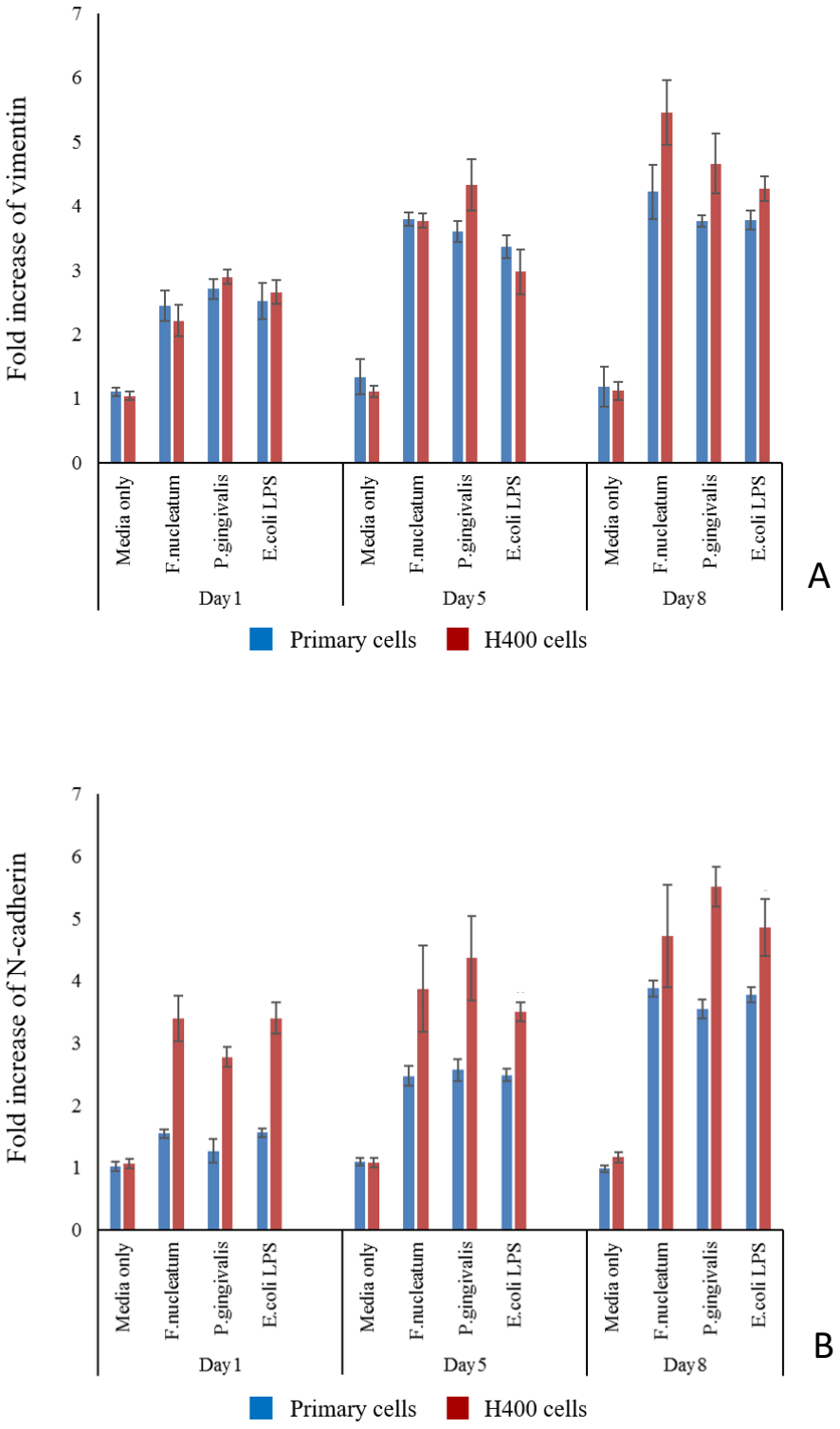

Figure 53. Expression of the mesenchymal transcript (A) vimentin and (B) N-cadherin in cultures, primary oral keratinocytes and H400 cells, stimulated with bacterial components showed that expression of vimentin and N-cadherin was almost 2-fold higher than primary cells at the end of the experiment.

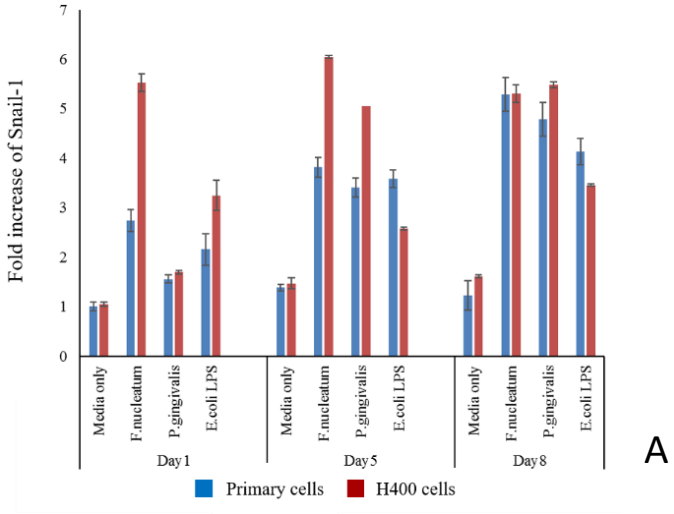

A

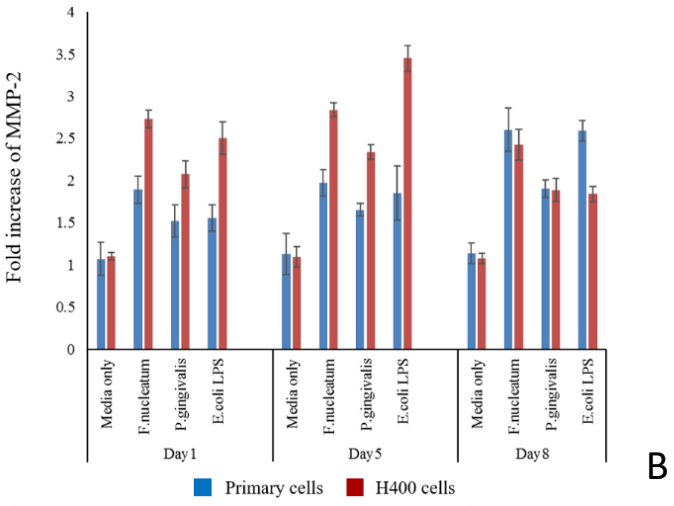

B

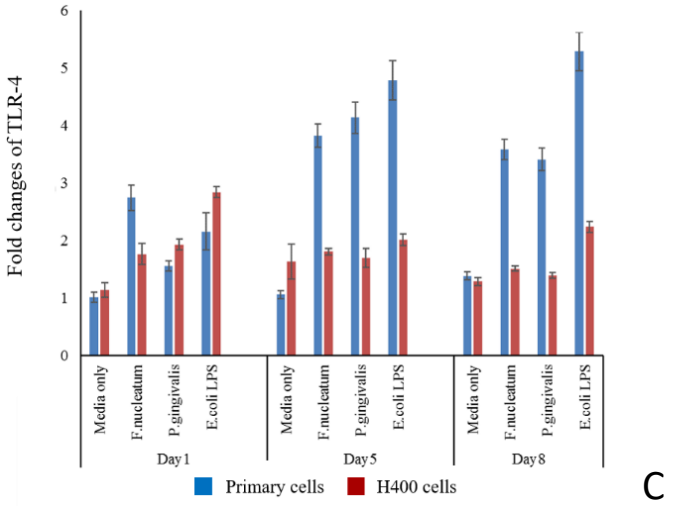

C

Figure 54. Comparison of primary oral keratinocytes and H400 cultures exposed to bacterial components demonstrated that (A) Snail-1 expression was 1- to 3-fold higher in H400 cultures than primary oral keratinocyte, the same trend was also apparent for the transcription levels of MMP-which showed higher expression (~1.5-fold) in H400 cultures compared with primary cells (B). However, stimulated primary cells cultures exhibited higher TLR-4 up-regulation (~4-fold) than H400 cells (C).

Analysis of immunofluorescence (IF) images (Figure 55) indicated a significant increase in the percentage of the oral epithelial cell population demonstrating vimentin positive staining in response to bacterial exposure ($P<0.05$) after 8-days culture (Figure 56). This increase in the expression of vimentin was concomitant with a decrease of E-cadherin expression on the cell membrane of stimulated cultures compared with controls. Similar to previous observations in H400 IF stained cultures, stimulated primary keratinocytes exhibited co-expression of E-cadherin and vimentin either in cell clusters or in individual fibroblast-like cells which may have indicated retention of some characteristics of their epithelial origin (Figure 55D). The percentage of vimentin-positive cells was significantly higher in H400 cultures, for all stimulated groups, when compared with primary cells (Figure 57).

3.3: Integrity of oral epithelial cultures stimulated with bacterial components

Analysis of Snail-1 immunocytochemistry (ICC) images showed that the number of Snail-translocation positive epithelial cells treated with bacterial components was higher compared with the control (Figure 58A). Snail activation during EMT is considered a key molecular event which is responsible for suppressing E-cadherin transcription with subsequent downstream loss of cellular adhesion (Wu and Zhou, 2010). ICC images (Figure 58B) showed an increase in nuclear and/or cytoplasmic Snail activity compared with controls (which were characterised by clear, violet nuclei). Stimulated cultures, at day 8 (Figure 58C) demonstrated increased Snail activity as well as cell dispersion representative of EMT. In contrast, control cultures retained their integrity with cells tightly packed, typical of epithelial culture.

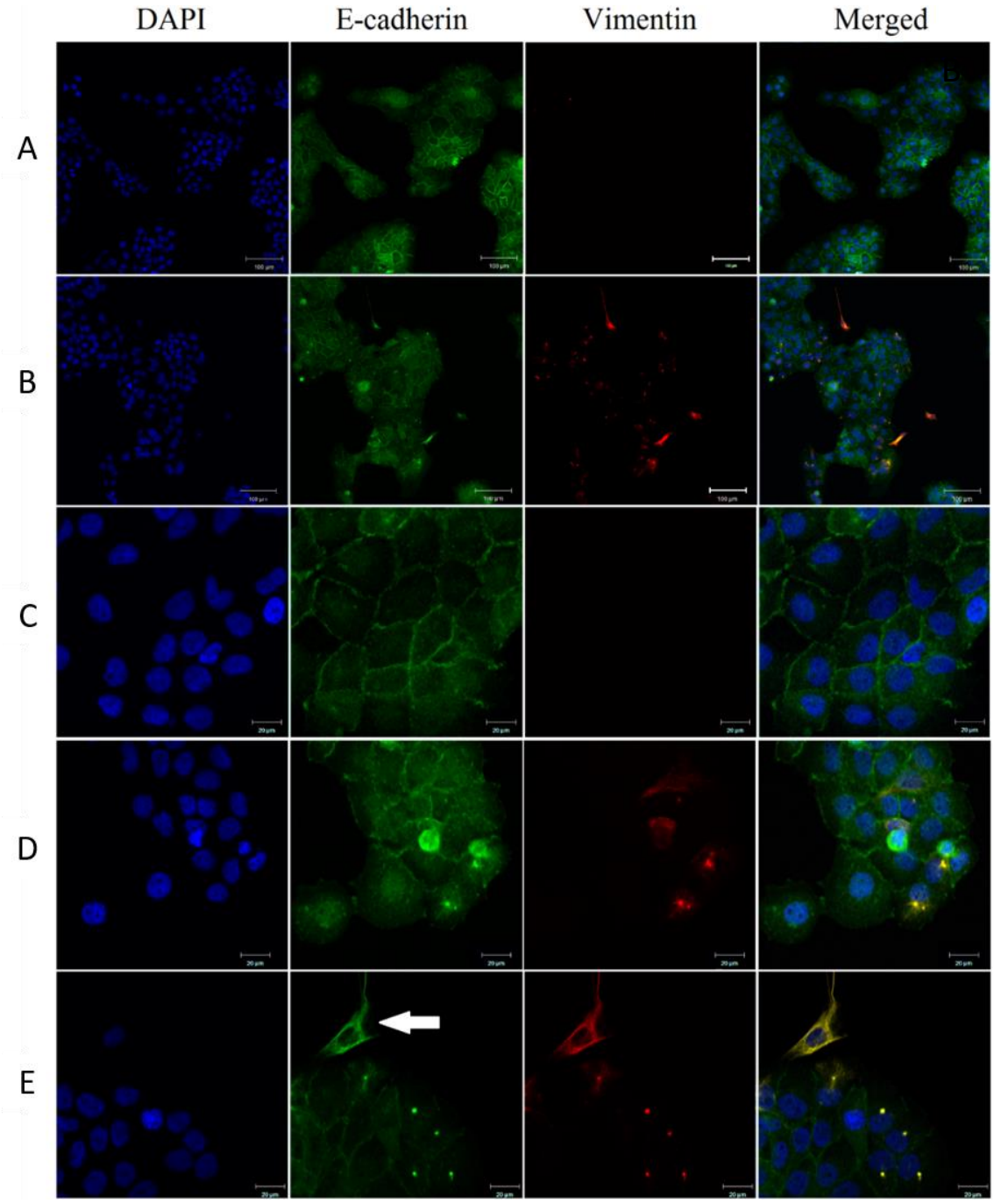

Figure 55. Confocal photomicrographs of IF staining presented at lower magnification of (A) cultures in media only and stimulated cultures, showed that vimentin (red) was expressed in oral keratinocytes following exposure to periodontal pathogens (B). Higher magnification of unstimulated (C) and stimulated cultures (D) provided evidence of transitioned cells which co-expressed E-cadherin, which indicated a potential epithelial origin, and vimentin and E-cadherin in two patterns; whilst remaining part of the epithelial sheet (D) or exhibiting fibroblast-like morphology (E). Images are representative of studies run in triplicate.

Data indicated an almost similar extent and pattern of Snail-1 activation by bacterial stimulation in both H400 cells and primary oral epithelial cells, except for the *P. gingivalis* exposed group which showed higher Snail-1 activation in H400 cells compared with the primary cells (Figure 59).

A further indication of the loss of epithelial barrier function was obtained from performing TEER analysis. Resistance of primary epithelial monolayers to the passage of AC-electric current was significantly decreased ($P<0.001$) in cultures exposed to bacteria compared with unstimulated controls (Figure 60). At day 4, only *P. gingivalis* exposure resulted in significant ($P<0.05$) reduction in TEER compared with controls. This was in contrast to previous TEER findings undertaken using H400 cells where resistance to electric current was significantly decreased in cultures treated with *F. nucleatum* and *E. coli* LPS but not in *P. gingivalis* exposure at the same time-point (Table 18). A significant decrease in electric impedance for primary epithelial monolayers began at day 5 following exposure to heat-killed *F. nucleatum*, *P. gingivalis* and *E. coli* LPS, and continued up to day 8. No significant difference was recorded when comparing primary cells and the H400 immortal cell line with respect to TEER results from days 5 - 8 (Table 18). These findings suggested that epithelial integrity was compromised in cultures exposed to periodontal pathogens.

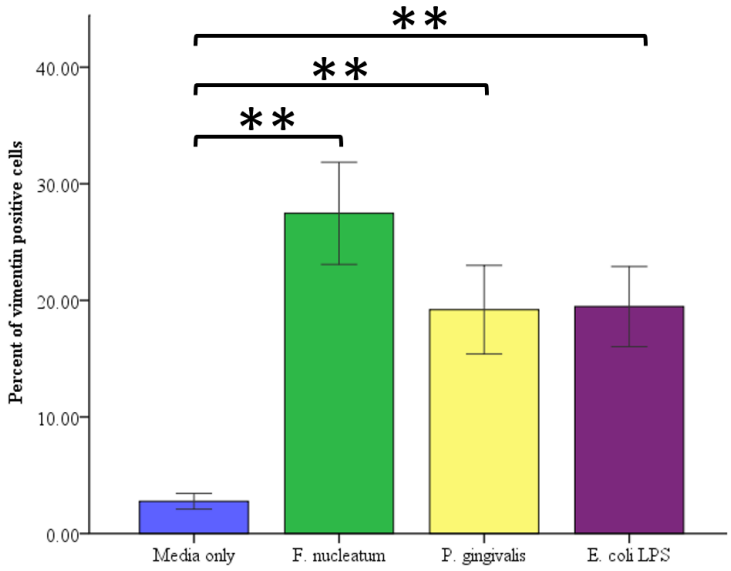

Figure 56. Culture of rat primary oral keratinocytes in the presence of bacterial components over 8 days exhibited altered vimentin and E-cadherin expression. Analysis of images demonstrated significant increases (up to 30%) of vimentin-positive cells within the population following exposure to periodontal pathogens compared with unstimulated control. Experiments were performed in triplicate, (**=P<0.001).

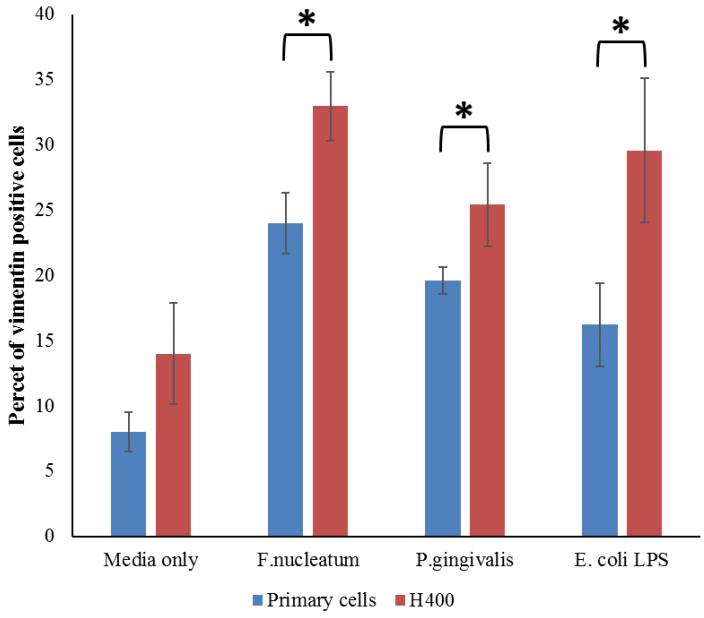

Figure 57. Expression of vimentin-positive cells was greater in primary oral keratinocyte and H400 cultures in response to bacterial stimulation. Notably the percentage of vimentin-positive cells was significantly greater in association with stimulated H400 cells. (*=P<0.05).

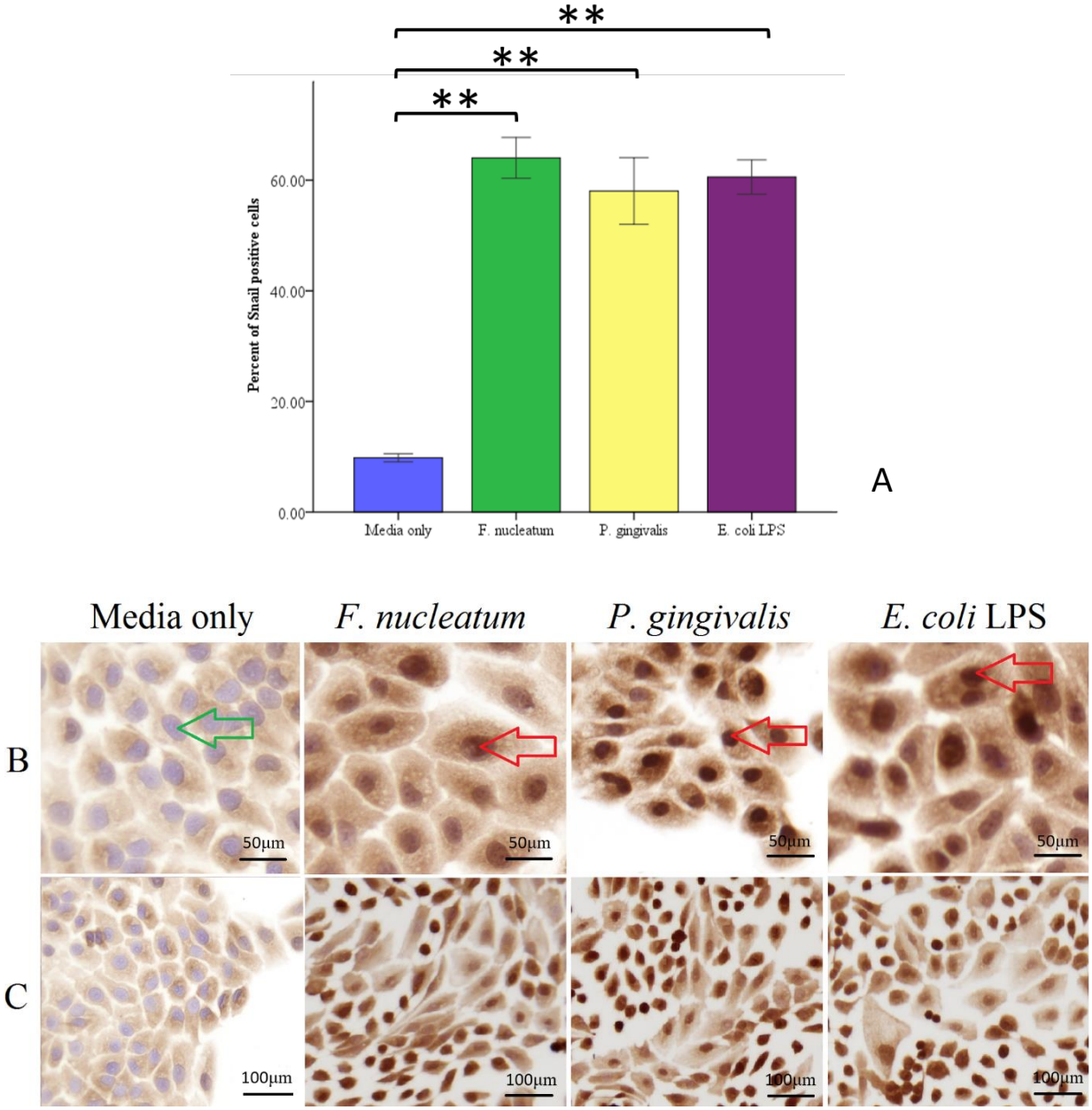

Figure 58. Treatment of oral keratinocytes with bacterial components resulted in Snail activation. (A) Analysis of the percentage of Snail-positive cells showed that periodontal pathogens induced significantly higher response (~60%) in comparison with unstimulated controls. (B) ICC staining images of primary oral epithelial cells, representative of 5 images, indicated an increased nuclear activity of Snail, dark brown discoloration of the nuclei and/or cytoplasm (red arrows), as compared with the dark blue colour characteristic of unstimulated cells (green arrow). (C) Cultures treated with bacteria, for 8-days, showed scattering and morphological alteration, while unstimulated controls exhibited tightly packed keratinocytes exhibiting the classical cobblestone appearance of the epithelial sheet. Experiments were undertaken in triplicate, (**=P<0.001).

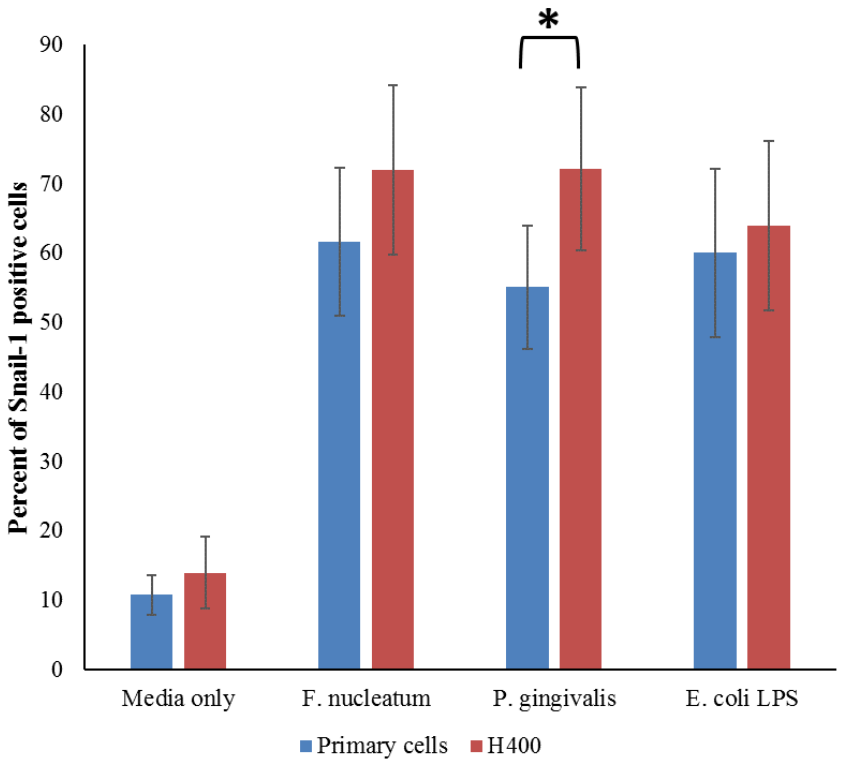

Figure 59. Comparison of primary oral epithelial cells and the H400 cell line with respect to Snail-1 activation. Data showed no significant difference between the two groups, except following *P. gingivalis* exposure where H400 cells exhibited higher Snail-positive cells compared with the primary cell response. (*=P<0.05).

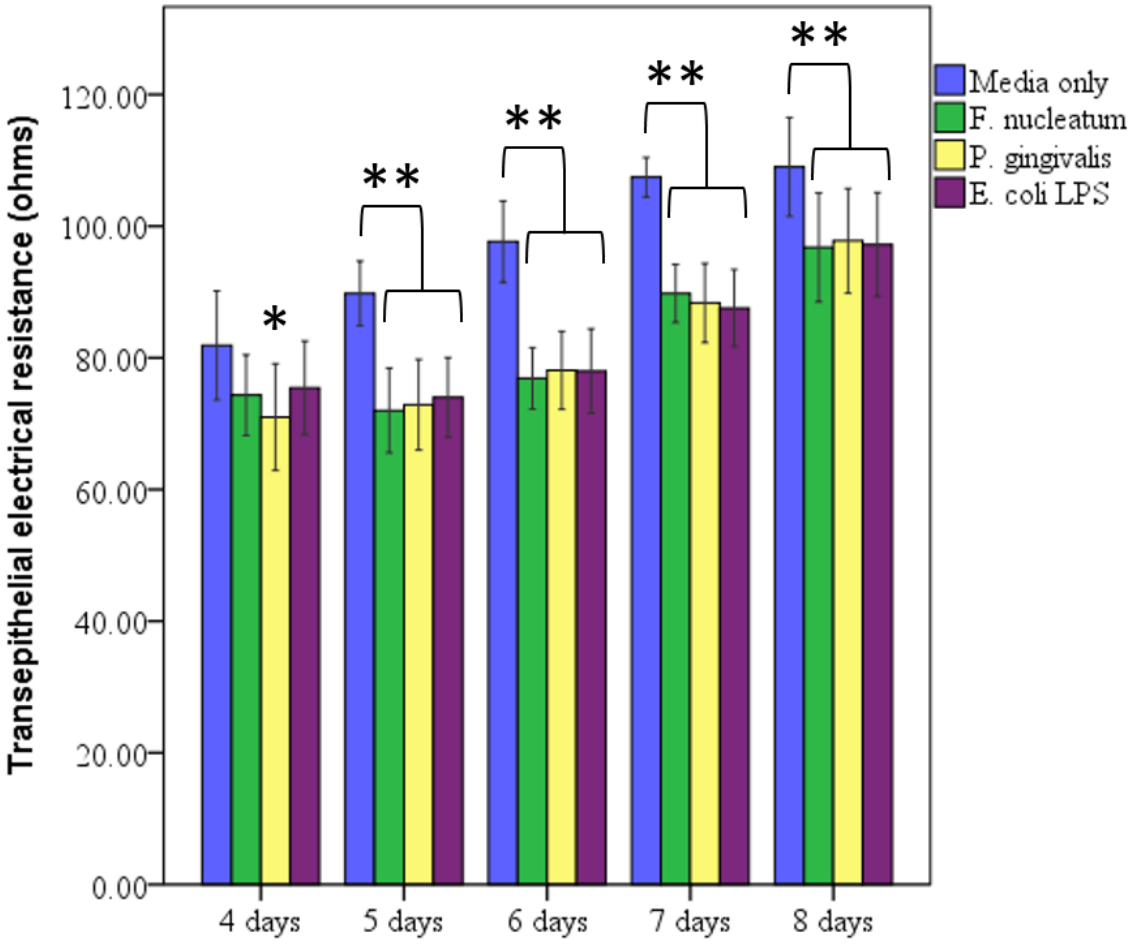

Figure 60. Resistance of primary oral keratinocytes monolayers to the passage of AC-electric current was significantly decreased following stimulation with bacteria. Analysis of TEER measurement showed that decrease resistance to AC-current began at day 4 and continued until day 8. Experiments were performed in triplicate, (*=P<0.05, **=P<0.001).

		4 days			5 days			6 days		
		Primary	H400	P-value	Primary	H400	P-value	Primary	H400	P-value
Mean TEER±SD	Media only	82.1±13.1	78.0±9.3	0.543	88.0±6.4	94.3±10.7	0.472	98.0±8.1	94.3±6.9	0.422
	F. nucleatum	72.0±8.6	57.3±6.7	0.008	73.1±10.1	75.5±13.6	0.626	77.8±6.8	73.6±7.5	0.342
	P. gingivalis	66.8±10.2	60.1±17.8	0.446	72.0±7.8	79.1±10.1	0.541	77.1±7.8	78.2±5.6	0.837
	E. coli LPS	76.0±9.4	61.5±5.8	0.009	74.4±7.3	77.3±7.2	0.311	80.6±9.2	77.3±7.3	0.492
		7 days		P-value	8 days		P-value			
		Primary	H400		Primary	H400				
	Media only	105.0±5.2	104.3±6.5	0.842	113.8±5.2	105.8±10.3	0.123			
	F. nucleatum	89.3±6.4	82.1±6.6	0.088	90.1±9.6	85.6±7.8	0.379			
	P. gingivalis	85.1±6.3	81.5±6.9	0.363	92.0±7.1	88.8±8.4	0.496			
	E. coli LPS	86.5±9.3	84.8±8.1	0.749	89.6±6.9	86.6±9.8	0.556			

Table 18. Comparison of TEER data from primary oral epithelial cells and H400 showed no significant differences other than at day 4 in association with the F. nucleatum and E. coli LPS exposure groups (shaded cells).

3.4: Effect of bacterial components on migratory ability of oral keratinocytes

EMT is accompanied with an increased motility of the cells which is considered an important indicator of mesenchymal phenotype acquisition. This cellular property was assessed utilizing a scratch assay on oral keratinocyte confluent monolayers treated with heat-killed bacteria (Figure 61A). The analysis showed no significant differences between stimulated and unstimulated control in the rate of gap closing at 12hr (except for *E. coli* LPS exposure) and 24hr (except for *P. gingivalis* exposure). However, after 36hr culture, stimulated cultures showed greater rates of gap closure ($P<0.05$) in comparison with unstimulated controls (Figure 61B). Comparison between primary oral epithelial cells and H400 cells showed that after 12hr, of stimulation with bacteria, only the *F. nucleatum* exposure group of the H400 cultures was significantly higher ($P<0.05$) than the primary cell gap closure rate. After 24hr, the rate of gap closure in H400 cultures was significantly higher ($P<0.001$) than primary epithelial cultures in association with all bacterial stimulants used (Table 19).

Migratory ability was further investigated using oral keratinocytes, pre-stimulated with bacteria for 8 days, in the transwell migration assay. The analysis showed that the migration rate of primary oral epithelial cells was significantly increased ($P<0.001$) in cultures treated with periodontal pathogens compared with unstimulated controls (Figure 62). No differences were observed in the number of migrated cells in response to bacterial stimulation between the H400 and primary oral keratinocytes (Figure 63).

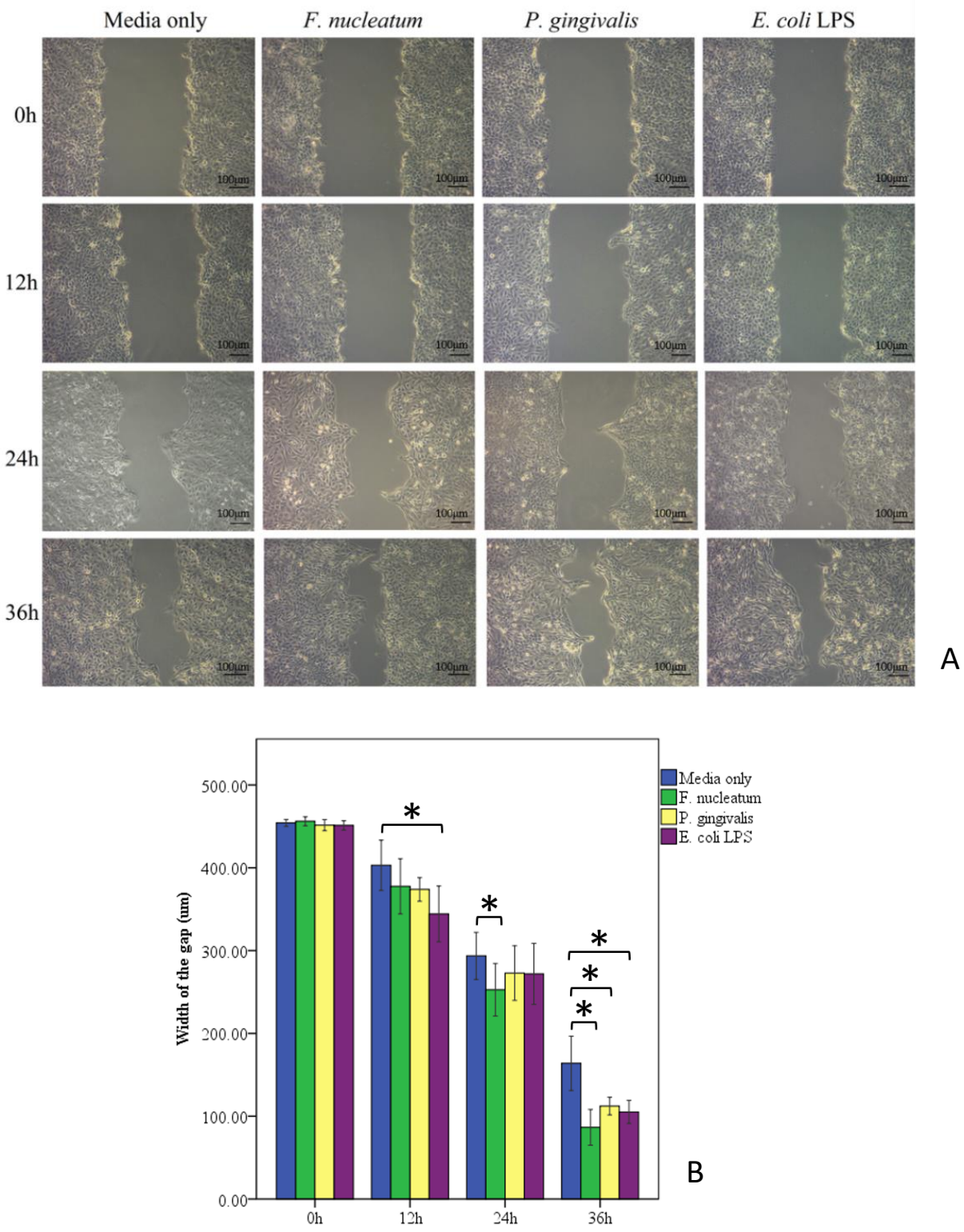

Figure 61. Phase contrast photomicrographs of scratched confluent monolayers of primary oral keratinocytes. (A) Images were captured immediately after scratching and then after 12, 24, and 36hr culture. Images are representative of studies performed in triplicate. Scale bars=100µm. (B) Analysis of gap width measurements showed no significant difference between stimulated and unstimulated cells at 12hr and 24hr; however, at 36hr the bridging of the gap was significantly increased in all cultures treated with bacterial components compared with unstimulated control. (*=P<0.05).

		0hr		P-value	12hr		P-value	24hr		P-value
		Primary	H400		Primary	H400		Primary	H400	
Mean gap width± SD	Media only	499.2±11.8	506.1±7.2	N.S	403.1±42.5	370.6±47.8	N.S	293.6±39.8	221.9±34.9	<0.001
	F. nucleatum	501.2±10.6	503.3±13.1	N.S	377.6±46.6	337.4±22.0	<0.05	252.7±44.4	124.3±19.6	<0.001
	P. gingivalis	502.3±9.4	506.0±9.6	N.S	373.9±19.9	382.6±31.1	N.S	272.8±46.0	158.9±15.5	<0.001
	E. coli LPS	504.8±9.8	504.1±9.6	N.S	344.2±47.1	366.0±20.1	N.S	271.9±51.5	110.6±21.1	<0.001

Table 19. Comparison of data from scratch assay of primary keratinocytes and H400 cells data showed that the closure rate in primary epithelial cell cultures was significantly lower than that detected in H400 cell cultures.

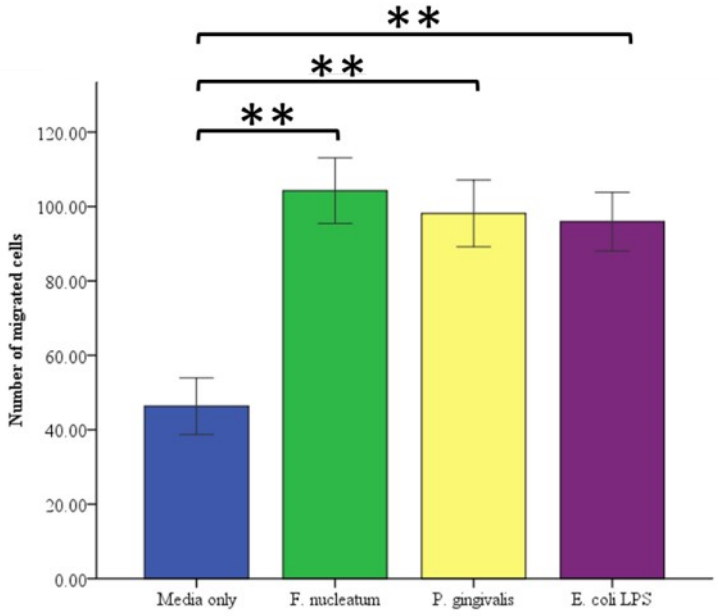

Figure 62. Analysis of transwell migration assay for primary oral keratinocytes exposed for eight days to heat-killed periodontal pathogens. The number of cells migrated, using FCS as chemoattractant, was significantly higher in bacteria stimulated cultures compared with the media only group. Experiments were undertaken in triplicate, (**=P<0.001).

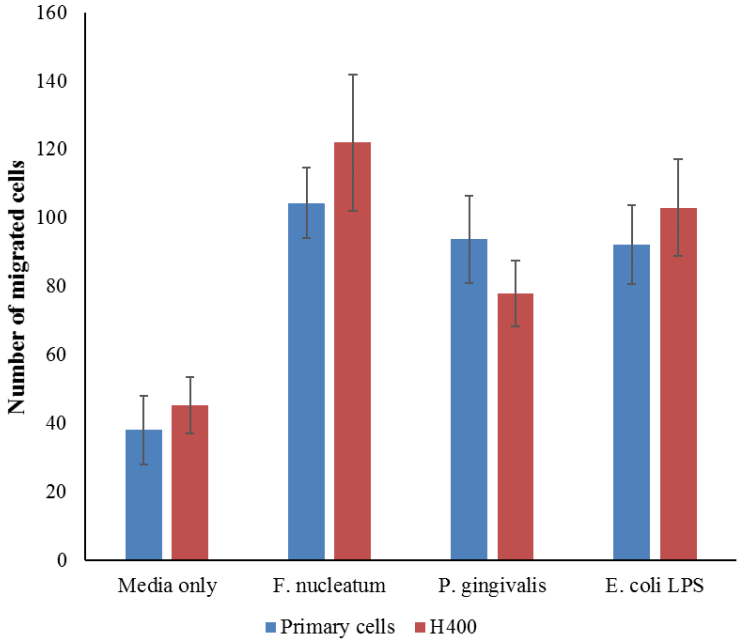

Figure 63. Number of migrated cells in primary and H400 oral keratinocytes cultures, following exposure to bacterial stimuli. There were no significant differences detected between the two cell types.

4: Discussion

Data from the previous studies on H400 cells indicated that the periodontal pathogens, *F. nucleatum* and *P. gingivalis*, altered the epithelial phenotype of the cells by inducing expression of mesenchymal-associated molecules, in addition to changes in behaviour and morphology. In the current chapter, selected markers and assays were utilised to investigate the effect of *F. nucleatum* and *P. gingivalis* exposure on primary oral keratinocytes and to compare findings with those obtained for the H400 immortal cell line. This work was based on the understanding that EMT-predisposing factors are reportedly present in the periodontal pocket microenvironment (Gram negative bacteria, cytokines, and hypoxia) (Hofman and Vouret-Craviari, 2012, Wang et al., 2013, Kao et al., 2016). Other clinical evidence such as bleeding upon probing of periodontal pockets due to micro-ulceration of the pocket lining could be also indicate interference of epithelial barrier function as a consequence of EMT.

The growth requirements of primary cells differ from those of immortal cell lines. Primary keratinocytes require the presence of a fibroblast feeder cell layer to enable growth and maintenance of viability. One important aspect of this technique therefore is that growth of fibroblasts would overwhelm primary cells, if the fibroblasts were not inhibited in terms of replication. One widely used inhibition method is that of MMC treatment (Lee et al., 2001) which inhibits fibroblast proliferation by cross-linking cellular DNA (Verweij and Pinedo, 1990). The population of 3T3 cells in the feeder layer subsequently tends to decrease with time after inhibition and requires replenishing with additional cells. A previous study reported that the inhibitory effect of this drug acts in a dose-dependent manner at relatively high (10μg/ml) and low (1μg/ml) concentrations (Kang et al., 2001). Findings from 3T3 growth curves presented here were consistent with previous studies which indicated that MMC inhibition is dose-dependent and even the lowest concentration used (1μg/ml) was sufficient to stop mitosis of cells. In addition, higher concentrations resulted in significantly

lower number of cells at the end point of the experiment compared with application of the lower concentration. These findings favored the use of 1μg/ml of MMC as an inhibitory concentration for use in this study.

EMT has been defined by down-regulation of key epithelial-adhesion proteins, increased motility, and increased expression of mesenchymal markers (Zeisberg and Neilson, 2009). PCR results from primary oral keratinocyte cultures, stimulated with bacterial components, indicated increased transcriptional activity of Snail (~5 fold) in stimulated cultures which associated with down-regulation of E-cadherin transcription (~3 fold) compared with unstimulated controls. These data were consistent with results from previous studies which have indicated down-regulation of E-cadherin levels in epithelium of periodontal pockets (Nagarakanti et al., 2007) and in response to co-culturing oral keratinocytes with *P. gingivalis*-LPS (Abe-Yutori et al., 2016). Furthermore, down-regulation of E-cadherin was also associated with up-regulation of N-cadherin transcription which is normally expressed in fibroblast. This may indicate the induction of the EMT process as cadherin-switching is regarded as a major indicator of EMT (Kalluri and Weinberg, 2009, Lamouille et al., 2014). Increased transcription of another important mesenchymal molecule, vimentin, was also detected in cells exposed to bacterial components. This protein is important in regulating cell motility and morphology (Mendez et al., 2010, Dmello et al., 2016). Increased expression of vimentin following stimulation of epithelial cells is considered by some to be a hallmark of EMT-induction (Kalluri and Weinberg, 2009). PCR data also identified up-regulation of MMP-2 compared with controls. This enzyme is involved in the breakdown of the basement membrane and tissue destruction during periodontitis and is reportedly expressed in periodontal tissues as a response to the presence of Gram-negative anaerobic bacteria (Grayson et al., 2003, Gursoy et al., 2008). LPS from Gram-negative bacteria is recognized by the cell-surface receptor TLR-4 (Ren et al., 2005, Li et al., 2014) and in this study, the

expression of TLR-4 was up-regulated upon exposing epithelial cells to suspensions of the heat-killed periodontal pathogens. This finding was similar to results previously reported (Milward et al., 2007) and may contribute to the chronic inflammation of periodontal diseases.

The association between E-cadherin down-regulation and Snail activity in primary oral keratinocytes was further explored utilising ICC. Cultures exposed to bacterial stimuli for 8 days exhibited activation of Snail-nuclear activity in ~60% of epithelial cells in response to *F. nucleatum* and *P. gingivalis* exposure. This process associated with morphological changes and cell dispersion, which indicated a potential loss of E-cadherin-mediated adhesion. TEER further supported the loss of cellular attachment as the electric resistance decreased in cultures challenged by bacteria.

The possibility of a loss of epithelial integrity due to cell death or a decrease in proliferation rate because of toxic effects of bacterial stimuli used in this study was indicated to be unlikely following determination of cell proliferation and viability throughout the experimental period. Furthermore, data derived from IF analysis showed up-regulation of vimentin expression following 8-days stimulation with bacterial components, which supported the potential acquisition of mesenchymal-phenotype as proposed by other studies (Kalluri and Weinberg, 2009, Zeisberg and Neilson, 2009). Notably, vimentin and E-cadherin co-existed in the transitioned cells, in a similar manner to that observed in stimulated H400 cells. Indeed, transitioned cells could be observed with two apparent patterns: i) elongated, vimentin-positive and associated with E-cadherin internalization, and ii) cells remained as part of epithelial sheets with E-cadherin normally distributed around the cell membrane with vimentin staining detectable in their cytoplasm.

Acquisition of a migratory-phenotype is an indicator of EMT-associated cell plasticity (Kalluri and Weinberg, 2009). Treatment of epithelial cultures with the periodontal pathogens resulted in an increased rate of scratch closure in confluent epithelial monolayers. These data were supported by the transwell migration assay that showed an increased number of migratory cells after bacterial stimulation. The increased cell mobility was also consistent with findings of the PCR and IF analyses that demonstrated down-regulation of E-cadherin expression. These results were consistent with previous findings which indicated that increased locomotion was associated with vimentin overexpression and decreased E-cadherin expression (Misra et al., 2012). In addition, vimentin expression has been demonstrated to increase in association with Snail up-regulated activity (Lee et al., 2008, Myong, 2012). Furthermore, the down-regulation of E-cadherin and other adherence molecules and subsequent loss of cellular junction may indicate the onset of EMT (Radisky, 2005).

Comparison of the effects of periodontal pathogens on H400 cells and primary oral keratinocytes showed that both cell types responded in a similar manner. Expression of epithelial proteins, E-cadherin and β-catenin, was down-regulated and associated with up-regulation of vimentin, N-cadherin, MMP-2, and Snail-1. However, these expression changes appeared greater in H400 cultures compared with primary cells. The same outcome was also true for the other assays applied including IF of E-cadherin and vimentin, ICC for Snail activation, TEER, and scratch-wound. As H400 cells are originally a cancer cell line, these results may reflect that healthy and diseased or abnormal, tissues of the same type could potentially react differently to the same stimuli which may indicate that cancerous cells are more prone to EMT than normal cells.

The current study of oral keratinocytes *in vitro* showed that cells acquire a range of EMT-like features following bacterial stimulation. These results also suggested the potential of periodontal pathogens in compromising epithelial-phenotype during periodontitis via

inducing the EMT process. Further study in experimental animals and clinical samples could clarify further the role of EMT in periodontal disease. Analysis could include longer-term studies and determination of the timing of events as well as further regulatory interactions with bacterial species. These data may provide further avenues for the development of new treatment modalities in periodontitis, including the potential to reverse EMT as has recently been suggested (Shimojo et al., 2013, Han et al., 2015).

5: Conclusions

- Primary oral keratinocytes exposed to Gram-negative periodontal pathogens exposure indicated molecular, functional and structural changes potentially representative of EMT. This suggested the possible implication of periodontal pathogen-mediated phenotypic alteration in compromising the integrity of pocket epithelial lining during periodontitis.
- Periodontal pathogens affect the phenotype and behavior of primary oral keratinocytes in a similar manner to an H400 OSCC cell line, yet the effect on the latter appears significantly higher and may be a function of cell derivation or species difference.

GENERAL DISCUSSION AND FUTURE WORK

Epithelia form physical barriers that line body cavities, external surfaces and act as a first line of defense. In health, epithelial cells form continuous epithelial sheets in which the cells adhere tightly to each other and to the underlying basement membrane by their specialised cellular junctions (Fritz et al., 2008, Marchiando et al., 2010). However, under certain physiological and pathological conditions, such as during chronic inflammation and tumour development, these cells may lose their phenotype and acquire migratory properties (Thiery, 2002b).

Although EMT was described in the 1960s, this process was not recognized as a distinct process until the early 1980s following several investigations performed in different adult and embryonic epithelial cell types (Greenburg and Hay, 1982). Furthermore, work by Stoker and Perryman (1985) indicated transition of MDCK cells, from an epithelial phenotype into elongated mesenchymal-like cells following culturing in fibroblast-conditioned medium. Notably however the role EMT in adult diseases took much longer to be recognized due to difficulties in following the EMT process *in vivo* due in part to the high cellular diversity which renders EMT cell tracking extremely difficult and open to ambiguity (Thiery, 2002). Recently, EMT, induced in response to inflammatory conditions is now considered as a possible mechanism affecting integrity of epithelial barrier function in many organs including the stomach, liver and kidney (Lamouille et al., 2014, Huang et al., 2012). The presence of EMT-predisposing factors such as bacteria, cytokines and hypoxia in periodontal pockets may therefore favour induction of this process which could contribute to initiation and progression of periodontitis although this has never been robustly investigated before in this context.

6.1: Bacterial exposure can drive EMT

Bacteria readily colonise the human body and are ten-fold more abundant than the human cells present. Notably areas having relatively high bacterial counts include the gastrointestinal tract and the oral cavity. Here the microbiota is highly diverse in composition and includes beneficial, opportunistic, and pathogenic bacteria. These bacteria play a crucial role in human life by influencing development, physiology, immunity, and regulation of nutrient uptake (Ley et al., 2006, Inagaki et al., 1996). The microbiota-immune system relationship can however become disturbed due to impaired growth of beneficial commensals leading to changes in composition of the microbial flora, subsequently favouring growth of pathogenic bacteria which are normally contained in a healthy state. These changes can result in activation of TLR-signaling pathways with subsequent up-regulation of inflammatory cytokines, such as TNF-α, TGF-β1 and interleukins (Round and Mazmanian, 2009), which could favour EMT-induction if this process becomes chronic (Kalluri and Weinberg, 2009). Indeed, *H. pylori* is a highly pathogenic Gram-negative bacterium which is considered the primary etiologic agent for gastritis and gastric ulcers. It is a well-recognized bacteria for its ability to disrupt cell-cell attachment, mainly by E-cadherin down-regulation, which disturbs barrier function (Amieva and El–Omar, 2008, Murata-Kamiya et al., 2007). In current study, it was hypothesised that well-recognized periodontal pathogens, *F. nucleatum* and *P. gingivalis*, may also have the potential to indirectly induce EMT during periodontitis.

6.2: Phenotypic-shifting alters epithelial barrier function

A hallmark of periodontal disease is the destruction of tooth supporting tissues which is mediated by an aberrant host response initiated and propagated by pathogenic bacteria. The presence of periodontal bacteria within the gingival tissue is a normal consequence of this destructive process and results in loss of barrier function (Allenspach-Petrzilka and Guggenheim, 1983, Christersson et al., 1987, Noiri et al., 1997, Thiha et al., 2007). As a

result, invasion of the connective tissues by periodontal pathogens occurs which further enhances the destructive inflammatory response seen in susceptible patients (Tribble and Lamont, 2010). Indeed, it has been reported that periodontopathogens are characterised by their ability to invade the connective tissues distant from the initial infection site following disruption of basement membrane integrity (Tribble and Lamont, 2010). Notably, the specific cellular mechanisms resulting in tissue destruction by periodontal pathogens remain largely undefined. Exposure of epithelial cells to periodontal pathogens results in features representative of that of EMT, including loss of attachment and rounding of the cells as a result of loss of cadherin and integrin junctions (Sheets et al., 2005). Indeed, down-regulation of E-cadherin in tissue samples collected from periodontally diseased sites has also been reported by other study (Nagarakanti et al., 2007) and challenge of gingival epithelium with *P. gingivalis* has been shown to induce cytoskeletal changes similar to those seen in EMT (Tribble and Lamont, 2010). It has also been reported that Gram-negative anaerobic periodontal pathogens such as *P. gingivalis*, can modulate apoptosis resulting in increased resistance to cell death (Urnowey et al., 2006, Mao et al., 2007, Nakhjiri et al., 2001) and cell viability is not affected following *P. gingivalis* exposure (Yilmaz, 2008). Consistently, results from this thesis indicated that viability of epithelial cultures (H400 and primary cells), were not affected by the presence of periodontal bacterial components. However, compromised epithelial barrier function of the periodontal pocket lining, due to EMT-induction potentially mediated by periodontal pathogens, may provide an explanation for the mechanism of tissue destruction and the impaired healing, observed in periodontitis. Indeed, refractory periodontitis which is a group of periodontal diseases characterized by low-plaque scores and which is unresponsive to conventional periodontal treatment (Magnusson and Walker, 1996). Interestingly serum from patients with refractory periodontitis showed elevated IgG level to a number of Gram-negative bacteria such as *P. gingivalis*, *T. forsythia*, *A.*

actinomycetemcomitans and *E. corrodens* (Magnusson et al., 1991, Magnusson and Walker, 1996). These bacteria have the potential for EMT-induction thus further supporting the possible role of EMT mechanisms in the pathogenesis of periodontitis. In addition, immunohistochemical analysis of gingival samples collected from gingivitis and periodontitis patients showed significant down-regulation of E-cadherin when compared with healthy individuals (Arun et al., 2010). Notably the treatment of periodontal pockets reportedly results in significant up-regulation of E-cadherin expression in comparison with diseased sites (Arun et al., 2010). These data add further support for the existence of EMT and for its potential in a range of disease process including periodontitis (Pierga et al., 2003).

6.3: Periodontal pathogens induced EMT in *in vitro* model systems

In the study presented here, the first challenge was to develop a 2D model that could be utilised for investigating EMT over an extended time-course. For this, an immortal OSCC cell line (H400) was utilised which expresses appropriate epithelial molecules to be investigated in addition to its relative homogeneity and low-maintenance requirements for culture. The main initial challenge was to carefully control the relatively high proliferation rate of these cells in order to ensure subconfluence was achieved during the experimental period (up to 8 days). This was accomplished by varying FCS concentration or cell seeding number or a combination of the two. Following a series of experiments, it was determined that variation in seeding number whilst maintaining conventionally used nutrient levels (10% FCS concentration) produced the most appropriate outcome. The ability of this model system to respond to periodontal pathogens was subsequently confirmed following investigations of NF-κB activation and TLR expression, in addition to determining vitality and proliferation rate following bacterial stimulation. EMT-related features, in H400 cells stimulated with bacteria, were determined by using a range of techniques widely applied to detect changes in phenotype including PCR, IF, ICC, scratch-wound assay, transwell migration, ELISA, SEM,

and TEER. Results from the H400 model system indicated that cellular changes occurred which were consistent with EMT. These data were supported by data generated in the primary cell system. Notably, primary oral keratinocytes harvested from rat labial gingivae and palate was used to investigate potential bacteria-mediated EMT using a similar model culture system with analysis of selected EMT markers.

The concept of phenotype-shifting and its implication in cancer progression and loss of epithelial barrier function remains under considerable debate. However, many studies have provided compelling evidence for EMT involvement in a range of different diseases (see Chapter 1). Investigation of tumor-invasive fronts in primary colon carcinoma demonstrate the presence of E-cadherin-negative cells which extended into the underlying stroma (Thiery, 2002a). Data from another study, using a mouse model of mammary carcinoma, proposed association of FSP-1-positive cells with acquisition of an invasive phenotype (Xue et al., 2003) which is consistent with results from this thesis which demonstrated up-regulation of this protein. Furthermore, data from this study have indicated that H400 and primary cells stimulated with bacterial components showed increased transcriptional activity of Snail-1 and -2, with both having been reported as major repressors of E-cadherin expression which has been reported to be associated with invasive malignancies such as gastric carcinoma (Rosivatz et al., 2002, Hajra et al., 2002). Association of key-EMT regulatory transcriptional factor, Snail-1, with loss of epithelial barrier function was recently investigated *in vitro* and in a zebrafish model infected with bacteria. Subsequent data generated showed that activation of Snail-1 by bacterial stimulation was accompanied by loss of epithelial attachment proteins with this effect being blocked when Snail-1-negative zebrafish were exposed to the same bacteria (Kim et al., 2015). Furthermore upper respiratory tract infection with *Haemophilus influenza* (*H. influenza*) (Gram-negative bacteria) resulted in an inflammatory response via activation of TLR signaling and subsequent up-regulation of TGF-β1, IL-6, and Snail-1

which are well-known molecules involved in compromising epithelial barrier function (Beisswenger et al., 2009).

Other interesting results obtained in this thesis using IF analysis of H400 and primary oral epithelial cells, showed co-existence of both mesenchymal and epithelial phenotype in stimulated cultures over 8-days. Notably most previous studies described EMT as a total transition of cells represented by complete loss of epithelial proteins and acquisition of mesenchymal molecules. However, data presented in this thesis indicated that transitioned cells preserved some of their epithelial-phenotype, retaining E-cadherin, together with the expression of molecules typically associated with mesenchymal cells such as vimentin. The complete absence of epithelial proteins was not observed in this study and subsequently this can be termed 'partial EMT'. The retaining of some of the parental cell proteins during the transition process is more consistent with the definition of EMT which states that cells can revert to their original phenotype following removal of stimulus (Kalluri and Weinberg, 2009). Indeed, EMT is different from terminal differentiation in which cells switch back and forth between epithelial to mesenchymal phenotype. The reasons underpinning these effects could be as a result of the types of cells used, culture conditions, and stimuli utilised. The immortal cell line used in this thesis showed a higher percent of vimentin-positive stained cells than the primary cell counterparts, this may indicate that H400 cells are more prone to EMT-induction due to genetic predisposition which increases their transition in response to bacterial stimulation and autocrine signaling. In addition, increased migratory ability could also be due to increased resistance to anoikis, type of apoptosis induced by disruption of cell-ECM attachment, which is crucial for cancer invasion and distant metastasis (Cao et al., 2016, Paoli et al., 2013). Primary keratinocytes are potentially more prone to anoikis (Gilmore, 2005) which could explain the limited invasive ability of transitioned primary epithelial cells when compared to keratinocytes derived from cancer.

Data derived from the scratch-wound, transwell migration assays and SEM images showed acquisition of a migratory-phenotype following physical trauma which was increased in the presence of heat-killed *F. nucleatum, P. gingivalis* and *E. coli* LPS. Increased cytokine production is a common feature of microbial or mechanical stimulation which could be responsible for the increased cell motility detected in these experiments. Most of the EMT studies tend to focus on particular cytokines, acting together or independently, to explain the triggering of the EMT process, and the key molecular modulators include TGF-β (Xu et al., 2009, Miyazono, 2009), TNF-α (Li et al., 2012a), and EGF (Buonato et al., 2015). Assaying supernatants collected from stimulated epithelial cultures utilised in this thesis indicated significantly increased levels of these cytokines.

The data generated from this thesis have indicated the ability of both H400 cells and primary oral epithelial cells to undergo EMT when exposed to periodontal pathogens *P. gingivalis* and *F. nucleatum.* As previously discussed this may have important ramifications in terms of malignant progression; however, this may also be of considerable interest in the pathogenesis of periodontal disease. Periodontal disease is characterised by loss of epithelial attachment, bacterial invasion of the connective tissues and establishment of a non-resolving chronic inflammatory lesion. The EMT process described in this thesis exhibits many aspects that potentially closely associate with pathogenesis of periodontitis.

6.4: Could anti-EMT drugs be used for periodontal therapy?

Treatment strategies for periodontitis have changed little over the last decades and centre on reducing the plaque biofilm by the patient and professional cleaning by the clinician, however this approach has its limitations (Carranza et al., 2014). In the case of aggressive periodontal disease antibiotic regimens are used to aid the elimination of bacterial pathogens (Kapoor et al., 2012, Prakasam et al., 2012). These approaches do not always provide successful outcomes and are responsible for local and systemic side-effects in addition to the increased

concern surrounding bacterial resistance (Slots and Rams, 1990, Davies and Davies, 2010). A further issue with periodontal disease management is the recolonization of the treated periodontal lesion from bacterial reservoirs within the oral cavity. Sbordone et al. (1990) evaluated the pattern of subgingival microflora derived from the same periodontal pockets before and after single mechanical debridement sessions. Results indicated that after 60 days the same sites were recolonised by pathogenic bacteria such as *F. nucleatum* and *P. gingivalis* with no significant difference between pre- and post-treatment clinical parameters or bacterial cultures. Current treatment of periodontal disease includes mechanical debridement which is sometimes supported with use of antibiotics that may affect beneficial flora beside well-known side effects of these drugs (Slots and Rams, 1990). To date there have been few clinical trials that have used interventions that aim to modulate the host response, however there have been a small number of studies in other diseases that have investigated several experimental and naturally derived anti-EMT drugs (Zhao et al., 2015, Wilson et al., 2014). Based on the data presented here this approach could provide a potential adjunct for use in managing periodontal disease. However, a better understanding of the EMT mechanism and how it relates to periodontitis pathogenesis may provide a potentially novel approach for treating this disease based on enhancing the innate immune response. Specifically, maintenance of the epithelial barrier function may prevent bacterial invasion of the connective tissues and subsequent aberrant host response which is implicated in tissue breakdown. Questions related to this include as to whether EMT is an integral part of cellular survival mechanism or is a failed component of the healing process. There are a number of other aspects of the EMT process that require further elucidation including determining the duration and frequency of cell stimulation required, the type and extent of stimulation, the specific cytokine(s) and their concentrations required, and other associated factors necessary to induce transition. These questions need to be addressed before a full understanding of the

importance of EMT in periodontal disease pathogenesis can be determined and only then will the potential for use of EMT blockers in disease management be fully realised.

Conclusions

- Data obtained from developing epithelial cells 2D model system showed that growth of cells can be controlled by varying cell seeding number and/or concentration of nutrients (FCS) in cultures. In addition, results indicated failure of image-based cell counter used in this study to produce consistent results, cell count and viability, in association with low cellular density samples.
- Heat-killed periodontal pathogens did not affect proliferation or viability of epithelial cells utilized in this study. In addition, dead bacterial suspension induced pro-inflammatory response in oral keratinocytes cultures which was evident by activating NF-κB nuclear translocation and altering transcription of different TLR. This provide safe alternative to avoid contamination of cultures when viable bacteria are used.
- OSCC H400 cell line showed changes representative to that of EMT following exposure to *P. gingivalis* and *F. nucleatum*. This may indicate a potential involvement of periodontal pathogens in cancer progression by dissociating epithelial cells and increasing migratory ability of the cells.
- Exposure of primary oral epithelial cells to periodontal pathogens resulted in EMT-like changes in similar pattern to H400 cells but to lesser extent. This may indicate that cells of cancerous origin are more susceptible to EMT-induction and acquisition of migratory-phenotype in response to bacterial stimulation.
- In general, the results of the current study indicated for the first time the possible implication of EMT in pathogenesis of periodontitis by compromising epithelial integrity of pockets lining, thereby causing further destruction to supporting tooth structures by facilitating invasion of pathogenic bacteria to deeper tissues.

Potential future studies

Data presented in this thesis have highlighted the potential of EMT as a key mechanism in the pathogenesis of periodontitis. However, significant additional work is required in order to further elucidate its role in the pathogenesis of periodontitis at a molecular and cellular level. Potential studies could include:

- Development of an improved model system such as the application of an organotypic model (3D) of oral keratinocytes to more closely mimic the periodontal pocket local environment which includes attachment between the basement membrane and underlying stroma *in vitro.* In addition, other factors associated with inflammation such as hypoxia, temperature and pH could be included in the model either in the presence of bacterial stimulation or alone. Furthermore, experimental periodontitis in an animal model could be studied which may better represent the situation in humans *in vivo*.
- The oral cavity harbours a large number of bacterial species (over 700 species) that can colonise tooth surfaces and subgingival area, many of which are pathogenic. More work is still required to investigate the potential ability of these species, particularly Gram-negative anaerobic bacteria, such as *A. actinomycetemcomitans*, *T. forsythia*, *P. intermedia*, *P. nigrescens*, and *E. corrodens* to induce EMT. Combined effects of multiple bacteria in oral keratinocyte cultures might reveal potentiation additional modulatory effects involved in the bacteria-host interactions. These could be determined by either co-culturing of epithelial with two or more bacteria (live versus dead) or by comparing effects of biofilm samples collected from periodontal pockets compared with biofilms derived from healthy periodontal sites.
- Results from the current and previous studies on EMT suggest that cytokines can play a major role in phenotypic alteration. The effect of different concentrations of potent cytokines, including TGF-β1 and TNF-α, independently or synergistically in a

periodontitis model, and their associated signaling downstream need to be studied further.

- Comparing healthy vs diseased tissues to investigate possible presence of EMT-indicators *in vivo* in periodontal disease by utilising range of assays to detect EMT-related indicators in gingival samples by PCR and immunohistochemistry in addition to measuring levels of EMT-inducing cytokines in gingival crevicular fluid by ELISA.
- Investigating the effect of drugs which have been previously reported to have an anti-EMT action in *in vitro* systems may indicate their potential clinical utility. These modulators include natural products such as curcumin, vitamins such as vitamin D and C, and antioxidants, e.g. superoxide dismutase 3, in addition to new experimental drugs, e.g. Sorafenib and U0126. Success of these drugs in reversing or preventing EMT may provide a useful adjunct in periodontal disease management.
- Ultimately once our understanding of EMT in periodontitis pathogenesis is better elucidated clinical trials could be conducted to determine efficacy alongside conventional periodontal treatment regimens.

References

ABERLE, H., BUTZ, S., STAPPERT, J., WEISSIG, H., KEMLER, R. & HOSCHUETZKY, H. 1994. Assembly of the cadherin-catenin complex in vitro with recombinant proteins. Journal of Cell Science, 107, 3655-3663.

ACAY, R. R., SANTOS, E. D. & MACHADO DE SOUSA, S. O. 2008. Correlation between c-Jun and human papillomavirus in oral premalignant and malignant lesions. Oral Oncology, 44, 698-702.

ACEVEDO, V. D., GANGULA, R. D., FREEMAN, K. W., LI, R., ZHANG, Y., WANG, F., AYALA, G. E., PETERSON, L. E., ITTMANN, M. & SPENCER, D. M. 2007. Inducible FGFR-1 activation leads to irreversible prostate adenocarcinoma and an epithelial-to-mesenchymal transition. Cancer Cell, 12, 559-71.

ACKLAND, M. L., NEWGREEN, D. F., FRIDMAN, M., WALTHAM, M. C., ARVANITIS, A., MINICHIELLO, J., PRICE, J. T. & THOMPSON, E. W. 2003. Epidermal growth factor-induced epithelio-mesenchymal transition in human breast carcinoma cells. Laboratory Investigation, 83, 435-48.

ALLENSPACH-PETRZILKA, G. E. & GUGGENHEIM, B. 1983. Bacterial invasion of the periodontium; an important factor in the pathogenesis of periodontitis? Journal of Clinical Periodontology, 10, 609-617.

AMAR, S. & HAN, X. 2003. The impact of periodontal infection on systemic diseases. Medical Science Monitor, 9, RA291-RA299.

AMBILI, R., SANTHI, W. S., JANAM, P., NANDAKUMAR, K. & PILLAI, M. R. 2005. Expression of activated transcription factor Nuclear Factor-κB in periodontally diseased tissues. Journal of Periodontology, 76, 1148-1153.

AMIEVA, M. R. & EL–OMAR, E. M. 2008. Host-bacterial interactions in Helicobacter pylori infection. Gastroenterology, 134, 306-323.

AMIEVA, M. R., VOGELMANN, R., COVACCI, A., TOMPKINS, L. S., NELSON, W. J. & FALKOW, S. 2003. Disruption of the epithelial apical-junctional complex by Helicobacter pylori CagA. Science, 300, 1430-1434.

AMIT, S., HATZUBAI, A., BIRMAN, Y., ANDERSEN, J. S., BEN-SHUSHAN, E., MANN, M., BEN-NERIAH, Y. & ALKALAY, I. 2002. Axin-mediated CKI phosphorylation of β-catenin at Ser 45: a molecular switch for the Wnt pathway. Genes & Development, 16, 1066-1076.

ARMITAGE, G. C. 1999. Development of a classification system for periodontal diseases and conditions. Annals of Periodontology, 4, 1-6.

ARNEMANN, J., SPURR, N. K., WHEELER, G. N., PARKER, A. E. & BUXTON, R. S. 1991. Chromosomal assignment of the human genes coding for the major proteins of the desmosome junction, desmoglein DGI (DSG), desmocollins DGIIIII (DSC), desmoplakins DPIII (DSP), and plakoglobin DPIII (JUP). Genomics, 10, 640-645.

ARUN, R., HEMALATHA, R., ARUN, K. & KUMAR, T. 2010. E-cadherin and CD1a expression in gingival epithelium in periodontal health, disease and post-treatment. Indian Journal of Dental Research, 21, 396-401.

AUMAILLEY, M., BRUCKNER-TUDERMAN, L., CARTER, W. G., DEUTZMANN, R., EDGAR, D., EKBLOM, P., ENGEL, J., ENGVALL, E., HOHENESTER, E. & JONES, J. C. 2005. A simplified laminin nomenclature. Matrix Biology, 24, 326-332.

AVERY, B. E. & SIMPSON, D. M. 1973. The baboon as a model system for the study of periodontal disease: clinical and light microscopic observations. Journal of periodontology, 44, 675-686.

BAGNOLI, F., BUTI, L., TOMPKINS, L., COVACCI, A. & AMIEVA, M. R. 2005. Helicobacter pylori CagA induces a transition from polarised to invasive phenotypes in MDCK cells. Proceedings of the National Academy of Sciences of the United States of America, 102, 16339-16344.

BAINBRIDGE, B. W., COATS, S. R. & DARVEAU, R. P. 2002. Porphyromonas gingivalis lipopolysaccharide displays functionally diverse interactions with the innate host defense system. Annals of Periodontology, 7, 29-37.

BAKHUBAIRA, S. 2013. Automated versus manual platelet count in Aden. Journal of Clinical & Experimental Pathology, 3, 1-4.

BALKWILL, F. 2006. TNF-α in promotion and progression of cancer. Cancer and Metastasis Reviews, 25, 409.

BALKWILL, F. 2009. Tumour necrosis factor and cancer. Nature Reviews Cancer, 9, 361-371.

BAO, X. L., SONG, H., CHEN, Z. & TANG, X. 2012. Wnt3a promotes epithelial-mesenchymal transition, migration, and proliferation of lens epithelial cells. Molecular Vision, 18, 1983-90.

BARBER, P. R., VOJNOVIC, B., KELLY, J., MAYES, C. R., BOULTON, P., WOODCOCK, M. & JOINER, M. C. 2001. Automated counting of mammalian cell colonies. Physics in Medicine and Biology, 46, 63.

BARRALLO-GIMENO, A. & NIETO, M. A. 2005. The Snail genes as inducers of cell movement and survival: implications in development and cancer. Development, 132, 3151-3161.

BATALLER, R. & BRENNER, D. A. 2005. Liver fibrosis. Journal of Clinical Investigation, 115, 209-218.

BATES, R. C. & MERCURIO, A. M. 2003. Tumor necrosis factor-α stimulates the epithelial-to-mesenchymal transition of human colonic organoids. Molecular Biology of the Cell, 14, 1790-1800.

BATLLE, E., SANCHO, E., FRANCI, C., DOMINGUEZ, D., MONFAR, M., BAULIDA, J. & GARCIA DE HERREROS, A. 2000. The transcription factor snail is a repressor of E-cadherin gene expression in epithelial tumour cells. Nature Cell Biology, 2, 84-9.

BAUD, J., VARON, C., CHABAS, S., CHAMBONNIER, L., DARFEUILLE, F. & STAEDEL, C. 2013. Helicobacter pylori initiates a mesenchymal transition through ZEB1 in gastric epithelial cells. PLoS ONE, 8, e60315.

BAUM, J. & DUFFY, H. S. 2011. Fibroblasts and myofibroblasts: what are we talking about? Journal of Cardiovascular Pharmacology, 57, 376-379.

BECK, J., GARCIA, R., HEISS, G., VOKONAS, P. S. & OFFENBACHER, S. 1996. Periodontal disease and cardiovascular disease. Journal of Periodontology, 67, 1123-1137.

BEISSWENGER, C., LYSENKO, E. S. & WEISER, J. N. 2009. Early bacterial colonization induces Toll-like receptor-dependent transforming growth factor β signaling in the epithelium. Infection and Immunity, 77, 2212-2220.

BERX, G., BECKER, K. F., HOFLER, H. & VAN ROY, F. 1998. Mutations of the human E-cadherin (CDH1) gene. Human Mutation, 12, 226-37.

BHATTACHARYA, R., XU, F., DONG, G., LI, S., TIAN, C., PONUGOTI, B. & GRAVES, D. T. 2014. Effect of bacteria on the wound healing behavior of oral epithelial cells. PLoS ONE, 9, e89475.

BIERNACKA, A., DOBACZEWSKI, M. & FRANGOGIANNIS, N. G. 2011. TGF-β signaling in fibrosis. Growth Factors, 29, 196-202.

BINDER GALLIMIDI, A., FISCHMAN, S., REVACH, B., BULVIK, R., MALIUTINA, A., RUBINSTEIN, A. M., NUSSBAUM, G. & ELKIN, M. 2015. Periodontal pathogens Porphyromonas gingivalis and Fusobacterium nucleatum promote tumor progression in an oral-specific chemical carcinogenesis model. Oncotarget, 6, 22613-22623.

BLASER, M. J. 2006. Who are we? Indigenous microbes and the ecology of human diseases. EMBO Reports, 7, 956-960.

BORTHWICK, L. A., SUNNY, S. S., OLIPHANT, V., PERRY, J., BRODLIE, M., JOHNSON, G. E., WARD, C., GOULD, K., CORRIS, P. A., DE SOYZA, A. & FISHER, A. J. 2011. Pseudomonas aeruginosa accentuates epithelial-to-mesenchymal transition in the airway. European Respiratory Society, 37, 1237-1247.

BOSE, S. K., MEYER, K., DI BISCEGLIE, A. M., RAY, R. B. & RAY, R. 2012. Hepatitis C Virus induces epithelial-mesenchymal transition in primary human hepatocytes. Journal of Virology, 86, 13621-13628.

BOUDREAU, N. J. & VARNER, J. A. 2004. The homeobox transcription factor Hox D3 promotes integrin α5β1 expression and function during angiogenesis. Journal of Biological Chemistry, 279, 4862-4868.

BOURBOULIA, D. & STETLER-STEVENSON, W. G. Matrix metalloproteinases (MMPs) and tissue inhibitors of metalloproteinases (TIMPs): Positive and negative regulators in tumor cell adhesion. Seminars in Cancer Biology, 2010. Elsevier, 161-168.

BRADLEY, J. 2008. TNF-mediated inflammatory disease. The Journal of Pathology, 214, 149-160.

BROWNLEE, M. 2005. The pathobiology of diabetic complications. A Unifying Mechanism, 54, 1615-1625.

BUCCIONE, R., CALDIERI, G. & AYALA, I. 2009. Invadopodia: specialised tumor cell structures for the focal degradation of the extracellular matrix. Cancer and Metastasis Reviews, 28, 137-149.

BULLIONS, L. C. & LEVINE, A. J. 1998. The role of beta-catenin in cell adhesion, signal transduction, and cancer. Current Opinion in Oncology, 10, 81-87.

BUONATO, J. M., LAN, I. S. & LAZZARA, M. J. 2015. EGF augments TGFβ-induced epithelial–mesenchymal transition by promoting SHP2 binding to GAB1. Journal of Cell Science, 128, 3898-3909.

CAO, Z., LIVAS, T. & KYPRIANOU, N. 2016. Anoikis and EMT: Lethal. Critical Reviews™ in Oncogenesis, 21, 155-168.

CARPENTER, G. and COHEN, S., 1990. Epidermal growth factor. J Biol Chem, 265, 7709-7712.

CARRANZA, F. A., NEWMAN, M. G., TAKEI, H. & KLOKKEVOLD, P. R. 2014. Clinical Periodontology, USA, Saunders.

CARSWELL, E., OLD, L. J., KASSEL, R., GREEN, S., FIORE, N. & WILLIAMSON, B. 1975. An endotoxin-induced serum factor that causes necrosis of tumors. Proceedings of the National Academy of Sciences, 72, 3666-3670.

CARVER, E. A., JIANG, R., LAN, Y., ORAM, K. F. & GRIDLEY, T. 2001. The mouse Snail gene encodes a key regulator of the epithelial-mesenchymal transition. Molecular and Cellular Biology, 21, 8184-8188.

CAVATORTA, A. L., GIRI, A. A., BANKS, L. & GARDIOL, D. 2008. Cloning and functional analysis of the promoter region of the human Disc large gene. Gene, 424, 87-95.

CEKICI, A., KANTARCI, A., HASTURK, H. & VAN DYKE, T. E. 2014. Inflammatory and immune pathways in the pathogenesis of periodontal disease. Periodontology 2000, 64, 57-80.

CHANDRAKESAN, P., HOUCHEN, C. W., ANANT, S. & UMAR, S. 2012. Bacterial infection-induced epithelial-to-mesenchymal transition (EMT) of colonic crypt cells with acquired characteristics of stem cells promotes spheroid/organoid formation in vitro and tumorigenesis in vivo. Cancer Research, 72, 1404-1404.

CHAPPLE, I. L. C., AND GILBERT, A. D. 2002. Understanding periodontal diseases: assessment and diagnostic procedures in practice. In: NORIN, H. F. W. (ed.) The role of the host response. London: Quintessence.

CHEA, H. K., WRIGHT, C. V. & SWALLA, B. J. 2005. Nodal signaling and the evolution of deuterostome gastrulation. Developmental Dynamics, 234, 269-278.

CHEN, G. & GOEDDEL, D. V. 2002. TNF-R1 signaling: a beautiful pathway. Science, 296, 1634-1635.

CHEN, Y.-S., HUANG, W.-L., CHANG, S.-H., CHANG, K.-W., KAO, S.-Y., LO, J.-F. & SU, P.-F. 2013a. Enhanced filopodium formation and stem-like phenotypes in a novel metastatic head and neck cancer cell model. Oncology Reports, 30, 2829-2837.

CHEN, Y., XIAO, Y., GE, W., ZHOU, K., WEN, J., YAN, W., WANG, Y., WANG, B., QU, C. & WU, J. 2013b. miR-200b inhibits TGF-β1-induced epithelial-mesenchymal transition and promotes growth of intestinal epithelial cells. Cell Death & Disease, 4, e541.

CHENG, S. & LOVETT, D. H. 2003. Gelatinase A (MMP-2) is necessary and sufficient for renal tubular cell epithelial-mesenchymal transformation. The American Journal of Pathology, 162, 1937-1949.

CHERNG, S., YOUNG, J. & MA, H. 2008. Alpha-smooth muscle actin (α-SMA). Journal of American Science, 4, 7-9.

CHINNERY, H. R., MCLENACHAN, S., BINZ, N., SUN, Y., FORRESTER, J. V., DEGLI-ESPOSTI, M. A., PEARLMAN, E. & MCMENAMIN, P. G. 2012. TLR9 ligand CpG-ODN applied to the injured mouse cornea elicits retinal inflammation. The American Journal of Pathology, 180, 209-220.

CHO, I., JANG, E.H., HONG, D., JUNG, B., PARK, M., & KIM, J. 2015. Suppression of LPS-induced epithelial-mesenchymal transition by aqueous extracts of Prunella vulgaris through inhibition of the NF-κB/Snail signaling pathway and regulation of EMT-related protein expression. Oncology Reports, 34, 2445-2450.

CHOI, S. S. & DIEHL, A. M. 2009. Epithelial-to-mesenchymal transitions in the liver. Hepatology, 50, 2007-2013.

CHRISTERSSON, L. A., WIKESJÖ, U. M. E., ALBINI, B., ZAMBON, J. J. & GENCO, R. J. 1987. Tissue localization of Actinobacillus actinomycetemcomitans in human periodontitis. Journal of Periodontology, 58, 540-545.

CHU, A. S., DIAZ, R., HUI, J.-J., YANGER, K., ZONG, Y., ALPINI, G., STANGER, B. Z. & WELLS, R. G. 2011. Lineage tracing demonstrates no evidence of cholangiocyte epithelial-to-mesenchymal transition in murine models of hepatic fibrosis. Hepatology (Baltimore, Md.), 53, 1685-1695.

CHUN, Y. H. P., CHUN, K. R. J., OLGUIN, D. A. & WANG, H. L. 2005. Biological foundation for periodontitis as a potential risk factor for atherosclerosis. Journal of Periodontal Research, 40, 87-95.

CLARKE, T. B., FRANCELLA, N., HUEGEL, A. & WEISER, J. N. 2011. Invasive bacterial pathogens exploit TLR-mediated downregulation of tight junction components to facilitate translocation across the epithelium. Cell Host & Microbe, 9, 404-414.

CLEVERS, H. 2006. Wnt/beta-Catenin signaling in development and disease. Cell, 127, 469-480.

COONS, A. H., CREECH, H., JONES, R. & BERLINER, E. 1942. The demonstration of pneumococcal antigen in tissues by the use of fluorescent antibody. The Journal of Immunology, 45, 159-70.

COONS, A. H., CREECH, H. J. & JONES, R. N. 1941. Immunological properties of an antibody containing a fluorescent group. Experimental Biology and Medicine, 47, 200-202.

COONS, A. H. & KAPLAN, M. H. 1950. Localization of antigen in tissue cells II. Improvements in a method for the detection of antigen by means of fluorescent antibody. The Journal of Experimental Medicine, 91, 1-13.

CORPECHOT, C., BARBU, V., WENDUM, D., KINNMAN, N., REY, C., POUPON, R., HOUSSET, C. & ROSMORDUC, O. 2002. Hypoxia-induced VEGF and collagen I expressions are associated with angiogenesis and fibrogenesis in experimental cirrhosis. Hepatology, 35, 1010-1021.

CORY, G. 2011. Scratch-Wound Assay. In: WELLS, C. M. & PARSONS, M. (eds.) Cell Migration: Developmental Methods and Protocols. Totowa, NJ: Humana Press.

COSTERTON, J., LEWANDOWSKI, Z., DEBEER, D., CALDWELL, D., KORBER, D. & JAMES, G. 1994. Biofilms, the customized microniche. Journal of Bacteriology, 176, 2137–2142.

COWIN, P., KAPPRELL, H.-P., FRANKE, W. W., TAMKUN, J. & HYNES, R. O. 1986. Plakoglobin: a protein common to different kinds of intercellular adhering junctions. Cell, 46, 1063-1073.

CROSNIER, C., STAMATAKI, D. & LEWIS, J. 2006. Organizing cell renewal in the intestine: stem cells, signals and combinatorial control. Nature Reviews Genetics, 7, 349-359.

D'AIUTO, F., PARKAR, M., ANDREOU, G., SUVAN, J., BRETT, P. M., READY, D. & TONETTI, M. S. 2004. Periodontitis and systemic inflammation: control of the local infection is associated with a reduction in serum inflammatory markers. Journal of Dental Research, 83, 156-160.

DAVE, J. M. & BAYLESS, K. J. 2014. Vimentin as an integral regulator of cell adhesion and endothelial sprouting. Microcirculation, 21, 333-344.

DAVENPORT, E., WILLIAMS, C., STERNE, J., MURAD, S., SIVAPATHASUNDRAM, V. & CURTIS, M. 2002. Maternal periodontal disease and preterm low birthweight: case-control study. Journal of Dental Research, 81, 313-318.

DAVIES, J. & DAVIES, D. 2010. Origins and evolution of antibiotic resistance. Microbiology and Molecular Biology Reviews: MMBR, 74, 417-433.

DAWSON, J. P., BERGER, M. B., LIN, C.-C., SCHLESSINGER, J., LEMMON, M. A. & FERGUSON, K. M. 2005. Epidermal growth factor receptor dimerization and activation require ligand-induced conformational changes in the dimer interface. Molecular and Cellular Biology, 25, 7734-7742.

DENNISON, D. K. & DYKE, T. E. 1997. The acute inflammatory response and the role of phagocytic cells in periodontal health and disease. Periodontology 2000, 14, 54-78.

DIERICKX, K., PAUWELS, M., VAN ELDERE, J., CASSIMAN, J. J., VAN STEENBERGHE, D. & QUIRYNEN, M. 2002. Viability of cultured periodontal pocket epithelium cells and Porphyromonas gingivalis association. Journal of Clinical Periodontology, 29, 987-96.

DING, L., ZHANG, Z., SHANG, D., CHENG, J., YUAN, H., WU, Y., SONG, X. & JIANG, H. 2014. α-Smooth muscle actin-positive myofibroblasts, in association with epithelial–mesenchymal transition and lymphogenesis, is a critical prognostic parameter in patients with oral tongue squamous cell carcinoma. Journal of Oral Pathology & Medicine, 43, 335-343.

DUANGKUMPHA, K., TECHASEN, A., LOILOME, W., NAMWAT, N., THANAN, R., KHUNTIKEO, N. & YONGVANIT, P. 2014. BMP-7 blocks the effects of TGF-β-induced EMT in cholangiocarcinoma. Tumor Biology, 35, 9667-9676.

ECKERT, M. A., LWIN, T. M., CHANG, A. T., KIM, J., DANIS, E., OHNO-MACHADO, L. & YANG, J. 2011. Twist1-induced invadopodia formation promotes tumor metastasis. Cancer Cell, 19, 372-386.

EKHLASSI, S., SCRUGGS, L. Y., GARZA, T., MONTUFAR-SOLIS, D., MORETTI, A. J. & KLEIN, J. R. 2008. Porphyromonas gingivalis lipopolysaccharide induces tumor necrosis factor-α and interleukin-6 secretion, and CCL25 gene expression, in mouse primary gingival cell lines: interleukin-6-driven activation of CCL2. Journal of Periodontal Research, 43, 431-439.

EURELL, J. A. & FRAPPIER, B. L. 2013. Dellmann's textbook of veterinary histology, John Wiley & Sons.

FALLON, J. H., SEROOGY, K. B., LOUGHLIN, S. E., MORRISON, R. S., BRADSHAW, R. A., KNAVER, D. & CUNNINGHAM, D. D. 1984. Epidermal growth factor immunoreactive material in the central nervous system: location and development. Science, 224, 1107-1109.

FELLER, L. & LEMMER, J. 2012. Oral squamous cell carcinoma: epidemiology, clinical presentation and treatment. Journal of Cancer Therapy, 3, 263-268.

FENG, X.-H. & DERYNCK, R. 2005. Specificity and versatility in TGF-β signaling through Smads. Annual Review of Cell and Developmental Biology, 21, 659-693.

FLIER, S. N., TANJORE, H., KOKKOTOU, E. G., SUGIMOTO, H., ZEISBERG, M. & KALLURI, R. 2010. Identification of epithelial to mesenchymal transition as a novel source of fibroblasts in intestinal fibrosis. Journal of Biological Chemistry, 285, 20202-20212.

FRAVALO, P., MÉNARD, C. & BONNAURE-MALLET, M. 1996. Effect of Porphyromonas gingivalis on epithelial cell MMP-9 type IV collagenase production. Infection and Immunity, 64, 4940-4945.

FRESHNEY, R. I. 2005. Culture of Animal Cells: A Manual of Basic Technique, New Jersey, Wiley-Liss.

FREUDENTHAL, R., LOCATELLI, F., HERMITTE, G., MALDONADO, H., LAFOURCADE, C., DELORENZI, A. & ROMANO, A. 1998. κ-B like DNA-binding activity is enhanced after spaced training that induces long-term memory in the crab Chasmagnathus. Neuroscience Letters, 242, 143-146.

FRITZ, J. H., LE BOURHIS, L., MAGALHAES, J. G. & PHILPOTT, D. J. 2008. Innate immune recognition at the epithelial barrier drives adaptive immunity: APCs take the back seat. Trends in Immunology, 29, 41-49.

FU, M. M., CHIN, Y.-T., FU, E., CHIU, H.-C., WANG, L.-Y., CHIANG, C.-Y. & TU, H.-P. 2015. Role of transforming growth factor-beta1 in Cyclosporine-induced epithelial-to-mesenchymal transition in gingival epithelium. Journal of Periodontology, 86, 120-128.

FURUSE, M., FUJITA, K., HIIRAGI, T., FUJIMOTO, K. & TSUKITA, S. 1998. Claudin-1 and-2: novel integral membrane proteins localizing at tight junctions with no sequence similarity to occludin. The Journal of Cell Biology, 141, 1539-1550.

FURUSE, M., HIRASE, T., ITOH, M., NAGAFUCHI, A., YONEMURA, S. & TSUKITA, S. 1993. Occludin: a novel integral membrane protein localizing at tight junctions. The Journal of Cell Biology, 123, 1777-1788.

GARRETT, S. C., VARNEY, K. M., WEBER, D. J. & BRESNICK, A. R. 2006. S100A4, a mediator of metastasis. Journal of Biological Chemistry, 281, 677-680.

GARROD, D. R., MERRITT, A. J. & NIE, Z. 2002. Desmosomal cadherins. Current Opinion in Cell Biology, 14, 537-545.

GEERTS, S. O., LEGRAND, V., CHARPENTIER, J., ALBERT, A. & ROMPEN, E. H. 2004. Further evidence of the association between periodontal conditions and coronary artery disease. Journal of Periodontology, 75, 1274-1280.

GETSIOS, S., HUEN, A. C. & GREEN, K. J. 2004. Working out the strength and flexibility of desmosomes. Nature reviews Molecular Cell Biology, 5, 271-281.

GHOSH, S. & KARIN, M. 2002. Missing pieces in the NF-kappaB puzzle. Cell, 109, S81-S96.

GILLES, C., POLETTE, M., MESTDAGT, M., NAWROCKI-RABY, B., RUGGERI, P., BIREMBAUT, P. & FOIDART, J.-M. 2003. Transactivation of vimentin by β-Catenin in human breast cancer cells. Cancer Research, 63, 2658-2664.

GILLES, C., POLETTE, M., ZAHM, J.-M., TOURNIER, J.-M., VOLDERS, L., FOIDART, J.-M. & BIREMBAUT, P. 1999. Vimentin contributes to human mammary epithelial cell migration. Journal of Cell Science, 112, 4615-4625.

GILLRIE, M. R., ZBYTNUIK, L., MCAVOY, E., KAPADIA, R., LEE, K., WATERHOUSE, C., DAVIS, S. P., MURUVE, D. A., KUBES, P. & HO, M. 2010. Divergent roles of Toll-like receptor 2 in response to lipoteichoic acid and Staphylococcus aureus in vivo. European Journal of Immunology, 40, 1639-1650.

GILMORE, A. P. 2005. Anoikis. Cell Death & Differentiation, 12, 1473-1477.

GOLDSTEIN, B. & MACARA, I. G. 2007. The PAR proteins: fundamental players in animal cell polarization. Developmental Cell, 13, 609-622.

GONÇALVES, M., CAPPELLARI, Á. R., SANTOS JUNIOR, A. A. D., MACHI, F. S., ANTUNES, K. H., SOUZA, A. P. D. D. & MORRONE, F. B. 2016. Effect of LPS on the viability and

proliferation of human oral and esophageal cancer cell lines. Brazilian Archives of Biology and Technology, 59.

GRAVDAL, K., HALVORSEN, O. J., HAUKAAS, S. A. & AKSLEN, L. A. 2007. A switch from E-Cadherin to N-Cadherin expression Indicates epithelial to mesenchymal transition and Is of strong and independent importance for the progress of prostate cancer. Clinical Cancer Research, 13, 7003-7011.

GRAVES, D. 2008. Cytokines that promote periodontal tissue destruction. Journal of Periodontology, 79, 1585-1591.

GREEN, K. J., GETSIOS, S., TROYANOVSKY, S. & GODSEL, L. M. 2010. Intercellular junction assembly, dynamics, and homeostasis. Cold Spring Harbor Perspectives in Biology, 2, a000125.

GREENBURG, G. & HAY, E. D. 1982. Epithelia suspended in collagen gels can lose polarity and express characteristics of migrating mesenchymal cells. The Journal of Cell Biology, 95, 333-339.

GROTEGUT, S., VON SCHWEINITZ, D., CHRISTOFORI, G. & LEHEMBRE, F. 2006. Hepatocyte growth factor induces cell scattering through MAPK/Egr-1-mediated upregulation of Snail. The EMBO Journal, 25, 3534-3545.

GUIJARRO-MUÑOZ, I., COMPTE, M., ÁLVAREZ-CIENFUEGOS, A., ÁLVAREZ-VALLINA, L. & SANZ, L. 2014. Lipopolysaccharide activates Toll-like receptor 4 (TLR4)-mediated NF-κB signaling pathway and proinflammatory response in human pericytes. The Journal of Biological Chemistry, 289, 2457-2468.

GUMBINER, B. M. 2005. Regulation of cadherin-mediated adhesion in morphogenesis. Nature Reviews Molecular Cell Biology, 6, 622-634.

GUO, R., SAKAMOTO, H., SUGIURA, S. & OGAWA, M. 2007. Endothelial cell motility is compatible with junctional integrity. Journal of Cellular Physiology, 211, 327-335.

GUO, S. & DIPIETRO, L. A. 2010. Factors affecting wound healing. Journal of Dental Research, 89, 219-229.

GURSOY, U. K., KÖNÖNEN, E. & UITTO, V. J. 2008. Stimulation of epithelial cell matrix metalloproteinase (MMP-2, -9, -13) and interleukin-8 secretion by fusobacteria. Oral Microbiology and Immunology, 23, 432-434.

HA, N. H., WOO, B. H., KIM DA, J., HA, E. S., CHOI, J. I., KIM, S. J., PARK, B. S., LEE, J. H. & PARK, H. R. 2015. Prolonged and repetitive exposure to Porphyromonas gingivalis increases aggressiveness of oral cancer cells by promoting acquisition of cancer stem cell properties. Tumour Biology, 36, 9947-60.

HAJRA, K. M., CHEN, D. Y.-S. & FEARON, E. R. 2002. The SLUG Zinc-Finger protein represses E-Cadherin in breast cancer. Cancer Research, 62, 1613-1618.

HALBLEIB, J. M. & NELSON, W. J. 2006. Cadherins in development: cell adhesion, sorting, and tissue morphogenesis. Genes & Development, 20, 3199-3214.

HANAHAN, D. & WEINBERG, R. A. 2000. The hallmarks of cancer. Cell, 100, 57-70.

HANNAS, A. R., PEREIRA, J. C., GRANJEIRO, J. M. & TJÄDERHANE, L. 2007. The role of matrix metalloproteinases in the oral environment. Acta Odontologica Scandinavica, 65, 1-13.

HARADA, K. I., MIYAKE, H., KUSUDA, Y. & FUJISAWA, M. 2012. Expression of epithelial–mesenchymal transition markers in renal cell carcinoma: impact on prognostic outcomes in patients undergoing radical nephrectomy. BJU International, 110, E1131-E1137.

HARASZTHY, V., ZAMBON, J., TREVISAN, M., ZEID, M. & GENCO, R. 2000. Identification of periodontal pathogens in atheromatous plaques. Journal of Periodontology, 71, 1554-1560.

HASAN, A. & PALMER, R. M. 2014. A clinical guide to periodontology: Pathology of periodontal disease. British Dental Journal, 216, 457-461.

HAUSMANN, M. 2010. How bacteria-induced apoptosis of intestinal epithelial cells contributes to mucosal inflammation. International Journal of Inflammation, 2010.

HAY, E. 1995. An overview of epithelio-mesenchymal transformation. Cells Tissues Organs, 154, 8-20.

HAY, E. D. 1968. Organization and fine structure of epithelium and mesenchyme in the developing chick embryo. Epithelial-Mesenchymal Interactions, 2, 31-35.

HAY, E. D. 2005. The mesenchymal cell, its role in the embryo, and the remarkable signaling mechanisms that create it. Developmental Dynamics, 233, 706-720.

HAY, E. D. & ZUK, A. 1995. Transformations between epithelium and mesenchyme: Normal, pathological, and experimentally induced. American Journal of Kidney Diseases, 26, 678-690.

HAYASHI, M., NINOMIYA, Y., HAYASHI, K., LINSENMAYER, T. F., OLSEN, B. R. & TRELSTAD, R. L. 1988. Secretion of collagen types I and II by epithelial and endothelial cells in the developing chick cornea demonstrated by in situ hybridization and immunohistochemistry. Development, 103, 27-36.

HAZAN, R. B., QIAO, R., KEREN, R., BADANO, I. & SUYAMA, K. 2004. Cadherin switch in tumor progression. Annals of the New York Academy of Sciences, 1014, 155-163.

HEMMI, H., TAKEUCHI, O., KAWAI, T., KAISHO, T., SATO, S., SANJO, H., MATSUMOTO, M., HOSHINO, K., WAGNER, H. & TAKEDA, K. 2000. A Toll-like receptor recognizes bacterial DNA. Nature, 408, 740-745.

HERTIG, A., VERINE, J., MOUGENOT, B., JOUANNEAU, C., OUALI, N., SEBE, P., GLOTZ, D., ANCEL, P. Y., RONDEAU, E. & XU-DUBOIS, Y. C. 2006. Risk factors for early epithelial to mesenchymal transition in renal grafts. American Journal of Transplantation, 6, 2937-2946.

HO, M.-Y., TANG, S.-J., CHUANG, M.-J., CHA, T.-L., LI, J.-Y., SUN, G.-H. & SUN, K.-H. 2012. TNF-α induces epithelial–mesenchymal transition of renal cell carcinoma cells via a GSK3β-dependent mechanism. Molecular Cancer Research, 10, 1109-1119.

HOFMAN, P. & VOURET-CRAVIARI, V. 2012. Microbes-induced EMT at the crossroad of inflammation and cancer. Gut Microbes, 3, 176-185.

HONJO, M., TANIHARA, H., SUZUKI, S., TANAKA, T., HONDA, Y. & TAKEICHI, M. 2000. Differential expression of cadherin adhesion receptors in neural retina of the postnatal mouse. Investigative Ophthalmology & Visual Science, 41, 546-551.

HUANG, M., WANG, Y. P., ZHU, L. Q., CAI, Q., LI, H. H. & YANG, H. F. 2015. MAPK pathway mediates epithelial-mesenchymal transition induced by paraquat in alveolar epithelial cells. Environmental Toxicology, 31, 1407-1414.

HUANG, R. Y.-J., GUILFORD, P. & THIERY, J. P. 2012. Early events in cell adhesion and polarity during epithelial-mesenchymal transition. The Company of Biologists Ltd.

HUBER, M. A., AZOITEI, N., BAUMANN, B., GRUNERT, S., SOMMER, A., PEHAMBERGER, H., KRAUT, N., BEUG, H. & WIRTH, T. 2004. NF-kappaB is essential for epithelial-mesenchymal

transition and metastasis in a model of breast cancer progression. The Journal of Clinical Investigation, 114, 569–581.

HUBER, O., BIERKAMP, C. & KEMLER, R. 1996. Cadherins and catenins in development. Current Opinion in Cell Biology, 8, 685-691.

HULPIAU, P. & VAN ROY, F. 2009. Molecular evolution of the cadherin superfamily. The International Journal of Biochemistry & Cell Biology, 41, 349-369.

IKENOUCHI, J., MATSUDA, M., FURUSE, M. & TSUKITA, S. 2003. Regulation of tight junctions during the epithelium-mesenchyme transition: direct repression of the gene expression of claudins/occludin by Snail. Journal of Cell Science, 116, 1959-1967.

INAGAKI, H., SUZUKI, T., NOMOTO, K. & YOSHIKAI, Y. 1996. Increased susceptibility to primary infection with Listeria monocytogenes in germfree mice may be due to lack of accumulation of L-selectin+ CD44+ T cells in sites of inflammation. Infection and Immunity, 64, 3280-3287.

INOUE, T., UMEZAWA, A., TAKENAKA, T., SUZUKI, H. & OKADA, H. 2015. The contribution of epithelial-mesenchymal transition to renal fibrosis differs among kidney disease models. Kidney International, 87, 233-238.

IWANO, M., PLIETH, D., DANOFF, T. M., XUE, C., OKADA, H. & NEILSON, E. G. 2002. Evidence that fibroblasts derive from epithelium during tissue fibrosis. The Journal of Clinical Investigation, 110, 341-350.

IZAWA, G., KOBAYASHI, W., HARAGUCHI, M., SUDO, A. & OZAWA, M. 2015. The ectopic expression of Snail in MDBK cells does not induce epithelial-mesenchymal transition. International Journal of Molecular Medicine, 36, 166-172.

JACOBS, M. D. & HARRISON, S. C. 1998. Structure of an IkappaB alpha/NF-kappaB complex. Cell, 95, 749-58.

JAMORA, C., LEE, P., KOCIENIEWSKI, P., AZHAR, M., HOSOKAWA, R., CHAI, Y. & FUCHS, E. 2004. A signaling pathway involving TGF-β2 and snail in hair follicle morphogenesis. PLoS Biol, 3, e11.

JANEWAY, C. A., JR. 1989. Approaching the asymptote? evolution and revolution in immunology. Cold Spring Harbor Symposia on Quantitative Biology, 54 Pt 1, 1-13.

JIANG, S.-B., HE, X.-J., XIA, Y.-J., HU, W.-J., LUO, J.-G., ZHANG, J. & TAO, H.-Q. 2016. Microrna-145-5p inhibits gastric cancer invasiveness through targeting n-cadherin and ZeB2 to suppress epithelial–mesenchymal transition. OncoTargets and therapy, 9, 2305.

JING, Y.-Y., HAN, Z.-P., SUN, K., ZHANG, S.-S., HOU, J., LIU, Y., LI, R., GAO, L., ZHAO, X., ZHAO, Q.-D., WU, M.-C. & WEI, L.-X. 2012. Toll-like receptor 4 signaling promotes epithelial-mesenchymal transition in human hepatocellular carcinoma induced by lipopolysaccharide. BMC Medicine, 10, 98.

KAIMORI, A., POTTER, J., KAIMORI, J.-Y., WANG, C., MEZEY, E. & KOTEISH, A. 2007. Transforming growth factor-β1 induces an epithelial-to-mesenchymal transition state in mouse hepatocytes in vitro. Journal of Biological Chemistry, 282, 22089-22101.

KALLURI, R. & NEILSON, E. G. 2003. Epithelial-mesenchymal transition and its implications for fibrosis. The Journal of Clinical Investigation, 112, 1776-1784.

KALLURI, R. & WEINBERG, R. A. 2009. The basics of epithelial-mesenchymal transition. The Journal of Clinical Investigation, 119, 1420-1428.

KAMIKIHARA, T., ISHIGAMI, S., ARIGAMI, T., MATSUMOTO, M., OKUMURA, H., UCHIKADO, Y., KITA, Y., KURAHARA, H., KIJIMA, Y., UENO, S. & NATSUGOE, S. 2012. Clinical implications of N-cadherin expression in gastric cancer. Pathology International, 62, 161-166.

KANTARCI, A., NSEIR, Z., KIM, Y. S., SUME, S. S. & TRACKMAN, P. C. 2011. Loss of Basement Membrane Integrity in Human Gingival Overgrowth. Journal of Dental Research, 90, 887-893.

KAPOOR, A., MALHOTRA, R., GROVER, V. & GROVER, D. 2012. Systemic antibiotic therapy in periodontics. Dental Research Journal, 9, 505-515.

KARDASSIS, D., MURPHY, C., FOTSIS, T., MOUSTAKAS, A. & STOURNARAS, C. 2009. Control of transforming growth factor β signal transduction by small GTPases. FEBS Journal, 276, 2947-2965.

KARIHTALA, P., AUVINEN, P., KAUPPILA, S., HAAPASAARI, K.-M., JUKKOLA-VUORINEN, A. & SOINI, Y. 2013. Vimentin, zeb1 and Sip1 are up-regulated in triple-negative and basal-like breast cancers: association with an aggressive tumour phenotype. Breast cancer Research and Treatment, 138, 81-90.

KARIN, M. & BEN-NERIAH, Y. 2000. Phosphorylation Meets Ubiquitination: The Control of NF-κB Activity. Annual Review of Immunology, 18, 621-663.

KATSUMOTO, T., MITSUSHIMA, A. & KURIMURA, T. 1990. The role of the vimentin intermediate filaments in rat 3Y1 cells elucidated by immunoelectron microscopy and computer-graphic reconstruction. Biology of the Cell, 68, 139-146.

KATZ, J., ONATE, M. D., PAULEY, K. M., BHATTACHARYYA, I. & CHA, S. 2011. Presence of Porphyromonas gingivalis in gingival squamous cell carcinoma. International Journal of Oral Science, 3, 209-215.

KAUFHOLD, S. & BONAVIDA, B. 2014. Central role of Snail1 in the regulation of EMT and resistance in cancer: a target for therapeutic intervention. Journal of Experimental & Clinical Cancer Research, 33, 1.

KAUR, G. & DUFOUR, J. M. 2012. Cell lines: Valuable tools or useless artifacts. Spermatogenesis, 2, 1-5.

KAWAI, T. & AKIRA, S. 2007. Signaling to NF-κB by Toll-like receptors. Trends in Molecular Medicine, 13, 460-469.

KIDD, M. E., SHUMAKER, D. K. & RIDGE, K. M. 2014. The Role of vimentin intermediate filaments in the progression of lung cancer. American Journal of Respiratory Cell and Molecular Biology, 50, 1-6.

KIKKAWA, Y., SANZEN, N., FUJIWARA, H., SONNENBERG, A. & SEKIGUCHI, K. 2000. Integrin binding specificity of laminin-10/11: laminin-10/11 are recognized by alpha 3 beta 1, alpha 6 beta 1 and alpha 6 beta 4 integrins. Journal of Cell Science, 113, 869-876.

KIM, B. J., HANCOCK, B. M., BERMUDEZ, A., CID, N. D., REYES, E., VAN SORGE, N. M., LAUTH, X., SMURTHWAITE, C. A., HILTON, B. J., STOTLAND, A., BANERJEE, A., BUCHANAN, J., WOLKOWICZ, R., TRAVER, D. & DORAN, K. S. 2015. Bacterial induction of Snail1 contributes to blood-brain barrier disruption. The Journal of Clinical Investigation, 125, 2473-2483.

KIM, K., LU, Z. & HAY, E. D. 2002. Direct evidence for a role of beta-catenin/LEF-1 signaling pathway in induction of EMT. Cell Biology International, 26, 463-76.

KIM, Y., KUGLER, M. C., WEI, Y., KIM, K. K., LI, X., BRUMWELL, A. N. & CHAPMAN, H. A. 2009. Integrin α3β1–dependent β-catenin phosphorylation links epithelial Smad signaling to cell contacts. The Journal of Cell Biology, 184, 309-322.

KIRSCHNER, N. & BRANDNER, J. M. 2012. Barriers and more: functions of tight junction proteins in the skin. Annals of the New York Academy of Sciences, 1257, 158-166.

KONDO, Y., HIGA-NAKAMINE, S., NOGUCHI, N., MAEDA, N., TOKU, S., ISOHAMA, Y., SUGAHARA, K., KUKITA, I. & YAMAMOTO, H. 2012. Induction of epithelial-mesenchymal transition by flagellin in cultured lung epithelial cells. American Journal of Physiology-Lung Cellular and Molecular Physiology, 303, L1057-L1069.

KORNMAN, K. S., PAGE, R. C. & TONETTI, M. S. 1997. The host response to the microbial challenge in periodontitis: assembling the players. Periodontology 2000, 14, 33-53.

KRISANAPRAKORNKIT, S. & IAMAROON, A. 2012. Epithelial-mesenchymal transition in oral Squamous cell carcinoma. ISRN Oncology, 2012, 10.

KRÜGER, M., HANSEN, T., KASAJ, A. & MOERGEL, M. 2013. The correlation between chronic periodontitis and oral cancer. Case Reports in Dentistry, 2013, 262410.

KUBICZKOVA, L., SEDLARIKOVA, L., HAJEK, R. & SEVCIKOVA, S. 2012. TGF-β–an excellent servant but a bad master. Journal of Translational Medicine, 10, 1.

KUBOTA, Y., KLEINMAN, H. K., MARTIN, G. R. & LAWLEY, T. J. 1988. Role of laminin and basement membrane in the morphological differentiation of human endothelial cells into capillary-like structures. The Journal of Cell Biology, 107, 1589-1598.

KURREY, N. K., JALGAONKAR, S. P., JOGLEKAR, A. V., GHANATE, A. D., CHASKAR, P. D., DOIPHODE, R. Y. & BAPAT, S. A. 2009. Snail and slug mediate radioresistance and chemoresistance by antagonizing p53-mediated apoptosis and acquiring a stem-like phenotype in ovarian cancer cells. Stem Cells, 27, 2059-2068.

KUSUMOTO, Y., HIRANO, H., SAITOH, K., YAMADA, S., TAKEDACHI, M., NOZAKI, T., OZAWA, Y., NAKAHIRA, Y., SAHO, T., OGO, H., SHIMABUKURO, Y., OKADA, H. & MURAKAMI, S. 2004. Human gingival epithelial cells produce chemotactic factors interleukin-8 and monocyte chemoattractant protein-1 after stimulation with Porphyromonas gingivalis via Toll-like receptor 2. Journal of Periodontology, 75, 370-379.

LAMOUILLE, S., CONNOLLY, E., SMYTH, J. W., AKHURST, R. J. & DERYNCK, R. 2012. TGF-β-induced activation of mTOR complex 2 drives epithelial–mesenchymal transition and cell invasion. Journal of Cell Science, 125, 1259-1273.

LAMOUILLE, S., XU, J. & DERYNCK, R. 2014. Molecular mechanisms of epithelial–mesenchymal transition. Nature reviews. Molecular Cell Biology, 15, 178-196.

LAWRENCE, D. A. 1996. Transforming growth factor-beta: a general review. European Cytokine Network, 7, 363-374.

LAX, A. J. & THOMAS, W. 2002. How bacteria could cause cancer: one step at a time. Trends in Microbiology, 10, 293-299.

LEE, S. H., HONG, H. S., LIU, Z. X., KIM, R. H., KANG, M. K., PARK, N.-H. & SHIN, K.-H. 2012. TNFα enhances cancer stem cell-like phenotype via Notch-Hes1 activation in oral squamous cell carcinoma cells. Biochemical and Biophysical Research Communications, 424, 58-64.

LEMAITRE, B., NICOLAS, E., MICHAUT, L., REICHHART, J.-M. & HOFFMANN, J. A. 1996. The Dorsoventral regulatory gene cassette spätzle/Toll/cactus controls the potent antifungal response in drosophila adults. Cell, 86, 973-983.

LEY, R. E., PETERSON, D. A. & GORDON, J. I. 2006. Ecological and evolutionary forces shaping microbial diversity in the human intestine. Cell, 124, 837-848.

LEYDON, C., IMAIZUMI, M., BARTLETT, R. S., WANG, S. F. & THIBEAULT, S. L. 2014. Epithelial cells are active participants in vocal fold wound healing: an in vivo animal model of injury. PLoS ONE, 9, e115389.

LI, C.-W., XIA, W., HUO, L., LIM, S.-O., WU, Y., HSU, J. L., CHAO, C.-H., YAMAGUCHI, H., YANG, N.-K., DING, Q., WANG, Y., LAI, Y.-J., LABAFF, A. M., WU, T.-J., LIN, B.-R., YANG, M.-H., HORTOBAGYI, G. N. & HUNG, M.-C. 2012a. Epithelial-mesenchyme transition induced by TNF-α requires NF-κB-mediated transcriptional upregulation of Twist1. Cancer Research, 72, 1290-1300.

LI, L., QI, L., LIANG, Z., SONG, W., LIU, Y., WANG, Y., SUN, B., ZHANG, B. I. N. & CAO, W. 2015. Transforming growth factor-β1 induces EMT by the transactivation of epidermal growth factor signaling through HA/CD44 in lung and breast cancer cells. International Journal of Molecular Medicine, 36, 113-122.

LI, Y., WANG, L., PAPPAN, L., GALLIHER-BECKLEY, A. & SHI, J. 2012b. IL-1β promotes stemness and invasiveness of colon cancer cells through Zeb1 activation. Molecular Cancer, 11, 87.

LI, Y., YANG, J., DAI, C., WU, C. & LIU, Y. 2003. Role for integrin-linked kinase in mediating tubular epithelial to mesenchymal transition and renal interstitial fibrogenesis. The Journal of Clinical Investigation, 112, 503-516.

LIANG, C.-C., PARK, A. Y. & GUAN, J.-L. 2007. In vitro scratch assay: a convenient and inexpensive method for analysis of cell migration in vitro. Nature Protocols, 2, 329-333.

LICKERT, H., BAUER, A., KEMLER, R. & STAPPERT, J. 2000. Casein Kinase II Phosphorylation of E-cadherin increases E-cadherin/β-Catenin interaction and strengthens cell-cell adhesion. Journal of Biological Chemistry, 275, 5090-5095.

LIEN, W.-H., KLEZOVITCH, O. & VASIOUKHIN, V. 2006. Cadherin–catenin proteins in vertebrate development. Current Opinion in Cell Biology, 18, 499-506.

LIM, M., CHUONG, C.-M. & ROY-BURMAN, P. 2011. PI3K, Erk signaling in BMP7-induced epithelial-mesenchymal transition (EMT) of PC-3 prostate cancer cells in 2- and 3-dimensional cultures. Hormones and Cancer, 2, 298.

LIN, C. Y., TSAI, P. H., KANDASWAMI, C. C., LEE, P. P., HUANG, C. J., HWANG, J. J. & LEE, M. T. 2011. Matrix metalloproteinase-9 cooperates with transcription factor Snail to induce epithelial–mesenchymal transition. Cancer Science, 102, 815-827.

LIN, S.-L., KISSELEVA, T., BRENNER, D. A. & DUFFIELD, J. S. 2008. Pericytes and perivascular fibroblasts are the primary source of collagen-producing cells in obstructive fibrosis of the kidney. The American Journal of Pathology, 173, 1617-1627.

LIOTTA, L., TRYGGVASON, K., GARBISA, S., HART, I., FOLTZ, C. & SHAFIE, S. 1980. Metastatic potential correlates with enzymatic degradation of basement membrane collagen. Nature, 284, 67-68.

LIU, D., XU, J., FIGLIOMENI, L., HUANG, L., PAVLOS, N., ROGERS, M., TAN, A., PRICE, P. & ZHENG, M. 2003. Expression of RANKL and OPG mRNA in periodontal disease: possible involvement in bone destruction. International Journal of Molecular Medicine, 11, 17-22.

LIU, P.-F., HAAKE, S. K., GALLO, R. L. & HUANG, C.-M. 2009. A novel vaccine targeting Fusobacterium nucleatum against abscesses and halitosis. Vaccine, 27, 1589-1595.

LIU, P., WAKAMIYA, M., SHEA, M. J., ALBRECHT, U., BEHRINGER, R. R. & BRADLEY, A. 1999. Requirement for Wnt3 in vertebrate axis formation. Nature Genetics, 22, 361-365.

LOCKE, D. & HARRIS, A. L. 2009. Connexin channels and phospholipids: association and modulation. BMC Biology, 7, 1.

LÓPEZ-NOVOA, J. M. & NIETO, M. A. 2009. Inflammation and EMT: an alliance towards organ fibrosis and cancer progression. EMBO Molecular Medicine, 1, 303-314.

LORENZ, K. J., KRAFT, K., GRAF, F., PRÖPPER, C. & STEINESTEL, K. 2015. Role of reflux-induced epithelial–mesenchymal transition in periprosthetic leakage after prosthetic voice rehabilitation. Head & Neck, 37, 530-536.

LOVEGROVE, J. 2003. Dental plaque revisited: bacteria associated with periodontal disease. Journal of the New Zealand Society of Periodontology, 87, 7-21.

LUO, W. & LIN, S. C. 2004. Axin: a master scaffold for multiple signaling pathways. Neurosignals, 13, 99-113.

MACDONALD, B. T., TAMAI, K. & HE, X. 2009. Wnt/β-catenin signaling: components, mechanisms, and diseases. Developmental Cell, 17, 9-26.

MACHADO, J. C., SOARES, P., CARNEIRO, F., ROCHA, A., BECK, S., BLIN, N., BERX, G. & SOBRINHO-SIMOES, M. 1999. E-cadherin gene mutations provide a genetic basis for the phenotypic divergence of mixed gastric carcinomas. Laboratory Investigation, 79, 459-65.

MAGER, D. L., HAFFAJEE, A. D., DEVLIN, P. M., NORRIS, C. M., POSNER, M. R. & GOODSON, J. M. 2005. The salivary microbiota as a diagnostic indicator of oral cancer: A descriptive, non-randomized study of cancer-free and oral squamous cell carcinoma subjects. Journal of Translational Medicine, 3, 27-27.

MAGNUSSON, I., MARKS, R. G., CLARK, W. B., WALKER, C. B., LOW, S. B. & MCARTHUR, W. P. 1991. Clinical, microbiological and immunological characteristics of subjects with “refractory” periodontal disease. Journal of Clinical Periodontology, 18, 291-299.

MAGNUSSON, I. & WALKER, C. B. 1996. Refractory periodontitis or recurrence of disease. Journal of Clinical Periodontology, 23, 289-292.

MAHLA, R. S., REDDY, M. C., PRASAD, D. V. R. & KUMAR, H. 2013. Sweeten PAMPs: role of sugar complexed PAMPs in innate immunity and vaccine biology. Frontiers in Immunology, 4, 248.

MAIER, H. J., SCHMIDT-STRABBURGER, U., HUBER, M. A., WIEDEMANN, E. M., BEUG, H. & WIRTH, T. 2010. NF-κB promotes epithelial–mesenchymal transition, migration and invasion of pancreatic carcinoma cells. Cancer Letters, 295, 214-228.

MAO, S., PARK, Y., HASEGAWA, Y., TRIBBLE, G. D., JAMES, C. E., HANDFIELD, M., STAVROPOULOS, M. F., YILMAZ, Ö. & LAMONT, R. J. 2007. Intrinsic apoptotic pathways of gingival epithelial cells modulated by Porphyromonas gingivalis. Cellular Microbiology, 9, 1997-2007.

MARCHIANDO, A. M., GRAHAM, W. V. & TURNER, J. R. 2010. Epithelial barriers in homeostasis and disease. Annual Review of Pathological Mechanical Disease, 5, 119-144.

MARSH, P. P. D., MARTIN, M. V., LEWIS, M. A. O., WILLIAMS, D. W. 2009. Oral microbiology, London, Churchill Livingstone.

MARTIN, J. A., PAGE, R. C., LOEB, C. F. & LEVI, P. A., JR. 2010. Tooth loss in 776 treated periodontal patients. Journal of Periodontology, 81, 244-50.

MARTíNEZ-ÁLVAREZ, C., BLANCO, M. A. J., PÉREZ, R., RABADÁN, M. A., APARICIO, M., RESEL, E., MARTíNEZ, T. & NIETO, M. A. 2004. Snail family members and cell survival in physiological and pathological cleft palates. Developmental Biology, 265, 207-218.

MASCHLER, S., WIRL, G., SPRING, H., BREDOW, D. V., SORDAT, I., BEUG, H. & REICHMANN, E. 2005. Tumor cell invasiveness correlates with changes in integrin expression and localization. Oncogene, 24, 2032-41.

MASSAGUÉ, J. 2008. TGF [beta] in cancer. Cell, 134.

MASSZI, A., FAN, L., ROSIVALL, L., MCCULLOCH, C. A., ROTSTEIN, O. D., MUCSI, I. & KAPUS, A. 2004. Integrity of cell-cell contacts is a critical regulator of TGF-β1-induced epithelial-to-myofibroblast transition: role for β-Catenin. The American Journal of Pathology, 165, 1955-1967.

MATTHEWS, D. C., SMITH, C. G. & HANSCOM, S. L. 2001. Tooth loss in periodontal patients. Journal-Canadian Dental Association, 67, 207-210.

MEALEY, B. L. & OATES, T. W. 2006. Diabetes mellitus and periodontal diseases. Journal of Periodontology, 77, 1289-1303.

MEDICI, D., HAY, E. D. & OLSEN, B. R. 2008. Snail and Slug promote epithelial-mesenchymal transition through β-catenin–T-cell factor-4-dependent expression of transforming growth factor-β3. Molecular Biology of the Cell, 19, 4875-4887.

MEDVEDEV, A. E., SABROE, I., HASDAY, J. D. & VOGEL, S. N. 2006. Invited review: Tolerance to microbial TLR ligands: molecular mechanisms and relevance to disease. Journal of Endotoxin Research, 12, 133-150.

MENDEZ, M. G., KOJIMA, S.-I. & GOLDMAN, R. D. 2010. Vimentin induces changes in cell shape, motility, and adhesion during the epithelial to mesenchymal transition. The FASEB Journal, 24, 1838-1851.

MERLO, E., FREUDENTHAL, R. & ROMANO, A. 2002. The IkappaB kinase inhibitor sulfasalazine impairs long-term memory in the crab Chasmagnathus. Neuroscience, 112, 161-72.

MIKAWA, T., POH, A. M., KELLY, K. A., ISHII, Y. & REESE, D. E. 2004. Induction and patterning of the primitive streak, an organizing center of gastrulation in the amniote. Developmental Dynamics, 229, 422-432.

MILWARD, M. R., CHAPPLE, I. L. C., WRIGHT, H. J., MILLARD, J. L., MATTHEWS, J. B. & COOPER, P. R. 2007. Differential activation of NF-κB and gene expression in oral epithelial cells by periodontal pathogens. Clinical and Experimental Immunology, 148, 307-324.

MINAFRA, L., BRAVATÀ, V., FORTE, G. I., CAMMARATA, F. P., GILARDI, M. C. & MESSA, C. 2014. Gene expression profiling of epithelial–mesenchymal transition in primary breast cancer cell culture. Anticancer Research, 34, 2173-2183.

MISRA, A., PANDEY, C., SZE, S. K. & THANABALU, T. 2012. Hypoxia activated EGFR signaling induces epithelial to mesenchymal transition (EMT). PLoS ONE, 7, e49766.

MIYAZAKI, K. 2006. Laminin-5 (laminin-332): unique biological activity and role in tumor growth and invasion. Cancer Science, 97, 91-98.

MIYAZONO, K. 2009. Transforming growth factor-β signaling in epithelial-mesenchymal transition and progression of cancer. Proceedings of the Japan Academy. Series B, Physical and Biological Sciences, 85, 314-323.

MIZE, T., SUNDARARAJ, K., LEITE, R. & HUANG, Y. 2015. Increased and correlated expression of connective tissue growth factor and transforming growth factor beta 1 in surgically removed periodontal tissues with chronic periodontitis. Journal of Periodontal Research, 50, 315-319.

MIZUMOTO, A., YAMAMOTO, K., NAKAYAMA, Y., TAKARA, K., NAKAGAWA, T., HIRANO, T. & HIRAI, M. 2015. Induction of epithelial-mesenchymal transition via activation of epidermal growth factor receptor contributes to Sunitinib resistance in human renal cell carcinoma cell lines. Journal of Pharmacology and Experimental Therapeutics, 355, 152-158.

MOLL, R., DIVO, M. & LANGBEIN, L. 2008. The human keratins: biology and pathology. Histochemistry and Cell Biology, 129, 705-733.

MOORE, W. & MOORE, L. V. 1994. The bacteria of periodontal diseases. Periodontology 2000, 5, 66-77.

MORI, Y., YOSHIMURA, A., UKAI, T., LIEN, E., ESPEVIK, T. & HARA, Y. 2003. Immunohistochemical localization of Toll-like receptors 2 and 4 in gingival tissue from patients with periodontitis. Oral Microbiology and Immunology, 18, 54-58.

MULHOLLAND, D. J., KOBAYASHI, N., RUSCETTI, M., ZHI, A., TRAN, L. M., HUANG, J., GLEAVE, M. & WU, H. 2012. Pten loss and RAS/MAPK activation cooperate to promote EMT and metastasis initiated from prostate cancer stem/progenitor cells. Cancer Research, 72, 1878-1889.

MURATA-KAMIYA, N., KURASHIMA, Y., TEISHIKATA, Y., YAMAHASHI, Y., SAITO, Y., HIGASHI, H., ABURATANI, H., AKIYAMA, T., PEEK, R. M., JR., AZUMA, T. & HATAKEYAMA, M. 2007. Helicobacter pylori CagA interacts with E-cadherin and deregulates the [beta]-catenin signal that promotes intestinal transdifferentiation in gastric epithelial cells. Oncogene, 26, 4617-4626.

MURRAY, C. J. & LOPEZ, A. D. 1997. Alternative projections of mortality and disability by cause 1990-2020: Global Burden of Disease Study. Lancet, 349, 1498-504.

NAGAI, T., ARAO, T., FURUTA, K., SAKAI, K., KUDO, K., KANEDA, H., TAMURA, D., AOMATSU, K., KIMURA, H. & FUJITA, Y. 2011. Sorafenib inhibits the hepatocyte growth factor–mediated epithelial mesenchymal transition in hepatocellular carcinoma. Molecular Cancer Therapeutics, 10, 169-177.

NAGARAKANTI, S., RAMYA, S., BABU, P., ARUN, K. V. & SUDARSAN, S. 2007. Differential expression of E-Cadherin and Cytokeratin 19 and net proliferative rate of gingival keratinocytes in oral epithelium in periodontal health and disease. Journal of Periodontology, 78, 2197-2202.

NAKAJIMA, S., DOI, R., TOYODA, E., TSUJI, S., WADA, M., KOIZUMI, M., TULACHAN, S. S., ITO, D., KAMI, K., MORI, T., KAWAGUCHI, Y., FUJIMOTO, K., HOSOTANI, R. & IMAMURA, M. 2004. N-Cadherin expression and epithelial-mesenchymal transition in pancreatic carcinoma. Clinical Cancer Research, 10, 4125-4133.

NAKHJIRI, S. F., PARK, Y., YILMAZ, O., CHUNG, W. O., WATANABE, K., EL-SABAENY, A., PARK, K. & LAMONT, R. J. 2001. Inhibition of epithelial cell apoptosis by Porphyromonas gingivalis. FEMS Microbiology Letters, 200, 145-149.

NARAYAN, T. V., REVANNA, G. M., HALLIKERI, U. & KURIAKOSE, M. A. 2014. Dental caries and periodontal disease status in patients with oral squamous cell carcinoma: a screening study in urban and semiurban population of Karnataka. Journal of Maxillofacial & Oral Surgery, 13, 435-443.

NAWSHAD, A., MEDICI, D., LIU, C.-C. & HAY, E. D. 2007. TGFβ3 inhibits E-cadherin gene expression in palate medial-edge epithelial cells through a Smad2-Smad4-LEF1 transcription complex. Journal of Cell Science, 120, 1646-1653.

NELSON, D. E., IHEKWABA, A. E. C., ELLIOTT, M., JOHNSON, J. R., GIBNEY, C. A., FOREMAN, B. E., NELSON, G., SEE, V., HORTON, C. A., SPILLER, D. G., EDWARDS, S. W., MCDOWELL, H. P., UNITT, J. F., SULLIVAN, E., GRIMLEY, R., BENSON, N., BROOMHEAD, D., KELL, D. B. & WHITE, M. R. H. 2004. Oscillations in NF-κB signaling control the dynamics of gene expression. Science, 306, 704-708.

NEMOTO, E., DARVEAU, R. P., FOSTER, B. L., NOGUEIRA-FILHO, G. R. & SOMERMAN, M. J. 2006. Regulation of cementoblast function by P. gingivalis lipopolysaccharide via TLR2. Journal of Dental Research, 85, 733-738.

NITTA, T., KIM, J.-S., MOHUCZY, D. & BEHRNS, K. E. 2008. Murine cirrhosis induces hepatocyte epithelial mesenchymal transition and alterations in survival signaling pathways. Hepatology (Baltimore, Md.), 48, 909-919.

NOACH, L. A., BOSMA, N. B., JANSEN, J., HOEK, F. J., VAN DEVENTER, S. J. & TYTGAT, G. N. 1994. Mucosal tumor necrosis factor-alpha, interleukin-1 beta, and interleukin-8 production in patients with Helicobacter pylori infection. Scandinavian Journal of Gastroenterology, 29, 425-429.

NOIRI, Y., OZAKI, K., NAKAE, H., MATSUO, T. & EBISU, S. 1997. An immunohistochemical study on the localization of Porphyromonas gingivalis, Campylobacter rectus and Actinomyces viscosus in human periodontal pockets. Journal of Periodontal Research, 32, 598-607.

O'CONNELL, P. A. A., TABA, M., NOMIZO, A., FOSS FREITAS, M. C., SUAID, F. A., UYEMURA, S. A., TREVISAN, G. L., NOVAES, A. B., SOUZA, S. L. S., PALIOTO, D. B. & GRISI, M. F. M. 2008. Effects of periodontal therapy on glycemic control and inflammatory markers. Journal of Periodontology, 79, 774-783.

OFFENBACHER, S. 1996. Periodontal diseases: pathogenesis. Annals of Periodontology, 1, 821-878.

OJI, C. & CHUKWUNEKE, F. 2012. Poor oral hygiene may be the sole cause of oral cancer. Journal of Maxillofacial & Oral Surgery, 11, 379-383.

OKADA, H., DANOFF, T. M., KALLURI, R. & NEILSON, E. G. 1997. Early role of Fsp1 in epithelial-mesenchymal transformation. American Journal of Physiology - Renal Physiology, 273, F563-F574.

OMENETTI, A., PORRELLO, A., JUNG, Y., YANG, L., POPOV, Y., CHOI, S. S., WITEK, R. P., ALPINI, G., VENTER, J. & VANDONGEN, H. M. 2008. Hedgehog signaling regulates epithelial-mesenchymal transition during biliary fibrosis in rodents and humans. The Journal of Clinical Investigation, 118, 3331-3342.

ONDER, T. T., GUPTA, P. B., MANI, S. A., YANG, J., LANDER, E. S. & WEINBERG, R. A. 2008. Loss of E-Cadherin promotes metastasis via multiple downstream transcriptional pathways. Cancer Research, 68, 3645-3654.

OVERDUIN, M., HARVEY, T. S., BAGBY, S. & TONG, K. I. 1995. Solution structure of the epithelial cadherin domain responsible for selective cell adhesion. Science, 267, 386.

PACCIONE, R. J., MIYAZAKI, H., PATEL, V., WASEEM, A., GUTKIND, J. S., ZEHNER, Z. E. & YEUDALL, W. A. 2008. Keratin down-regulation in vimentin-positive cancer cells is reversible by vimentin RNA interference, which inhibits growth and motility. American Association for Cancer Research, 7, 2894-2903.

PAGE, R. C. & KORNMAN, K. S. 1997. The pathogenesis of human periodontitis: an introduction. Periodontology 2000, 14, 9-11.

PALENA, C., HAMILTON, D. H. & FERNANDO, R. I. 2012. Influence of IL-8 on the epithelial–mesenchymal transition and the tumor microenvironment. Future oncology (London, England), 8, 713-722.

PANDIT, N. K. 2007. Introduction to the pharmaceutical sciences, Lippincott Williams & Wilkins.

PANKOV, R. & YAMADA, K. M. 2002. Fibronectin at a glance. Journal of Cell Science, 115, 3861-3863.

PAOLI, P., GIANNONI, E. & CHIARUGI, P. 2013. Anoikis molecular pathways and its role in cancer progression. Biochimica et Biophysica Acta (BBA)-Molecular Cell Research, 1833, 3481-3498.

PARASKEVAS, S., HUIZINGA, J. D. & LOOS, B. G. 2008. A systematic review and meta-analyses on C-reactive protein in relation to periodontitis. Journal of Clinical Periodontology, 35, 277-290.

PASTER, B. J., BOCHES, S. K., GALVIN, J. L., ERICSON, R. E., LAU, C. N., LEVANOS, V. A., SAHASRABUDHE, A. & DEWHIRST, F. E. 2001. bacterial diversity in human subgingival plaque. Journal of Bacteriology, 183, 3770-3783.

PATTAMAPUN, K., TIRANATHANAGUL, S., YONGCHAITRAKUL, T., KUWATANASUCHAT, J. & PAVASANT, P. 2003. Activation of MMP-2 by Porphyromonas gingivalis in human periodontal ligament cells. Journal of Periodontal Research, 38, 115-121.

PAULSSON, M. 2008. Basement membrane proteins: structure, assembly, and cellular interactions. Critical Reviews in Biochemistry and Molecular Biology, 27, 93-127.

PEINADO, H., BALLESTAR, E., ESTELLER, M. & CANO, A. 2004. Snail mediates E-Cadherin repression by the recruitment of the Sin3A/Histone Deacetylase 1 (HDAC1)/HDAC2 complex. Molecular and Cellular Biology, 24, 306-319.

PEINADO, H., OLMEDA, D. & CANO, A. 2007. Snail, Zeb and bHLH factors in tumour progression: an alliance against the epithelial phenotype? Nature Reviews Cancer, 7, 415-428.

PHILIP, S., BULBULE, A. & KUNDU, G. C. 2004. Matrix metalloproteinase-2: mechanism and regulation of NF-kappaB-mediated activation and its role in cell motility and ECM-invasion. Glycoconjugate Journal, 21, 429-441.

PICARD, N., BAUM, O., VOGETSEDER, A., KAISSLING, B. & LE HIR, M. 2008. Origin of renal myofibroblasts in the model of unilateral ureter obstruction in the rat. Histochemistry and Cell Biology, 130, 141-155.

PICKUP, M., NOVITSKIY, S. & MOSES, H. L. 2013. The roles of TGF [beta] in the tumour microenvironment. Nature Reviews Cancer, 13, 788-799.

PIERGA, J. Y., BONNETON, C., MAGDELÉNAT, H., VINCENT-SALOMON, A., NOS, C., POUILLART, P. & THIERY, J. P. 2003. Clinical significance of proliferative potential of occult metastatic cells in bone marrow of patients with breast cancer. British Journal of Cancer, 89, 539-545.

PISOSCHI, C., STANCIULESCU, C., MUNTEANU, C., FUSARU, A. M. & BANITA, M. 2012. Evidence for the epithelial-mesenchymal transition as a pathogenic mechanism of phenytoin-induced gingival overgrowth. Farmacia, 60, 168-176.

POHLERS, D., BRENMOEHL, J., LÖFFLER, I., MÜLLER, C. K., LEIPNER, C., SCHULTZE-MOSGAU, S., STALLMACH, A., KINNE, R. W. & WOLF, G. 2009. TGF-β and fibrosis in different organs—molecular pathway imprints. Biochimica et Biophysica Acta (BBA)-Molecular Basis of Disease, 1792, 746-756.

POLETTE, M., MESTDAGT, M., BINDELS, S., NAWROCKI-RABY, B., HUNZIKER, W., FOIDART, J.-M., BIREMBAUT, P. & GILLES, C. 2007. β-catenin and ZO-1: shuttle molecules involved in tumor invasion-associated epithelial-mesenchymal transition processes. Cells Tissues Organs, 185, 61-65.

PÖLLÄNEN, M. T., GURSOY, U. K., KÖNÖNEN, E. & UITTO, V.-J. 2012. Fusobacterium nucleatum biofilm induces epithelial migration in an organotypic model of dento-gingival junction. Journal of Periodontology, 83, 1329-1335.

POLTORAK, A., HE, X., SMIRNOVA, I., LIU, M. Y., VAN HUFFEL, C., DU, X., BIRDWELL, D., ALEJOS, E., SILVA, M., GALANOS, C., FREUDENBERG, M., RICCIARDI-CASTAGNOLI, P., LAYTON, B. & BEUTLER, B. 1998. Defective LPS signaling in C3H/HeJ and C57BL/10ScCr mice: mutations in Tlr4 gene. Science, 282, 2085-8.

POPPERL, H., SCHMIDT, C., WILSON, V., HUME, C. R., DODD, J., KRUMLAUF, R. & BEDDINGTON, R. S. 1997. Misexpression of Cwnt8C in the mouse induces an ectopic embryonic axis and causes a truncation of the anterior neuroectoderm. Development, 124, 2997-3005.

PRAKASAM, A., ELAVARASU, S. S. & NATARAJAN, R. K. 2012. Antibiotics in the management of aggressive periodontitis. Journal of Pharmacy & Bioallied Sciences, 4, S252-S255.

PRESHAW, P. M., ALBA, A. L., HERRERA, D., JEPSEN, S., KONSTANTINIDIS, A., MAKRILAKIS, K. & TAYLOR, R. 2012. Periodontitis and diabetes: a two-way relationship. Diabetologia, 55, 21-31.

PRICE, S. R., GARCIA, N. V. D. M., RANSCHT, B. & JESSELL, T. M. 2002. Regulation of motor neuron pool sorting by differential expression of type II cadherins. Cell, 109, 205-216.

PRIME, S. S., NIXON, S. V. R., CRANE, I. J., STONE, A., MATTHEWS, J. B., MAITLAND, N. J., REMNANT, L., POWELL, S. K., GAME, S. M. & SCULLY, C. 1990. The behaviour of human oral squamous cell carcinoma in cell culture. The Journal of Pathology, 160, 259-269.

PULENDRAN, B., KUMAR, P., CUTLER, C. W., MOHAMADZADEH, M., VAN DYKE, T. & BANCHEREAU, J. 2001. Lipopolysaccharides from distinct pathogens induce different classes of immune responses in vivo. Journal of Immunology, 167, 5067-5076.

QUELLHORST, G., PRABHAKAR, S., HAN, Y. & YANG, J. 2006. PCR Array: A simple and quantitative method for gene expression profiling. Frederick, MD: SuperArray Bioscience Corp.

RADISKY, D. C. 2005. Epithelial-mesenchymal transition. Journal of Cell Science, 118, 4325-4326.

RASBAND, W. 2016. ImageJ [Online]. Bethesda, Maryland, USA: U. S. National Institutes of Health. Available: http://imagej.nih.gov/ij/ [Accessed 2016].

RASTALDI, M. P., FERRARIO, F., GIARDINO, L., DELL'ANTONIO, G., GRILLO, C., GRILLO, P., STRUTZ, F., MULLER, G. A., COLASANTI, G. & D'AMICO, G. 2002. Epithelial-mesenchymal transition of tubular epithelial cells in human renal biopsies. Kidney International, 62, 137-46.

RAVANTI, L., HÄKKINEN, L., LARJAVA, H., SAARIALHO-KERE, U., FOSCHI, M., HAN, J. & KÄHÄRI, V.-M. 1999. Transforming growth factor-β induces collagenase-3 expression by human gingival fibroblasts via p38 mitogen-activated protein kinase. Journal of Biological Chemistry, 274, 37292-37300.

REIFE, R. A., SHAPIRO, R. A., BAMBER, B. A., BERRY, K. K., MICK, G. E. & DARVEAU, R. P. 1995. Porphyromonas gingivalis lipopolysaccharide is poorly recognized by molecular components of innate host defense in a mouse model of early inflammation. Infection and Immunity, 63, 4686-4694.

REN, L., LEUNG, W. K., DARVEAU, R. P. & JIN, L. 2005. The expression profile of lipopolysaccharide-binding protein, membrane-bound CD14, and Toll-like receptors 2 and 4 in chronic periodontitis. Journal of Periodontology, 76, 1950-1959.

REZAEI, M., ZARKESH-ESFAHANI, S. H. & GHARAGOZLOO, M. 2013. The effect of different media composition and temperatures on the production of recombinant human growth hormone by CHO cells. Research in Pharmaceutical Sciences, 8, 211-217.

RHEE, J. W., LEE, K. W., KIM, D., LEE, Y., JEON, O. H., KWON, H. J. & KIM, D. S. 2007. NF-kappaB-dependent regulation of matrix metalloproteinase-9 gene expression by lipopolysaccharide in a macrophage cell line RAW 264.7. Journal of Biochemistry and Molecular Biology, 40, 88-94.

RHEINWALD, J. G. & GREEN, H. 1975. Serial cultivation of strains of human epidermal keratinocytes: the formation of keratinizing colonies from single cells. Cell, 6, 331-343.

RIDLEY, A. J. 2011. Life at the leading edge. Cell, 145, 1012-1022.

RIETSCHEL, E. T., KIRIKAE, T., SCHADE, F. U., MAMAT, U., SCHMIDT, G., LOPPNOW, H., ULMER, A. J., ZÄHRINGER, U., SEYDEL, U. & DI PADOVA, F. 1994. Bacterial endotoxin: molecular relationships of structure to activity and function. The FASEB Journal, 8, 217-225.

ROCKEY, D. C., BELL, P. D. & HILL, J. A. 2015. Fibrosis—a common pathway to organ injury and failure. New England Journal of Medicine, 372, 1138-1149.

RODRIGUEZ, E. N., PEREZ, M., CASANOVA, P. & MARTINEZ, L. 2001. Effect of Seed Cell Density on Specific Growth Rate Using CHO Cells as Model. In: LINDNER-OLSSON, E., CHATZISSAVIDOU, N. & LÜLLAU, E. (eds.) Animal Cell Technology: From Target to Market: Proceedings of the 17th ESACT Meeting Tylösand, Sweden, June 10–14, 2001. Dordrecht: Springer Netherlands.

ROMANO, L. A. & RUNYAN, R. B. 2000. Slug is an essential target of TGFβ2 signaling in the developing chicken heart. Developmental Biology, 223, 91-102.

ROSENQUIST, K., WENNERBERG, J., SCHILDT, E.-B., BLADSTRÖM, A., GÖRAN HANSSON, B. & ANDERSSON, G. 2005. Oral status, oral infections and some lifestyle factors as risk factors for oral and oropharyngeal squamous cell carcinoma. A population-based case-control study in southern Sweden. Acta Oto-Laryngologica, 125, 1327-1336.

ROSIVATZ, E., BECKER, I., SPECHT, K., FRICKE, E., LUBER, B., BUSCH, R., HÖFLER, H. & BECKER, K.-F. 2002. Differential expression of the epithelial-mesenchymal transition regulators Snail, SIP1, and Twist in gastric cancer. The American Journal of Pathology, 161, 1881-1891.

ROSS, M. H. & PAWLINA, W. 2006. Histology: a text and atlas: with correlated cell and molecular biology 5th ed. Baltimore, MD: Lippincott Wiliams & Wilkins.

ROSSINI, M., CHEUNSUCHON, B., DONNERT, E., MA, L. J., THOMAS, J. W., NEILSON, E. G. & FOGO, A. B. 2005. Immunolocalization of fibroblast growth factor-1 (FGF-1), its receptor (FGFR-1), and fibroblast-specific protein-1 (FSP-1) in inflammatory renal disease. Kidney International, 68, 2621-2628.

ROUND, J. L. & MAZMANIAN, S. K. 2009. The gut microbiome shapes intestinal immune responses during health and disease. Nature reviews. Immunology, 9, 313-323.

RYGIEL, K. A., ROBERTSON, H., MARSHALL, H. L., PEKALSKI, M., ZHAO, L., BOOTH, T. A., JONES, D. E., BURT, A. D. & KIRBY, J. A. 2008. Epithelial–mesenchymal transition contributes to portal tract fibrogenesis during human chronic liver disease. Laboratory investigation, 88, 112-123.

SALINAS, M., ROSAS, J., IBORRA, J., MANERO, H. & PASCUAL, E. 1997. Comparison of manual and automated cell counts in EDTA preserved synovial fluids. Storage has little influence on the results. Annals of the Rheumatic Diseases, 56, 622-626.

SANTIBAÑEZ, JUAN F., QUINTANILLA, M. & BERNABEU, C. 2011. TGF-β/TGF-β receptor system and its role in physiological and pathological conditions. Clinical Science, 121, 233-251.

SAVAGNER, P. 2010. The epithelial–mesenchymal transition (EMT) phenomenon. Annals of Oncology, 21, vii89-vii92.

SAVAGNER, P., YAMADA, K. M. & THIERY, J. P. 1997. The zinc-finger protein slug causes desmosome dissociation, an initial and necessary step for growth factor–induced epithelial–mesenchymal transition. The Journal of Cell Biology, 137, 1403-1419.

SBORDONE, L., RAMAGLIA, L., GULLETTA, E. & IACONO, V. 1990. Recolonization of the subgingival microflora after scaling and root planing in human periodontitis. Journal of Periodontology, 61, 579-584.

SCANLON, C. S., VAN TUBERGEN, E. A., INGLEHART, R. C. & D'SILVA, N. J. 2013. Biomarkers of epithelial-mesenchymal transition in squamous cell carcinoma. Journal of Dental Research, 92, 114-121.

SCHAEFFER, D., SOMARELLI, J. A., HANNA, G., PALMER, G. M. & GARCIA-BLANCO, M. A. 2014. Cellular migration and invasion uncoupled: increased migration is not an inexorable consequence of epithelial-to-mesenchymal transition. Molecular and Cellular Biology, 34, 3486-3499.

SCHARL, M., HUBER, N., LANG, S., FÜRST, A., JEHLE, E. & ROGLER, G. 2015. Hallmarks of epithelial to mesenchymal transition are detectable in Crohn's disease associated intestinal fibrosis. Clinical and Translational Medicine, 4, 1.

SCHAUER, D. B., ZABEL, B. A., PEDRAZA, I. F., O'HARA, C. M., STEIGERWALT, A. G. & BRENNER, D. J. 1995. Genetic and biochemical characterization of Citrobacter rodentium sp. nov. Journal of Clinical Microbiology, 33, 2064-2068.

SCHLANGE, T., MATSUDA, Y., LIENHARD, S., HUBER, A. & HYNES, N. E. 2007. Autocrine WNT signaling contributes to breast cancer cell proliferation via the canonical WNT pathway and EGFR transactivation. Breast Cancer Research: BCR, 9, R63-R63.

SCHOLTEN, D., ÖSTERREICHER, C. H., SCHOLTEN, A., IWAISAKO, K., GU, G., BRENNER, D. A. & KISSELEVA, T. 2010. Genetic labeling does not detect epithelial-to-mesenchymal transition (EMT) of cholangiocytes in liver fibrosis in mice. Gastroenterology, 139, 987-998.

SCHOUMACHER, M., GOLDMAN, R. D., LOUVARD, D. & VIGNJEVIC, D. M. 2010. Actin, microtubules, and vimentin intermediate filaments cooperate for elongation of invadopodia. The Journal of Cell Biology, 189, 541-556.

SCHRÖDER, N. W. J., MORATH, S., ALEXANDER, C., HAMANN, L., HARTUNG, T., ZÄHRINGER, U., GÖBEL, U. B., WEBER, J. R. & SCHUMANN, R. R. 2003. Lipoteichoic acid (LTA) of Streptococcus pneumoniaeand Staphylococcus aureus activates immune cells via Toll-like receptor (TLR)-2, Lipopolysaccharide-binding protein (LBP), and CD14, whereas TLR-4 and MD-2 are not Involved. Journal of Biological Chemistry, 278, 15587-15594.

SCHROEDER, H. & PAGE, R. 1972. Lymphocyte-fibroblast interaction in the pathogenesis of inflammatory gingival disease. Experientia, 28, 1228-1230.

SERRANO, M. J., ORTEGA, F. G., ALVAREZ-CUBERO, M. J., NADAL, R., SANCHEZ-ROVIRA, P., SALIDO, M., RODRÍGUEZ, M., GARCÍA-PUCHE, J. L., DELGADO-RODRIGUEZ, M. & SOLÉ, F. 2014. EMT and EGFR in CTCs cytokeratin negative non-metastatic breast cancer. Oncotarget, 5, 7486–7497.

SHAH, P. P., FONG, M. Y. & KAKAR, S. S. 2012. PTTG induces EMT through integrin αVβ3-focal adhesion kinase signaling in lung cancer cells. Oncogene, 31, 3124-3135.

SHAPIRO, L., FANNON, A. M., KWONG, P. D., THOMPSON, A., LEHMANN, M. S., GRÜBEL, G., LEGRAND, J.-F., ALS-NIELSEN, J., COLMAN, D. R. & HENDRICKSON, W. A. 1995. Structural basis of cell-cell adhesion by cadherins. Nature, 374, 327-337.

SHAPIRO, L. & WEIS, W. I. 2009. Structure and biochemistry of cadherins and catenins. Cold Spring Harbor perspectives in biology, 1, a003053.

SHARIFI, A. M., HODA, F. E. & NOOR, A. M. 2010. Studying the effect of LPS on cytotoxicity and apoptosis in PC12 neuronal cells: role of Bax, Bcl-2, and Caspase-3 protein expression. Toxicology Mechanisms and Methods, 20, 316-320.

SHEETS, S. M., POTEMPA, J., TRAVIS, J., CASIANO, C. A. & FLETCHER, H. M. 2005. Gingipains from Porphyromonas gingivalis W83 induce cell adhesion molecule cleavage and apoptosis in endothelial cells. Infection and Immunity, 73, 1543-1552.

SHERMAN, V. R., YANG, W. & MEYERS, M. A. 2015. The materials science of collagen. Journal of the Mechanical Behavior of Biomedical Materials, 52, 22-50.

SHI, Y. & MASSAGUÉ, J. 2003. Mechanisms of TGF-β signaling from cell membrane to the nucleus. Cell, 113, 685-700.

SHINTANI, Y., MAEDA, M., CHAIKA, N., JOHNSON, K. R. & WHEELOCK, M. J. 2008. Collagen I promote epithelial-to-mesenchymal transition in lung cancer cells via transforming growth factor–β signaling. American Journal of Respiratory Cell and Molecular Biology, 38, 95-104.

SHIRAKIHARA, T., SAITOH, M. & MIYAZONO, K. 2007. Differential regulation of epithelial and mesenchymal markers by δEF1 proteins in epithelial–mesenchymal transition induced by TGF-β. Molecular Biology of the Cell, 18, 3533-3544.

SILETZ, A., SCHNABEL, M., KNIAZEVA, E., SCHUMACHER, A. J., SHIN, S., JERUSS, J. S. & SHEA, L. D. 2013. Dynamic transcription factor networks in epithelial-mesenchymal transition in breast cancer models. PloS ONE, 8, e57180.

SILVA, N., ABUSLEME, L., BRAVO, D., DUTZAN, N., GARCIA-SESNICH, J., VERNAL, R., HERNÁNDEZ, M. & GAMONAL, J. 2015. Host response mechanisms in periodontal diseases. Journal of Applied Oral Science, 23, 329-355.

SIMONSON, M. S. 2007. Phenotypic transitions and fibrosis in diabetic nephropathy. Kidney International, 71, 846-854.

SIMPSON, D. M. & AVERY, B. E. 1974. Histopathologic and ultrastructural features of inflamed gingiva in the baboon. Journal of Periodontology, 45, 500-510.

SINGH, A. & SETTLEMAN, J. 2010. EMT, cancer stem cells and drug resistance: an emerging axis of evil in the war on cancer. Oncogene, 29, 4741-4751.

SKROMNE, I. & STERN, C. D. 2001. Interactions between Wnt and Vg1 signalling pathways initiate primitive streak formation in the chick embryo. Development, 128, 2915-2927.

SKROMNE, I. & STERN, C. D. 2002. A hierarchy of gene expression accompanying induction of the primitive streak by Vg1 in the chick embryo. Mechanisms of Development, 114, 115-118.

SLOTS, J. & RAMS, T. E. 1990. Antibiotics in periodontal therapy: advantages and disadvantages. Journal of Clinical Periodontology, 17, 479-493.

SMIT, M. A., GEIGER, T. R., SONG, J.-Y., GITELMAN, I. & PEEPER, D. S. 2009. A Twist-Snail axis critical for TrkB-induced epithelial-mesenchymal transition-like transformation, anoikis resistance, and metastasis. Molecular and Cellular Biology, 29, 3722-3737.

SOBRAL, L. M., KELLERMANN, M. G., GRANER, E., MARTELLI-JUNIOR, H. & COLETTA, R. D. 2010. Cyclosporin induced gingival overgrowth is not associated with myofibroblast transdifferentiation. Brazilian Oral Research, 24, 182-188.

SOCRANSKY, S. S., HAFFAJEE, A. D., CUGINI, M. A., SMITH, C. & KENT, R. L., JR. 1998. Microbial complexes in subgingival plaque. Journal of Clinical Periodontology, 25, 134-44.

SONG, W., JACKSON, K. & MCGUIRE, P. G. 2000. Degradation of type IV collagen by matrix metalloproteinases is an important step in the epithelial-mesenchymal transformation of the endocardial cushions. Developmental Biology, 227, 606-617.

STEINESTEL, K., BRÜDERLEIN, S., LENNERZ, J. K., STEINESTEL, J., KRAFT, K., PRÖPPER, C., MEINEKE, V. & MÖLLER, P. 2014. Expression and Y435-phosphorylation of Abelson interactor 1 (Abi1) promotes tumour cell adhesion, extracellular matrix degradation and invasion by colorectal carcinoma cells. Molecular Cancer, 13, 145-145.

STOKER, M. & PERRYMAN, M. 1985. An epithelial scatter factor released by embryo fibroblasts. Journal of Cell Science, 77, 209-223.

STRUM, J., GARTNER, L. & HIATT, J. 2007. Cell biology and histology. Hagerstwon, MD: Lippincott Williams & Wilkins, 83.

STRUTZ, F., OKADA, H., LO, C. W., DANOFF, T., CARONE, R. L., TOMASZEWSKI, J. E. & NEILSON, E. G. 1995. Identification and characterization of a fibroblast marker: FSP1. The Journal of Cell Biology, 130, 393-405.

STRUTZ, F., ZEISBERG, M., ZIYADEH, F. N., YANG, C. Q., KALLURI, R., MULLER, G. A. & NEILSON, E. G. 2002. Role of basic fibroblast growth factor-2 in epithelial-mesenchymal transformation. Kidney International, 61, 1714-1728.

SULLIVAN, N. J., SASSER, A. K., AXEL, A. E., VESUNA, F., RAMAN, V., RAMIREZ, N., OBERYSZYN, T. M. & HALL, B. M. 2009. Interleukin-6 induces an epithelial-mesenchymal transition phenotype in human breast cancer cells. Oncogene, 28, 2940-2947.

SUME, S. S., KANTARCI, A., LEE, A., HASTURK, H. & TRACKMAN, P. C. 2010. Epithelial to mesenchymal transition in gingival overgrowth. The American Journal of Pathology, 177, 208-218.

SZLOSAREK, P., CHARLES, K. A. & BALKWILL, F. R. 2006. Tumour necrosis factor-α as a tumour promoter. European Journal of Cancer, 42, 745-750.

TABETA, K., YAMAZAKI, K., AKASHI, S., MIYAKE, K., KUMADA, H., UMEMOTO, T. & YOSHIE, H. 2000. Toll-like receptors confer responsiveness to lipopolysaccharide from Porphyromonas gingivalis in human gingival fibroblasts. Infection and Immunity, 68, 3731-3735.

TAKEICHI, M. 1990. Cadherins: a molecular family important in selective cell-cell adhesion. Annual Review of Biochemistry, 59, 237-252.

TAKEICHI, M. 1995. Morphogenetic roles of classic cadherins. Current Opinion in Cell Biology, 7, 619-627.

TAKKUNEN, M., GRENMAN, R., HUKKANEN, M., KORHONEN, M., GARCIA DE HERREROS, A. & VIRTANEN, I. 2006. Snail-dependent and -independent epithelial-mesenchymal transition in oral squamous carcinoma cells. Journal of Histochemistry and Cytochemistry, 54, 1263-1275.

TAN, X., LI, Y. & LIU, Y. 2007. Therapeutic role and potential mechanisms of active Vitamin D in renal interstitial fibrosis. The Journal of Steroid Biochemistry and Molecular Biology, 103, 491-496.

TANAKA, S.-I., SUMIOKA, T., FUJITA, N., KITANO, A., OKADA, Y., YAMANAKA, O., FLANDERS, K. C., MIYAJIMA, M. & SAIKA, S. 2010. Suppression of injury-induced epithelial-mesenchymal transition in a mouse lens epithelium lacking tenascin-C. Molecular Vision, 16, 1194-1205.

TANG, P., HUNG, M.-C. & KLOSTERGAARD, J. 1996. Human pro-tumor necrosis factor is a homotrimer. Biochemistry, 35, 8216-8225.

TAURA, K., IWAISAKO, K., HATANO, E. & UEMOTO, S. 2016. Controversies over the epithelial-to-mesenchymal transition in liver fibrosis. Journal of Clinical Medicine, 5, 9.

TAURA, K., MIURA, K., IWAISAKO, K., ÖSTERREICHER, C. H., KODAMA, Y., PENZ-ÖSTERREICHER, M. & BRENNER, D. A. 2010. Hepatocytes do not undergo epithelial-mesenchymal transition in liver fibrosis in mice. Hepatology, 51, 1027-1036.

TAVERNITI, V. & GUGLIELMETTI, S. 2011. The immunomodulatory properties of probiotic microorganisms beyond their viability (ghost probiotics: proposal of paraprobiotic concept). Genes & Nutrition, 6, 261-274.

TECHASEN, A., LOILOME, W., NAMWAT, N., DOKDUANG, H., JONGTHAWIN, J. & YONGVANIT, P. 2012. Cytokines released from activated human macrophages induce epithelial mesenchymal transition markers of cholangiocarcinoma cells. Asian Pacific Journal of Cancer Prevention, 13, 115-118.

TENG, Y., ZEISBERG, M. & KALLURI, R. 2007. Transcriptional regulation of epithelial-mesenchymal transition. The Journal of Clinical Investigation, 117, 304-306.

THIERY, J. P. 2002. Epithelial-mesenchymal transitions in tumour progression. Nature Reviews Cancer, 2, 442-54.

THIERY, J. P. & HUANG, R. 2005. Linking epithelial-mesenchymal transition to the well-known polarity protein Par6. Developmental Cell, 8, 456-458.

THIERY, J. P. & SLEEMAN, J. P. 2006. Complex networks orchestrate epithelial-mesenchymal transitions. Nature Reviews Molecular Cell Biology, 7, 131-142.

THIHA, K., TAKEUCHI, Y., UMEDA, M., HUANG, Y., OHNISHI, M. & ISHIKAWA, I. 2007. Identification of periodontopathic bacteria in gingival tissue of Japanese periodontitis patients. Oral Microbiology and Immunology, 22, 201-207.

THOMAS, P., BRICKMAN, J., PÖOPPERL, H., KRUMLAUF, R. & BEDDINGTON, R. Axis duplication and anterior identity in the mouse embryo. Cold Spring Harbor symposia on quantitative biology, 1997. Cold Spring Harbor Laboratory Press, 115-125.

TORTORA, G. J. & DERRICKSON, B. 2010. Essentials of anatomy and physiology, Wiley New Jersey.

TRIBBLE, G. D. & LAMONT, R. J. 2010. Bacterial invasion of epithelial cells and spreading in periodontal tissue. Periodontology 2000, 52, 68-83.

TSUJIMURA, H., TAMURA, T., KONG, H. J., NISHIYAMA, A., ISHII, K. J., KLINMAN, D. M. & OZATO, K. 2004. Toll-like receptor 9 signaling activates NF-κB through IFN regulatory factor-8/IFN consensus sequence binding protein in dendritic cells. The Journal of Immunology, 172, 6820-6827.

URNOWEY, S., ANSAI, T., BITKO, V., NAKAYAMA, K., TAKEHARA, T. & BARIK, S. 2006. Temporal activation of anti- and pro-apoptotic factors in human gingival fibroblasts infected with the periodontal pathogen, Porphyromonas gingivalis: potential role of bacterial proteases in host signalling. BMC Microbiology, 6, 26-26.

VAN DER FLIER, L. G. & CLEVERS, H. 2009. Stem cells, self-renewal, and differentiation in the intestinal epithelium. Annual Review of Physiology, 71, 241-260.

VAN DYKE, T. E. & DAVE, S. 2005. Risk factors for periodontitis. Journal of the International Academy of Periodontology, 7, 3.

VAN ROY, F. & BERX, G. 2008. The cell-cell adhesion molecule E-cadherin. Cellular and Molecular Life Sciences, 65, 3756-3788.

VASIOUKHIN, V., BOWERS, E., BAUER, C., DEGENSTEIN, L. & FUCHS, E. 2001. Desmoplakin is essential in epidermal sheet formation. Nature Cell Biology, 3, 1076-1085.

VINCENT, T., NEVE, E. P. A., JOHNSON, J. R., KUKALEV, A., ROJO, F., ALBANELL, J., PIETRAS, K., VIRTANEN, I., PHILIPSON, L., LEOPOLD, P. L., CRYSTAL, R. G., DE HERREROS, A. G., MOUSTAKAS, A., PETTERSSON, R. F. & FUXE, J. 2009. A SNAIL1-SMAD3/4 transcriptional repressor complex promotes TGF-β mediated epithelial-mesenchymal transition. Nature Cell Biology, 11, 943-950.

VIRCHOW, R. L. K. 1871. Die Cellularpathologie: in ihrer Begründung auf physiologische und pathologische Gewebelehre, Verlag von August Hirschwald, Unter den Linden No. 68.

VITTAL, R., FAN, L., GREENSPAN, D. S., MICKLER, E. A., GOPALAKRISHNAN, B., GU, H., BENSON, H. L., ZHANG, C., BURLINGHAM, W. & CUMMINGS, O. W. 2013. IL-17 induces type V collagen overexpression and EMT via TGF-β-dependent pathways in obliterative bronchiolitis. American Journal of Physiology-Lung Cellular and Molecular Physiology, 304, L401-L414.

WAJANT, H., PFIZENMAIER, K. & SCHEURICH, P. 2003. Tumor necrosis factor signaling. Cell Death & Differentiation, 10, 45-65.

WANG, H., WANG, H.-S., ZHOU, B.-H., LI, C.-L., ZHANG, F., WANG, X.-F., ZHANG, G., BU, X.-Z., CAI, S.-H. & DU, J. 2013. Epithelial–mesenchymal transition (EMT) induced by TNF-α requires AKT/GSK-3β-mediated stabilization of Snail in colorectal cancer. PLoS ONE, 8, e56664.

WANG, J. H., DOYLE, M., MANNING, B. J., DI WU, Q., BLANKSON, S. & REDMOND, H. P. 2002. Induction of bacterial lipoprotein tolerance is associated with suppression of toll-like receptor 2 expression. Journal of Biological Chemistry, 277, 36068-36075.

WARA-ASWAPATI, N., SURARIT, R., CHAYASADOM, A., BOCH, J. A. & PITIPHAT, W. 2007. RANKL upregulation associated with periodontitis and Porphyromonas gingivalis. Journal of Periodontology, 78, 1062-1069.

WEI, J., XU, G., WU, M., ZHANG, Y., LI, Q., LIU, P., ZHU, T., SONG, A., ZHAO, L., HAN, Z., CHEN, G., WANG, S., MENG, L., ZHOU, J., LU, Y., WANG, S. & MA, D. 2008. Overexpression of vimentin contributes to prostate cancer invasion and metastasis via Src regulation. Anticancer Research, 28, 327-334.

WELLS, R. G. 2010. The epithelial-to-mesenchymal transition in liver fibrosis: Here today, gone tomorrow? Hepatology, 51, 737-740.

WENDT, M. K., SMITH, J. A. & SCHIEMANN, W. P. 2010. Transforming growth factor-β-induced epithelial-mesenchymal transition facilitates epidermal growth factor-dependent breast cancer progression. Oncogene, 29, 6485-6498.

WENDT, M. K., TAYLOR, M. A., SCHIEMANN, B. J. & SCHIEMANN, W. P. 2011. Down-regulation of epithelial cadherin is required to initiate metastatic outgrowth of breast cancer. Molecular Biology of the Cell, 22, 2423-2435.

WHITE, D. A., TSAKOS, G., PITTS, N. B., FULLER, E., DOUGLAS, G. V. A., MURRAY, J. J. & STEELE, J. G. 2012. Adult Dental Health Survey 2009: common oral health conditions and their impact on the population. British Dental Journal, 213, 567-572.

WHITEMAN, E., LIU, C., FEARON, E. & MARGOLIS, B. 2008. The transcription factor snail represses Crumbs3 expression and disrupts apico-basal polarity complexes. Oncogene, 27, 3875-3879.

WIDYANTORO, B., EMOTO, N., NAKAYAMA, K., ANGGRAHINI, D. W., ADIARTO, S., IWASA, N., YAGI, K., MIYAGAWA, K., RIKITAKE, Y. & SUZUKI, T. 2010. Endothelial cell–derived endothelin-1 promotes cardiac fibrosis in diabetic hearts through stimulation of endothelial-to-mesenchymal transition. Circulation, 121, 2407-2418.

WILLIS, B. C. & BOROK, Z. 2007. TGF-β-induced EMT: mechanisms and implications for fibrotic lung disease. American Journal of Physiology-Lung Cellular and Molecular Physiology, 293, L525-L534.

WILSON, C., NICHOLES, K., BUSTOS, D., LIN, E., SONG, Q., STEPHAN, J.-P., KIRKPATRICK, D. S. & SETTLEMAN, J. 2014. Overcoming EMT-associated resistance to anti-cancer drugs via Src/FAK pathway inhibition. Oncotarget, 5, 7328-7341.

WU, Y., DENG, J., RYCHAHOU, P. G., QIU, S., EVERS, B. M. & ZHOU, B. P. 2009. Stabilization of Snail by NF-κB is required for inflammation-induced cell migration and invasion. Cancer Cell, 15, 416-428.

WU, Y. & ZHOU, B. P. 2010. Snail: More than EMT. Cell Adhesion & Migration, 4, 199-203.

WYNN, T. 2008. Cellular and molecular mechanisms of fibrosis. The Journal of Pathology, 214, 199-210.

XU, J., LAMOUILLE, S. & DERYNCK, R. 2009. TGF-β-induced epithelial to mesenchymal transition. Cell Research, 19, 156-172.

XUE, C., PLIETH, D., VENKOV, C., XU, C. & NEILSON, E. G. 2003. The gatekeeper effect of epithelial-mesenchymal transition regulates the frequency of breast cancer metastasis. Cancer Research, 63, 3386-3394.

YADAV, A., KUMAR, B., DATTA, J., TEKNOS, T. N. & KUMAR, P. 2011. IL-6 promotes head and neck tumor metastasis by inducing epithelial-mesenchymal transition via the JAK-STAT3-SNAIL signaling pathway. Molecular Cancer Research: MCR, 9, 1658-1667.

YAMANAKA, T., HORIKOSHI, Y., SUZUKI, A., SUGIYAMA, Y., KITAMURA, K., MANIWA, R., NAGAI, Y., YAMASHITA, A., HIROSE, T. & ISHIKAWA, H. 2001. PAR-6 regulates aPKC activity in a novel way and mediates cell-cell contact-induced formation of the epithelial junctional complex. Genes to Cells, 6, 721-731.

YAMAOKA, K., NOUCHI, T., MARUMO, F. & SATO, C. 1993. α-Smooth-muscle actin expression in normal and fibrotic human livers. Digestive Diseases and Sciences, 38, 1473-1479.

YAN, WA, G., WL, G., L, Q., T, T., N, T. & YP, H. 2010. Epithelial to mesenchymal transition in human skin wound healing is induced by tumor necrosis factor-alpha through bone morphogenic protein-2. American Journal of Pathology, 176, 2247-2258.

YAN, D., AVTANSKI, D., SAXENA, N. K. & SHARMA, D. 2012. Leptin-induced epithelial-mesenchymal transition in breast cancer cells requires β-catenin activation via Akt/GSK3-and MTA1/Wnt1 protein-dependent pathways. Journal of Biological Chemistry, 287, 8598-8612.

YANAKA, A., SUZUKI, H., SHIBAHARA, T., MATSUI, H., NAKAHARA, A., TANAKA, N. 2002. EGF promotes gastric mucosal restitution by activating Na+/H+ exchange of epithelial cells. American Journal of Physiology-Gastrointestinal and Liver Physiology, 282, G866-G876.

YÁÑEZ-MÓ, M., LARA-PEZZI, E., SELGAS, R., RAMÍREZ-HUESCA, M., DOMÍNGUEZ-JIMÉNEZ, C., JIMÉNEZ-HEFFERNAN, J. A., AGUILERA, A., SÁNCHEZ-TOMERO, J. A., BAJO, M. A. & ÁLVAREZ, V. 2003. Peritoneal dialysis and epithelial-to-mesenchymal transition of mesothelial cells. New England Journal of Medicine, 348, 403-413.

YANG, J. & WEINBERG, R. A. 2008. Epithelial-mesenchymal transition: at the crossroads of development and tumor metastasis. Developmental Cell, 14, 818-829.

YILMAZ, Ö. 2008. The chronicles of Porphyromonas gingivalis: the microbium, the human oral epithelium and their interplay. Microbiology, 154, 2897-2903.

YOO, Y. A., KANG, M. H., LEE, H. J., KIM, B.-H., PARK, J. K., KIM, H. K., KIM, J. S. & OH, S. C. 2011. Sonic hedgehog pathway promotes metastasis and lymphangiogenesis via activation of Akt, EMT, and MMP-9 pathway in gastric cancer. Cancer Research, 71, 7061-7070.

YOSHIDA, K., SAITO, T., KAMIDA, A., MATSUMOTO, K., SAEKI, K., MOCHIZUKI, M., SASAKI, N. & NAKAGAWA, T. 2013. Transforming growth factor-β transiently induces vimentin expression and invasive capacity in a canine mammary gland tumor cell line. Research in Veterinary Science, 94, 539-541.

YU, H., ZENG, J., LIANG, X., WANG, W., ZHOU, Y., SUN, Y., LIU, S., LI, W., CHEN, C. & JIA, J. 2014. Helicobacter pylori promotes epithelial–mesenchymal transition in gastric cancer by downregulating programmed cell death protein 4 (PDCD4). PLoS ONE, 9, e105306.

YUCEL-LINDBERG, T. & BÅGE, T. 2013. Inflammatory mediators in the pathogenesis of periodontitis. Expert Reviews in Molecular Medicine, 15, e7.

ZANDI, E., ROTHWARF, D. M., DELHASE, M., HAYAKAWA, M. & KARIN, M. 1997. The IκB Kinase complex (IKK) contains two kinase subunits, IKKα and IKKβ, necessary for IκB phosphorylation and NF-κB activation. Cell, 91, 243-252.

ZAVADIL, J. & BÖTTINGER, E. P. 2005. TGF-β and epithelial-to-mesenchymal transitions. Oncogene, 24, 5764-5774.

ZEISBERG, M., HANAI, J.-I., SUGIMOTO, H., MAMMOTO, T., CHARYTAN, D., STRUTZ, F. & KALLURI, R. 2003. BMP-7 counteracts TGF-[beta]1-induced epithelial-to-mesenchymal transition and reverses chronic renal injury. Nature Medicine, 9, 964-968.

ZEISBERG, M. & NEILSON, E. G. 2009. Biomarkers for epithelial-mesenchymal transitions. The Journal of Clinical Investigation, 119, 1429-1437.

ZEISBERG, M., YANG, C., MARTINO, M., DUNCAN, M. B., RIEDER, F., TANJORE, H. & KALLURI, R. 2007. Fibroblasts derive from hepatocytes in liver fibrosis via epithelial to mesenchymal transition. Journal of Biological Chemistry, 282, 23337-23347.

ZHANG, J., CHEN, Y.-L., JI, G., FANG, W., GAO, Z., LIU, Y., WANG, J., DING, X. & GAO, F. 2013a. Sorafenib inhibits epithelial-mesenchymal transition through an epigenetic-based mechanism in human lung epithelial cells. PLoS ONE, 8, e64954.

ZHANG, S., WANG, X., IQBAL, S., WANG, Y., OSUNKOYA, A. O., CHEN, Z., CHEN, Z., SHIN, D. M., YUAN, H., WANG, Y. A., ZHAU, H. E., CHUNG, L. W. K., RITENOUR, C., KUCUK, O. & WU, D. 2013b. Epidermal growth factor promotes protein degradation of epithelial protein lost in neoplasm (EPLIN), a putative metastasis suppressor, during epithelial-mesenchymal transition. The Journal of Biological Chemistry, 288, 1469-1479.

ZHANG, W., JU, J., RIGNEY, T. & TRIBBLE, G. 2014. Porphyromonas gingivalis infection increases osteoclastic bone resorption and osteoblastic bone formation in a periodontitis mouse model. BMC Oral Health, 14, 89.

ZHANG, X., LIU, S., HU, T., HE, Y. & SUN, S. 2009. Up-regulated microRNA-143 transcribed by nuclear factor kappa B enhances hepatocarcinoma metastasis by repressing fibronectin expression. Hepatology, 50.

ZHAO, L., QUAN, Y., WANG, J., WANG, F., ZHENG, Y. & ZHOU, A. 2015. Vitamin C inhibit the proliferation, migration and epithelial-mesenchymal-transition of lens epithelial cells by destabilizing HIF-1α. International Journal of Clinical and Experimental Medicine, 8, 15155-15163.

ZHAO, L., YANG, R., CHENG, L., WANG, M., JIANG, Y. & WANG, S. 2011. LPS-induced epithelial-mesenchymal transition of intrahepatic biliary epithelial cells. Journal of Surgical Research, 171, 819-825.

ZHOU, B., VON GISE, A., MA, Q., HU, Y. W. & PU, W. T. 2010. Genetic fate mapping demonstrates contribution of epicardium-derived cells to the annulus fibrosis of the mammalian heart. Developmental Biology, 338, 251-261.

Appendix

Outputs from this thesis

1. A. A. Abdulkareem, G. Landini, R. M. Shelton, P. R. Cooper, M. R. Milward. The potential role of EMT in the pathogenesis of chronic periodontitis (Poster). BSP Autumn Conference 21-23 September 2014, Birmingham.

   Introduction:

   Crevicular epithelium protects the periodontal tissues from bacterial invasion. Disruption of epithelial integrity may predispose patients to periodontitis. Epithelial-mesenchymal transition (EMT) results in a switch from an epithelial to mesenchymal cellular/tissue phenotype resulting in barrier function loss, frustrated tissue healing and fibrosis, all characteristic of periodontitis.

   Inducers of EMT including bacteria, hypoxia, reactive oxygen species, and pro-inflammatory cytokines all present in the periodontal pocket.

   Aim:

   To investigate a potential role of periodontal pathogens to induce EMT

   Methods:

   Oral epithelial cells (H400 cells) were grown to a sub-confluence in 5% CO2 at 37°C and exposed to heat-killed F. nucleatum (FN), P. gingivalis (PG) or E. coli LPS (positive control) for up to 8-days. RNA was harvested on days 1, 5 and 8. RT-PCR was performed to determine the relative gene expression of key EMT markers (vimentin, FSP-1, β-catenin, E-cadherin, and N-cadherin) in comparison with non-exposed cultures

   Results:

   'Chronic' exposure of oral epithelial cells (up to 8-days) to PG & FN resulted in up-regulation of vimentin and FSP-1 and down-regulation of β-catenin and E-cadherin in comparison with un-exposed controls.

   Conclusion:

   Heat-killed periodontal pathogens induced expression and inhibition of genes associated with EMT suggesting a possible role in periodontal disease pathogenesis. This could offer a new target in disease management.

2. Ali A Abdulkareem. Potential role of Epithelial- Mesenchymal Transition (EMT) in the Pathogenesis of Periodontitis (Seminar). College of Dentistry/ University of Birmingham May 2015.

3. A. A. Abdulkareem, G. Landini, R. M. Shelton, P. R. Cooper, M. R. Milward. Bacterially stimulated TGF-β1 potentially induces epithelial-mesenchymal transition in a chronic periodontitis model system (Poster). EUROPERIO conference of the European federation of periodontology 3-6 June 2015, London. Published in Journal of Clinical Periodontology Volume 42, Issue Supplement S17 Pages 1–467, 2015.

   Aim:

   TGF-β1 is a potent inducer of epithelial-mesenchymal transition (EMT) in various diseases including drug-induced gingival overgrowth. Periodontal pathogens provoke changes in molecular expression in pocket epithelial cells. The aim of this study was to

investigate TGF-β1 expression in an EMT in vitro model system which utilised cultured oral keratinocytes and periodontal pathogens.

Materials and Methods:

Oral keratinocytes (H400) were grown to sub-confluence in an atmosphere of 5% CO2 at 37°C and exposed to heat-killed F. nucleatum (FN), P. gingivalis (PG) (100 bacteria per keratinocyte) or 20 µg/ml E. coli lipopolysaccharide (LPS) for up to 8-days.

Culture supernatants were collected on days 1, 5, and 8 to determine TGF-β1 protein levels (ELISA) and RNA was also isolated from cultures using the RNeasy mini-kit. Reverse transcription polymerase chain reaction was performed to determine the relative gene expression levels of TGF-β1 and the key EMT markers (vimentin, S100A4, β-catenin, E-cadherin and N-cadherin) compared with non-exposed cultures.

Results:

'Chronic' exposure of oral keratinocytes to PG, FN & LPS resulted in a significant increased TGF-β1 protein production (ANOVA, $P<0.05$) at days 1, 5, and 8. In addition there was up-regulation of TGF-β1 transcript and key mesenchymal markers (N-cadherin, vimentin and S100A4), associated with down-regulation of epithelial markers (β-catenin and E-cadherin) over this period compared with non-exposed controls.

Conclusion:

Prolonged exposure of oral keratinocytes to periodontal pathogens increased TGF-β1 levels which potentially promoted EMT. These cellular changes may result in disruption of epithelial barrier function in periodontal pockets and may contribute to periodontitis pathogenesis.

4. A. A. Abdulkareem, G. Landini, R. M. Shelton, P. R. Cooper, M. R. Milward. Epithelial mesenchymal transition: a novel mechanism potentially involved in the pathogenesis of periodontitis (Poster). BSP Spring Conference 2016 7-9 April 2016, Oxford.

Introduction

Periodontitis is a chronic inflammatory condition usually associated with non-resolving inflammation and breakdown of the crevicular epithelium. The ability of periodontal pathogens to induce epithelial mesenchymal transition (EMT); by reprogramming cells from an epithelial to mesenchymal-like phenotype, in the crevicular epithelium potentially provides a novel mechanism for periodontitis pathogenesis.

Aim

To identify whether periodontal pathogens can trigger features of EMT in periodontitis models in vitro.

Material and Methods

Rat primary oral keratinocytes, (passage 1-4) were cultured to sub-confluence in 5% CO2 at 37°C; then exposed to heat-killed F. nucleatum (FN), P. gingivalis (PG) (100 bacteria/cell) or E. coli lipopolysaccharide (LPS) (20µg/ml) for up to 8-days. Molecular and phenotypic changes were investigated using RT-PCR for key EMT markers (vimentin, FSP-1, β-catenin, E-cadherin, and N-cadherin), transwell migration, wound healing assays and immunostaining for E-cadherin and vimentin. Controls were non-exposed cultures.

Results

Cells exposed to bacteria demonstrated up-regulation of vimentin, N-cadherin and FSP-1 and down-regulation of β-catenin and E-cadherin using RT-PCR after 1, 5, and 8 days. Cells also exhibited increases in migratory activity and the number of vimentin positive and E-cadherin negative cells in comparison with non-exposed controls.

Conclusion

Periodontal pathogens induced EMT-like changes which may contribute to compromised epithelial integrity, indicating a possible role of this mechanism in the pathogenesis of periodontitis.

5. A. A. Abdulkareem, G. Landini, R. M. Shelton, P. R. Cooper, M. R. Milward. Potential role of periodontal pathogens to induce epithelial mesenchymal transition in periodontitis model *in vitro* (Poster). Research Poster Conference 2016, University of Birmingham.

Aim:

Transforming growth factor-β1 (TGF-β1) is a potent inducer of epithelial-mesenchymal transition (EMT) in various diseases including drug-induced gingival overgrowth. Periodontal pathogens provoke changes in molecular expression in pocket epithelial cells. The aim of this study was to investigate TGF-β1 expression in an EMT in vitro model system which utilised cultured oral keratinocytes and periodontal pathogens.

Materials and Methods:

Oral keratinocytes (H400) were grown to sub-confluence in an atmosphere of 5% CO2 at 37°C and exposed to heat-killed F. nucleatum (FN), P. gingivalis (PG) (100 bacteria per keratinocyte) or 20 µg/ml E. coli lipopolysaccharide (LPS) for up to 8-days.

Culture supernatants were collected on days 1, 5, and 8 to determine TGF-β1 protein levels (ELISA) and RNA was isolated from cultures using the RNeasy mini-kit. Reverse transcription polymerase chain reaction was performed to determine the relative gene expression levels of TGF-β1 and the key EMT markers (vimentin, S100A4, β-catenin, E-cadherin and N-cadherin) compared with non-exposed cultures.

Results:

'Chronic' exposure of oral keratinocytes to PG, FN & LPS resulted in a significant increased TGF-β1 protein production (ANOVA, $P<0.05$) at days 1, 5, and 8. In addition there was up-regulation of TGF-β1 transcript and key mesenchymal markers (N-cadherin, vimentin and S100A4), associated with down-regulation of epithelial markers (β-catenin and E-cadherin) over this period compared with non-exposed controls.

Conclusion:

Prolonged exposure of oral keratinocytes to periodontal pathogens potentially promoted EMT. Also, these bacteria caused upregulation of TGF-β1 level, which could be involved in EMT induction. These cellular changes may result in disruption of epithelial barrier function in periodontal pockets and may contribute to periodontitis pathogenesis.